US Army Corps of Engineers

AD-A167 447

(12)

TECHNICAL REPORT SL-86-2

EFFECTS OF EDGE RESTRAINT ON SLAB BEHAVIOR

by

L. K. Guice

Structures Laboratory

DEPARTMENT OF THE ARMY
Waterways Experiment Station, Corps of Engineers
PO Box 631, Vicksburg, Mississippi 39180-0631

DTIC
ELECTE
MAY 05 1986
S D

February 1986
Final Report

Approved For Public Release, Distribution Unlimited

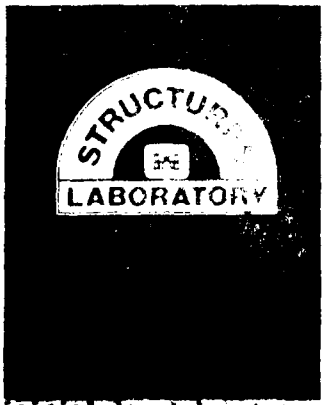

DTIC FILE COPY

Prepared for
Federal Emergency Management Agency
Washington, DC 20472

86 5 5 016

TECHNICAL REPORT SL-86-2

EFFECTS OF EDGE RESTRAINT ON SLAB BEHAVIOR

by

L. K. Guice

Structures Laboratory

DEPARTMENT OF THE ARMY
Waterways Experiment Station, Corps of Engineers
PO Box 631, Vicksburg, Mississippi 39180-0631

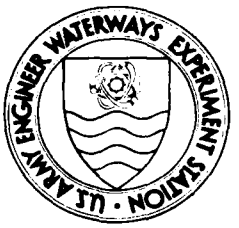

February 1986
Final Report

Approved For Public Release; Distribution Unlimited

This report has been reviewed in the Federal Emergency Management Agency and approved for publication. Approval does not signify that the contents necessarily reflect the views and policies of the Federal Emergency Management Agency.

Prepared for

Federal Emergency Management Agency
Washington, DC 20472

DISCLAIMER NOTICE

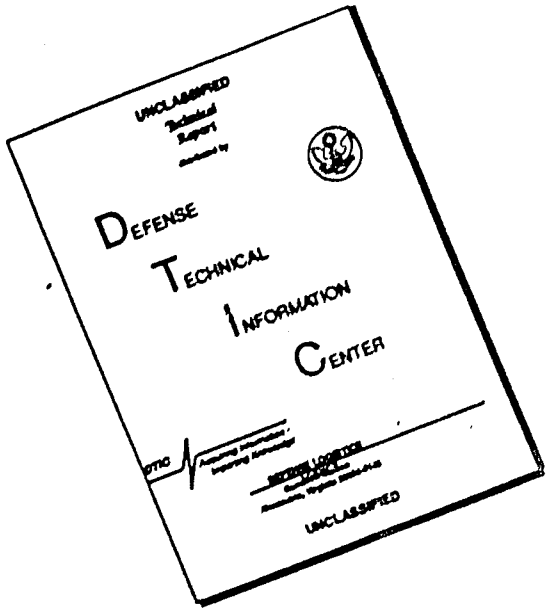

THIS DOCUMENT IS BEST QUALITY AVAILABLE. THE COPY FURNISHED TO DTIC CONTAINED A SIGNIFICANT NUMBER OF PAGES WHICH DO NOT REPRODUCE LEGIBLY.

Unclassified

SECURITY CLASSIFICATION OF THIS PAGE *(When Data Entered)*

REPORT DOCUMENTATION PAGE		READ INSTRUCTIONS BEFORE COMPLETING FORM
1 REPORT NUMBER Technical Report SL-86-2	2. GOVT ACCESSION NO. ADA 167447	3. RECIPIENT'S CATALOG NUMBER
4. TITLE *(and Subtitle)* EFFECTS OF EDGE RESTRAINT ON SLAB BEHAVIOR		5. TYPE OF REPORT & PERIOD COVERED Final report 6. PERFORMING ORG. REPORT NUMBER
7. AUTHOR(s) L. K. Guice		8. CONTRACT OR GRANT NUMBER(s)
9. PERFORMING ORGANIZATION NAME AND ADDRESS US Army Engineer Waterways Experiment Station Structures Laboratory PO Box 631, Vicksburg, Mississippi 39180-0631		10. PROGRAM ELEMENT, PROJECT, TASK AREA & WORK UNIT NUMBERS
11. CONTROLLING OFFICE NAME AND ADDRESS Federal Emergency Management Agency 500 C Street, SW, Room 716 Washington, DC 20472		12. REPORT DATE February 1986 13. NUMBER OF PAGE 251
14. MONITORING AGENCY NAME & ADDRESS *(if different from Controlling Office)*		15. SECURITY CLASS. *(of this report)* 15a. DECLASSIFICATION/DOWNGRADING SCHEDULE

16. DISTRIBUTION STATEMENT *(of this Report)*

Approved for public release; distribution unlimited.

17. DISTRIBUTION STATEMENT *(of the abstract entered in Block 20, if different from Report)*

18. SUPPLEMENTARY NOTES

Available from National Technical Information Service, 5285 Port Royal Road, Springfield, Virginia 22161.

19. KEY WORDS *(Continue on reverse side if necessary and identify by block number)*

Atomic bomb shelters--Design and construction (LC)
Concrete slabs--Blast effect (LC)
Reinforced concrete construction (LC)
Slabs--Blast effect (LC)

20. ABSTRACT *(Continue on reverse side if necessary and identify by block number)*

This study was performed in conjunction with a Federal Emergency Management Agency program to plan, design, and construct keyworker blast shelters which would be used in high-risk areas of the country during and after a nuclear attack. The shelters considered in this study were box-type structures in which damage is much more likely to occur in the roof slab than in the walls or floor. In this part of the program, the effect of edge restraint on slab

(Continued)

DD FORM 1 JAN 73 1473 EDITION OF 1 NOV 65 IS OBSOLETE

Unclassified

SECURITY CLASSIFICATION OF THIS PAGE *(When Data Entered)*

20. Abstract (Continued).

behavior was investigated. The primary objective was to determine the effects of partial rotational restraint on slab strength, ductility, and mechanism of failure.

Sixteen one-way, reinforced concrete plate elements were tested in a reaction structure under uniform static water pressure. A "thick-slab" group consisted of eight slabs with span-thickness ratios of 10.4, while eight slabs in the "thin-slab" group had span-thickness ratios of 14.8. The following conclusions were reached at the completion of testing:

1. Thrusts enhanced the flexural capacities of slabs with small rotational freedoms as long as the lateral stiffness was sufficient to develop in-plane forces.
2. The deflections at which the peak capacities were achieved were significantly different for slabs with varied rotational freedoms.
3. For larger rotational freedoms, the peak capacities occurred at large deflections, were significantly lower than the capacities which were predicted by compressive membrane theory, and in some cases, the slabs had no definitive flexural capacity at all.
4. Smaller rotational freedoms were necessary to induce a stability failure in the thin slabs.
5. Significantly more tensile membrane response occurred in the thin-slab group than in the thick-slab group.
6. In those slabs which were reinforced with ductile No. 2 bars, average incipient collapse deflection occurred at approximately one-eighth of the span for the thick-slab group and somewhat more than that for the thin-slab group.

PREFACE

The research reported herein was sponsored by the Federal Emergency Management Agency (FEMA) through the US Army Engineer Huntsville Division (HND).

Construction and testing were conducted by personnel of the Structures Laboratory (SL), US Army Engineer Waterways Experiment Station (WES), under the general supervision of Mr. Bryant Mather, Chief, SL, and Mr. J. T. Ballard, Assistant Chief, SL. Chief of the Structural Mechanics Division (SMD) during this investigation was Dr. J. P. Balsara. The project was managed by Dr. S. A. Kiger, and Mr. S. C. Woodson supervised the experiments. This report was prepared by Mr. L. K. Guice and was edited by Ms. Janean Shirley, Publications and Graphic Arts Division.

COL Allen F. Grum, USA, was Director of WES during the preparation and publication of this report. Dr. Robert W. Whalin was Technical Director.

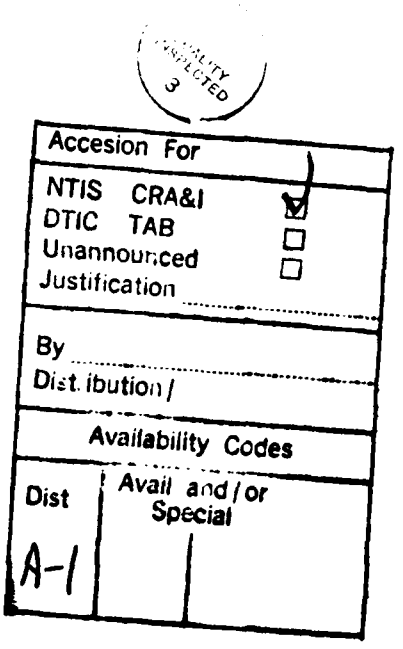

CONTENTS

LIST OF ILLUSTRATIONS

LIST OF TABLES

CONVERSION FACTORS, NON-SI TO SI (METRIC)
UNITS OF MEASUREMENT

Non-SI units of measurement used in this report can be converted to SI (metric) units as follows:

Multiply	By	To Obtain
degrees	0.01745	radians
feet	0.3048	metres
inches	2.54	centimetres
inch-pounds	0.1129848	newton-metres
kips (force) per inch	175.1268	kilonewtons per metre
kips per square inch	6.894757	megapascals
pounds (force)	4.448222	newtons
pounds (force) per square inch	6.894757	kilopascals
square inches	6.4516	square centimetres

CHAPTER 1

INTRODUCTION

1.1 BACKGROUND

At the time of this study, civil defense planning called for the evacuation of nonessential personnel to safe host areas during a time of crisis, and the construction of shelters to protect the keyworkers remaining in the risk areas. The Federal Emergency Management Agency (FEMA) tasked the US Army Engineer Huntsville Division (HND) to develop Keyworker Blast Shelter designs. The research reported herein is in support of the HND design effort.

Economic considerations in the design of these structures are very important. Design alterations that result in a reduction of materials or a simplification in construction can have a significant impact on the total cost of the program. However, design modifications that reduce the structural capacity below a specified safety threshold are not considered to be valid.

Both conventional and nuclear blast simulation procedures have been used to evaluate the structural capacity of these facilities. The conventional design criteria have undergone repeated verification through laboratory experimentation and through the construction of facilities by the public sector. However, nuclear design procedures have not been rigorously verified but are continuously investigated. Methods have been developed to analyze the response of structures under the exponentially decayed pressure histories produced by nuclear weapons, but those methods are not consistently in agreement with the test data for simulated low-yield nuclear weapons effects.

For box-type structures such as the keyworker blast shelters, the roof slab is much more likely to see significant structural damage than the walls or floor. Consequently, analytical and experimental investigations of the overall structural behavior are generally not necessary. Models which accurately represent the response of the roof slab should sufficiently represent the controlling response of the whole structure.

Predicting the flexural response of structural slabs under blast loads requires a thorough understanding of their behavior under similarly distributed static loads. Unless an alternate mode of response is invoked, e.g.,

shear, then the dynamically loaded slab is typically assumed to provide a pattern of resistance, i.e., response similar to a statically loaded slab. However, some differences in resistance magnitude may be noted because of strain-rate effects in the material properties.

1.2 OBJECTIVES

The major purpose of this program was to investigate the effects of edge restraint on slab behavior. In the past, both static and dynamic analyses have been based on the idealized conditions of perfect lateral and rotational restraint. However, prototype structures are seldom adequately represented by the idealized boundary conditions used in analytical and experimental models.

Recent static tests of rigidly restrained, one-way reinforced concrete slab strips at WES have produced some behavioral patterns which in some ways were considered to be undesirable. For example, failure was characterized by relatively narrow crack bands, and by little, if any, tensile membrane capacity. Although the peak flexural capacities were quite predictable using compressive membrane theory, the unpredictable behavior beyond the point of maximum capacity led to a lack of confidence in the existing analytical capabilities for determining overall slab strength and ductility. Consequently, one of the major objectives of this investigation was to improve understanding of the load-deflection relationships for slabs with geometric proportions, reinforcement patterns, and boundary conditions similar to those used in the keyworker blast shelter design.

It was anticipated that slabs with partial rotational restraint would not have significantly different initial behavior than slabs with rigid restraint, but that the failure mechanisms could be different, particularly if rotations were significant enough to allow structural instability. If this were true, and if the structural configuration of the keyworker blast shelter did permit sufficient rotations, then analytical models could be improved to provide a more realistic analysis. An improvement in analytical capabilities always leads to a greater confidence in the integrity of design and provides a basis for making design alterations.

Certain geometric slab parameters, such as reinforcement ratio and span-thickness ratio, were also known to have a significant effect on slab behavior. Previous tests had revealed that a minimum reinforcement ratio was required in order to achieve an enhanced tensile membrane capacity. There

was also a suggestion that slabs with smaller span-thickness ratios would generally have a better tendency to exhibit reserve strength. Because both of these parameters were under investigation in the final design of the shelter, it was considered necessary to bound the most probable solution with the slabs used in this experimental program.

Finally, in order to properly evaluate the effects of each parameter on the behavior of the slabs, an instrumentation program was needed which would provide accurate measurements of slab end actions. Measurements of end rotations, moments, and thrusts were considered necessary to suitably define the boundary conditions of the slab.

In summary, the objectives of this investigation were:

1. To determine the effects of partial rotational restraint on slab strength, ductility, and mechanism of failure.

2. To determine the behavioral characteristics of slabs with different reinforcement ratios and span-thickness ratios.

3. To improve analytical procedures for predicting slab resistance.

4. To validate and/or enhance design criteria for slabs used in the keyworker blast shelters.

1.3 SCOPE

Sixteen one-way, reinforced concrete plate elements were loaded in a reaction structure under uniform static water pressure. The slabs were approximately 1:4-scale models of slabs with geometric parameters similar to the prototype keyworker blast shelters. Overall dimensions of the slabs were 24 inches[1] by 36 inches with an effective loaded area of 24 inches by 24 inches. All slabs had the same percentage of steel in both compression and tension.

The span-thickness ratio, reinforcement ratio, and degree of rotational restraint were the primary parameters varied in the tests. Tests were conducted on eight slabs with span-thickness ratios of approximately 10.4 and reinforcement ratios of 0.52 percent, 0.74 percent, and 1.06 percent in each face. The eight remaining slabs had span-thickness ratios of 14.8 and reinforcement ratios of 0.58 percent, 1.14 percent, and 1.47 percent.

The reaction structure was designed to permit partial rotation at the

[1] A table of factors for converting non-SI units of measurement to SI (metric) units is presented on page 5.

supports. Rotations were varied within a range expected to simulate elastic rotations in a box-type structure. Average support rotations were varied between approximately 0.4 and 2.8 degrees.

CHAPTER 2

EXPERIMENTAL INVESTIGATION

2.1 OVERVIEW

The experimental phase of the project consisted of the testing of 16 scaled models of one-way reinforced concrete slabs. Slabs with an effective loaded area of 24 inches by 24 inches but supported on only two edges were tested under uniform static pressure. The intent of performing tests on slab strips was to isolate the primary action of one-way slabs and eliminate any contributary effects due to two-way action. In addition, the choice of slab strips enabled the tests to be conducted on much larger models than would otherwise have been possible.

All slabs had equal percentages of steel in the top and bottom faces. Temperature steel was provided in the transverse direction. Single-leg stirrups were spaced along the length of the longitudinal bars at the locations of the transverse reinforcement. This steel configuration resulted in a structural cage which provided confinement for the inner core of concrete. A study of the effects of shear stirrup details on slab behavior was presented by Woodson (Reference 1). That report and recommendations from the shelter design group were used as a basis for the selection of the reinforcement configurations for this program.

It was necessary to design and construct a reaction structure which would meet the objective of permitting partial rotational restraint as established for this program. It was also deemed necessary to provide additional capability for measuring actions at the ends of the slabs. A reaction structure was constructed which allowed the slabs to be mounted in rigid steel support racks which were permitted to rotate within the confines of a solid steel reaction structure. Efforts were made to eliminate undesirable friction forces and to isolate the various member-end actions of the slab. Figures 2.1 and 2.2 illustrate the overall design of the reaction structure in its test configuration.

Measurements of support displacements, thrusts, and moments were made to allow accurate evaluation of slab behavior. Recorded data also included water pressure, steel strains, early time concrete strains, and slab deflections.

Descriptions of the element construction details, material properties,

test configuration, instrumentation, and test procedure are provided in the following sections.

2.2 SLAB CONSTRUCTION DETAILS

One-half of the 16 slabs were constructed with a span-thickness ratio of 10.4, providing a direct correlation with previous tests performed for the prototype structure. The rest of the slabs were constructed with a span-thickness ratio of 14.8, representing more recent enhancements to the design of the prototype slabs.

Actual dimensions of the slabs were 24 inches by 36 inches. However, 6 inches on each supported end of the slab were clamped between flat plates to provide continuity between the slab and support racks. Since the ends of the slabs acted integrally with the supports, only 24 inches by 24 inches of the slabs were effectively loaded by the surface pressure.

The slab thickness was 2-5/16 inches for the thick-slab group and 1-5/8 inches for the thin slabs. The distance from the outer face of the slab to the center of the reinforcement was held to 3/8 inch in every case, resulting in effective depths of 1-15/16 inches and 1-1/4 inches, respectively.

Three steel percentages were selected for each of the two slab groups. The slabs with larger span-thickness ratios had steel ratios of 0.52 percent, 0.74 percent, and 1.06 percent. The slabs with smaller span-thickness ratios had a higher limiting steel ratio of 1.47 percent and other ratios of 0.58 percent and 1.14 percent. The actual variances in design parameters are specified in Table 2.1. Slab construction details are listed in Table 2.2 and illustrated in Figure 2.3.

Selection and placement of reinforcement was based on an objective to achieve the specified steel percentages while minimizing the variance of bar size and spacing. Recent tests have indicated that bar spacings greater than the slab thickness do not have a significant effect on slab behavior. Consequently, primary reinforcement spacings were controlled within the limits of 1 to 2.5 times the slab thickness. Bar diameters for the principal reinforcement were varied from 0.183 inch to 0.25 inch, with the latter diameter being used for 75 percent of the slabs.

Small-diameter wire was used for temperature steel in all slabs and was equally spaced at 3 inches along the top and bottom mats. Both mats were tied together with single-leg, 0.11-inch-diameter wire stirrups placed at the

locations where the temperature steel crossed the longitudinal steel. This configuration resulted in temperature steel percentages of 0.27 percent and 0.41 percent for both slab thicknesses. Shear steel percentage varied according to the spacing of the longitudinal steel. Small-gage tie wire was used to hold the stirrups, temperature steel, and primary steel in position.

2.3 REACTION STRUCTURE DETAILS

The reaction structure was designed with the objective of permitting partial rotations at the supports while satisfying the size constraints of (1) using the standardized slab size of 24 inches by 36 inches and (2) using the existing 6-foot-diameter load-generator facility. Other major considerations in the design of the structure were to keep the size of the gaps between the slab reaction structure as small as possible, to provide adequate room for the adjustment of instrumentation, to provide for the capability to test slabs of various thicknesses, and to use the most readily available construction materials.

Six-inch-thick plate steel was selected as the construction material for the reaction structure because of its strength, stiffness, adaptability, and availability. Because high stress concentrations were expected in the areas of localized support reactions and because numerous openings for instrumentation were required, the structure was constructed of steel rather than a composite of steel and concrete. Also, facilities were available for cutting, welding, and machining of heavy steel plate, making the selection of the material even more appropriate. Detailed drawings of the reaction structure are provided in Appendix A.

Rigid steel support racks were designed to transmit slab reactions to the major portion of the reaction structure through symmetrically placed shafts and spring assemblies. The large-diameter cylindrical shafts located at each end of the support racks were machined and fitted into roller bearings. The spring assemblies were mounted to the long edge of each support rack through ball-and-socket connectors, and then fitted into slots of the reaction structure.

The spring assemblies were conceptually designed as soft load cells. By using disk springs, each assembly could be controlled to deflect by a predetermined amount and with a given stiffness. This particular design offered the advantage of providing the capability to alter the assembly deflection and

stiffness, and consequently, the rack rotation parameters, simply by modifying the configuration of the disks. Also, load washers inserted with each group of disk springs were capable of monitoring the magnitude of the load passing through the assemblies.

In addition to the load washers used in the spring assemblies, other load washers were used between the support racks and the reaction structure at the location of the cylindrical shafts. These load washers, located on each side of the shafts, were used to measure the thrusts and tensile forces generated from the restained lateral movement of the slab.

Thrusts and moments were transmitted from the slab to the support racks by bearing and friction forces developed along the steel plate and concrete slab interfaces. High-strength steel bolts were countersunk into steel plates on top of the slab, inserted through small holes at the end of the slab, and screwed into threaded openings in the support racks. Small steel plates were also inserted between the ends of the slab and the support racks to provide bearing resistance to lateral movement of the slab.

The design of the reaction structure allowed for the use of variable slab thicknesses and permitted relatively large tolerances in construction of the slabs. The support racks were designed to handle slabs with thicknesses up to 4 inches.

2.4 INSTRUMENTATION

Approximately 30 channels of analog data were recorded on magnetic tape for each test. The data for each channel were later digitized, processed, and plotted. Most of the channels were used to record data from instruments which were common to all tests. However, some channels were varied from test to test in an effort to obtain a broader range of data and still remain within the limits of a 32-channel recorder. A summary of the recorded channels and related instrumentation is provided in Table 2.3. Figure 2.4 shows the location of the instrumentation in the test configuration.

Two water-pressure gages (Kulite Model HKM-375) were mounted inside the bonnet of the load-generator facility to record the pressure applied to the slab. One of those gages was used as a reference channel for all subsequent data.

Position/displacement transducers (Celesco Model PT-101) with a full-scale range of 10 inches and an accuracy of 0.1 percent were used to record

the quarterspan and midspan slab deflections. These transducers measured the displacement of the slab by means of a potentiometer which detected the extension and retraction of a cable attached to a spring inside the transducer. The body of each transducer was mounted to the floor of the reaction structure and the cable was attached to wires projecting from the slab.

Linear variable differential transformers (LVDT's) (Trans-Tek Model 244-000) were used to measure the lateral movement of the bottom portion of the support racks. One LVDT was mounted to each end of the reaction structure with its probe attached to the associated support rack. Rotations were computed from the measured displacements and known geometries.

Two types of load washers were used in the tests. Eaton Model 3711-500 load sensors were used in the spring assemblies which were attached to the support racks. These 20,000-pound-capacity sensors had a maximum calibrated nonlinearity of 3.4 percent. Large-diameter and high-capacity force washers (Houston Scientific Model 2054V-100) were used to measure the thrusts transmitted to the reaction structure at the location of the large shafts at the ends of the support racks. A maximum calibration nonlinearity of 12.4 percent was computed within the working range of the 100,000-pound-capacity washers. At least one high-capacity washer was placed in a position to measure the vertical load being transmitted through the support racks.

Single-axis, metal-film, 350-ohm strain gages (Micro-Measurements Model EA-06-125 BZ-350) were mounted on the principal reinforcement at the midspan, quarterspan, and support. In every slab, two pairs of bars (two at the top and two at the bottom) were instrumented with strain gages. However, only one pair was monitored for strains during each test, except for the cases in which alternate bars were tested for verification.

Epoxy-coated concrete strain gages (Tokyo Sokki Kenkyujo Types PML-60 and PMC-60) were mounted on the surface of several slabs in the compression zones at midspan and near the support. The latter type of concrete gage had filaments in mutually perpendicular directions and was used to provide information on the biaxial stresses in the concrete.

In addition to the electronic data, visual data were recorded in several of the tests with the use of a remote-controlled camera. The camera was mounted in the bottom of the reaction structure and focused on the bottom of the slab to provide information on the sequence of formation of cracks. All slabs were painted white and marked with a reference line at quarterspan to

enhance visibility and establish orientation.

2.5 PROCEDURE

The steel reinforcement for all slabs was measured, cut, bent, and formed into a cage. The cage was then placed into wood forms which had been coated with a thin film of oil. All reinforcement was adjusted and tied into position. Next, the concrete was mixed and placed into the forms. A vibrating table was used to support the forms and compact the concrete during placement. The slabs were finished with hand trowels and placed under wet burlap. Water was applied to the burlap for approximately 7 days. Finally, the forms were removed and the slabs were stacked into position until the time of testing.

Tests were performed over a period of approximately 6 weeks beginning on August 13, 1984, nearly 75 days after the date of concrete placement. Slabs were tested in somewhat of a random order with several of the thick slabs tested first, followed by some of the thin slabs, and then the remainder of both slab groups. It was intended to conduct the tests with close controls on the degree of rotational restraint. However, because of construction tolerances in the reaction structure and difficulties in accurately measuring the pretest configurations, evaluations of rotational restraint could only be made after each test was completed.

In preparation for the test series, the load-generator facility was filled with sand to within about 40 inches from the top. Then the reaction structure was carefully positioned into the generator. The support racks were put in place and the spring assemblies were installed. Instrumentation which was to remain in position for all tests was connected to the main instrument panel. The LVDT'S and load washers were installed as semipermanent instrumentation for all of the tests.

For each test, a slab was placed into the support racks and held in position by partially tightening the bolts which passed through the holes in the ends of the slab. All strain gages were connected and verified at the instrument panel. For most of the tests, the assemblies at the ends of the support racks which provided lateral restraint were preloaded to about 20,000 pounds to insure that full lateral restraint would be provided. After the assemblies were preloaded, the support rack bolts were tightened, and all of the instrumentation channels were balanced to zero.

A specially constructed table was placed around the reaction structure to

provide support for the water pressure. A 1/2-inch-thick rubber mat and three 1-1/2-inch-thick layers of styrofoam were cut to be approximately the same size as the loaded area of the slab. The purpose of these mats was to raise the height of the loading surface and, consequently, minimize the amount of stretching in the rubber membranes.

Two thin, fiber-reinforced, rubber membranes were used to isolate the slab and reaction structure from the volume of water in the upper cavity of the generator. The membranes were clamped between two steel rings which perfectly fit the inside diameter of the generator. Slack was placed in the membranes to prevent the development of any significant tensile loads during the stage of large slab deflections.

After the rings and membranes were placed into the generator, the bonnet was lowered into position and the generator facility was moved into the central firing station. All instrumentation channels were taken through a final verification of calibration and then water was pumped into the upper cavity of the generator. Approximately 20 minutes was required to fill the chamber with water and raise the bonnet to bear against the massive portion of the central firing station. During that time the pressure was gradually increased to about 10 psi. Until the bonnet was firmly seated against the central firing station, a constant pressure of about 10 psi was maintained inside the chamber. As the pressure began to increase again, the pumping rate was reduced. Pumping rates were selected to control the rate of deflection to be slow and uniform throughout the test.

Upon completion of each test, the bonnet was taken off, all remaining water was discharged, and the membranes were removed. Posttest activities included an inspection of crack and spall behavior, the recording of steel rupture, and photography. Results of the individual tests are presented in the next chapter.

2.6 MATERIAL PROPERTIES

The design compressive strength of the concrete was selected to be 4,000 psi. A mix was designed using Portland cement type I, a 3/8-inch maximum-size limestone coarse aggregate, and a manufactured limestone sand fine aggregate. Two batches were prepared, one for each of the different thickness slab groups. A total of thirty-eight 4-inch-diameter cylinders were collected from the two batches. The average 28-day compressive strength for

the first batch was 3,420 psi and for the second batch was 4,760 psi. The remaining cylinders were tested at approximately the same time as the slab elements. Results of those compressive tests are provided in Table 2.4. It should be noted that standard tests correlating cylinders of various sizes suggest that a 4-inch-diameter cylinder should have a strength which is on the order of 3 percent greater than the strength of a 6-inch-diameter cylinder.

A regression analysis was performed on each batch of concrete cylinder data. The method of least squares was used to establish a second-order regression equation for the first batch and a linear regression equation for the second batch. Higher-order equations were generated for each batch, but those equations did not sufficiently characterize the behavior of concrete. The relationships between the equations and the raw data are illustrated in Figures 2.5 and 2.6.

Six of the cylinders were instrumented with strain gages to allow the constitutive relationships of the concrete under uniaxial compression to be evaluated. The modulus of elasticity and Poisson's ratio were determined for each cylinder according to the American Society for Testing and Materials Standards (ASTM C469). The average moduli of elasticity for Batches 1 and 2 were 3.98E6 psi and 4.92E6 psi, respectively. Average Poisson's ratios for each group were determined to be 0.19 and 0.21, respectively.

Most of the slabs were reinforced with standard No. 2 deformed reinforcing bars. However, in order to provide the desired steel percentages and to maintain appropriate bar spacings, a few of the slabs were constructed with small-diameter, heat-treated, deformed wire. The heat treatment of the wire was performed at WES. By controlling oven temperatures and time of heating, a steel wire was produced with a substantially lower but more definitive yield strength and with an increased ductility. The yield strength and ultimate strength were the primary parameters which were observed during the initial heat-treatment trials. Because of malfunctioning instrumentation, measurements of the ultimate deformations could not be made during the treatment process. The treated wire was later found to have a significantly lower rupture strain than No. 2 reinforcing bars.

Random samples of all reinforcement were tested to rupture in an Instrom tensile testing apparatus. An extensometer was used to monitor the deformation of each specimen. Plots of the load-deformation characteristics of the specimens were generated. The yield and ultimate strengths of the

reinforcement were computed by dividing the appropriate load by the original cross-sectional area. The corresponding strains were determined by dividing the measured deformations by the gage lengths. A comparison of typical curves from the deformed bar group and the heat-treated wire group is illustrated in Figure 2.7. Tabular results from the steel reinforcement tests are presented in Table 2.5.

Table 2.1. Slab design parameters.

Slab	Span/Thickness Ratio	Longitudinal Steel Percentage[a]	Bar Type[b]	Bar Spacing in
1	10.4	0.52	D3	3
2		0.52	D3	3
3		0.74	No. 2	3.75
4		0.74		3.75
4A		0.74		3.75
4B		0.74		3.75
5		1.06		2.5
6		1.06		2.5
7	14.8	0.58	D2.5	3.75
8		0.58	D2.5	
9		1.14	No. 2	
9A		1.14		
10		1.14		
10A		1.14		
11		1.47		
12		1.47		

[a]Steel percentages were the same in top and bottom.
[b]Corresponding areas and diameters of bars are: D3; area = 0.030 in^2; diameter = 0.195 in; D2.5; area = 0.025 in^2; diameter = 0.178 in; No. 2; area = 0.049 in^2; diameter = 0.250 in.

Table 2.2. Slab construction details.

Slab	Thickness t, in	Depth d, in	Bar Diameter db, in	Bar Spacing s, in	Edge Spacing se, in
1	2-5/16	1-15/16	0.195	3	1-1/2
2			0.195	3	1-1/2
3			0.25	3-3/4	3/4
4				3-3/4	
4A				3-3/4	
4B				3-3/4	
5				2-1/2	
6				2-1/2	
7	1-5/8	1-1/4	0.178	3-3/4	
8			0.178		
9			0.25		
9A					
10					
10A					
11				2-3/4	1
12				2-3/4	1

Table 2.3. Instrumentation details.[a]

Slab / Channel	1	2	3	4	4A	4B	5	6	7	8	9	9A	10	10A	11	12
1	P1	P1	P1	P1	P1	P1	P1	P1	P1	P1	P1	P1	P1	P1	P1	P1
2	P2	P2	P2	P2	P2	P2	P2	P2	P2	P2	P2	P2	P2	P2	P2	P2
3	D1	D1	D1	D1	D1	D1	D1	D1	D1	D1	D1	D1	D1	D1	D1	D1
4	D2	D2	D2	D2	D2	D2	D2	D2	D2	D2	D2	D2	D2	D2	D2	D2
5	D3	D3	D3	D3	D3	D3	D3	D3	D3	D3	D3	D3	D3	D3	D3	D3
6	D4	D4	D4	D4	D4	D4	D4	D4	D4	D4	D4	D4	D4	D4	D4	D4
7	LW1	LW1	LW1	LW1	LW1	LW1	LW1	LW1	b	b	LW1	LW1	LW1	LW1	LW1	LW1
8	LW2	LW2	LW2	LW2	LW2	LW2	LW2	LW2	LW2	LW2	LW2	LW2	LW2	LW2	LW2	LW2
9	LW3	LW3	LW3	LW3	LW3	LW3	LW3	LW3	LW3	LW3	LW3	LW3	LW3	LW3	LW3	LW3
10	LW4	LW4	LW4	LW4	LW4	LW4	LW4	LW4	b	LW4	LW4	LW4	LW4	LW4	LW4	LW4
11	LW5	LW5	LW5	LW5	LW5	LW5	LW5	LW5	b	LW5	LW5	LW5	LW5	LW5	b	LW5
12	LW6	LW6	LW6	LW6	LW6	LW6	LW6	LW6	LW6	LW6	LW6	LW6	LW6	LW6	LW6	LW6
13	LW7	LW7	LW7	LW7	LW7	LW7	LW7	LW7	LW7	LW7	LW7	LW7	LW7	LW7	LW7	LW7
14	LW8	LW8	LW8	LW8	LW11	LW8	LW8	LW8	LW8	LW8	LW8	LW8	LW8	LW8	LW8	LW8
15	LW9	LW9	LW9	LW9	ST1	LW9	LW9	LW9	LW9	LW9	LW9	LW9	LW9	LW9	LW9	b
16	LW10	LW10	LW10	LW11	ST2	LW11	LW10	LW10	LW10	LW10	LW10	LW10	LW10	LW10	LW10	LW10
17	LW11	LW11	LW11	LW12	ST3	LW12	LW11	LW11	LW11	LW11	LW11	LW11	LW11	LW11	LW11	LW11
18	LW13	LW12	b	LW13	SB1	LW13	LW13	LW12	LW13	LW12	LW13	LW13	LW12	LW12	LW13	LW12
19	LW14	LW13	LW13	LW15	SB2	ST1	LW14	LW13	LW14	LW13	LW14	b	LW13	LW13	LW14	LW13
20	LW15	LW14	LW14	ST1	SB3	ST2	LW15	LW14	LW15	LW14	LW15	LW15	LW14	LW14	LW15	LW14
21	ST1	LW15	LW15	ST2	b	ST3	ST1	LW15	ST1	LW15	ST1	ST1	LW15	LW15	ST1	LW15
22	ST2	LW16	ST1	ST3	D3S	SB1	ST2	LW16	ST2	LW16	ST2	ST2	LW16	LW16	ST2	b
23	ST3	ST1	ST2	SB1	D4S	SB2	ST3	ST1	ST3	ST1	ST3	ST3	ST1	ST1	ST3	ST1
24	SB1A	ST2	ST3	SB2	b	SB3	SB1	ST2	SB1	ST2	SB1	SB1	ST2	ST2	SB1	ST2
25	SB2	ST3	SB1	SB3	b	D3S	SB2	ST3	SB2	ST3	SB2	SB2	ST3	ST3	SB2	ST3
26	SB3	SB1	SB2	D3S	ST1S	D4S	SB3	SB1	SB3	SB1	SB3	SB3	SB1	SB1	SB3	SB1
27	CT1	SB2	SB3	D4S	ST3S	ST1S	CT1	SB2	ST1A	SB2	CT1	CT1	SB2	SB2	CT1	SB2
28	CB3	SB3	CT1	ST1S	SB1S	ST3S	CB3	SB3	ST3A	SB3	CB3	CB3	SB3	SB3	CB3	SB3
29	CB3P	b	CB3P	ST3S	SB3S	SB1S	CB3P	b	CT1	CB3	ST1A	ST1A	ST1A	b	SB1A	CB3
30	ST1A	b	CB3	SB1S	b	SB3S	ST1A	b	CB3	CT1	SB1A	SB1A	SB1A	SB1A	SB3A	CT1
31	b	b	ST1A	SB3S	b	b	b	b	SB3A	CT1P	ST3A	SB3A	SB3A	SB3A	ST3A	CT1P

[a] Prefix descriptors: P = water pressure gages; D = displacement transducers; LW = load washers; ST = steel strain gages in top of slab; SB = steel strain gages in bottom of slab; CT = concrete strain gages on top of slab; and CB = concrete strain gages on bottom of slab. Suffix descriptors: A = alternate strain gage; P = strain gage perpendicular to major slab axis; and S = split calibration step channel.

[b] Indicates non-instrumented channels.

Table 2.4. Experimental concrete properties.

Cylinder	Compressive Strength, psi	Age When Tested, days	Average Strength, psi
		Batch 1	
1	3,420	29	
2	3,420	29	3,420
3	3,950	75	
4	4,220	75	4,090
5	4,340	77	
6	4,140	77	4,240
7	4,610	82	
8	3,920	82	4,270
9[a]	4,230	88	
10[a]	4,720	88	
11[a]	4,160	88	4,370
12	4,220	103	
13	4,550		
14	4,610		
15	4,720		
16	4,140		
17	4,310		
18	4,500		4,440
		Batch 2	
19	4,770	29	
20	4,750	29	4,760
21	3,700	12	3,700
22	3,840	14	3,840
23	5,290	89	
24	5,390	89	5,340
25	4,380	106	
26	4,130	106	
27	5,210	106	4,570
28	4,380	109	
29	5,500	109	
30	4,770	109	4,880
31[a]	5,180	110	
32[a]	5,230	110	
33[a]	5,030	110	5,150
34	5,510	111	
35	5,230	111	
36	4,660	111	5,130
37	5,110	112	
38	5,270	112	5,190

[a]Cylinder instrumented with strain gages.

Table 2.5. Experimental steel properties.

Bar Type	Yield Load lb	Yield Stress psi	Yield Strain in/in	Ultimate Load lb	Ultimate Stress psi	Rupture Strain in/in
No. 2[a]	2,920	59,590	0.0020	3,880	79,180	0.165
	2,780	56,730	0.0015	3,700	75,510	0.188
	2,880	58,780	0.0017	3,700	75,510	0.135[b]
	2,880	58,780	0.0015	3,750	76,530	0.170
Average	2,865	58,470	0.0017	3,760	76,680	0.174
D3	1,600	53,330	0.0015	1,950	65,000	0.091
	1,180	39,330	0.0015	1,520	50,670	0.198
	1,500	50,000	0.0016	1,780	59,330	0.039
	1,720	57,330	0.0014	2,120	70,670	0.075
Average	1,500	50,000	0.0015	1,840	61,420	0.101
D2.5	1,600	64,000	0.0019	1,900	76,000	0.053
	1,900	76,000	0.0020	2,060	82,400	0.109
	1,550	62,000	0.0019	1,870	74,800	0.073
Average	1,680	67,330	0.0019	1,940	77,730	0.078
D1	950	95,000	0.0028	970	97,000	0.058
	870	87,000	0.0028	860	86,000	0.029
	860	86,000	0.0038	860	86,000	0.017
	890	89,000	0.0028	890	89,000	0.020
	960	96,000	0.0030	970	97,000	0.015
Average	906	90,600	0.0030	910	91,000	0.028

[a]Corresponding areas and diameters of bars are: D3; area = 0.030 in^2; diameter = 0.195 in; D2.5; area = 0.025 in^2; diameter = 0.178 in; D1; area = 0.010 in^2; diameter = 0.110 in; No. 2; area = 0.049 in^2; diameter = 0.250 in.

[b]Failure occurred outside gage length.

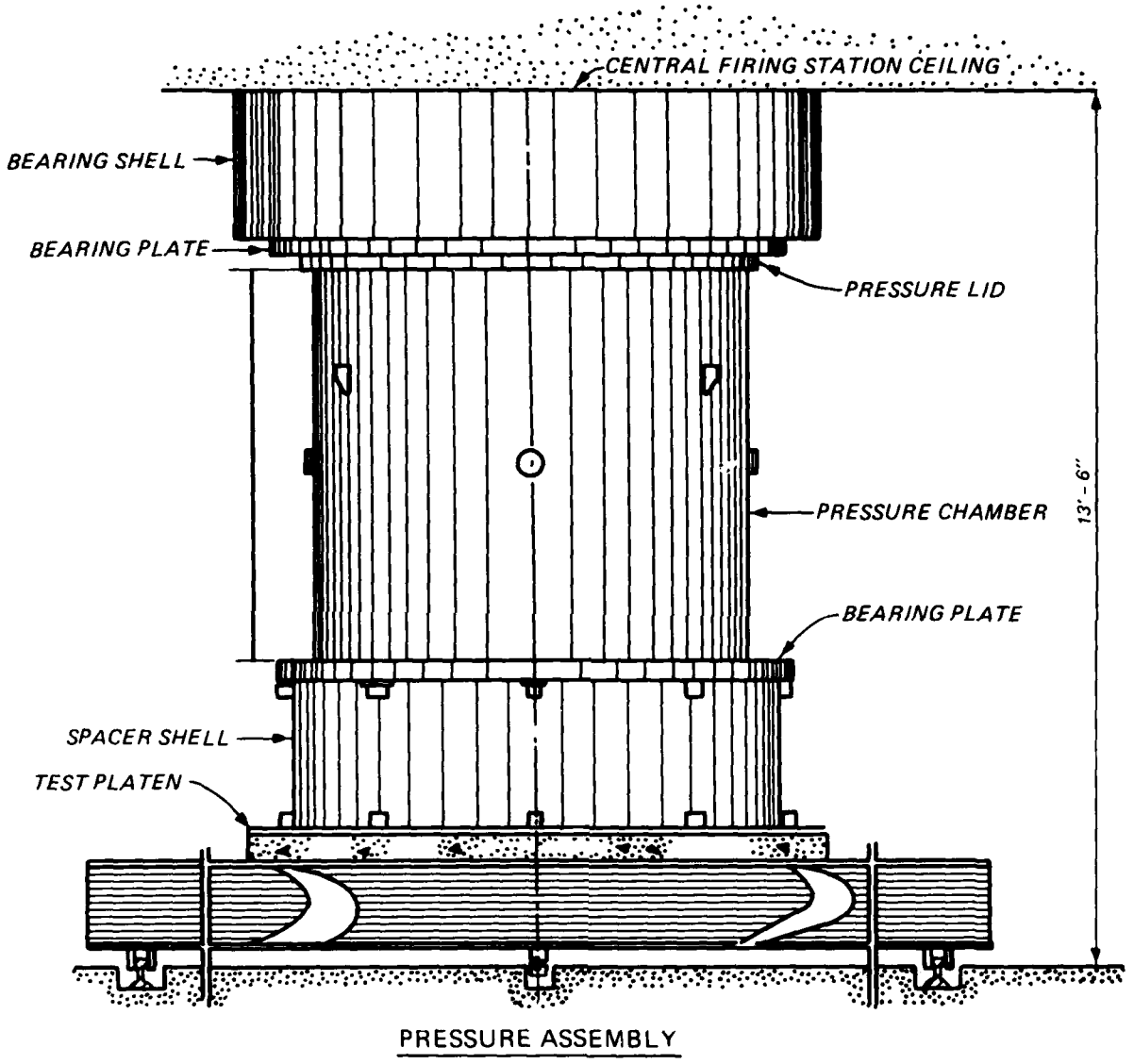

Figure 2.1. Elevation view of load generator facility.

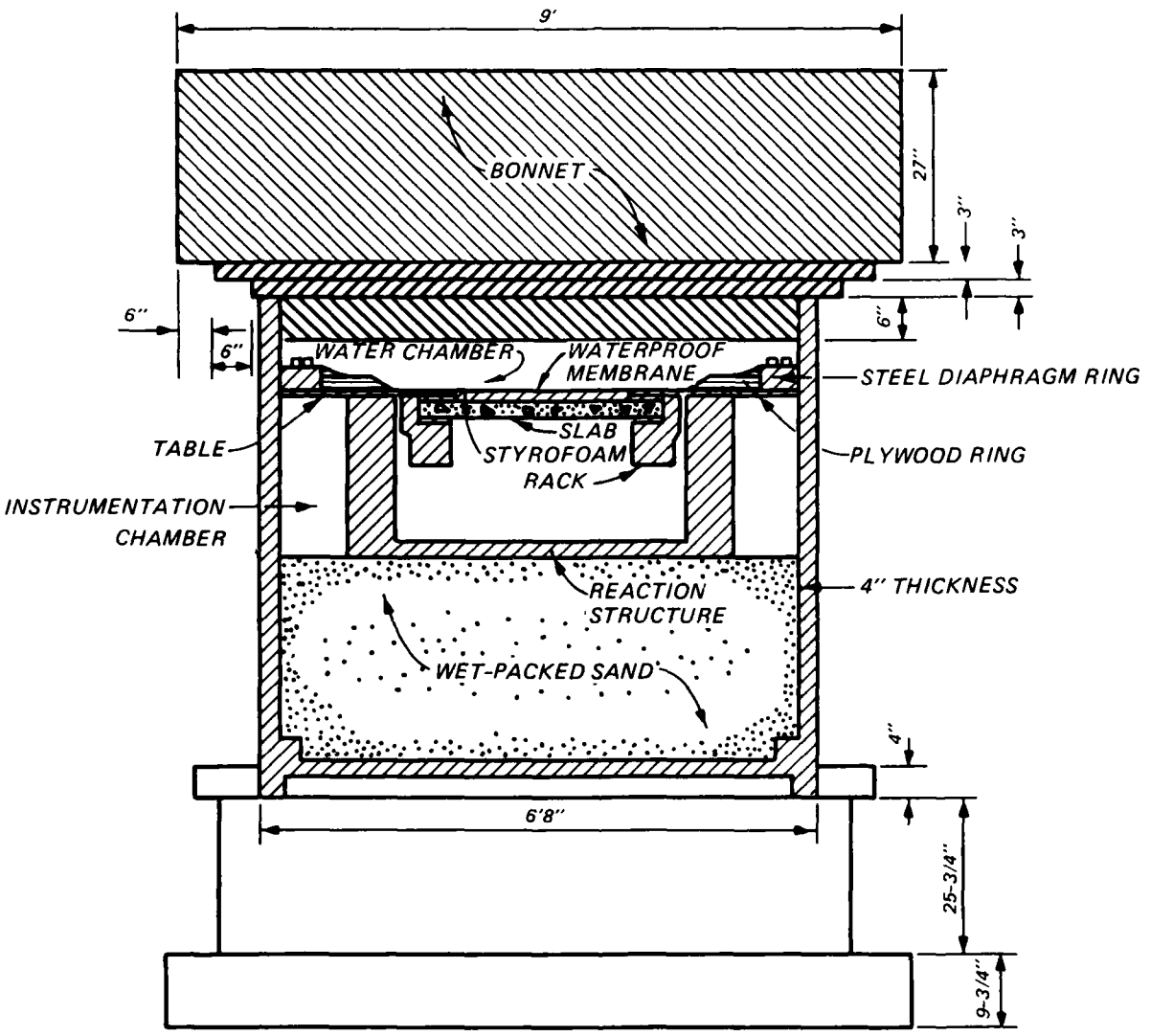

Figure 2.2. Cross section of reaction structure in test configuration.

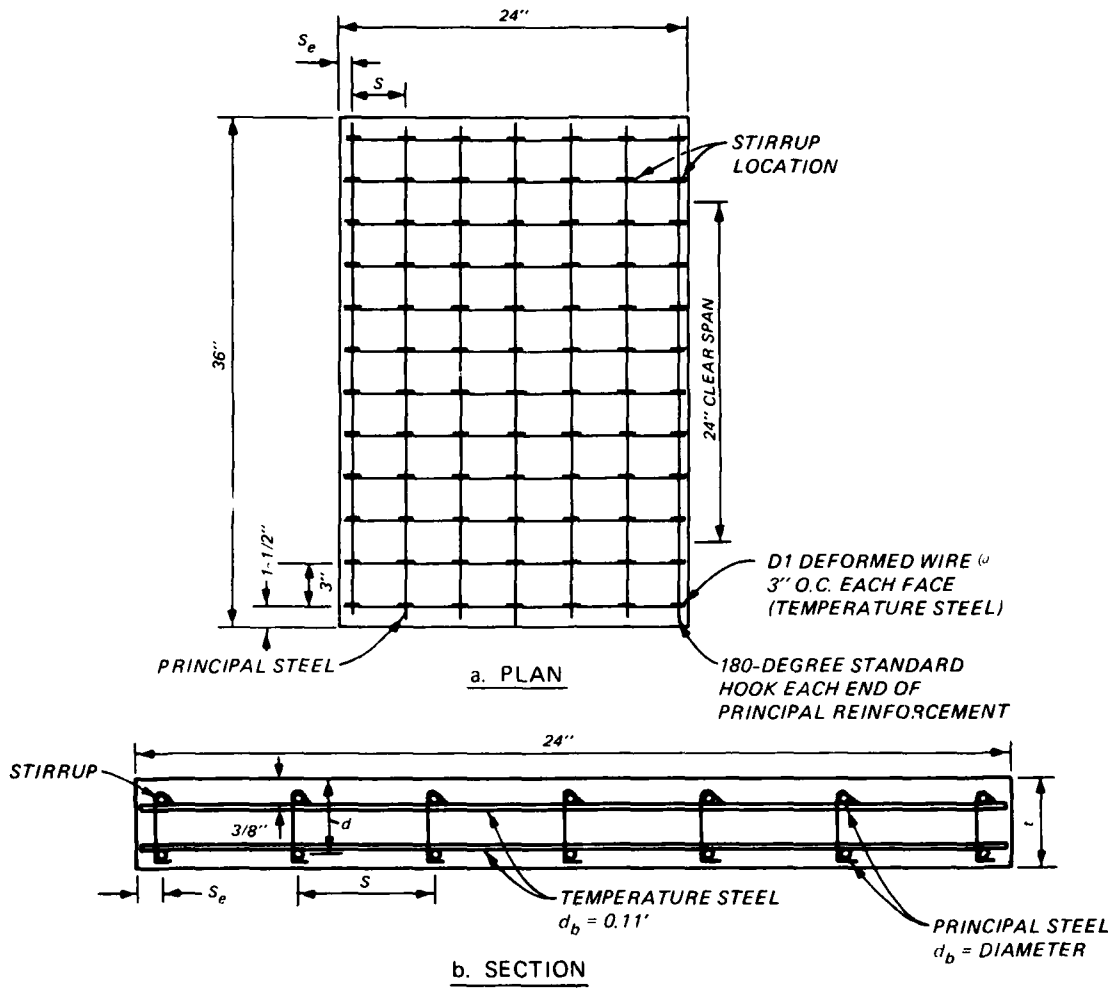

Figure 2.3. Slab construction details.

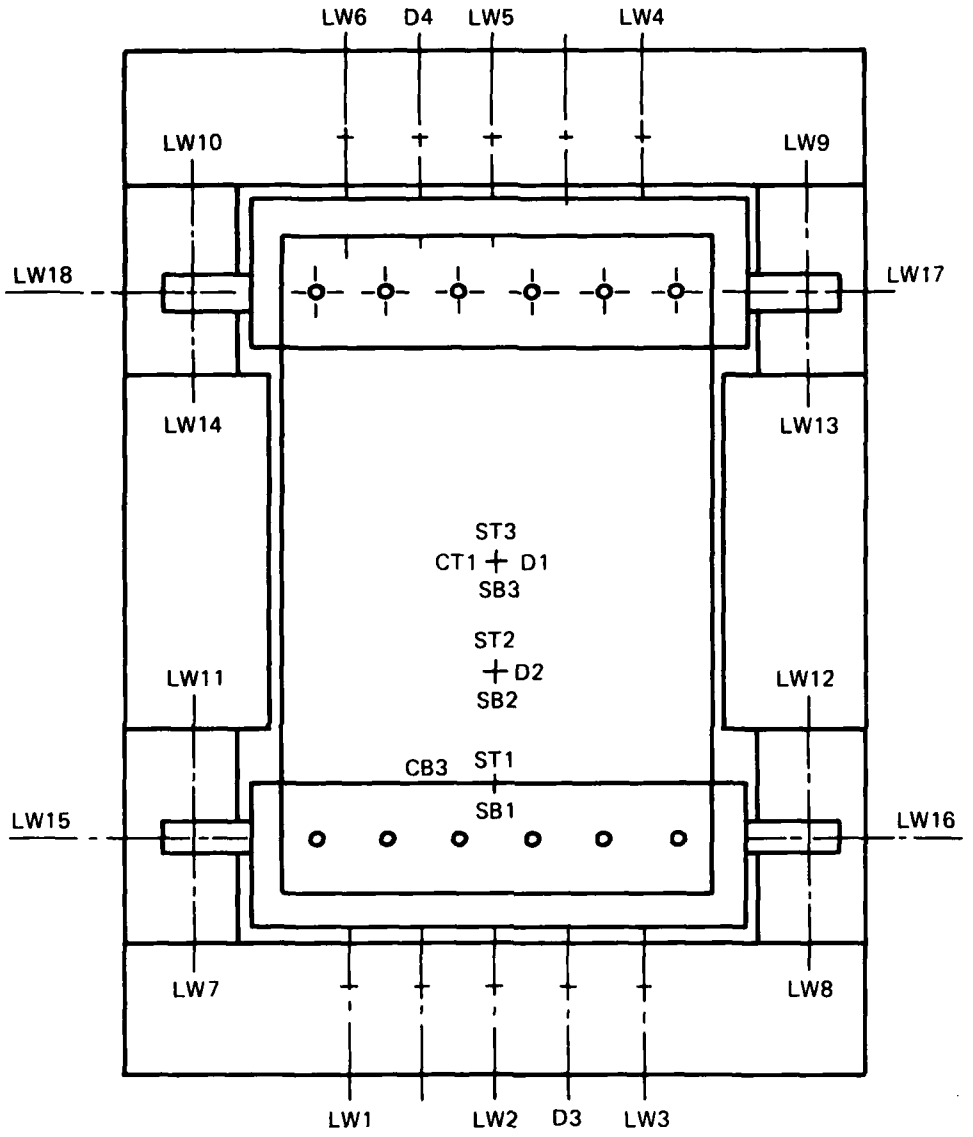

NOTE: SEE TABLE 2.2 FOR DESCRIPTIONS OF INSTRUMENTATION ACRONYMS

Figure 2.4. Instrumentation layout.

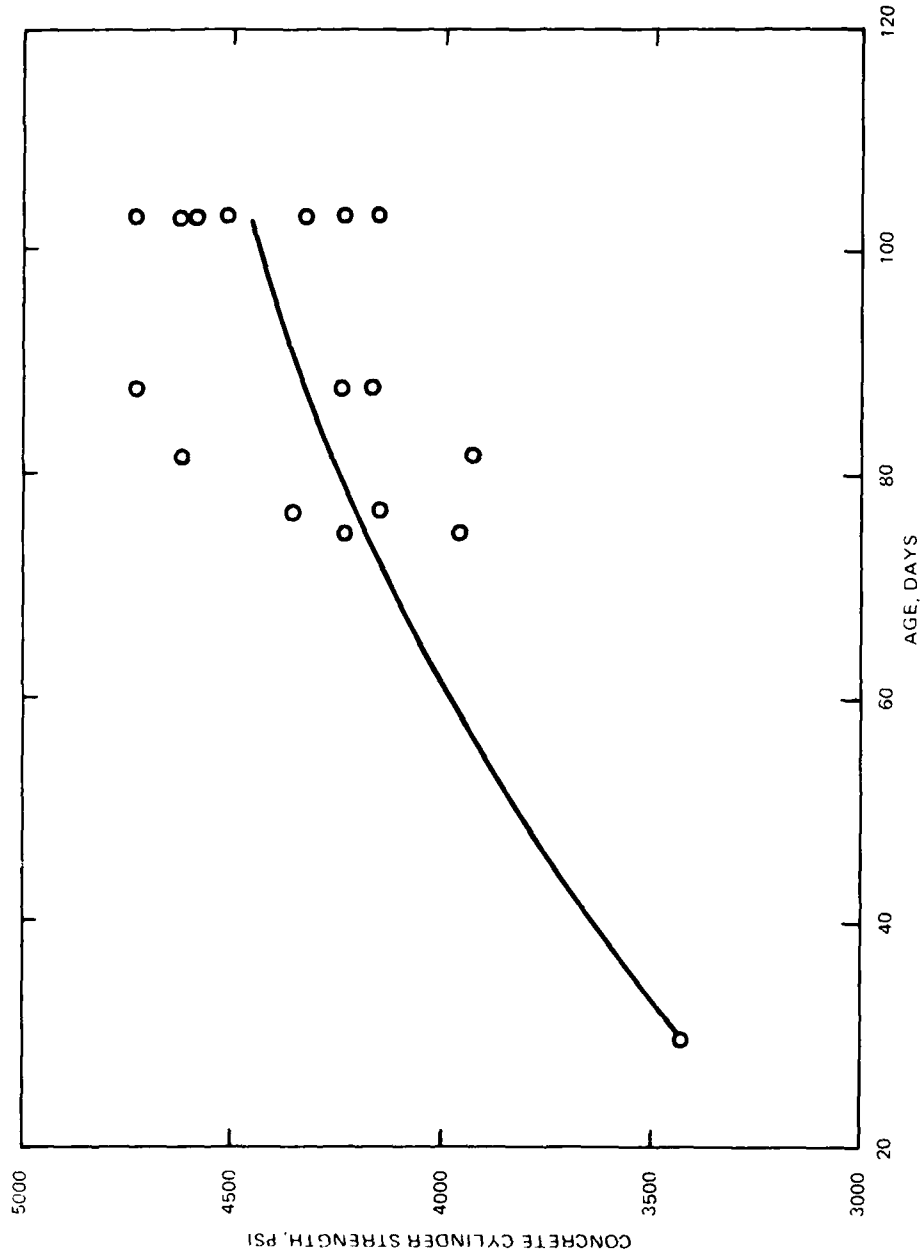

Figure 2.5. Relationship between experimental concrete strengths and regression curve for Batch 1.

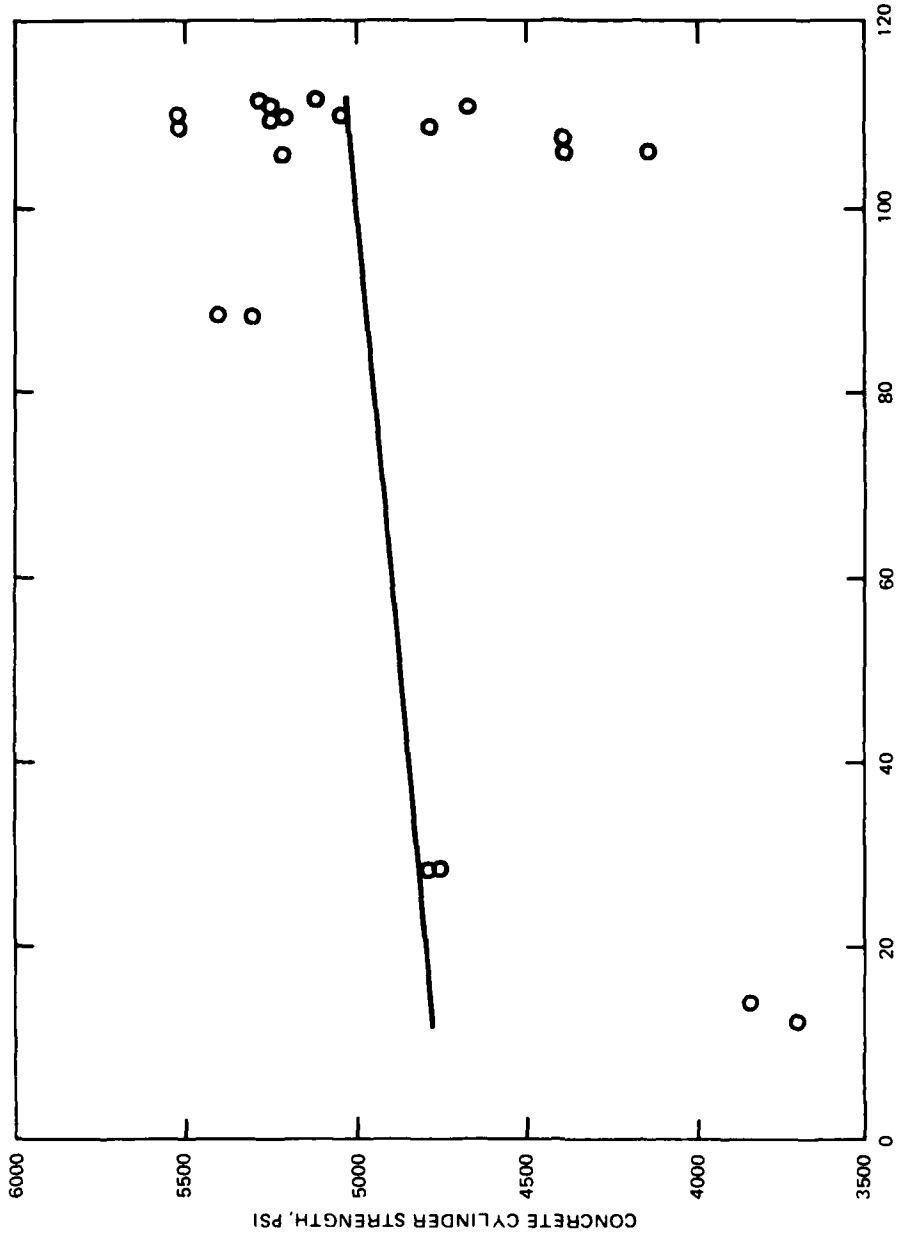

Figure 2.6. Relationship between experimental concrete strengths and regession curve for Batch 2.

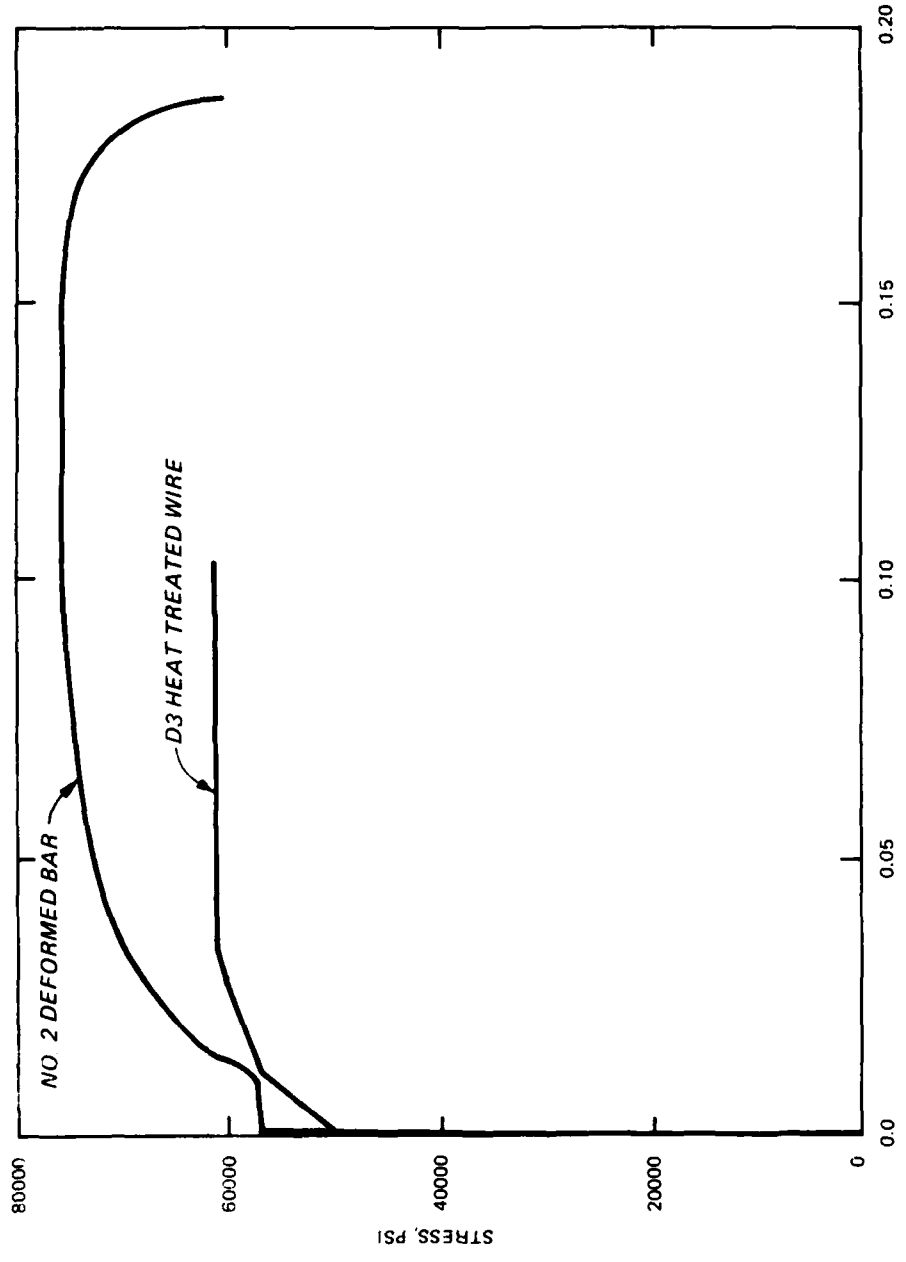

Figure 2.7. Representative steel curves for deformed bar and wire groups.

CHAPTER 3

EXPERIMENTAL RESULTS

3.1 OBSERVATIONS

The recording of general observations after conducting an experiment has proven to be as important as the recording of electronic data during the test. A careful inspection may provide a verification or contradiction of the recorded data. Also, the use of certain analytical procedures or the disallowance of others may be evident from posttest observations of the specimens. For those reasons, both descriptive and photographic records of all slabs have been provided for this program.

Crack patterns and failures of reinforcement were the most significant behavioral characteristics to be observed from the slab specimens. Tabular descriptions of those posttest observations are provided in Table 3.1.

The bottoms of all slabs were painted white and marked with a quarterspan reference line prior to testing. Immediately after each test, all visible cracks in the slabs were highlighted with markers. Records were kept of the widths of the crack bands in the tensile zones at midspan and supports, and the width of the spall band in the compression zone at midspan. Approximate dimensions for the bands of spalling and cracking were computed by averaging the widths of the patterns at 6-inch intervals across the span. Since small cracks developed over nearly the whole slab in practically every case, the specified widths were subjectively determined from only the most significant flexural cracks. In most tests, the widths of the patterns were substantially greater at the edges of the slabs than near the center. To minimize the effect of biased data due to edge effects, only dimensions in the center portion of the slab were used to determine band widths. A graphical representation of the damage assessment criteria is presented in Figure 3.1. The reader should be advised to use the approximations of band width dimensions only within the context of which they were determined.

The percentage of ruptured steel was recorded at both midspan and supports. Percentages were computed at midspan by dividing the number of broken bars by the total number of bars in each layer. At the supports, the average number of broken bars for both sections was divided by the number of bars at one section. Since the bottom bars at the support were not ruptured in any

test, no data were tabularized for that location. Although the broken bar counts were taken from careful examinations of the slabs, some of the reinforcement was still covered by the concrete and could not be observed.

Photographs were taken of both sides of each slab and have been included in Appendix B. In addition to the individual slab photographs, group pictures were taken of each slab series and the total collection. A posttest view of the bottoms of all slabs is provided in Figure 3.2.

3.2 INSTRUMENTED DATA

As stated previously, all of the analog signals which were received from the instrumentation during each test were recorded on magnetic tape, digitized by computer, and output on a plotter. The analog-digital sampling rate for digitization of the data was established by the acquisition of 1,000 points selected at equal time intervals over the duration of each test.

The results of the instrumented data are discussed in this chapter and the plotted data are presented in Appendix C. More detailed discussions of the experimental results and comparisons with the analytical results are presented in Chapter 4.

3.3 LOAD-DEFLECTION DATA

The midspan deflection was plotted with respect to the reference channel water pressure for each test, resulting in a load-deflection curve. Because fundamental behavior of each slab could be readily interpreted through a careful examination of the load-deflection curve, those data were plotted and monitored as each test progressed. Decisions to change the rate of loading and to terminate each test were based on observations of the real-time load-deflection curve.

The termination of each test was, in general, based on the objective to observe the state of the slab just prior to the incipient collapse deflection. However, the actual decision to terminate a test was governed by one or more of the following criteria:

1. Large decreases in pressure with little, if any, increase in deflection, indicating significant deterioration of slab capacity.

2. Very large deflections, approaching the stretchable limits of the rubber membranes.

3. Very high pressures, significantly exceeding the calibrated limits of the instrumentation.

4. Malfunction of equipment or instrumentation.

The character of the load-deflection data was, in general, similar to the idealized curve in Figure 3.3(a). The typical curve exhibited a peak in load capacity at relatively small deflections, followed by a sharp decline in capacity with still larger deflections, and then another increase in capacity until the incipient collapse deflection was approached. The initial rise in load was due to compressive membrane action; the flexural capacity of the slab was enhanced by thrusts generated from the restricted lateral movement of the ends of the slab. The ensuing decline in capacity corresponded with a reduction in thrust and instabilities of the slab. Because the ends of the slab were restrained from lateral movement in either direction, tensile stresses could be developed throughout the slab at very large deflections. That action, known as tensile membrane behavior, resulted in both the top and bottom layers of reinforcement acting as a tensile net with a capacity primarily determined by the rupture strength of the steel.

Those slabs that had substantially different behavior than that described above can be divided into two groups. First, the slabs with the the smallest reinforcement ratio in each span-thickness group (Slabs 1, 2, 7, 8) did not demonstrate an enhanced capacity in the tensile membrane stage. Second, two thin slabs with large support rotations (Slabs 10, 10A) did not exhibit a definitive compressive membrane peak.

One atypical characteristic of the load-deflection curves for this test program was a noticeable change in slope at relatively small deflections. That change correlated with an increase in support rotations and resulted in a decrease of slab stiffness. In nearly every test, the most substantial portion of the support rotations occurred prior to the initial peak in capacity. As planned, the full effects of support rotations were felt before any significant damage occurred to the slabs.

3.4 SUPPORT ROTATIONS

Support rotations were computed by measuring the lateral movement of a particular point located on the side and near the bottom of the support rack. As illustrated in Figure 3.4, support rotations could be approximated by using trigonometric relationships and by knowing the center of rotation, the

geometry of the support rack, and a component of displacement.

As stated previously, it was very difficult to provide accurate control of support rotations. However, the amount of rotation which did occur could be accurately evaluated after each test was completed and the results were processed. Due to the lack of control, rotations at one support could be substantially different than at the other.

As a point of reference, rotations for each support were computed at the time each slab reached its compressive membrane capacity. Those results are presented in Table 3.2.

3.5 SUPPORT MOMENTS

The design of the reaction structure was such that the various member end action components such as lateral thrust, vertical reactions, rotations, and moments could essentially be isolated from each other. In the previous section, support rotations were shown to be computed by considering the lateral displacement of a point on a support rack. The moments at the supports were found by monitoring the loads which passed through the spring assemblies. Utilizing the same concept as for rotations, i.e., knowing the center of rotation and geometry, the moment resistance provided by external sources at the supports could be determined. It should be noted, however, that the moment so computed was only one component of the total moment resisted at the ends of the slab.

Load washers were placed in each of the spring assemblies along the support racks to determine the coupling forces for the support moments. Three load washers were associated with the total coupling force for each supported end of the slab. An inability to adequately balance the initial loads and precisely control the deflections in the spring assemblies led to an unequal distribution of loads in each of the washers. However, because of the extreme stiffness of the support racks, the distribution of moments to the ends of the slabs was considered to be uniform.

Since the support moments were linearly related to the coupling forces detected by the load washers, discussions of the moment resistance have been expressed in terms of the actual loads which were measured. Those loads, as monitored by LW1-LW6, typically resulted in the idealized curve of Figure 3.3(b). The general character of that curve was found to occur in most

tests, particularly when the load-deflection curve of the slab was similar to the one illustrated in Figure 3.3(a).

As the applied pressure was initially increased, the support rotations occurred, the spring assemblies were seated, and some load was transmitted to the washers. When the disc springs closed completely, the coupling forces significantly increased until the peak flexural capacity was reached. From that point until the applied pressure was decreased to terminate the test, the coupling forces remained nearly constant. That action indicated that plastic hinges had been formed at the supports and plastic rotations occurred with a small change in support moments.

3.6 LATERAL LOADS

A primary objective for the experimental phase of this project was to measure the axial forces generated from the restrained lateral movement of the slabs. During the initial phase of loading, the geometry of deformation of the slabs caused in-plane forces to act outward at the support and resulted in compressive membrane behavior. As the slabs underwent very large deflections, the in-plane forces changed directions and resulted in tensile membrane behavior. Load washers were used to measure both the compressive and tensile in-plane forces which were generated as the slab deformed.

The load washers were positioned in specially designed assemblies located on the large shafts at the ends of the support racks. Each of the four support shafts was capable of utilizing the load cells; however, to minimize data channels, load cells were not used at every support.

The design of the reaction structure permitted the thrusts to be measured at the mid-thickness of each slab. By varying the thickness of the plates between the slab and the support rack, the central axis of each different slab was made to correspond with the center of the support shafts. The load washers were positioned on studs located at the same level as the center of each shaft.

Observations of the load washer records after the initial tests led to concerns about the magnitudes of thrusts being generated. Several attempts were made to improve the quality of the recorded thrust data including (1) the use of precision-machined washers adjacent to the load washers to improve the load transfer, (2) the use of lubricated, stainless steel bearings to minimize the effects of friction, and (3) preloading of the load washers by the

tightening of adjustment screws in order to reduce losses in thrust from seating between the load cells and reaction structure. The latter change resulted in some irregularities in the format of data from test to test because each washer could actually measure both tensile and compressive in-plane loads.

3.7 STRAIN GAGE DATA

Steel strain gages were placed on the principal reinforcement in every slab. Top and bottom bars located nearest the middle portion of each slab were instrumented with strain gages at midspan, quarterspan, and one support. Alternate strain gages were mounted on an adjacent pair of bars to provide backup instrumentation and, in some cases, to provide duplicate records for verification of the major strain-gage records.

Because the strain gages could not be located in advance exactly at the critical sections and because of the bond characteristics between the strain gage and adjacent materials, the preciseness of the strain-gage records is of little value. However, the general character of the strain plots can be of assistance in determining the overall behavior of the steel in the general vicinity of the critical sections. For example, evidence of tension or compression in the reinforcement can be observed from the data. Also, the records may reveal whether or not the reinforcement yielded. However, records that do not indicate yielding of the steel may not accurately reflect the actual conditions at the critical sections.

Concrete strain gages were attached to the exterior surfaces of several of the slabs. Although the gages were capable of being mounted internally, there was concern that the gages might induce spalling or otherwise influence the behavior of the slabs.

Table 3.1. Posttest observations of slab behavior.

Slab	Ruptured Steel, %			Average Crack Zone, in		Average Spall Zone, in Midspan, Top
	Midspan		Support	Midspan	Support	
	Top	Bottom	Top	Bottom	Top	
1	100.0	100.0	87.5	4	0.5-1.0	4.0
2	87.5	100.0	87.5	3	0.5-1.0	3.0
3	0.0	71.4	28.6	12	0.5-1.0	2.0
4	↓	42.9	14.3	8	0.5-1.0	1.0
4A		57.1	0.0	8	2.0-2.5	2.5
4B		28.6	0.0	6	0.5-1.0	1.5
5		30.0	40.0	12	1.0-2.0	1.5
6		20.0	0.0	10	2.0-2.5	1.5
7	85.7	85.7	92.9	10	0.5-1.0	3.0
8	85.7	100.0	92.9	4	0.5-1.0	2.5
9	0.0	0.0	14.3	20	1.0-2.0	1.5
9A	↓	0.0	14.3	20	1.0-2.0	2.0
10		0.0	0.0	12	1.0-2.0	1.5
10A		57.1	0.0	8	0.5-1.0	1.5
11		0.0	0.0	18	1.0-2.0	1.5
12		0.0	0.0	12	2.0-2.5	2.5

Table 3.2. Support rotations.

Slab	Lateral Deflection, in			Rack Rotation, deg		
	D3	D4	Average	D3	D4	Average
1	0.14	0.20	0.17	1.50	2.14	1.82
2	0.10	0.19	0.145	1.08	2.04	1.56
3	0.01	0.22	0.115	0.14	2.36	1.24
4	0.10	0.18	0.14	1.08	1.93	1.50
4A	0.19	0.28	0.235	2.04	3.00	2.52
4B	0.12	0.29	0.205	1.29	3.12	2.20
5	0.05	0.05	0.05	0.55	0.55	0.55
6	0.14	0.24	0.19	1.50	2.57	2.04
7	0.10	0.01	0.055	1.08	0.14	0.61
8	0.21	0.20	0.205	2.25	2.14	2.20
9	0.04	0.20	0.12	0.45	2.14	1.29
9A	0.01	0.06	0.035	0.14	0.66	0.40
10	0.30	0.22	0.26	3.22	2.36	2.79
10A	0.20	0.18	0.19	2.14	1.93	2.04
11	0.12	0.02	0.07	1.29	0.24	0.76
12[a]	0.21	0.16	0.19	2.25	1.72	2.04

[a]Denotes slabs with substantial rotations after peak capacity.

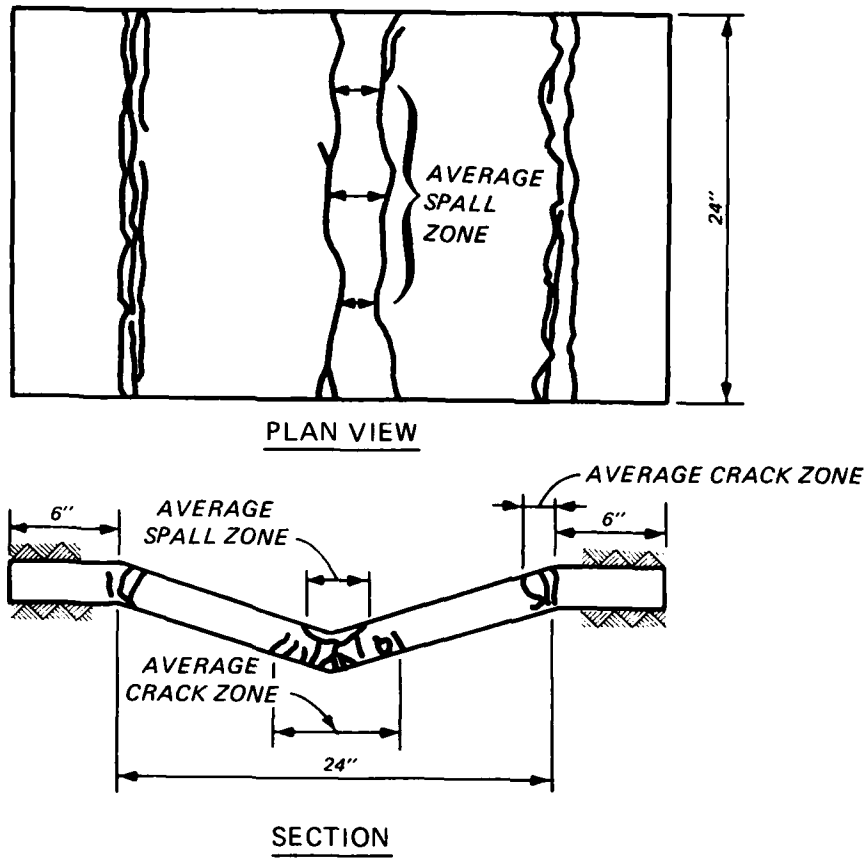

Figure 3.1. Crack damage assessment criteria.

Figure 3.2. Posttest view of undersurface of slabs.

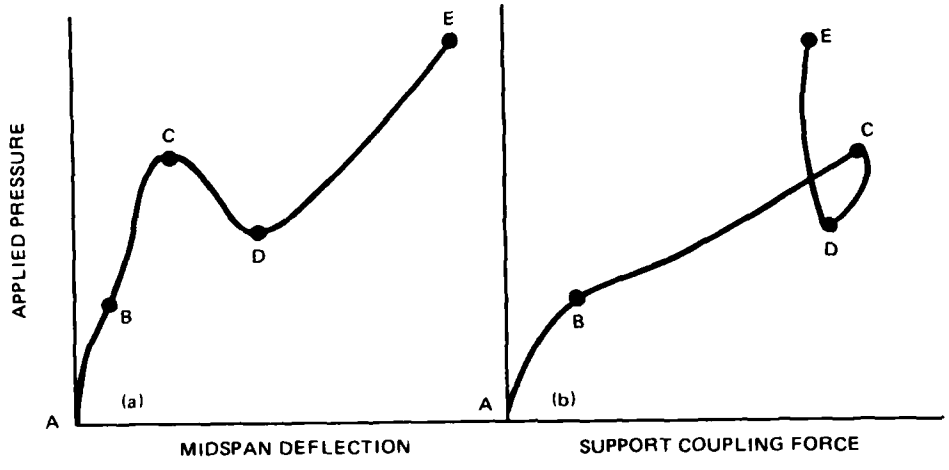

PHASE	SLAB BEHAVIOR
A-B	COMPRESSIVE MEMBRANE; MAJOR SUPPORT ROTATIONS
B-C	COMPRESSIVE MEMBRANE; MINOR SUPPORT ROTATIONS
C-D	PLASTIC DECAY
D-E	TENSILE MEMBRANE

Figure 3.3. Typical relationship between experimental deflections and coupling forces.

NOTE: Δ - MEASURED LATERAL DISPLACEMENT
θ - COMPUTED SUPPORT ROTATION

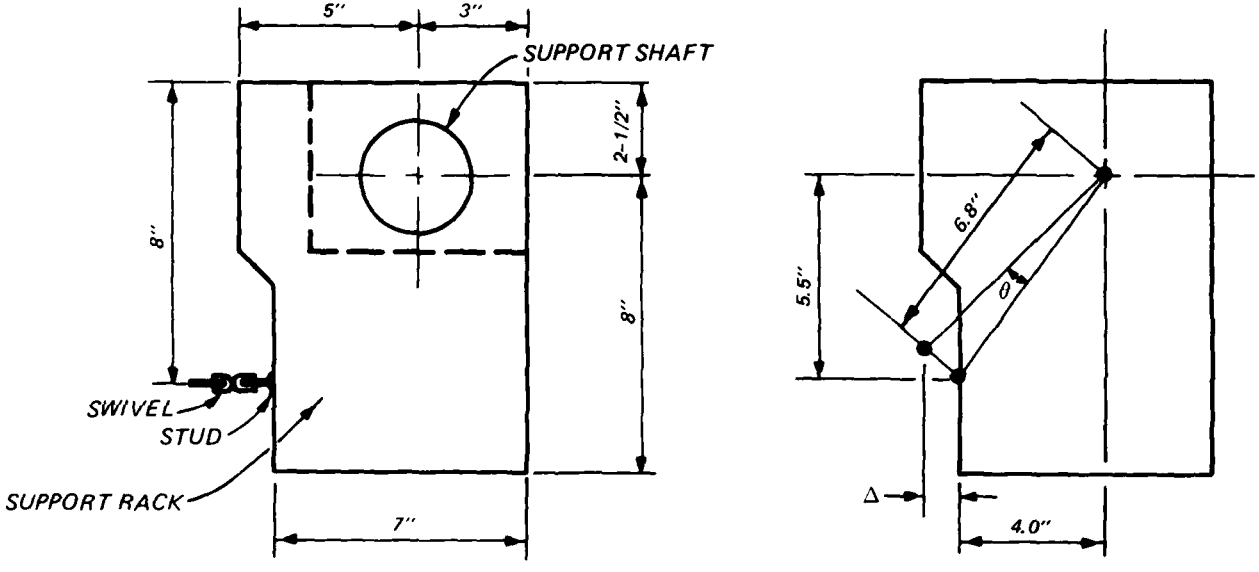

a. Actual support rack configuration.

b. Support rack geometry for computing rotations.

Figure 3.4. Methods of approximating support rotations.

CHAPTER 4

ANALYSIS

4.1 INTRODUCTION

One of the major objectives of this program was to understand the behavioral characteristics of slabs with the given parameters. To meet that objective, analyses of the slabs were performed using existing theoretical relationships. The aspects of the slabs' response which were considered to be most important for analysis were the peak flexural capacity and the tensile membrane behavior.

Existing analytical techniques do not permit full consideration of imperfect boundary conditions. However, the actual behavior of slabs can be significantly affected by those types of boundary conditions, as evidenced from the results of this test program. The analytical efforts of this program thus far have been to determine bounds for the capacities of slabs with variable boundary conditions. Future efforts will be focused on the development of theory for predicting the actual response of partially restrained slabs.

4.2 FLEXURAL BEHAVIOR

The flexural behavior of reinforced concrete slabs has been investigated by engineers since the first of the century. Elastic theories were first applied to the analysis of slabs. However, it was soon recognized that stresses, strains, and deflections of slabs were too difficult to predict by elasticity concepts, particularly at higher load levels. Engineers recognized that the predominant response of slabs under large loads was controlled by plastic behavior at various sections. In recent years, plasticity theories have become the most prevalent methods of slab analysis.

Johansen's yield-line plasticity theory (Reference 2) has offered a means for determining the pure ultimate flexural capacity of slabs, i.e., the capacity neglecting in-plane forces in the slab. The yield-line theory is based on the plastic moment capacities of a slab's critical cross sections. When the moment capacities of enough sections have been exceeded to permit a mechanism to form, the slab is considered to have achieved its limiting capacity. Portions of the slab between yield lines are considered to behave elastically and have a negligible effect on the ultimate capacity. Provided a correct failure

mechanism is assumed, and neglecting thrusts, the yield-line method will provide an upper-bound solution for the ultimate capacity of a slab.

Yield-line analyses were performed for the one-way slab strips which were tested in the experimental program. The geometric characteristics of the slab strips were such that the correct failure mechanism could be postulated with confidence. However, because free rotations were permitted at supports, the formation of plastic hinges at those locations could not be insured. If hinges did not form at the supports during the initial stage of loading, then the slabs would have essentially behaved as simply supported slabs. On the other hand, if free rotations were small enough to require plastic hinges to form at the supports, then the slabs would have been considered to be fixed. Consequently, yield-line values were computed for both simply supported and fixed boundary conditions.

The ultimate flexural load for a slab may be derived by equilibrating the work caused by external forces to the internal work performed along the hinge lines. The ultimate capacity for a uniformly loaded, simply supported, one-way slab may be expressed as follows:

$$w = \frac{8}{L^2} \frac{M_n}{B} \qquad (4.1)$$

where

w = uniform load on the slab at peak capacity, psi

L = length of the slab in the principal direction, inches

M_n = ultimate moment of resistance along the plastic hinge line at midspan, in-lb

B = width of the slab, inches

For a one-way slab with fixed boundary conditions, the sum of the ultimate moments of resistance along the hinge lines at midspan and one support would replace the term M_n in Equation 4.1.

The nominal moment capacities for the critical cross sections were calculated in accordance with the procedure embodied in the 1983 American Concrete Institute Code (Reference 3). The analyses accounted for the contributions of the compression reinforcement to the total moment of resistance. Because the same areas of steel were used in the top and bottom of each slab, the theoretical resisting moments at midspan and supports were identical. Specific quantities used in computing the nominal moments are presented in Table 4.1.

Results of the yield-line flexural analyses are provided in Table 4.2.

4.3 COMPRESSIVE MEMBRANE BEHAVIOR

Recent tests (References 4, 5, and 7) have confirmed that the yield-line theory significantly underpredicts the ultimate capacity of slabs, particularly if the slabs are laterally restrained. The enhancement in strength over the yield-line capacity is attributable to compressive membrane action. Compressive membrane thrusts resulting from the restricted movement of the slab's edges increase the moment capacities of the critical cross sections and consequently enhance the total capacity of the slab. Several investigators have confirmed the existence of compressive membrane action in both models and actual structures. A summary of the tests and their references can be found in Reference 4.

Theories have been developed to predict the peak capacity of slabs with compressive membrane forces (References 5, 6, and 7). By considering the equilibrium and deformations of a slab strip as in Figure 4.1, Park and Gamble (Reference 5) have shown that the sum of internal moments including thrusts can be expressed as follows:

$$M'_n + M_n - n_n\delta = 0.85f'_c\beta_1 h\left[\frac{h}{2}\left(1 - \frac{\beta_1}{2}\right) + \frac{\delta}{4}(\beta_1 - 3)\right.$$

$$+ \frac{\beta\ell^2}{4\delta}(\beta_1 - 1)\left(\varepsilon + \frac{2t}{\ell}\right) + \frac{\delta^2}{8h}\left(2 - \frac{\beta_1}{2}\right) + \frac{\beta\ell^2}{4h}\left(1 - \frac{\beta_1}{2}\right)\left(\varepsilon + \frac{2t}{\ell}\right)$$

$$\left. - \frac{\beta_1\beta^2\ell^4}{16h\delta^2}\left(\varepsilon + \frac{2t}{\ell}\right)^2\right] - \frac{1}{3.4f'_c}\left(T' - T - C_s + C_s\right)^2$$

$$+ \left(C'_s + C_s\right)\left(\frac{h}{2} - d' - \frac{\delta}{2}\right) + (T' + T)\left(d - \frac{h}{2} + \frac{\delta}{2}\right) \quad (4.2)$$

in which ε = the sum of elastic, creep, and shrinkage strains, t = lateral movement of one support, and all other previously undefined terms are represented in Figure 4.1.

Equation 4.2 accounts for the effects of axial shortening and support movements. As is the case for actual slabs, the equation is very sensitive to those secondary effects. The magnitude of thrust is reduced as supports are displaced and as elastic, creep, and shrinkage axial strains occur.

Accompanying that relief in thrust is a reduction in the internal moment of resistance.

By including external forces and applying the principle of virtual work, an equation may be derived to determine the resistance of a slab to a uniform load. That equation, expressing the uniform load w in pounds per square inch, may be written as:

$$w = \frac{8}{L^2 B} (M_n' + M_n - n\delta) \tag{4.3}$$

The application of Equation 4.3 in predicting the peak capacities of rigidly restrained experimental slabs has been quite satisfactory provided the deflection at which the peak capacity occurs is known. That suggests that either the equation may be applied only after a test has been conducted or that the peak capacity deflection must somehow be determined prior to the test. Most authors suggest that using an ultimate deflection of one-half of the slab thickness ($\delta/t = 0.5$) will yield satisfactory results. However, Keenan (Reference 6) has shown that the ultimate deflection is dependent on the geometric characteristics and boundary conditions of the slab. He derived the expression below for predicting the central deflection required to crush the concrete along the hinge lines of a slab strip.

$$\delta = \frac{\varepsilon_c L^2}{8c'} \left(1 + \frac{2t}{L}\right) \tag{4.4}$$

Equation 4.4 is very sensitive to the strain, $2t/L$, associated with movement of the supports, which is in turn dependent on the stiffness of the supports. Since there is very little information on the lateral stiffness of the supports for most experimental programs, including the previous programs at WES, Equation 4.4 has not been rigorously verified. However, analyses of rigidly restrained slabs which were tested at WES have revealed that an upper bound solution for the peak capacity can be obtained by using Equation 4.4 and assuming an infinite lateral stiffness at the supports.

A computer code was developed incorporating an iterative solution scheme for Equations 4.2 through 4.4. Solutions for the ultimate capacities and corresponding deflections were obtained for each experimental slab and are presented in Table 4.3. To obtain an upper bound compressive membrane solution, an extremely large support stiffness was assumed, effectively permitting

no support movement. Only elastic shortening due to the large thrusts was considered in reducing the magnitudes of the computed thrusts and resisting moments.

Other solutions were determined for support stiffnesses which were assumed to be more representative of the experimental conditions. To obtain those stiffnesses, a portion of the shaft assembly (Figure A.6) was loaded in a uniaxial compression device. It was determined that the assembly had a lower stiffness during the initial stage of loading due to seating between the threaded bolt and cylinder. Consequently, in the tests where the shaft assemblies were preloaded, a slightly higher support stiffness would be expected. Results of the analyses for the different support stiffnesses have been included in Table 4.3.

4.4 TENSILE MEMBRANE BEHAVIOR

Another phenomenon of slab behavior that has received considerable attention in recent years is tensile membrane action. Such action typically occurs after the slab has exceeded its compressive membrane capacity and has begun to undergo large deflections. If sufficient lateral restraint is provided, the tensile strength of the steel can supply a reserve capacity that will defer the progressive collapse of the slab. Tensile membrane action is usually accompanied with full-depth cracking, inward support movement, and large deflections. The largest deflection that a slab can withstand before there is a loss in tensile membrane capacity is referred to as the incipient collapse deflection.

Several investigators have recorded tensile membrane action in two-way slabs (References 4, 5, 6, 7). However, most of the records were results of studies of compressive membrane action, and the tensile membrane capacity received only secondary attention. Very few tests have been carried to the point of incipient collapse deflection.

Park and Gamble (Reference 5) used standard plastic membrane theory to establish relationships between load and deflection for rectangular slabs. The theory assumes that tensile membrane action is solely dependent on the yield forces in the steel. It does not account for combined bending and tensile membrane action, which would serve to enhance the capacity of the slab. For slabs with large aspect ratios, as idealized with one-way slab strips, the standard plastic tensile membrane theory formula can be written:

$$\frac{w}{\delta} = \frac{8T}{L^2} \tag{4.5}$$

where T equals the total tensile force carried by the steel for a unit width.

Since the strains in the reinforcement at the critical sections would be quite large at large deflections, it is probable that some strain hardening would occur as tensile membrane action is induced. Strain hardening would have definitely occurred prior to the incipient collapse deflection. Therefore, Equation 4.5 has been computed for the parameters of the experimental slabs and by using both the yield stress and ultimate stress of the steel in determining the tensile force T . Those results are presented in Table 4.4.

4.5 ANALYSIS OF LOAD WASHER DATA

Load washers were positioned in each spring assembly and in each shaft assembly to measure the loads which were transmitted from the slab to the rigid reaction structure. The magnitude of the resisting moment at each end of the slab could be approximated by computing the moment which resulted from the forces in the spring assemblies. To obtain an accurate representation of the in-plane loads, the coupling forces from the spring assemblies had to be added to the forces from the shaft assemblies. The conversion of measured lateral loads to an equivalent force-couple system is represented in Figure 4.2. The records provided qualitative, if not quantitative, data to substantiate the findings of this report.

4.6 COMPARISON OF EXPERIMENTAL AND ANALYTICAL RESULTS

Lines representing Johansen's load (Equation 4.1), the compressive membrane capacity (Equation 4.3), and the tensile membrane response (Equation 4.5) have been constructed on the plots of the experimental load-deflection curves in Figures 4.3-4.18. Johansen's load for both fixed (wjf) and simple (wjs) boundary conditions have been included. The tensile membrane slopes for both the yield strain, $(w/\delta)y$, and rupture strain, $(w/\delta)r$, have also been shown.

With the exception of Slab G1, the compressive membrane capacity predicted by Equation 4.3, together with the ultimate deflection predicted by

Equation 4.4, provided an upper bound to the experimental flexural capacity. The analytical capacity was exceeded by less than 5 percent in Slab G1. With the exception of Slab G12, every slab which had a definitive flexural capacity was bounded from the low side by Johansen's load for fixed boundary conditions.

Another observation from the curves was that the change in load-deflection curvature, which resulted from rotation of the support racks, generally occurred at a load between the two Johansen's loads for different boundary conditions. Although that phenomenon was primarily a function of the test facility, it supported the concept that the slab followed the path of least resistance. It generally took less energy to exceed the yield section at midspan than to compress the springs providing resistance to rotation at the supports. It took less energy to compress the springs at the supports than to form a three-hinge mechanism in the slab.

Because most of the slabs exhibited an ultimate capacity beyond Johansen's load for fixed boundary conditions, it was apparent that thrusts acted to enhance the flexural capacities. The enhancement ratio, $(w_u - w_{jf})/w_{jf}$, ranged from a low of approximately 25 percent in Slab G8 to a high of about 180 percent in Slab G1. The slabs which showed no definitive peak capacity (G10, G10A) were thin and had large free rotations at the supports. Those conditions probably induced stability failures before large thrusts were developed. The relatively small enhancements in flexural capacities for Slabs G8 and G12 could be attributed to stability failures after significant thrusts had developed. Analysis of the load washer data substantiated the sudden reduction in thrust as the peak capacities were approached for those slabs.

The initial portions of the experimental load-deflection curves representing tensile membrane behavior were usually bounded or closely approached by the analytical curves from Equation 4.5. As deflections became larger and reinforcement ruptured, the curves began to follow sloped lines representing membrane behavior for lower percentages of steel. The slabs which exhibited the poorest tensile membrane behavior (G1, G2, G7, G8) were slabs which were constructed of a less-ductile reinforcement. In each case, the reinforcement appeared to rupture before any significant tensile membrane action occurred.

4.7 EFFECTS OF SUPPORT ROTATION ON SLAB BEHAVIOR

Comparisons between slabs with the same geometric and material characteristics but different boundary conditions have led to some distinguishable patterns of behavior. A discussion of the effects of support rotation on each series of slabs follows.

Slabs G1 and G2 were from the thick-slab group and contained the lowest percentage of reinforcement of all slabs. The behavior of this slab pair was different from any of the others in that Slab G1 had a much higher peak capacity, even though the support rotations were significantly greater than for Slab G2. An inspection of the load washer data led to a conclusion that there was a probable compression preloading of Slab G1 which resulted in an enhancement in the compressive membrane capacity. The preloading probably occurred because the slab was fixed in the support racks while the large screws in the shaft assembly were tightened. Nevertheless, both slabs exhibited similar post-peak behavior in that there were very rapid decays, i.e., abrupt losses in capacity after the initial peaks. Excessive bar breakage prevented any significant tensile membrane action from occurring. The failure of each slab was characterized by well-defined yield lines, narrow crack bands, and practically total steel rupture.

Although average support rotations varied between 1.24 and 2.52 degrees, there appeared to be no significant difference in the peak capacities of Slabs G3, G4, and G4A. However, an apparent initial compression in Slab G4B led to a slightly higher capacity. The peak capacities of Slabs G3, G4, and G4A were less than 5 percent different from the capacities of the similarly constructed, rigidly fixed slabs of Woodson (Reference 1). The initial tensile membrane responses of all four slabs were almost identical. The points where plastic decay ended and tensile membrane action began were the same, except for Slab G4B, which initiated the tensile behavior at a slightly higher load. G3 had the earliest deviation from the membrane slope, followed by G4 and G4A. G3 also had more bars ruptured at the end of the test than either of the other two. All slabs exhibited significantly better tensile membrane behavior than Woodson's slabs.

Slabs G5 and G6 had the largest percentage of steel of the thick-slab group. Even though Slab G5 had much smaller support rotations, the peak capacity was only about 7 percent greater than for Slab G6. Slab G6 exhibited

practically no plastic decay, indicating a probable stability failure. The slopes of the tensile membrane responses were initially very close. However, Slab G6 was able to achieve a much higher tensile capacity with significantly less steel breakage.

Slabs G7 and G8 were from the thin-slab group, and like G1 and G2, were constructed with low percentages of a nonductile heat-treated wire. The average support rotation was significantly less in Slab G7 and resulted in a significant compressive membrane enhancement. The apparent instability of Slab G8 seemed to have little effect on the tensile membrane behavior.

Four slabs (G9, G9A, G10, and G10A) had approximately 1 percent of steel in a relatively thin cross section. The overall behavior of Slabs G9 and G9A was remarkably similar, even though the average support rotation was more than three times greater in Slab G9 (1.29 degrees) than in G9A (0.4 degree). Peak capacities were accurately predicted by the upper bound compressive membrane solution. The tensile membrane slopes and capacities, as well as percentages of steel breakage and formation of crack patterns, were almost identical in both slabs. On the other hand, Slabs G10 and G10A had quite different behavior. No peak flexural capacities were apparent in these slabs, although Slab G10A exhibited some flexural response. The instability for this series occurred between the support rotations of 1.29 degrees in Slab G9 and 2.04 degrees in Slab G10A. The tensile membrane slopes were significantly less in Slabs G10 and G10A, and appeared to follow the slope of the lower bound tensile membrane curves. Reinforcement ruptured at the supports in the two slabs with the smallest rotations. No reinforcement ruptured in the slab with the greatest rotations.

Slabs G11 and G12 were the slabs with the largest steel ratios and largest span-thickness ratios. As was the case with most of the other slabs, an instability occurred in the slab with the largest support rotations. A significant difference in the tensile membrane slopes was also apparent. Slab G11 apparently had a higher tensile slope as a result of the initial flexural response. There was no steel breakage in either slab, but the effects of strain hardening in the reinforcement were apparent in the latter parts of the curves.

Slabs G3, G4, G4A, G4B, G9, G9A, G10, and G10A all had the same gross area of steel. However, the last four slabs had thin cross sections, which resulted in a higher percentage of steel. In general, the thick-slab series

exhibited a much better flexural behavior, with peak capacities of around 70 psi. The highest flexural capacity of the thin-slab series was approximately 41 psi. Most of the slabs tended to follow similar tensile membrane slopes, although tensile responses were initiated at much smaller deflections for the thin slabs.

Slabs G3 and G9 had the same areas of steel, approximately the same support rotations, and each slab exhibited significant flexural action. However, the tensile membrane capacity was somewhat higher in the thin slab. On the other hand, Slabs G4 and G10 also had the same areas of steel and about the same rotational freedoms, but the tensile response was lower in the thin slab. The fact that the thicker slab responded in combined flexure and tension accounted for the difference in behavior.

Table 4.1. Values for parameters used in analytical computations.

All slabs had lengths = 24 inches and widths = 24 inches. All slabs had depth to compression steel = 0.375 inch. The areas and percentages of steel were the same for each face. The ultimate strain in concrete was assumed = 0.003.

	Reinforcement		Slab		Materials		
Slab	Area in^2	Ratio	Thickness in	Depth in	Steel Strength psi	Concrete Strength psi	Steel Modulus ksi
1	0.240	0.0052	2.3125	1.9375	50,000	4,414	33,300
2	0.240	0.0052			50,000	4,269	33,300
3	0.343	0.0074			58,470	4,443	34,300
4	0.343	0.0074				4,258	
4A	0.343	0.0074				4,165	
4B	0.343	0.0074				4,201	
5	0.490	0.0106				4,450	
6	0.490	0.0106				4,279	
7	0.175	0.0058	1.625	1.25	67,330	5,023	35,400
8	0.175	0.0058			67,330	4,968	35,400
9	0.343	0.0114			58,470	5,015	34,300
9A	0.343	0.0114				5,005	
10	0.343	0.0114				4,965	
10A	0.343	0.0114				4,963	
11	0.441	0.0147				5,018	
12	0.441	0.0147				4,973	

Table 4.2. Results of yield-line analyses.

Slab	Cross-sectional Moment Capacity M_n, kip-in	Johansen's Load	
		Simple Supports wjs, psi	Fixed Supports wjf, psi
1	24.1	14.0	28.0
2	24.0	13.9	27.8
3	37.2	21.6	43.2
4	37.0	21.4	42.8
4A	37.0	21.4	42.8
4B	37.0	21.4	42.8
5	51.0	29.5	59.0
6	50.8	29.4	58.8
7	16.0	9.2	18.4
8	16.0	9.2	18.4
9	24.0	13.9	27.8
9A	24.0	13.9	27.8
10	24.0	13.9	27.8
10A	24.0	13.9	27.8
11	29.3	17.0	34.0
12	29.3	16.9	33.8

Table 4.3. Results of compressive membrane analyses.

Condition A: support stiffness = 1.0E20 lb/in. Condition B: support stiffness = 5.4E6 lb/in. Condition C: support stiffness = 3.0E6 lb/in.

	Analytical Results						Experimental Results	
	Condition A		Condition B		Condition C			
Slab	wua , psi	δ/t	wub , psi	δ/t	wuc , psi	δ/t	wu , psi	δ/t
1	74.4	0.11	66.6	0.16	63.5	0.17	78	0.32
2	72.9		65.4		62.5		52	0.37
3	89.3		81.3		78.2		72	0.52
4	89.3		79.9		77.0		71	0.65
4A	86.2		79.1		76.3		69	0.58
4B	86.6		79.4		76.6		77	0.56
5	105.1		97.1		94.0		98	0.37
6	103.5		96.0		93.1		91	0.65
7	32.6	0.25	28.2	0.32	26.2	0.35	32	0.37
8	32.4		28.0		25.7	0.36	23	0.62
9	40.9		37.4		34.1	0.33	40	0.43
9A	40.9		37.4		34.1	0.33	41	0.31
10	40.7		37.2		34.1	0.33	--	--
10A	40.7		37.2		33.9	0.33	--	--
11	46.6		43.3		39.7	0.32	46	0.40
12	46.4		43.1		39.7	0.32	22	0.31

Table 4.4. Results of tensile membrane analyses.

		Membrane Slope		
	Yield Force	Ultimate Force		Membrane Slope
Slab	Per Unit Width, lb	(w/δ)y psi/in	Per Unit Width, lb	(w/δ)r psi/in
1	1,000	13.9	1,228	17.1
2	1,000	13.9	1,228	17.1
3	1,671	23.2	2,192	30.4
4	1,671	23.2	2,192	30.4
4A	1,671	23.2	2,192	30.4
4B	1,671	23.2	2,192	30.4
5	2,388	33.2	3,131	43.5
6	2,388	33.2	3,131	43.5
7	982	13.6	1,134	15.7
8	982	13.6	1,134	15.7
9	1,671	23.2	2,192	30.4
9A	1,671	23.2	2,192	30.4
10	1,671	23.2	2,192	30.4
10A	1,671	23.2	2,192	30.4
11	2,149	29.8	2,818	39.1
12	2,149	29.8	2,818	39.1

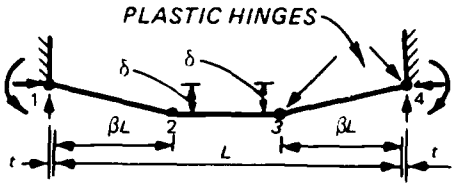

a. Geometry for deformation of restrained strip.

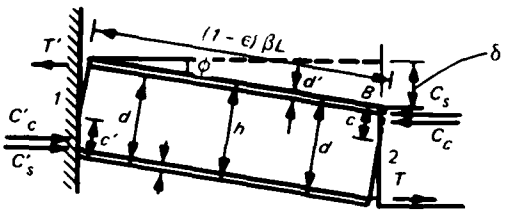

b. Portion of strip between yield sections.

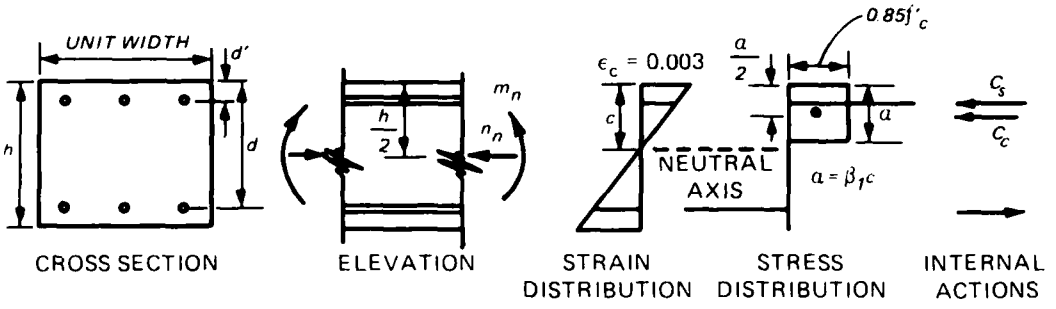

c. Assumed conditions at yield section.

Figure 4.1. Equilibrium and deformations of a slab strip.

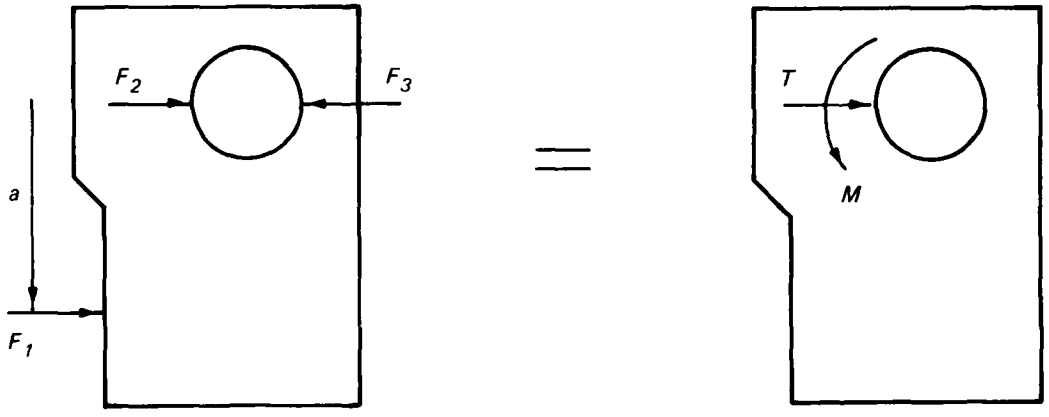

$$M = F_1 \cdot a$$

$$T = F_3 = F_1 + F_2$$

F_1 = SUM OF FORCES IN SPRING ASSEMBLIES

F_2 = SUM OF FORCES IN SHAFT ASSEMBLIES

Figure 4.2. Equivalent force-couple at support rack.

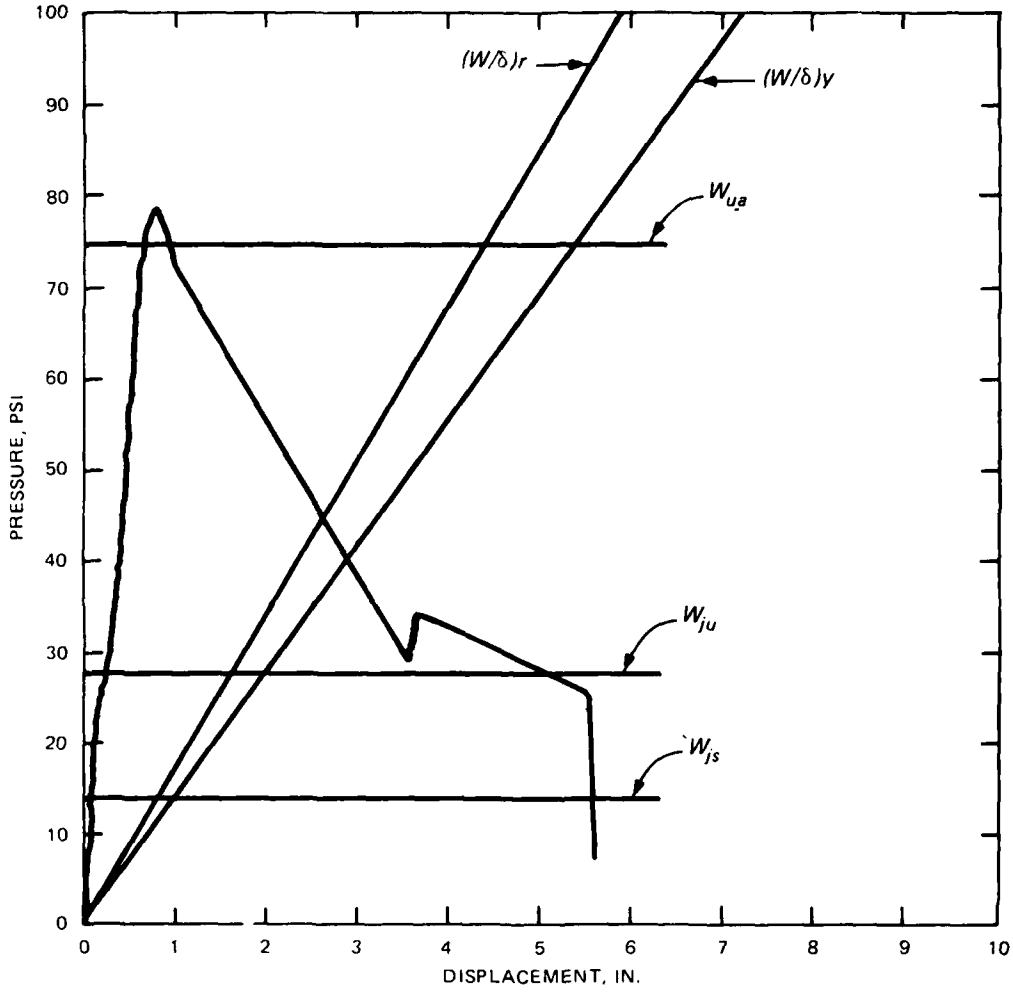

Figure 4.3. Experimental and analytical comparisons for Slab G1.

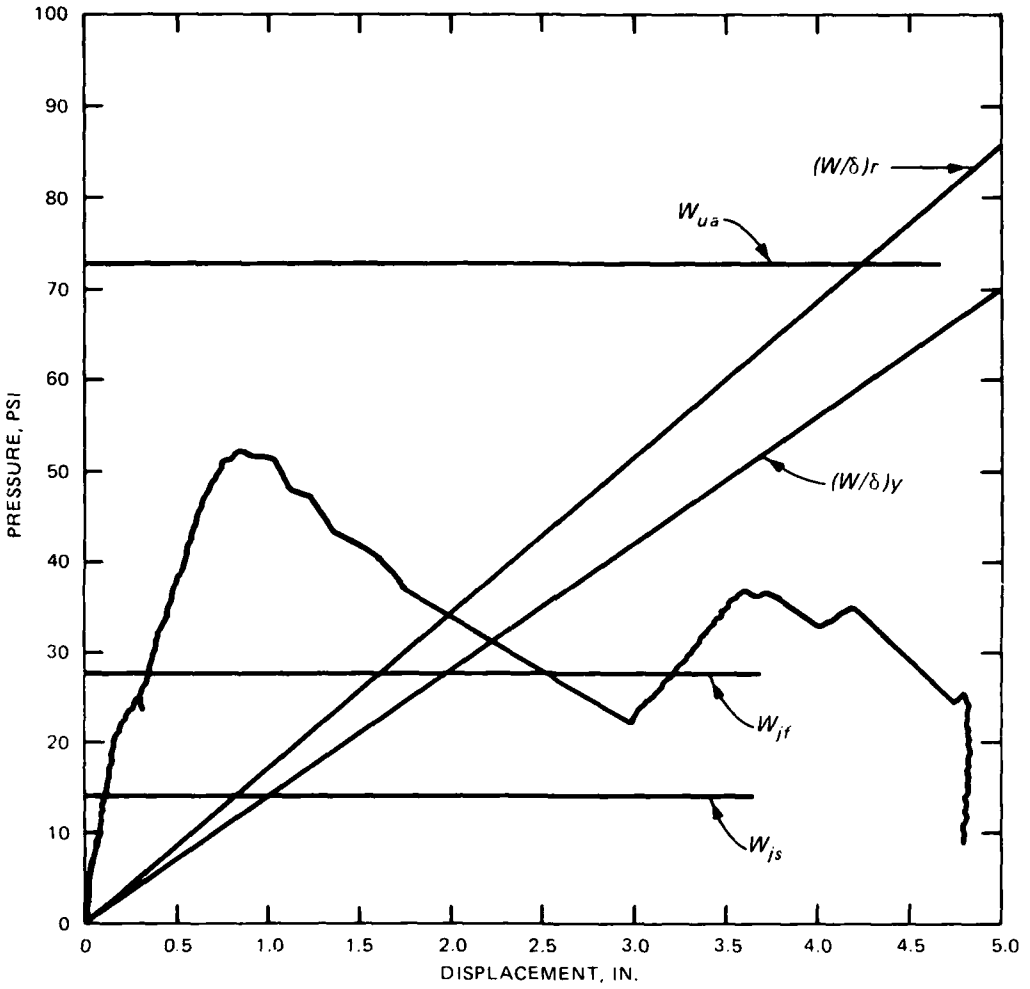

Figure 4.4. Experimental and analytical comparisons for Slab G2.

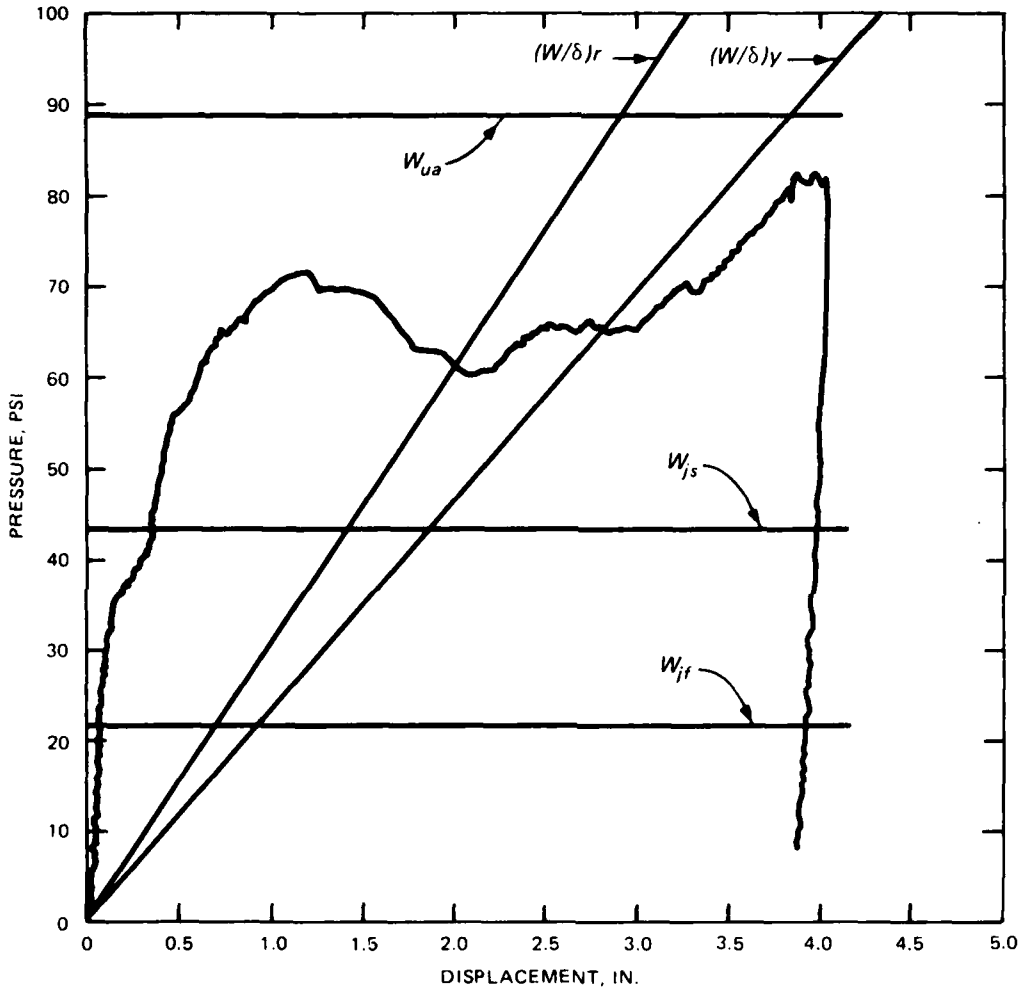

Figure 4.5. Experimental and analytical comparisons for Slab G3.

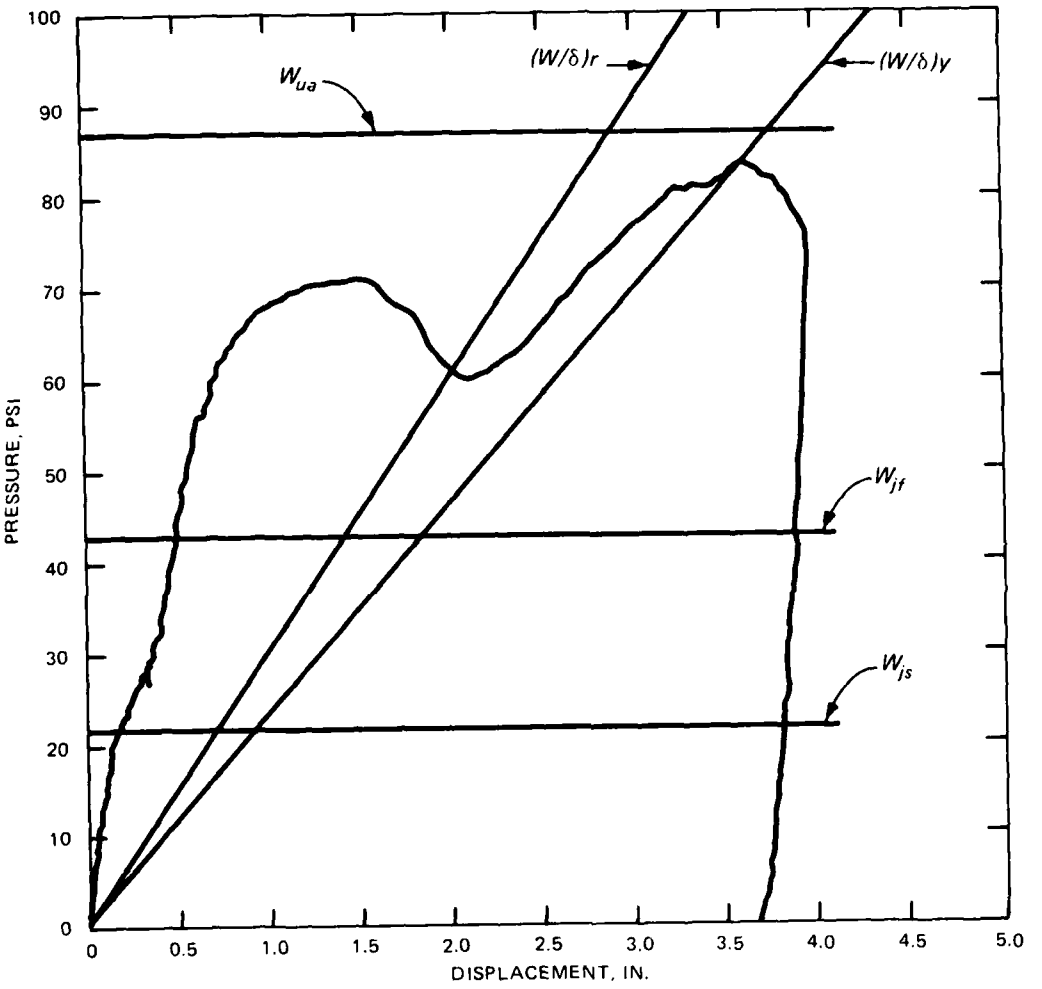

Figure 4.6. Experimental and analytical comparisons for Slab G4.

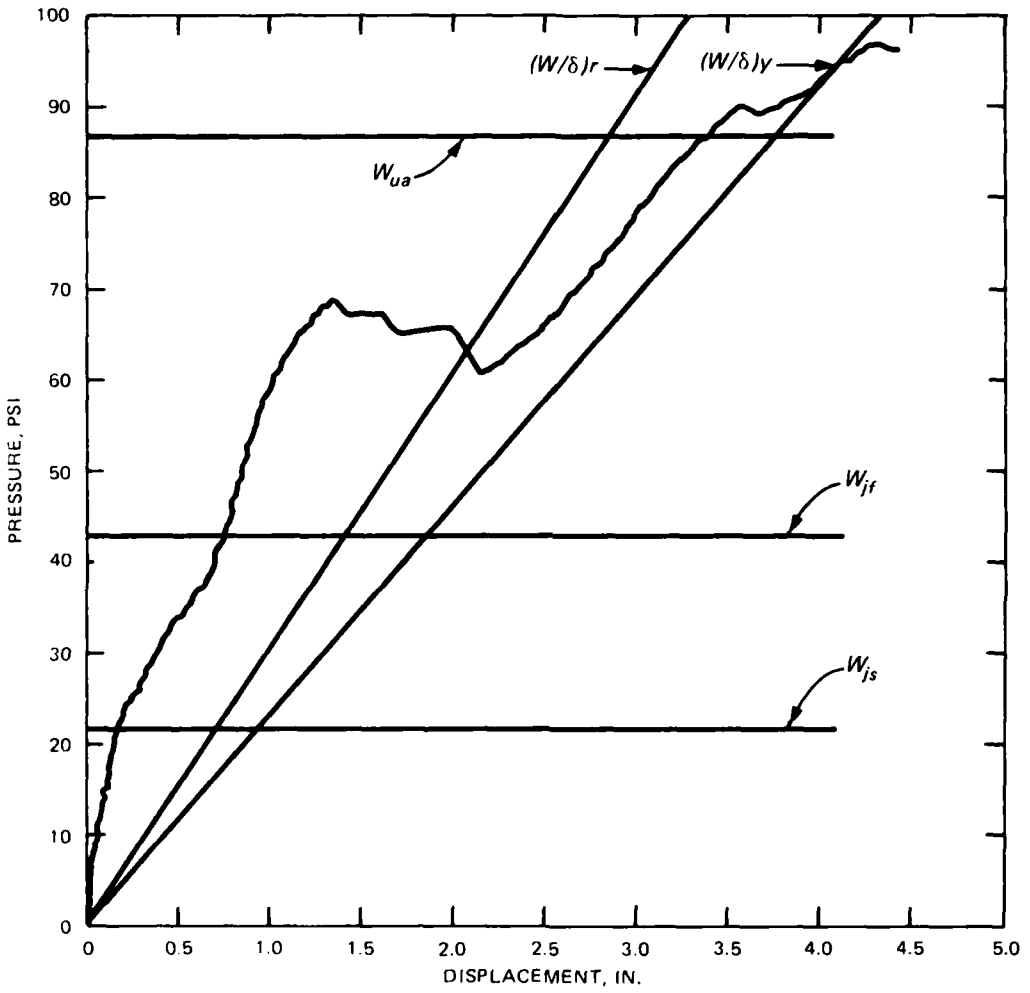

Figure 4.7. Experimental and analytical comparisons for Slab G4A.

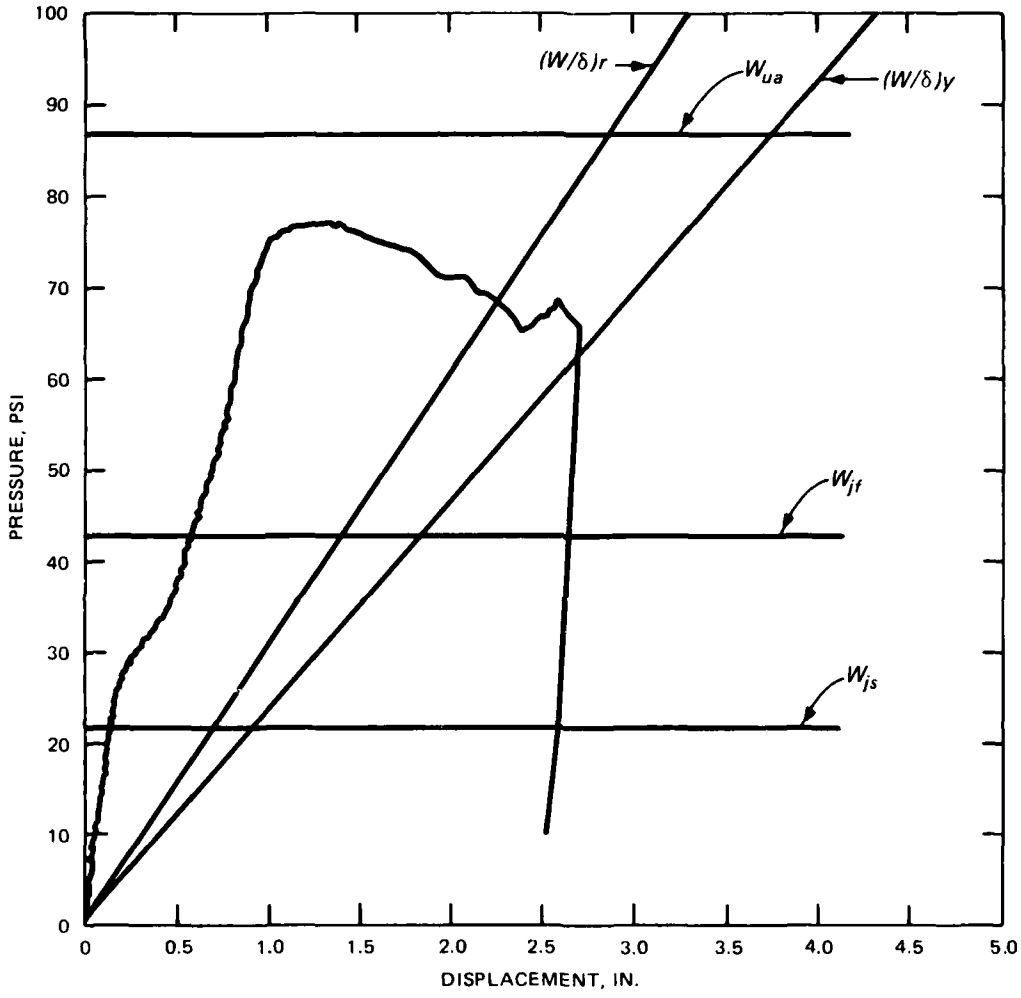

Figure 4.8. Experimental and analytical comparisons for Slab G4B.

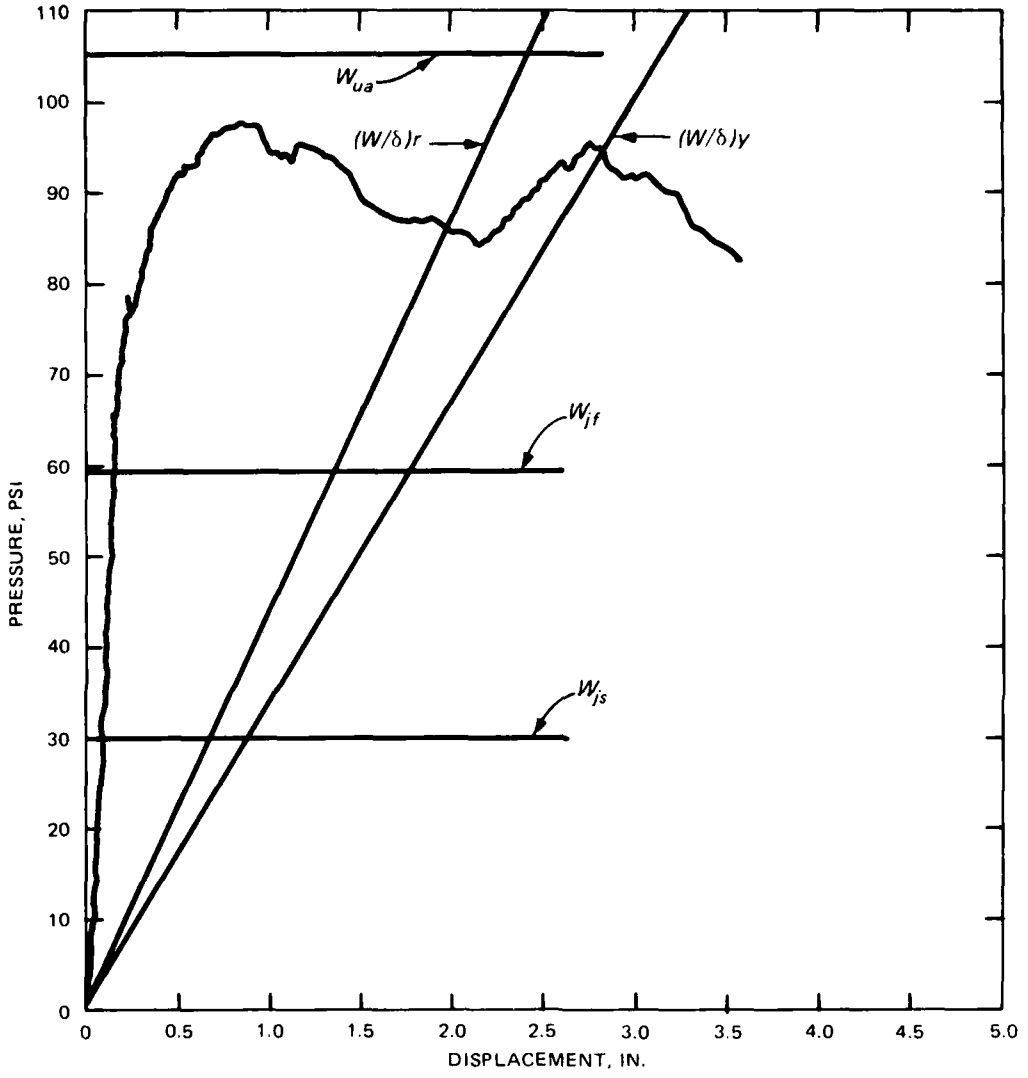

Figure 4.9. Experimental and analytical comparisons for Slab G5.

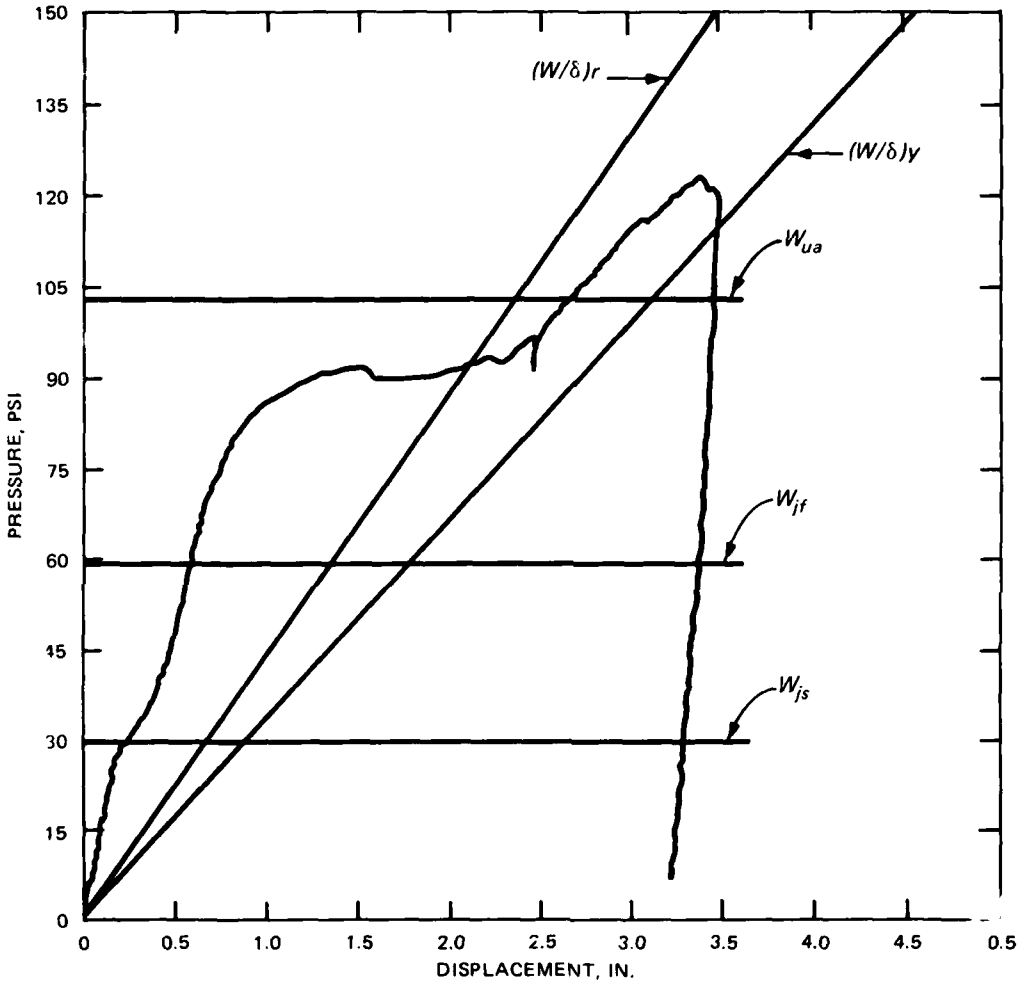

Figure 4.10. Experimental and analytical comparisons for Slab G6.

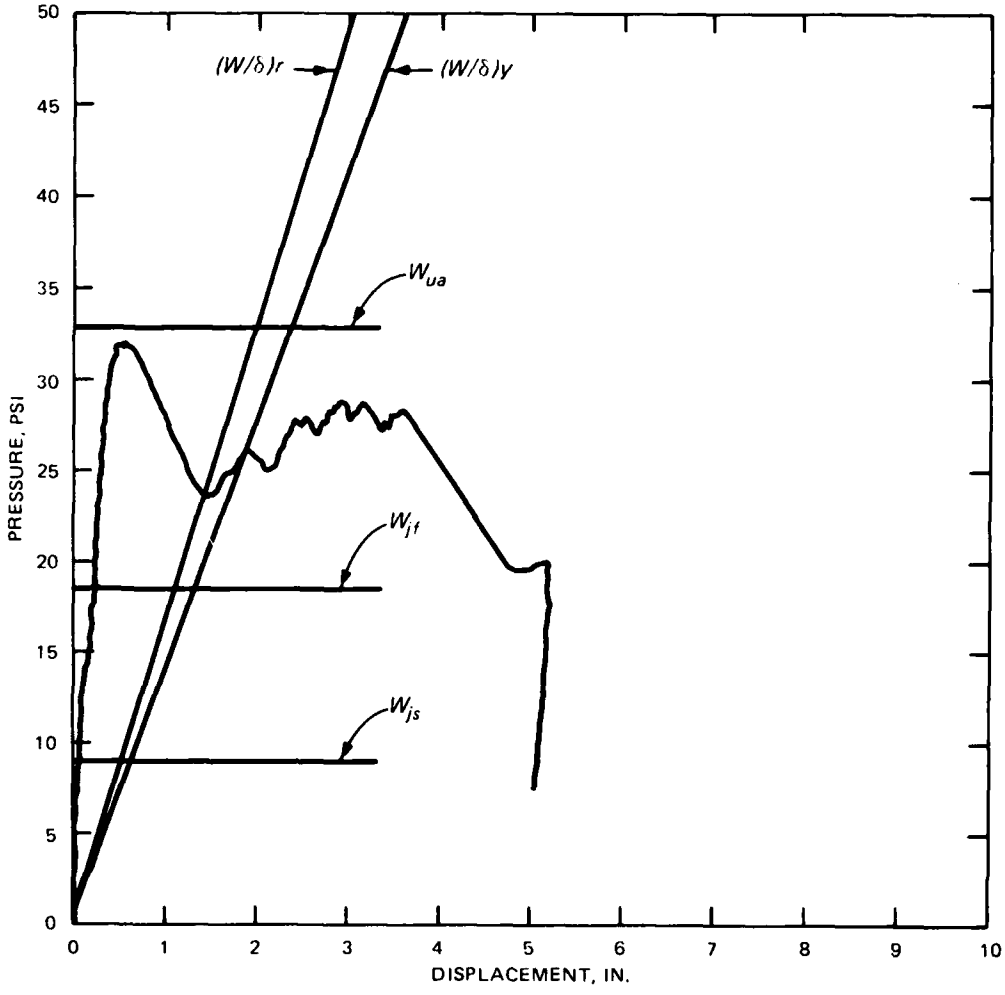

Figure 4.11. Experimental and analytical comparisons for Slab G7.

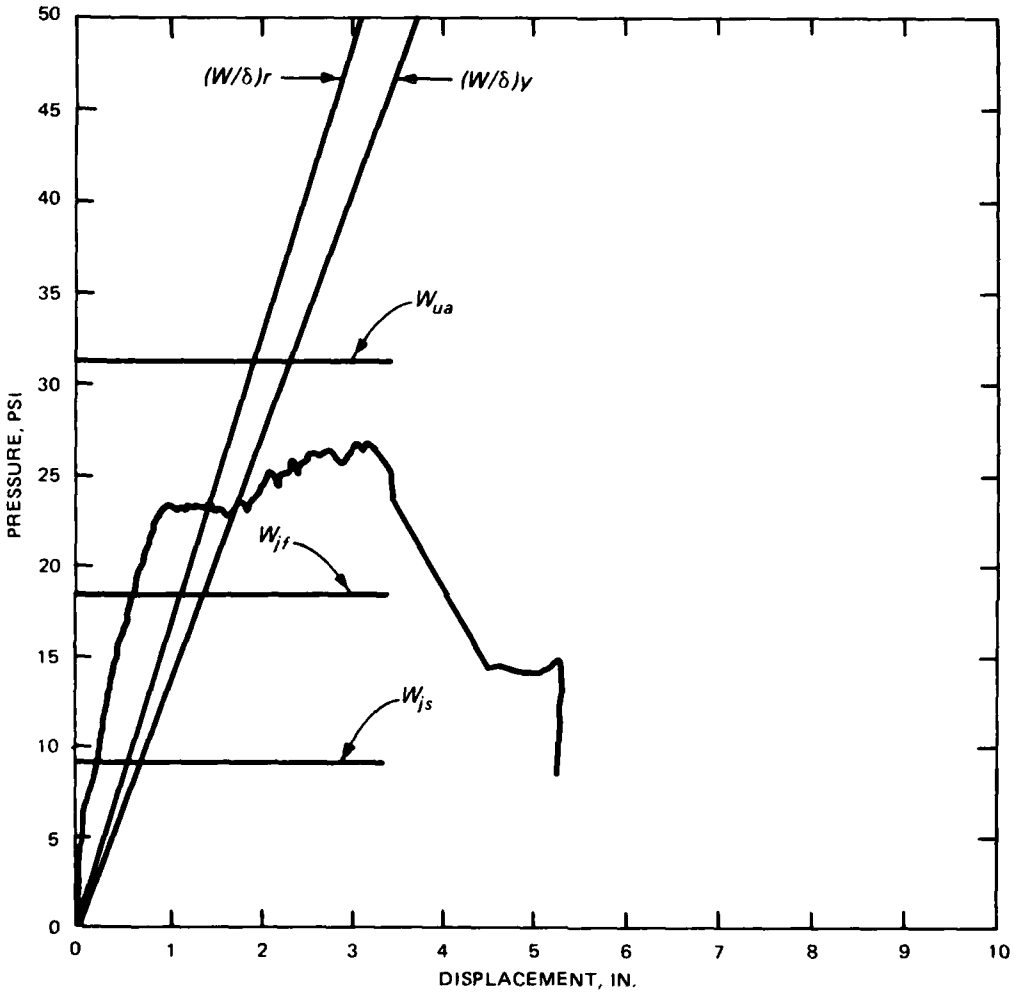

Figure 4.12. Experimental and analytical comparisons for Slab G8.

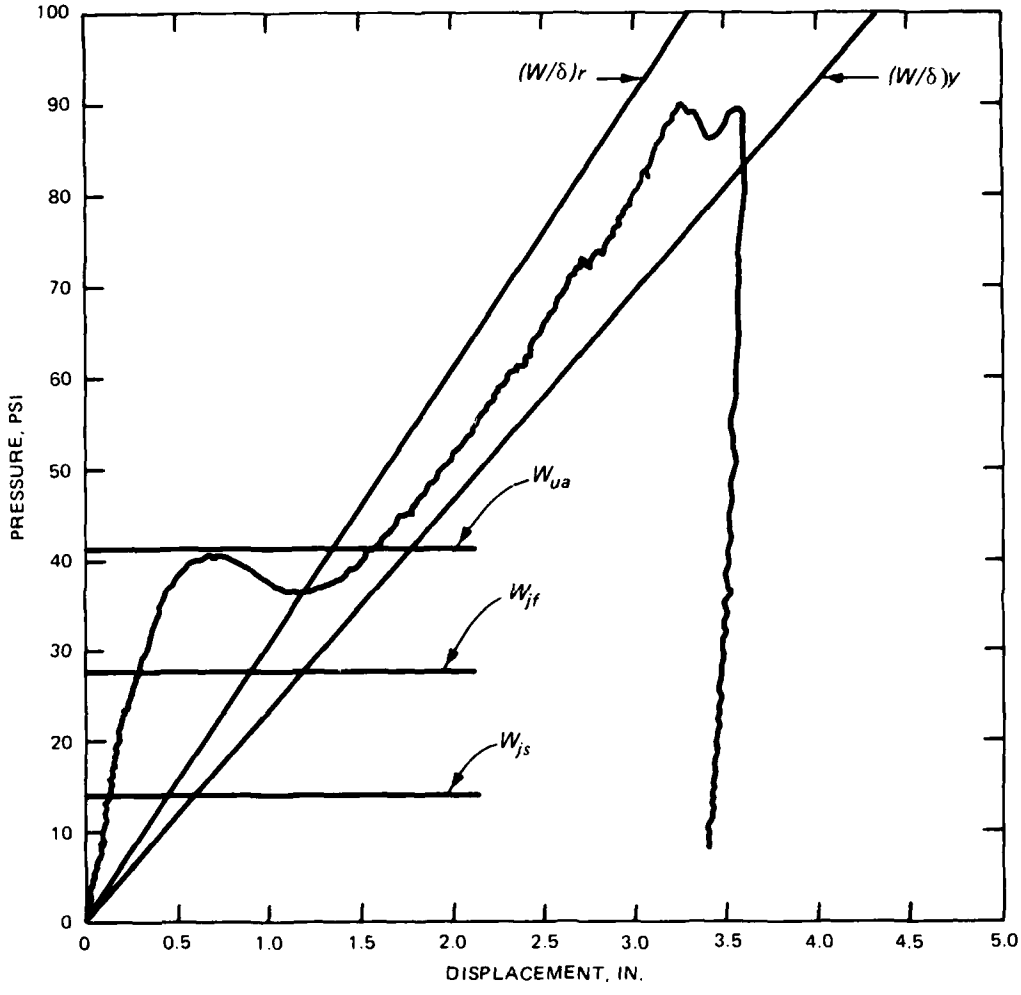

Figure 4.13. Experimental and analytical comparisons for Slab G9.

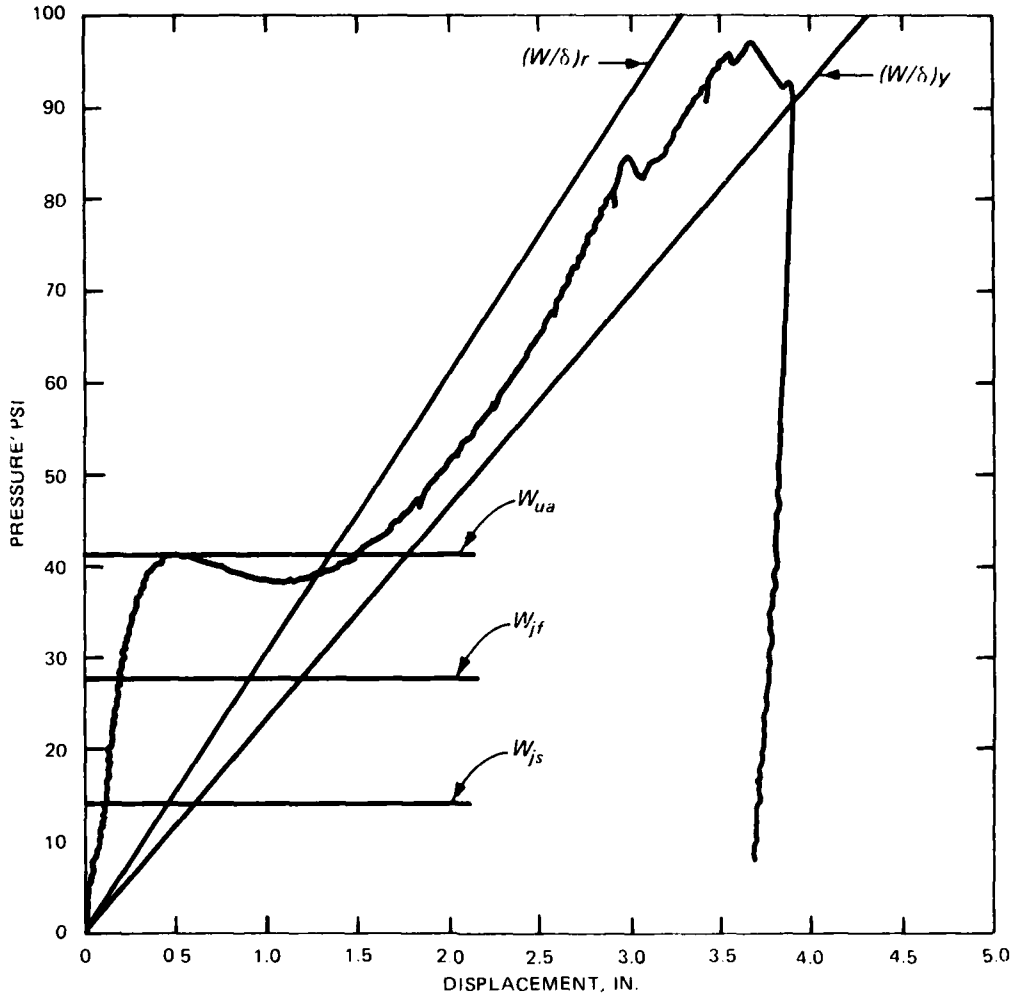

Figure 4.14. Experimental and analytical comparisons for Slab G9A.

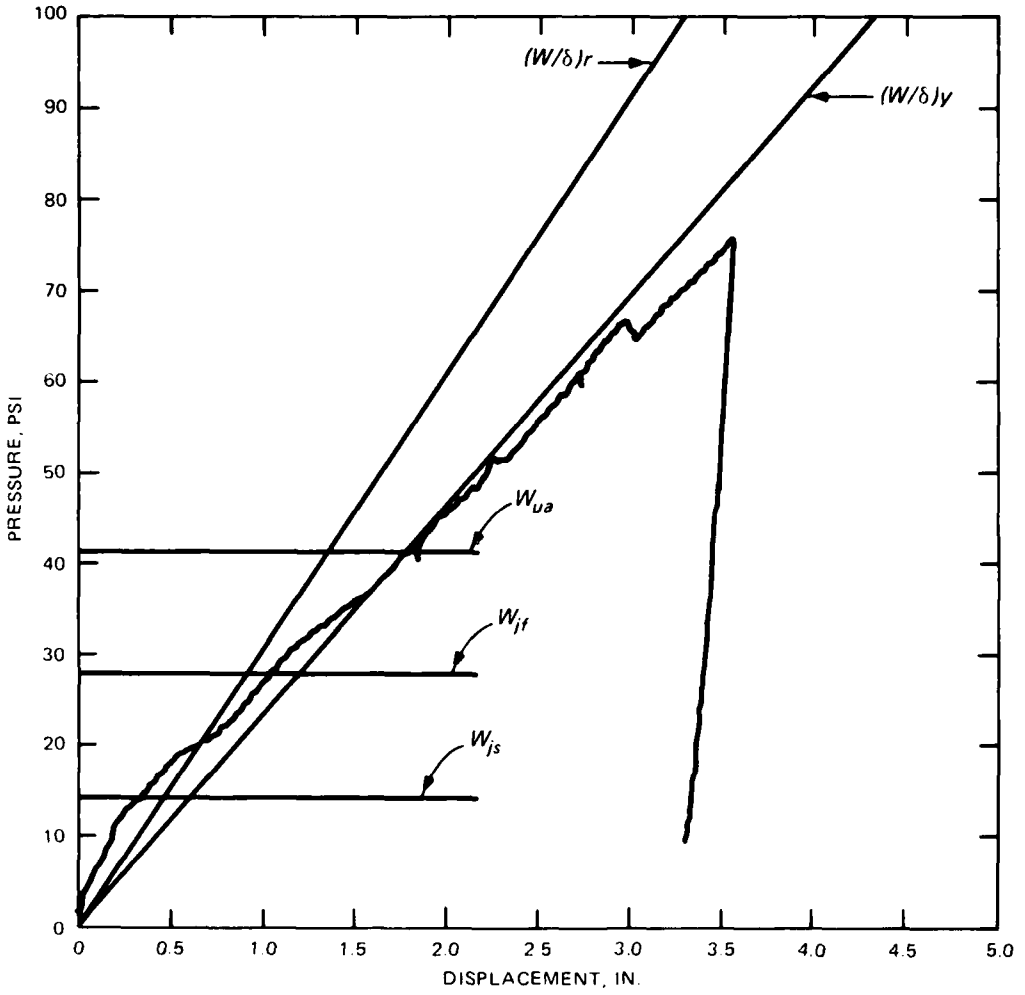

Figure 4.15. Experimental and analytical comparisons for Slab G10.

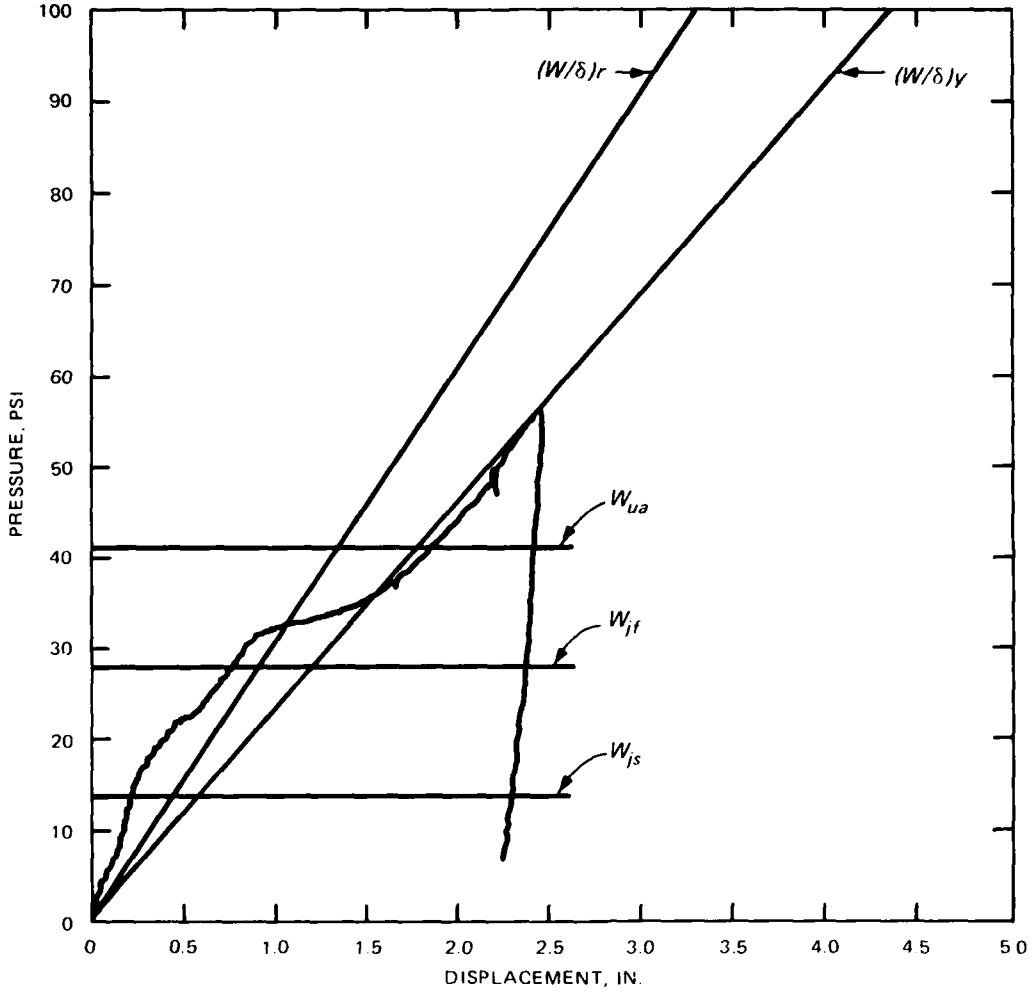

Figure 4.16. Experimental and analytical comparisons for Slab G10A.

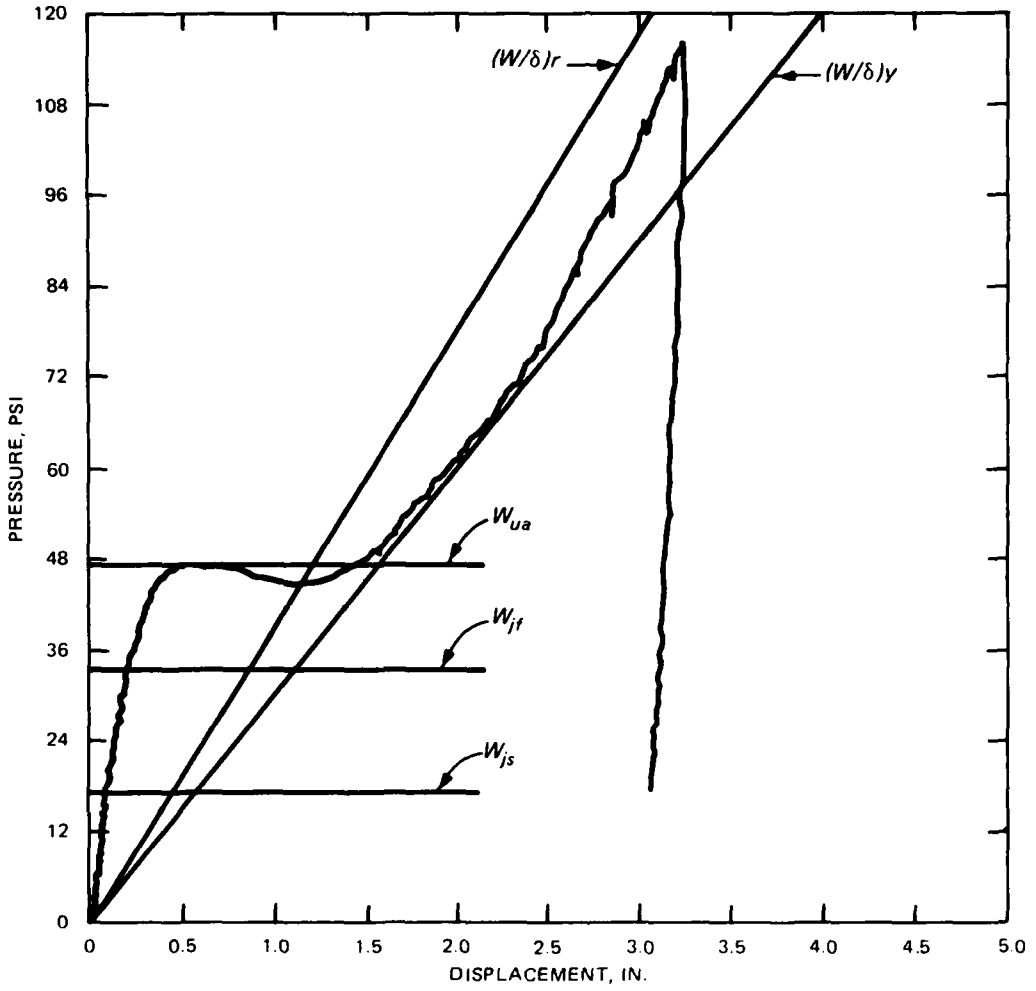

Figure 4.17. Experimental and analytical comparisons for Slab G11.

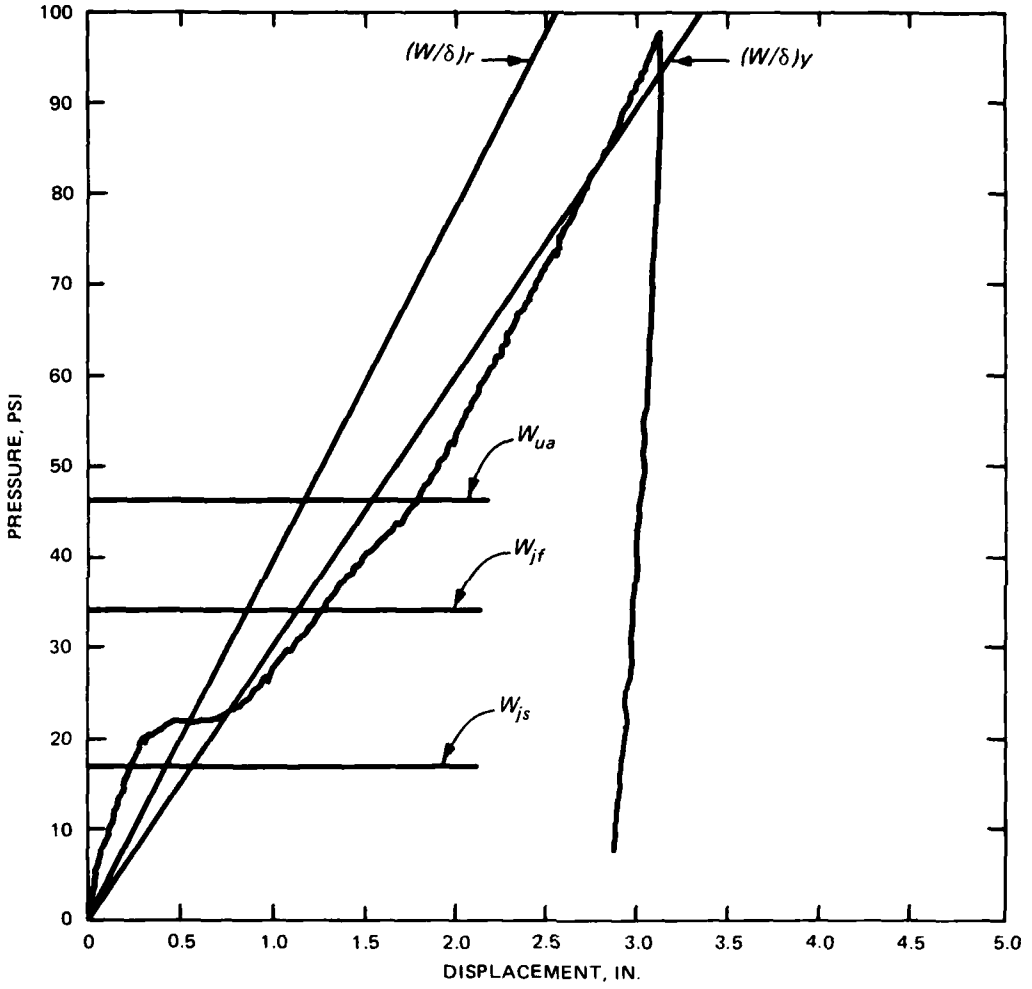

Figure 4.18. Experimental and analytical comparisons for Slab G12.

CHAPTER 5

SUMMARY, CONCLUSIONS, AND RECOMMENDATIONS

5.1 SUMMARY

From observations of the physical specimens, examinations of experimental data, and comparisons with analytical results, a better understanding of slab behavior has been achieved. Of primary interest in this test program was the determination of the effects of partial rotational restraint on slabs with different geometric characteristics. The slab parameters which were considered were the span/thickness ratio and the reinforcement ratio.

At least two slabs for each of six slab configurations were constructed and tested. Each slab was permitted different degrees of rotational freedom. A specially designed reaction structure permitted measurements of the various member end actions, including thrusts and rotations. The following conclusions are based on the results of the 16 slabs from this test program, and where appropriate, from Woodson's tests of rigidly restrained slabs (Reference 1).

5.2 CONCLUSIONS

Compressive membrane theory (References 5 and 6) using an assumed infinite lateral stiffness overpredicted the flexural capacity of slabs with partial rotational restraint when no external in-plane loads were present. For slabs which underwent relatively small rotations, the same theory (combined with a realistic value for lateral stiffness) predicted the peak capacity within approximately 10 percent, and was a significantly better predictor for peak capacity than yield-line theory. Therefore, thrusts did act to enhance the flexural capacities of slabs with small rotational freedoms as long as the lateral stiffness was sufficient to develop in-plane forces.

The deflections at which the peak capacities were achieved were significantly different for slabs with varied rotational freedoms. However, as long as the rotational freedoms were small, the peak capacities were relatively unaffected and were not substantially different from the peak capacities of rigidly restrained slabs. The peak capacity deflections were significantly underpredicted by the Johansen's load from Equation 4.1.

For larger rotational freedoms, the peak capacities occurred at large

deflections, were significantly lower than the capacities which were predicted by compressive membrane theory, and in some cases, the slabs had no definitive flexural capacity at all. The distinct difference in behavior was attributed to geometric instability. In other words, because the rotations were large, the slab snapped through to the tensile membrane stage before significant thrusts were developed to enhance the flexural capacity.

Smaller rotational freedoms were necessary to induce a stability failure in the thin slabs. The range of average support rotational freedoms at which stability failures were induced was approximately 2.0 to 2.5 degrees. All three series of the thin-slab group had developed instabilities at rotations of less than 2.2 degrees, and in two cases, at rotations of less than 2.04 degrees. Slab G9 appeared to be stable at a rotation of 1.29 degrees. Even though Slab G6 experienced an instability at approximately 2.04 degrees, none of the other thick slabs demonstrated similar responses. Slab G4A did show appreciable signs of unstable action at a rotation of 2.52 degrees. Overall, the effects of instability were more apparent for the thin slabs.

There are insufficient data to draw conclusions on the effects of steel percentage on the flexural stability of partially restrained slabs.

There was significantly more tensile membrane response in the thin-slab group than in the thick-slab group. Under similar ranges of loading, the thin slabs carried a larger percentage of the load by tensile membrane action. The tensile response was apparent in that the crack patterns for the thin slabs were much broader and the cracks were significantly narrower. The yielding of the reinforcement appeared to be less confined to the central yield zone and more evenly distributed throughout the whole slab.

The tensile membrane theory (Equation 4.5), based on both yield strains and rupture strains, usually bounded the tensile response of the slabs prior to rupturing of the reinforcement. After some of the reinforcement ruptured, the load-deflection curve followed a reduced tensile slope.

For the thick-slab group, higher tensile capacities were achieved as the rotational freedoms increased. The probable explanation for this behavior was that with small rotational freedoms, more strain energy was required at the critical sections in the flexural stage, causing more of the reinforcement to rupture in earlier portions of the tensile membrane stage.

For given deflections, the tensile capacities of the thin slabs were generally higher as rotational freedoms decreased. With smaller rotational

freedoms, the slabs carried the load by combined flexure and tension, which resulted in a higher capacity than could be achieved in pure tension. Also, plastic rotations acted to increase the strains in the reinforcement such that strain-hardening contributed to the tensile capacities.

When instability was not a factor, the thin slabs came closer to approaching the maximum analytical compressive membrane capacity. Even though the actual support stiffnesses were approximately the same for all slabs, the relative lateral stiffness of the supports was greater for the thin slabs, making the peak capacity approach that for an infinitely stiff support.

Most slabs initiated the tensile membrane response at a deflection which fell between the slab's effective depth and thickness.

Only considering slabs which were reinforced with the ductile No. 2 bars, the average incipient collapse deflection occurred at approximately one-eighth of the span for the thick-slab group and somewhat more than that for the thin-slab group. Since no reinforcement rupture was apparent in three of the thin slabs, the average incipient collapse deflection was not computed. However, an examination of the data indicated that the deflection at which the reinforcement first ruptured was somewhat greater for the thin slabs than for the thick slabs.

5.3 RECOMMENDATIONS FOR DESIGN

The following design recommendations have been based on the results of this test program and should be considered in the development of keyworker blast shelters. Since designs are frequently based on different criteria, the recommendations have been stated in terms of the particular performance affected.

1. Regardless of rotational freedoms, adequate lateral stiffness must be provided to develop compressive and tensile membrane enhancements.

2. Increases in the area of steel or the slab thickness act separately to enhance the compressive membrane capacity and energy-absorption capacity of the slab, as long as rotational freedoms do not induce stability failures.

3. Small rotational freedoms do not significantly affect the compressive membrane capacity, but do enhance the tensile membrane capacity and incipient collapse deflection. For design purposes, the largest possible rotational freedom which permits an enhanced peak capacity without inducing a premature stability failure generally results in the most favorable overall response.

That rotational freedom appears to be between 2.0 and 2.5 degrees for the thicker slabs and from 1.5 to 2.0 degrees for the thin slabs.

4. If allowed small rotations, thicker slabs provide a substantial increase in flexural capacity and a decrease in tensile capacity with respect to thin slabs with the same total steel area. As a result of the larger area under the initial portion of the load-deflection curves, the energy absorption capacity of the thicker slabs is greater.

5. Regardless of the rotational freedom, thin slabs carry a much larger percentage of the load by tensile membrane action. The failure of a thin slab is characterized by a broad band of relatively small cracks. In terms of the resistance, thin slabs are much more likely to "catch" the load after the initial compressive membrane peak.

6. Sufficient reinforcement ductility must be provided to develop any tensile membrane resistance. In general, Grade 60 or lower reinforcement should provide adequate ductility.

Roof slabs which have a span-thickness ratio of about 15, have from 1.0 to 1.5 percent of steel in each face, and are supported with a relatively large lateral stiffness and a moderate rotational stiffness will probably result in a structure which best combines the characteristics of strength, ductility, and economy.

5.4 RECOMMENDATIONS FOR FURTHER STUDY

A more in-depth analysis of each slab, including a finite element analysis and a stability analysis, is needed to verify the findings of this study and to further explain the reasons for the experimental slabs' behavior.

Additional tests should be conducted to determine the rotational instability deflection for each span/thickness ratio and reinforcement ratio. Such tests would also serve to confirm the previous experimental results.

REFERENCES

1. S. C. Woodson; "Effects of Shear Stirrup Details on Ultimate Capacity and Tensile Membrane Behavior of Reinforced Concrete Slabs"; Technical Report SL-85-4, August 1985; US Army Engineer Waterways Experiment Station, Vicksburg, Miss.

2. K. W. Johansen; "Brudlinieteorier" (English translation, "Yield-Line Theory"); 1962; Cement and Concrete Association, London.

3. American Concrete Institute; "ACI 318-83, Building Code Requirements"; 1983; Detroit, Mich.

4. T. Takehira, A. T. Derecho, and M. Iqbal; "Design Criteria for Deflection Capacity of Conventionally Reinforced Concrete Slabs, State-of-the-Art Report"; Contract Reports CR80.026-CR 80.028, 1979-1980; Portland Cement Association, Skokie, Ill.

5. R. Park and W. L. Gamble; "Reinforced Concrete Slabs"; 1980; John Wiley and Sons, New York, N.Y.; pages 562-610.

6. W. A. Keenan; "Strength and Behavior of Restrained Reinforced Concrete Slabs Under Static and Dynamic Loading"; Technical Report R621, April 1969; US Naval Civil Engineering Laboratory, Port Hueneme, Calif.

7. J. F. Brotchie, A. Jacobson, and S. Okabo; "Effect of Membrane Action on Slab Behavior"; Research Report R65-25, 1965; Department of Civil Engineering, Massachusetts Institute of Technology, Cambridge, Mass.

APPENDIX A

REACTION STRUCTURE DETAILS

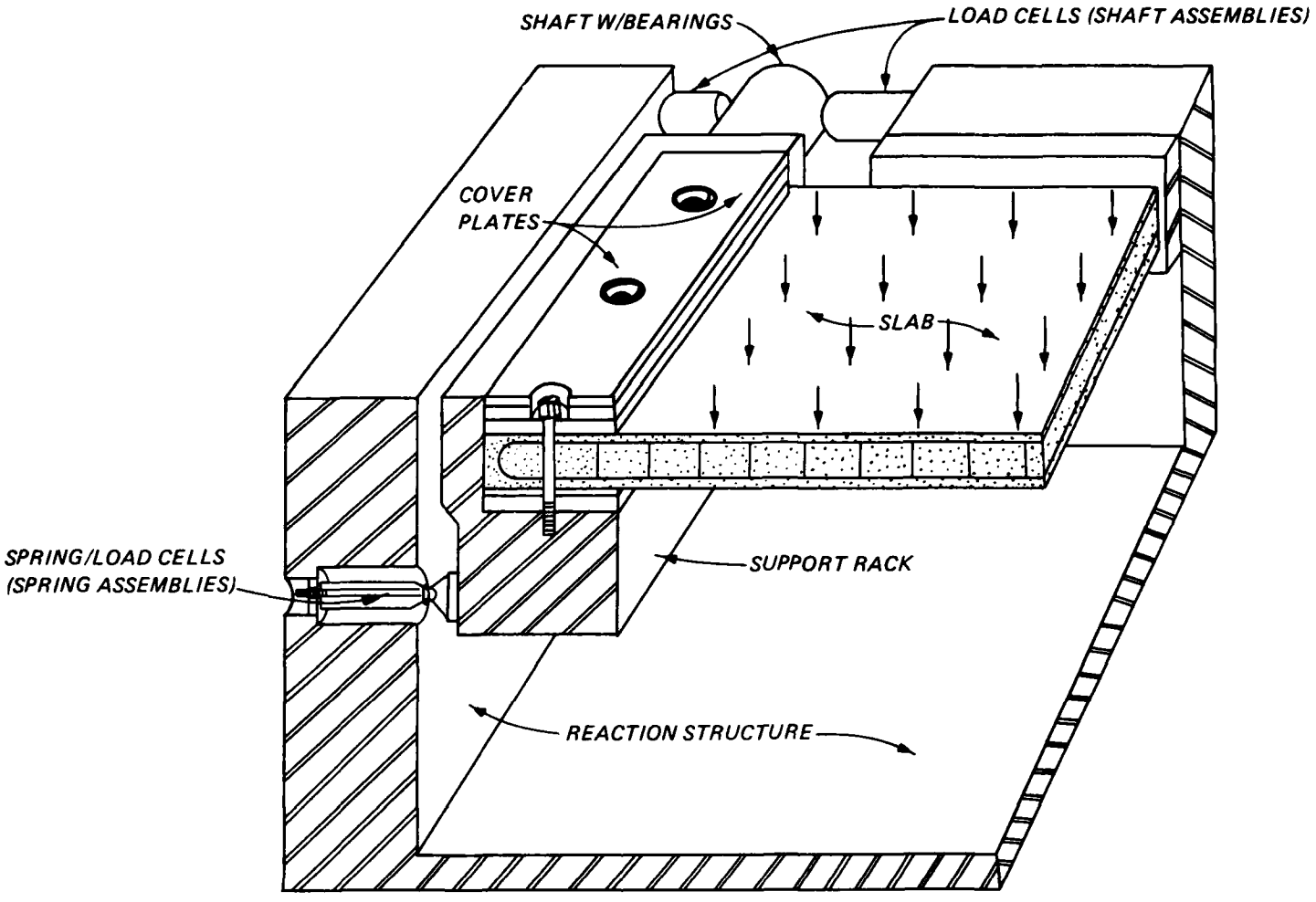

Figure A.1. Quarter-section view of reaction structure with slab in place.

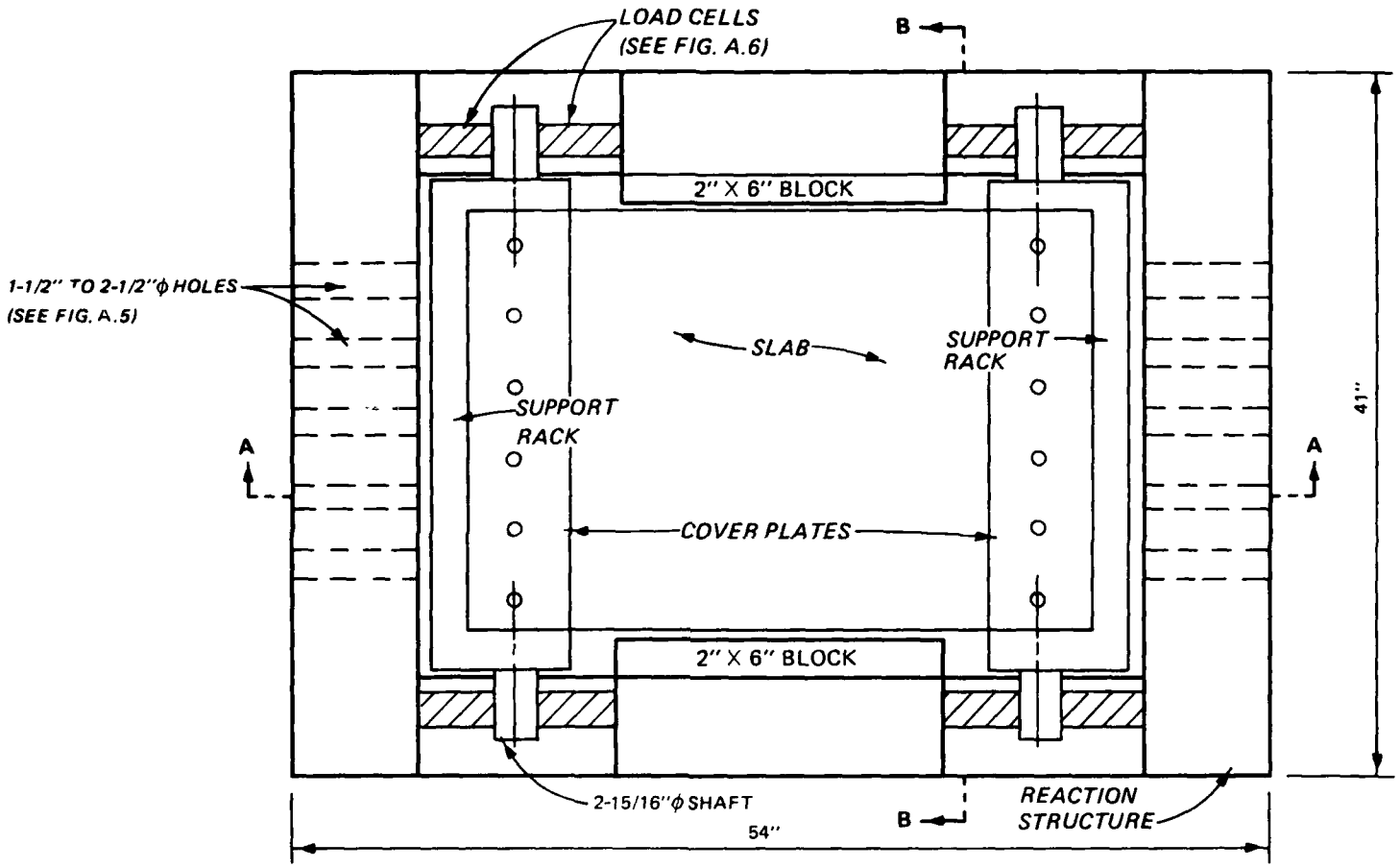

Figure A.2. Plan view of reaction structure and assemblies.

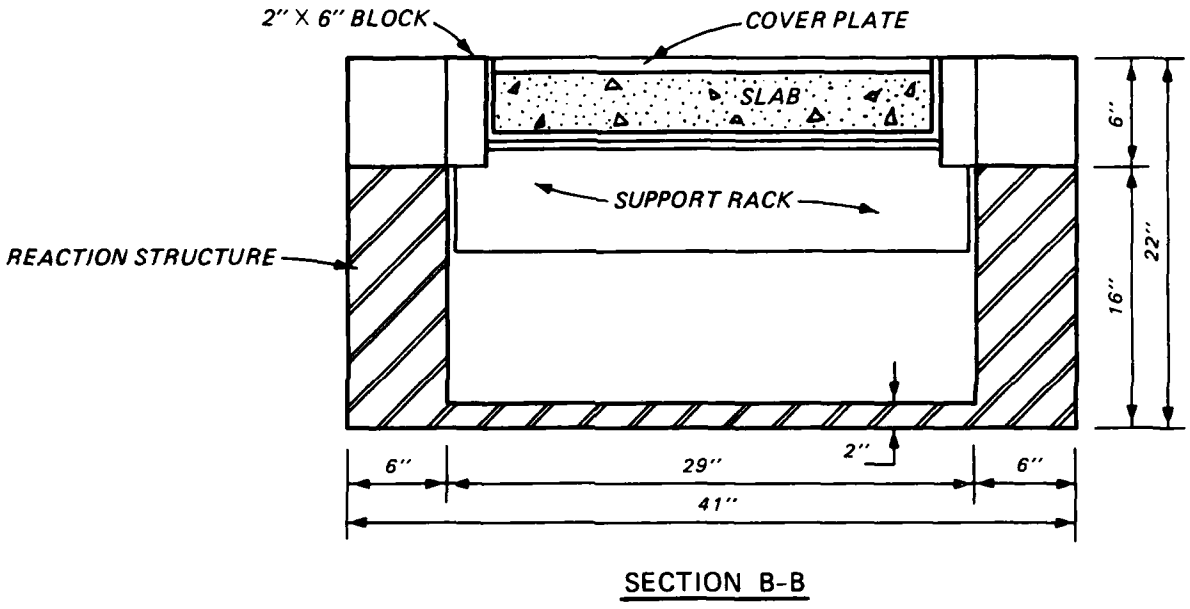

SECTION B-B

Figure A.3. Sections through reaction structure (Sheet 1 of 2).

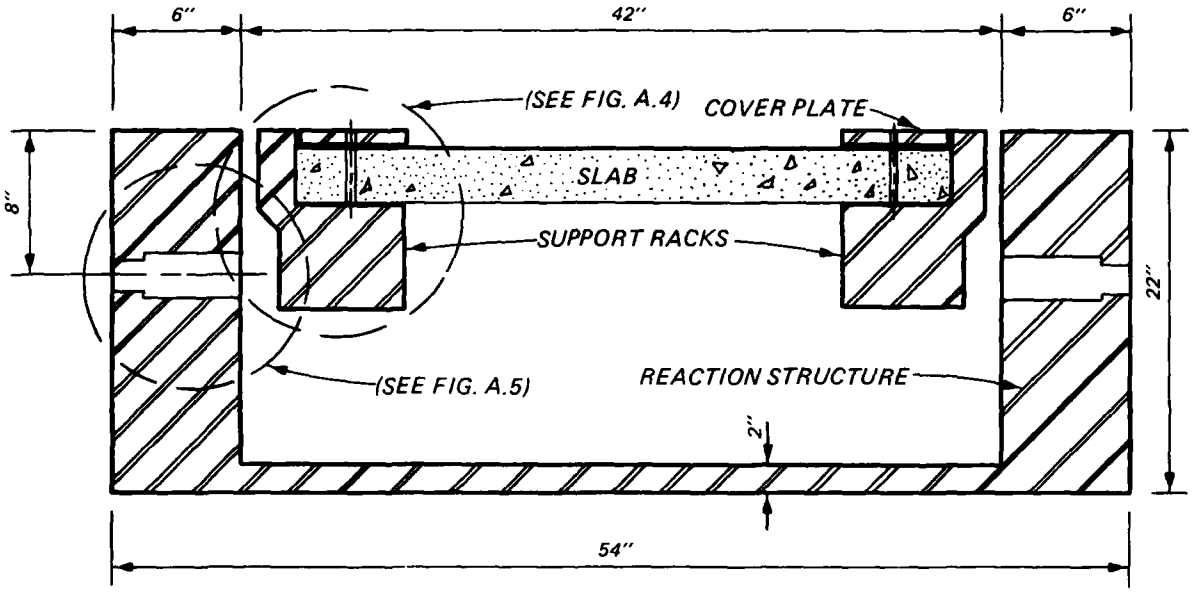

SECTION A-A

Figure A.3. (Sheet 2 of 2).

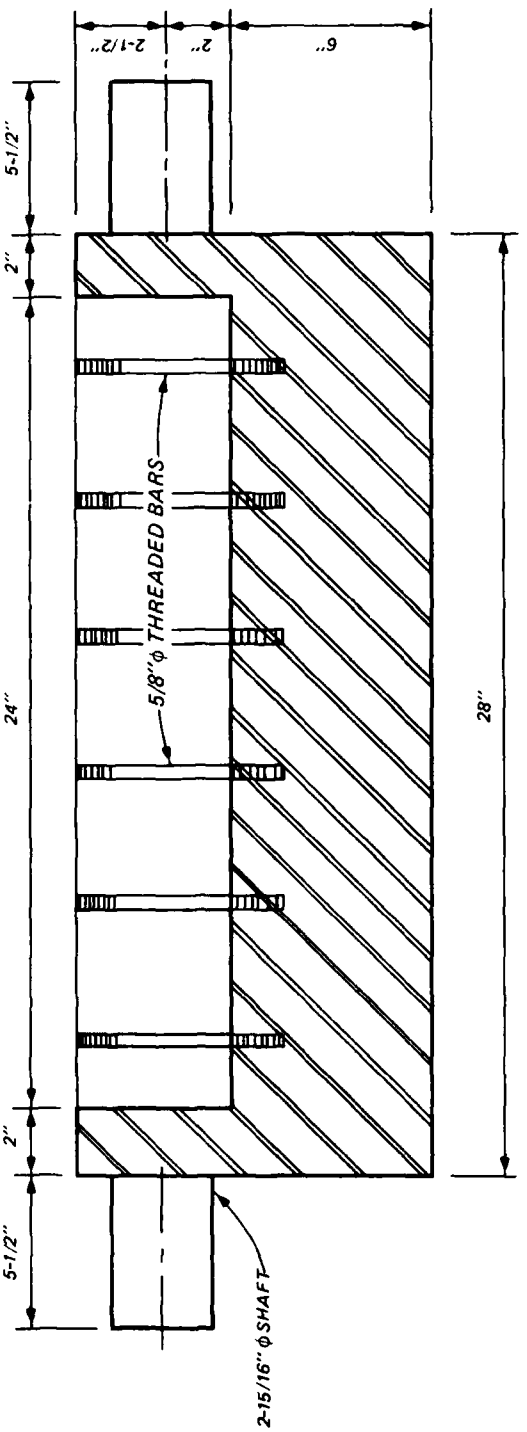

Figure A.4. Support rack details (Sheet 1 of 2).

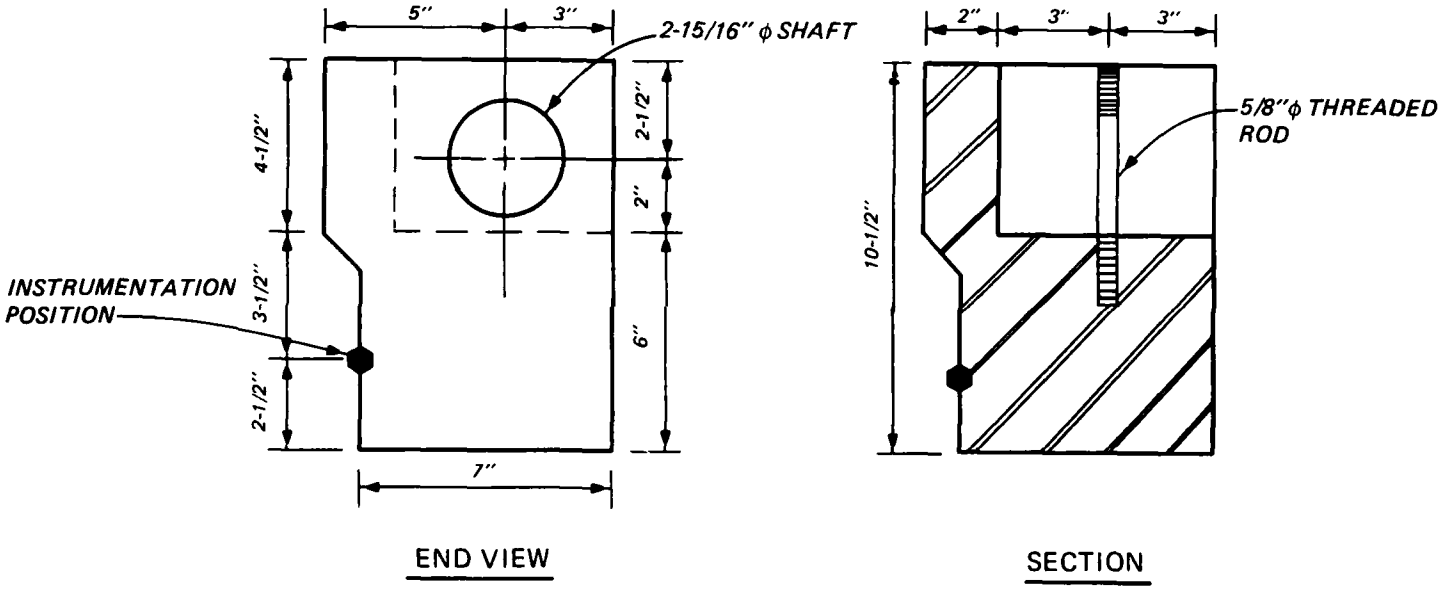

Figure A.4. (Sheet 2 of 2).

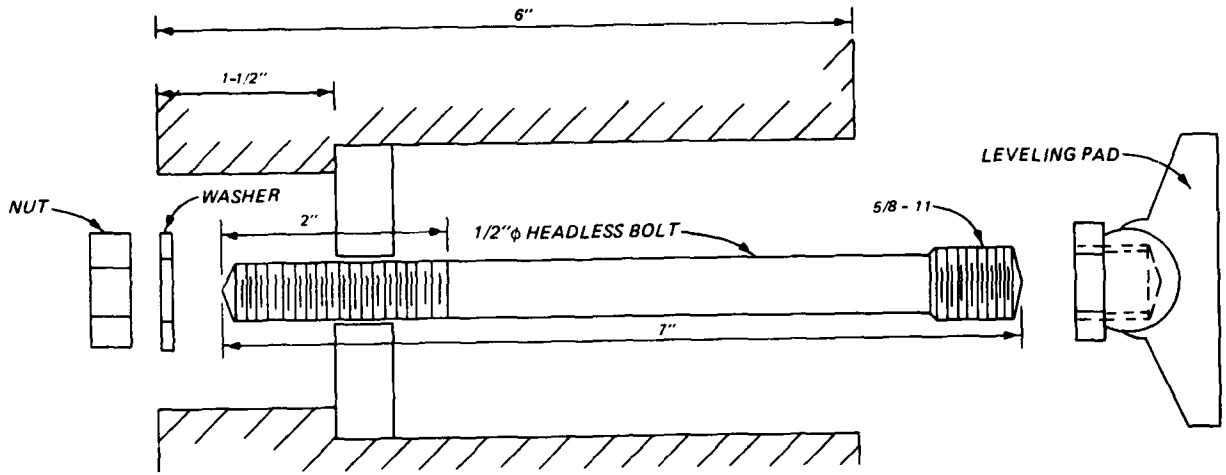

SPRING DETAIL

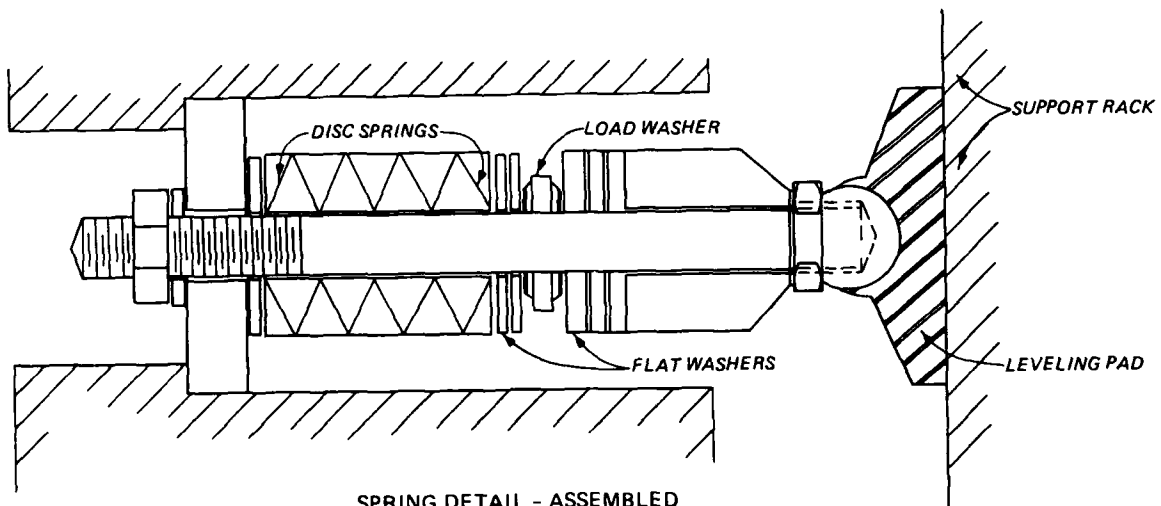

SPRING DETAIL - ASSEMBLED

Figure A.5. Spring assembly details.

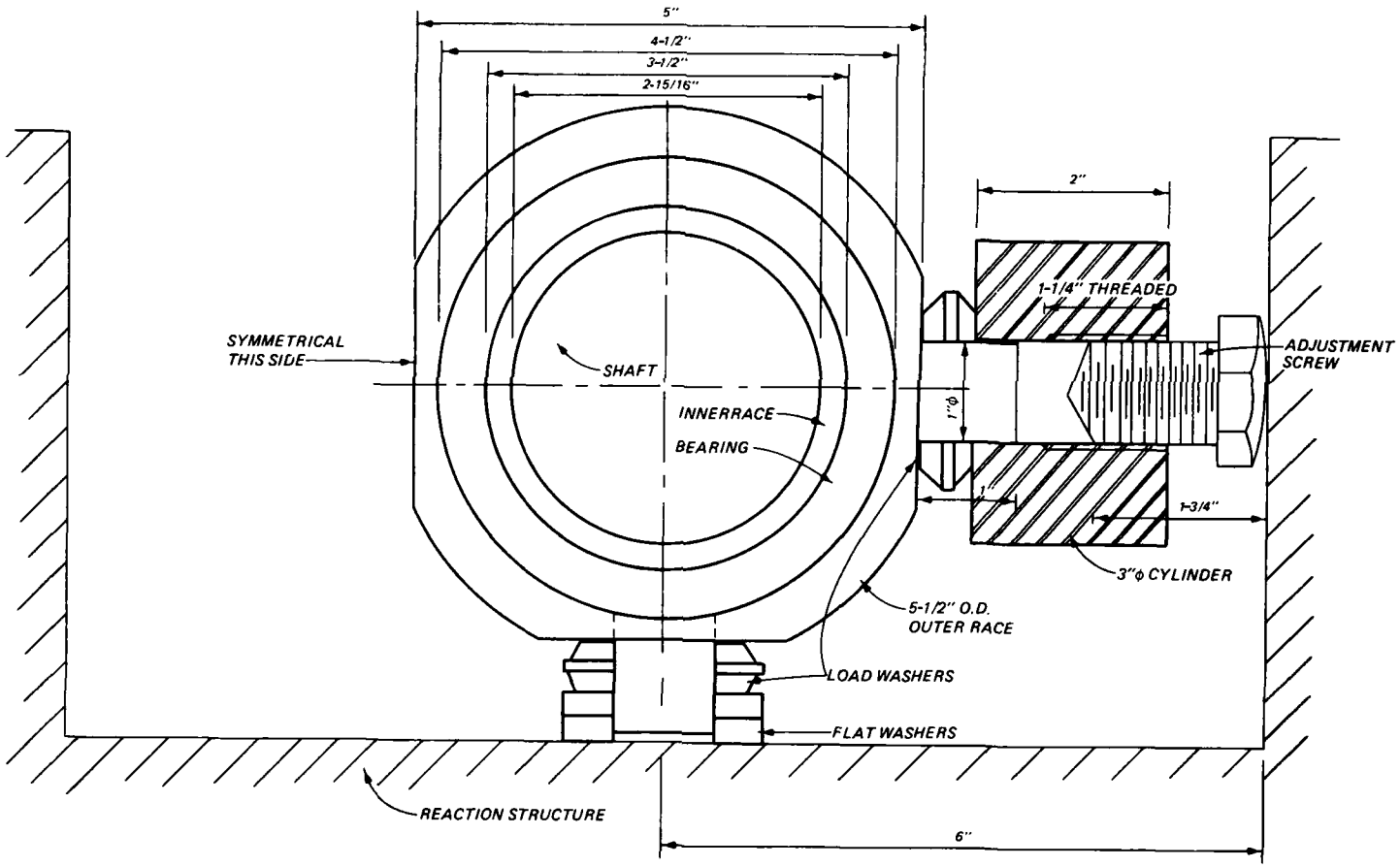

Figure A.6. Shaft assembly details.

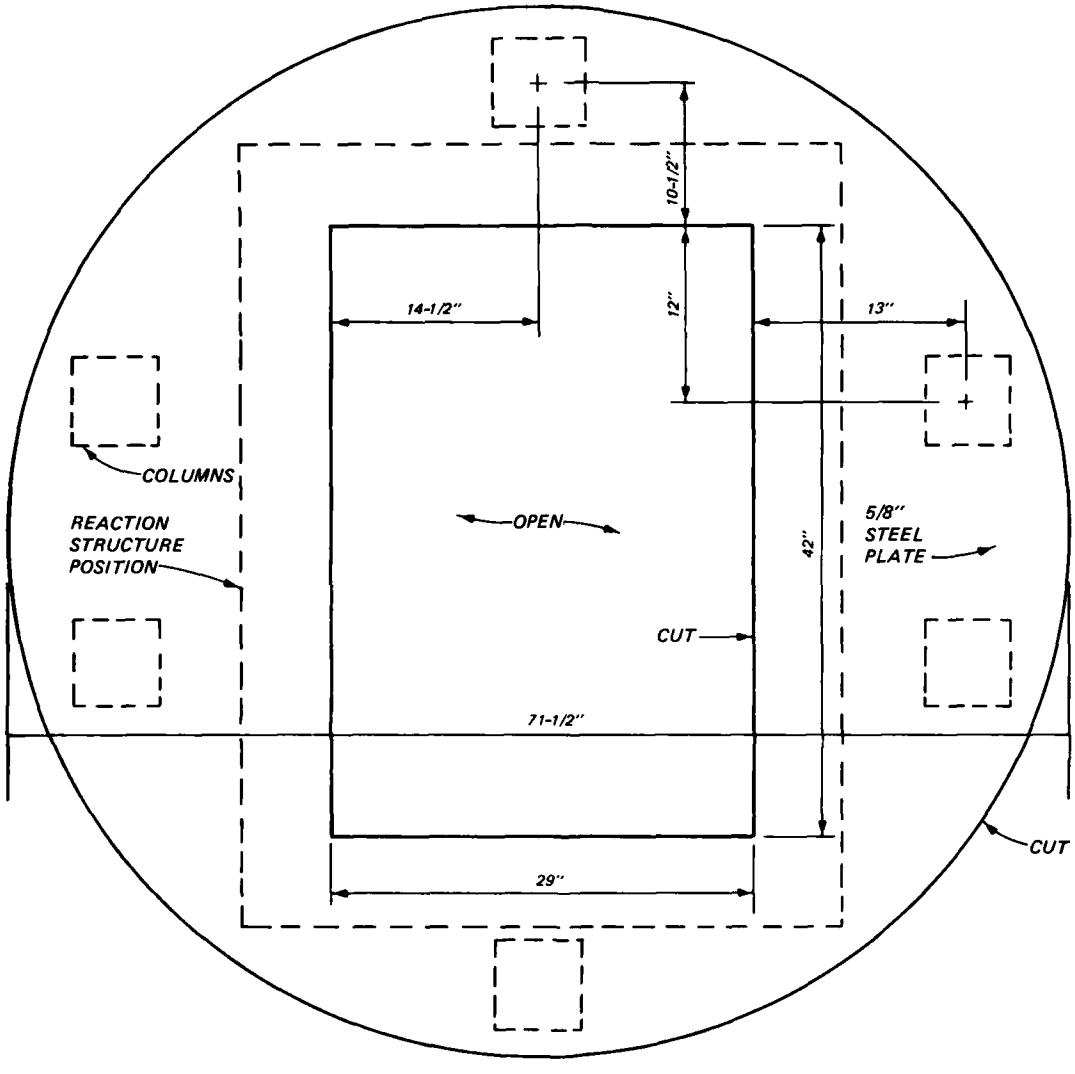

Figure A.7. Details for protective tables (Sheet 1 of 2).

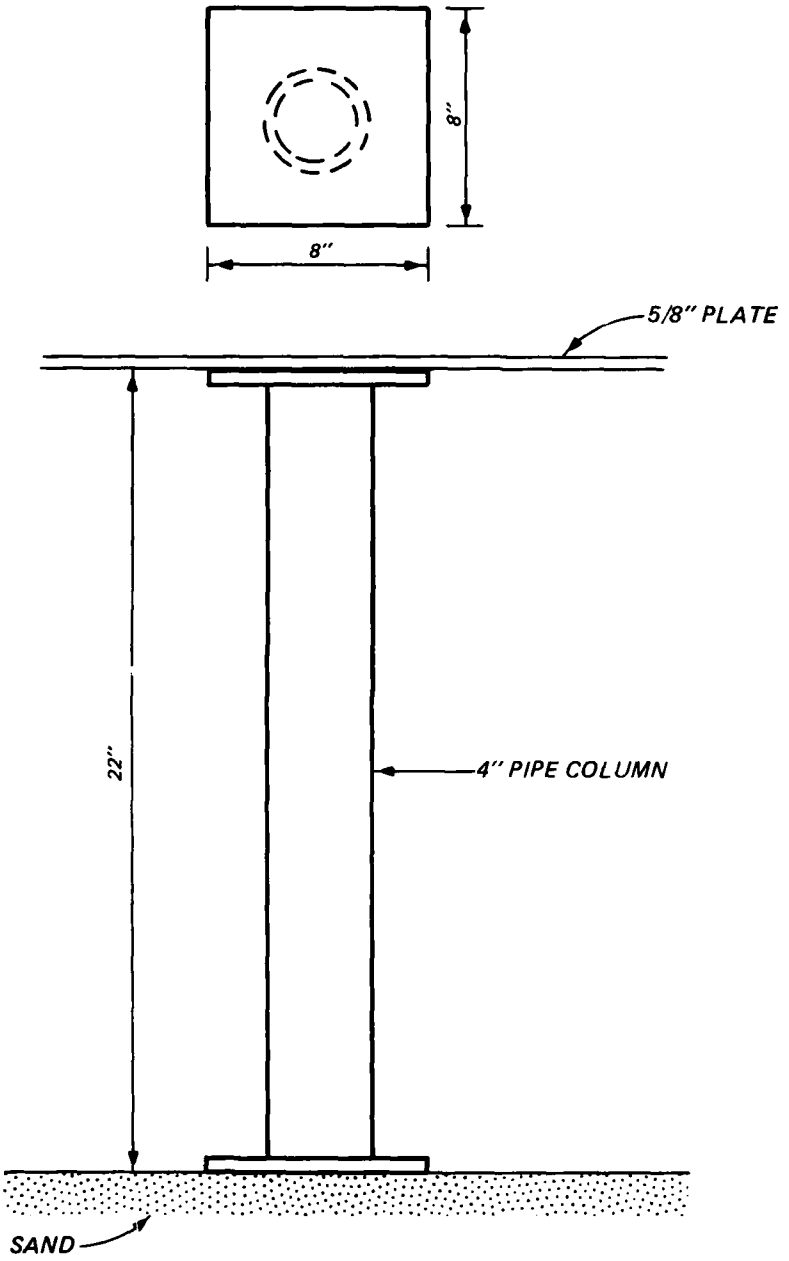

COLUMN DETAIL

Figure A.7. (Sheet 2 of 2).

APPENDIX B

PHOTOGRAPHS

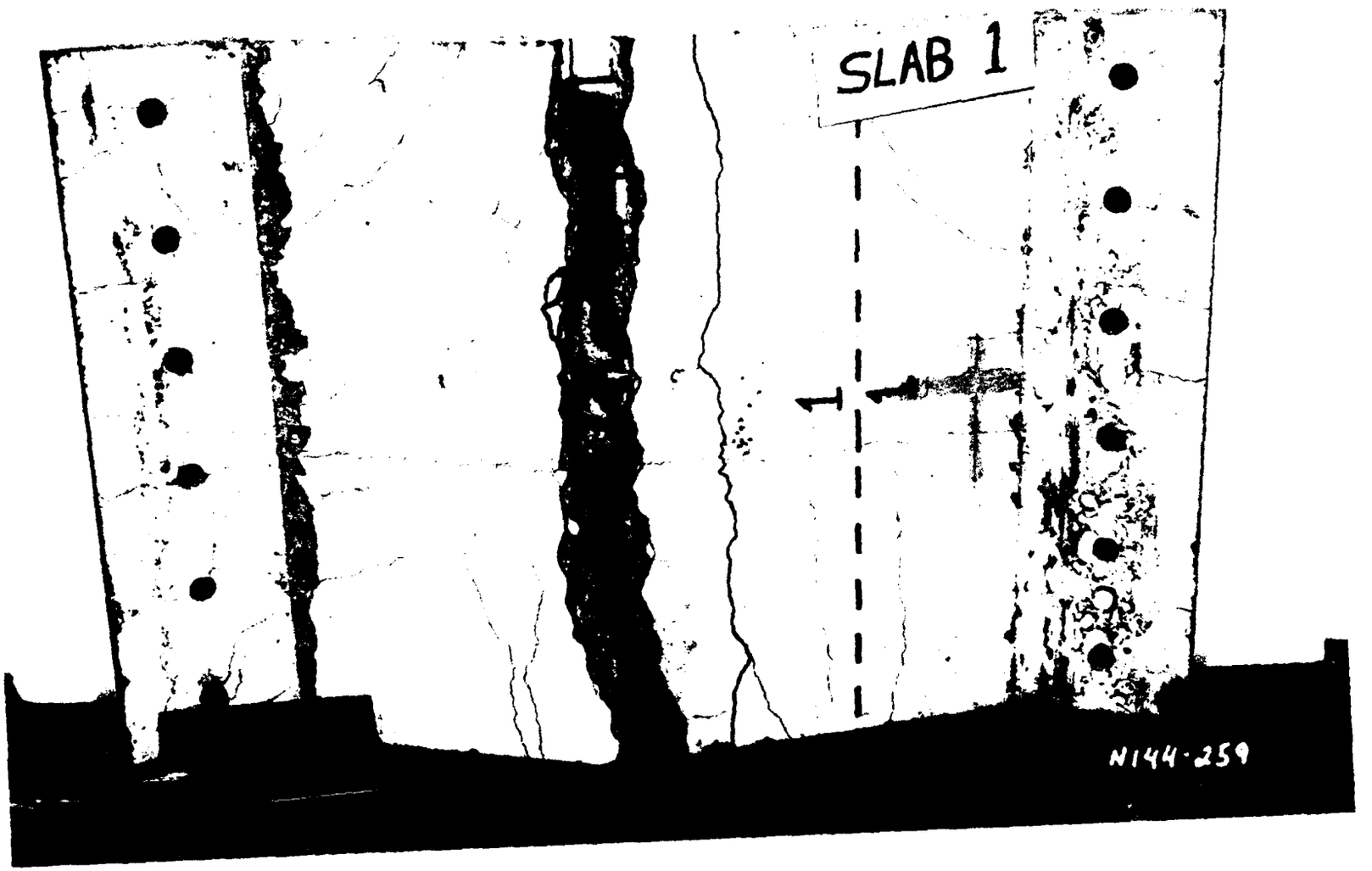
SLAB 1
N144-259

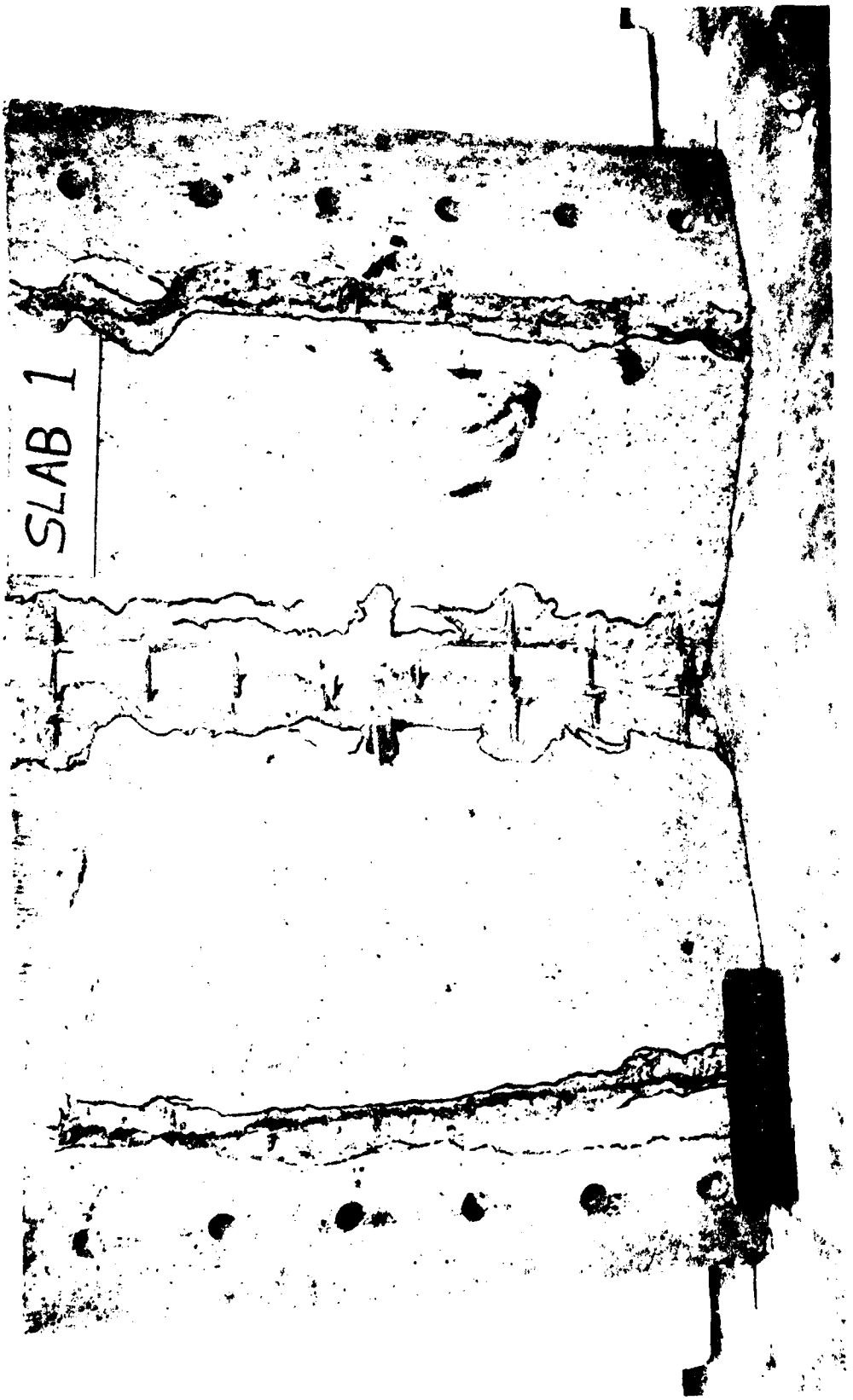
SLAB 1

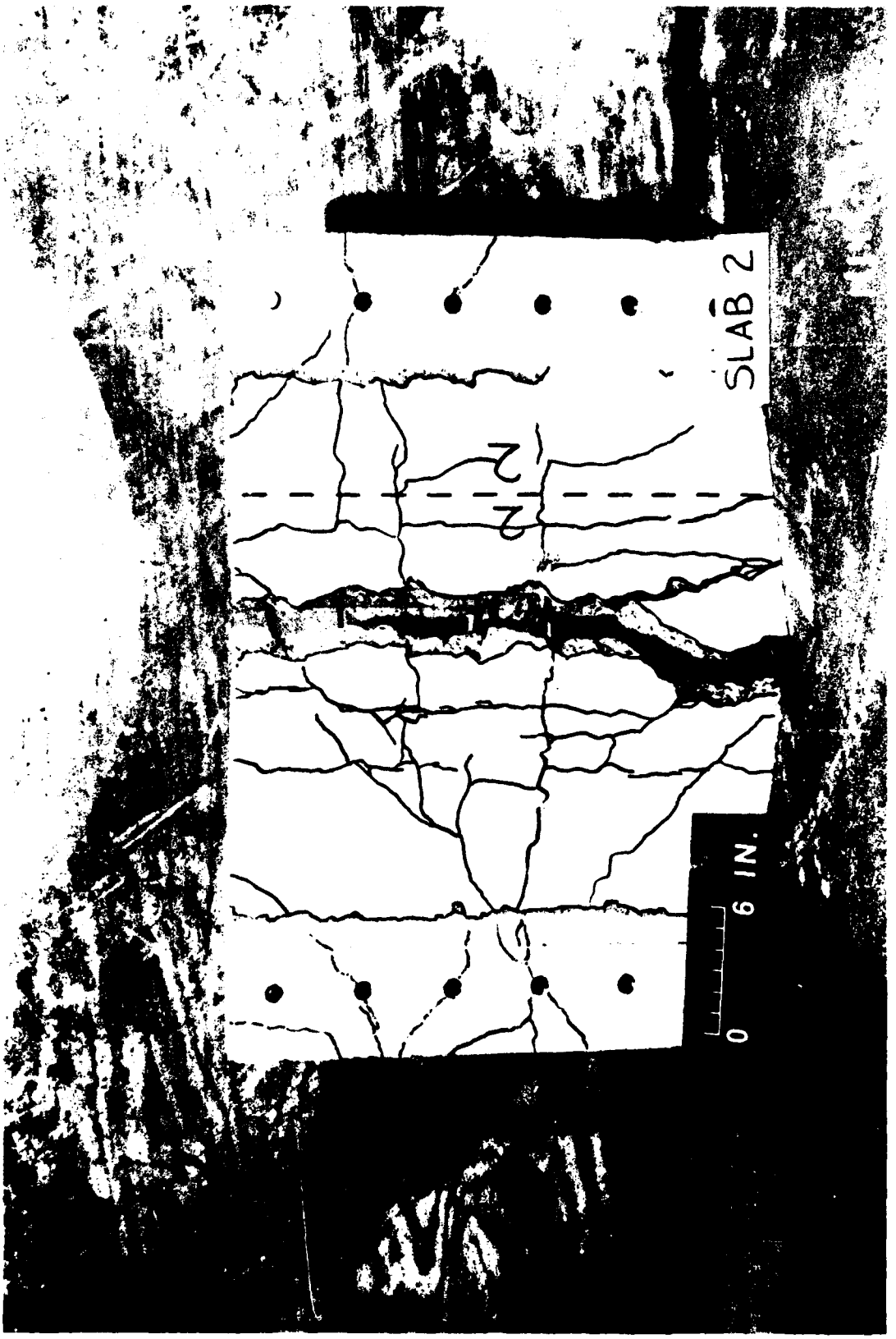
SLAB 2
2
2
0
6 IN.

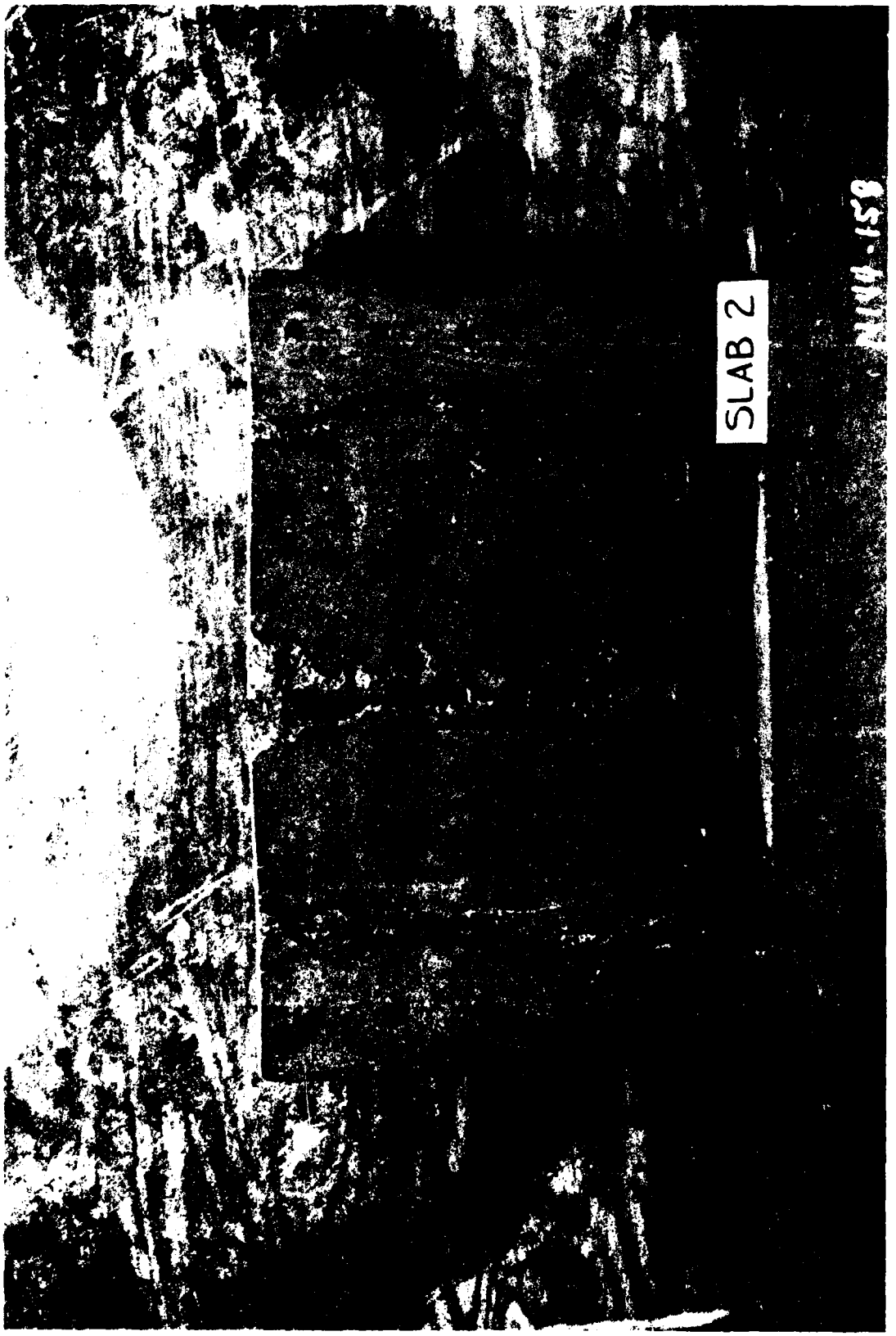
SLAB 2

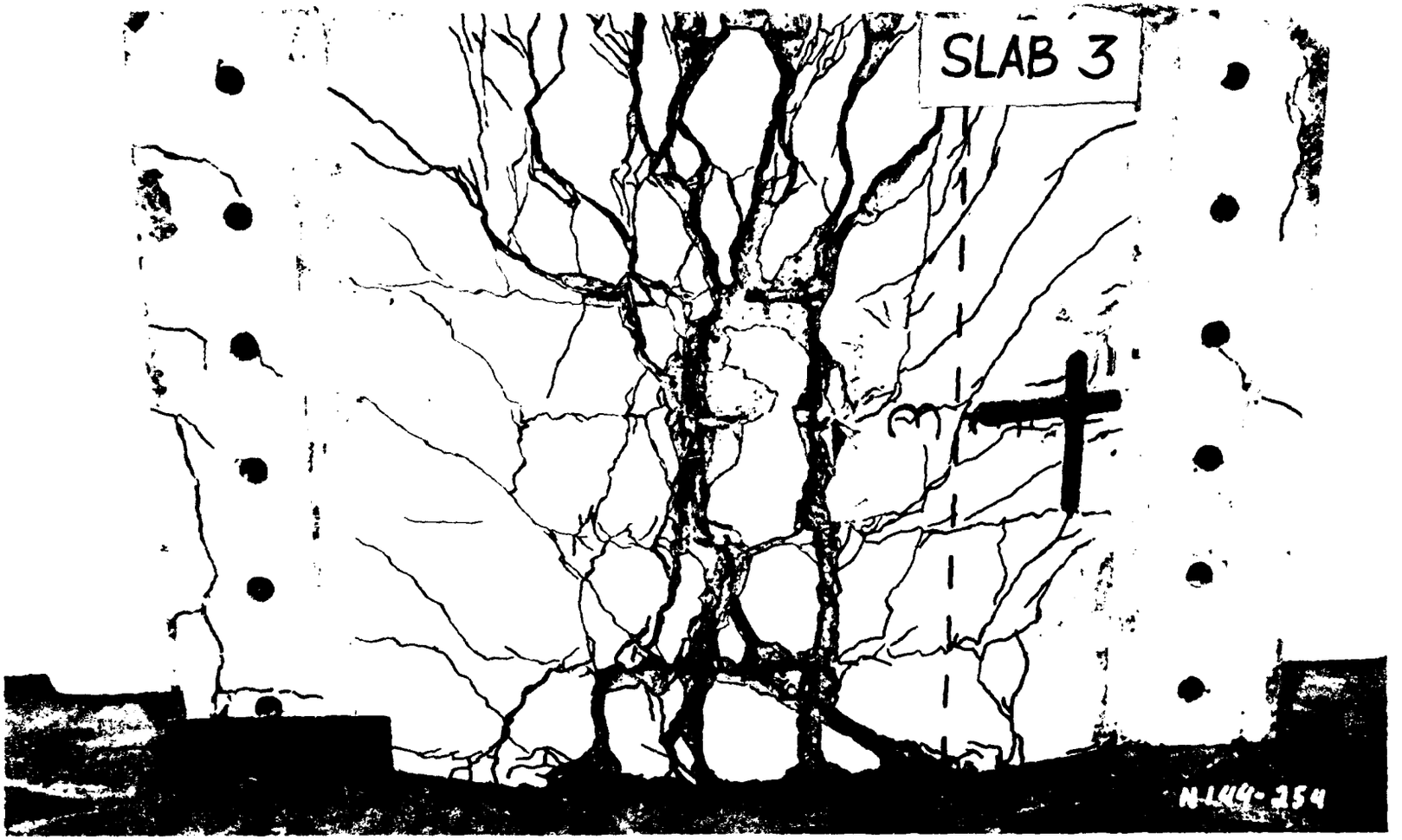
SLAB 3
N-LLL-254

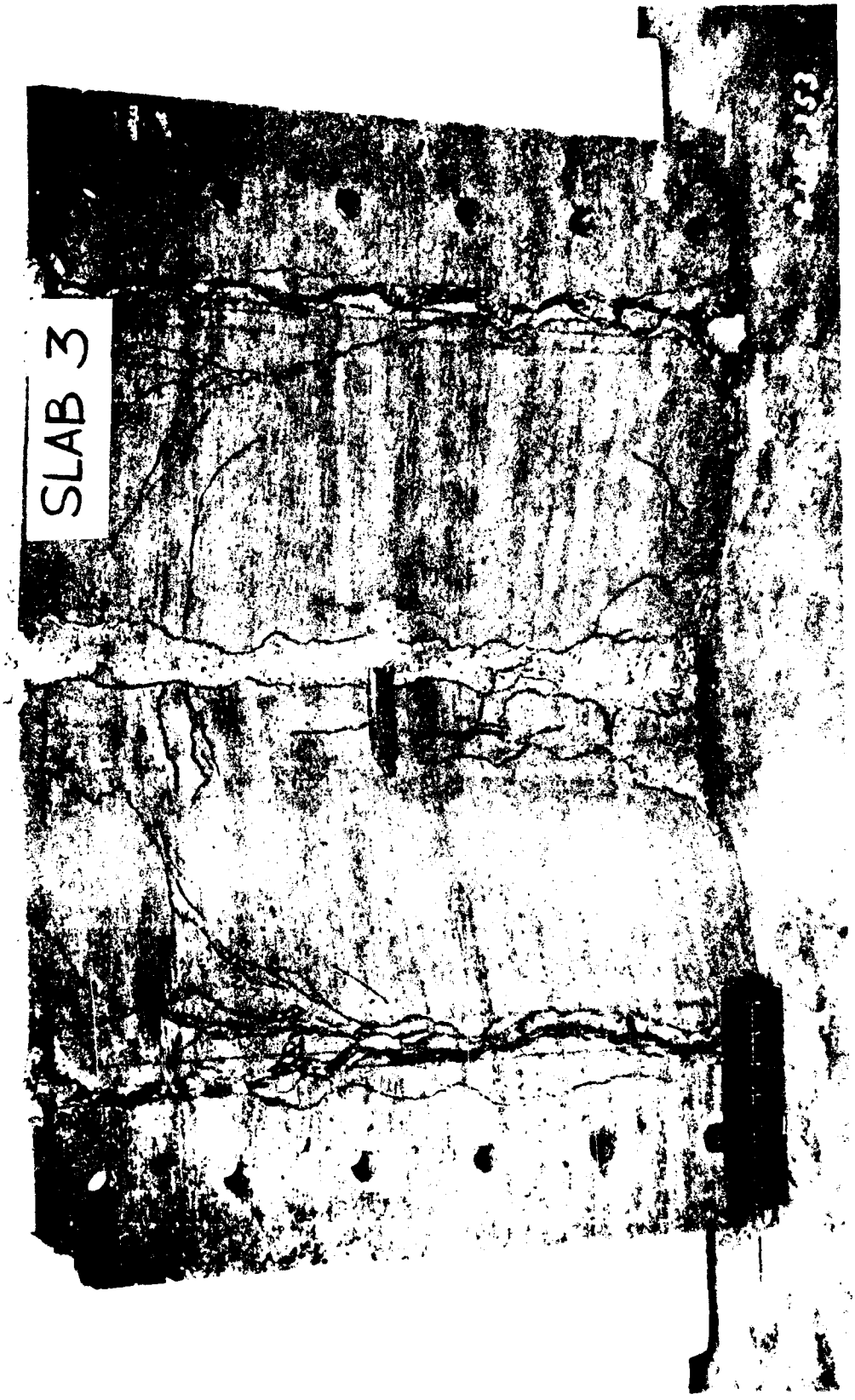
SLAB 3

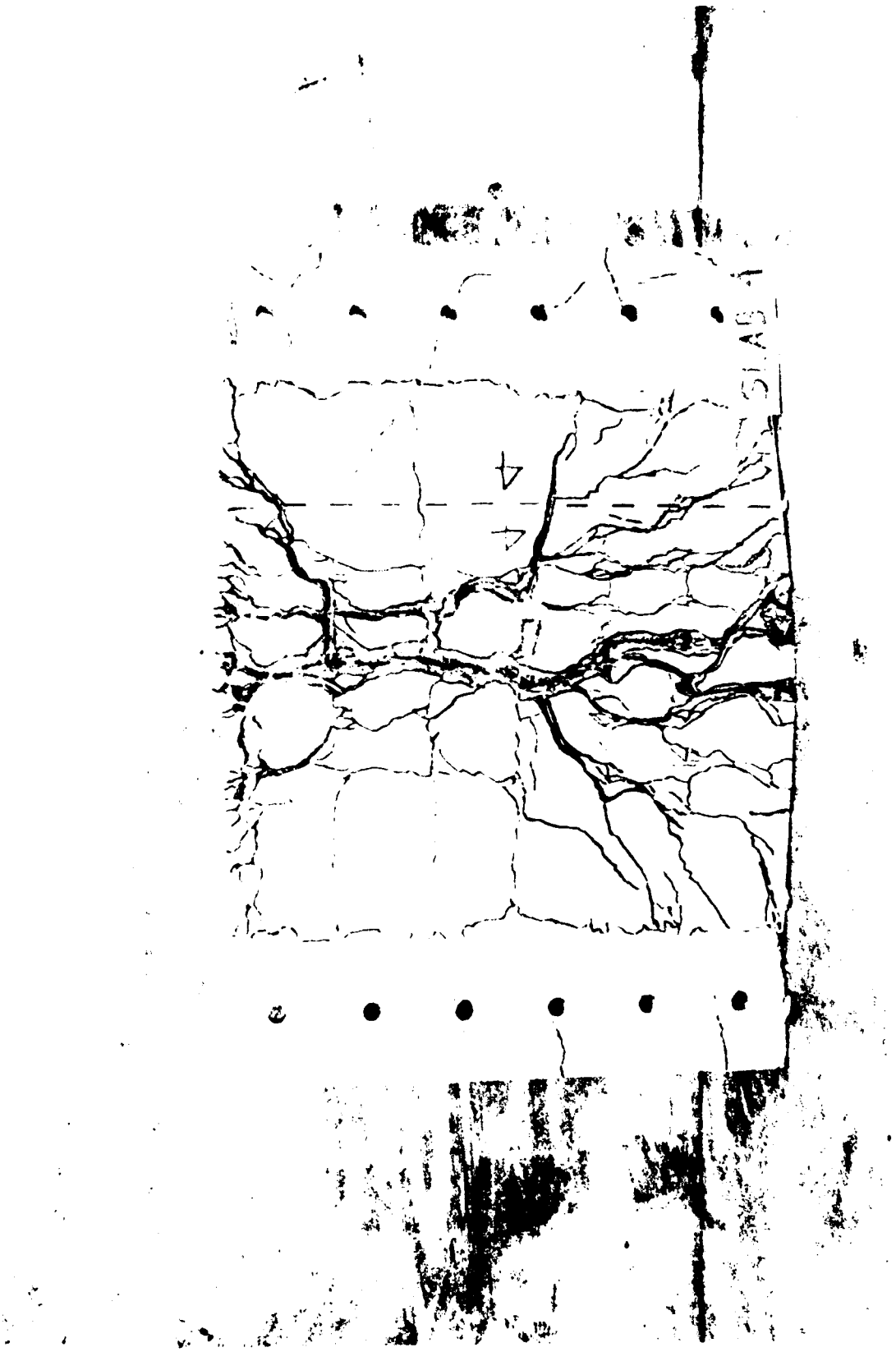
STA 8

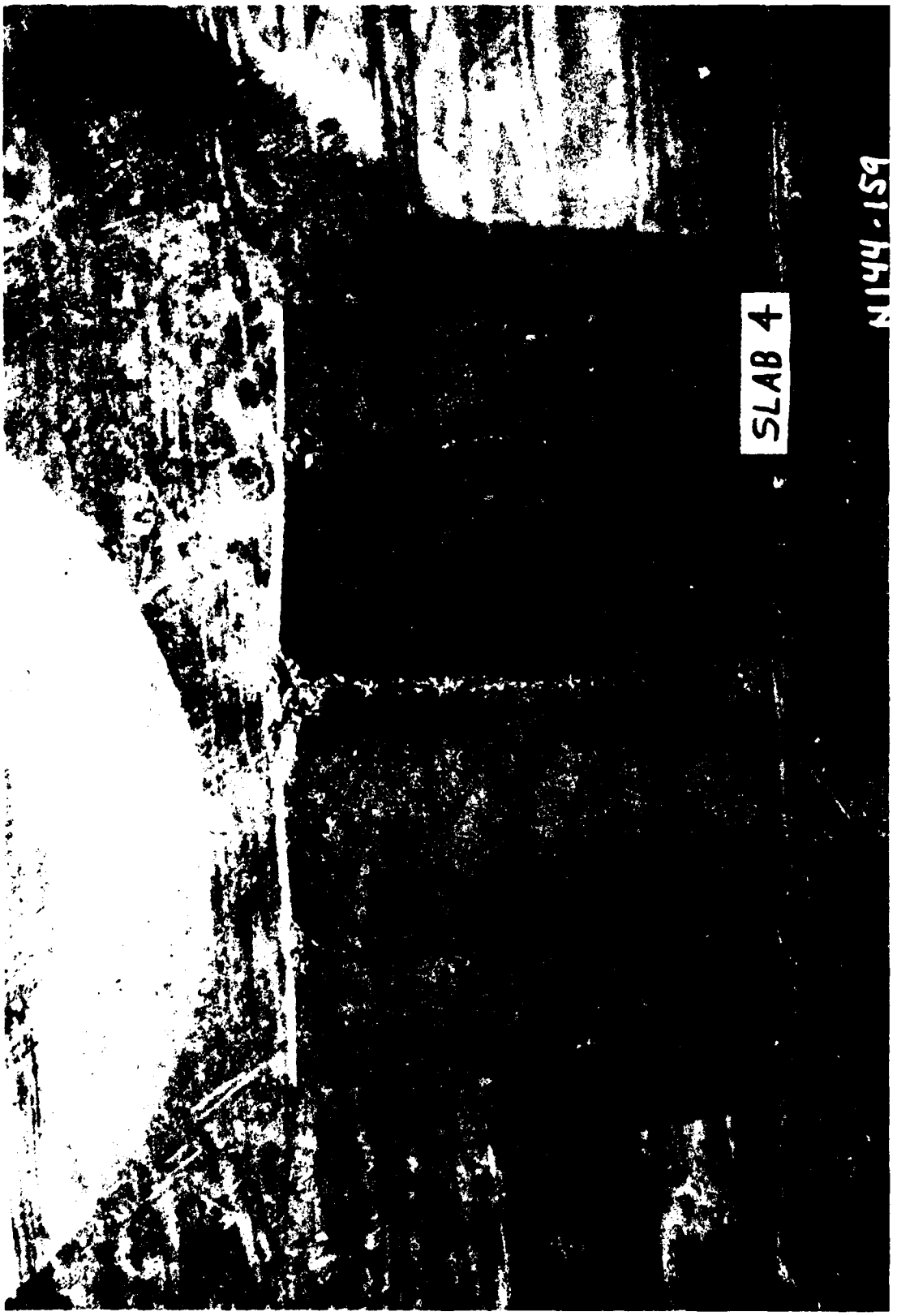
SLAB 4
N144-159

SLAB-A
A-A
A-A

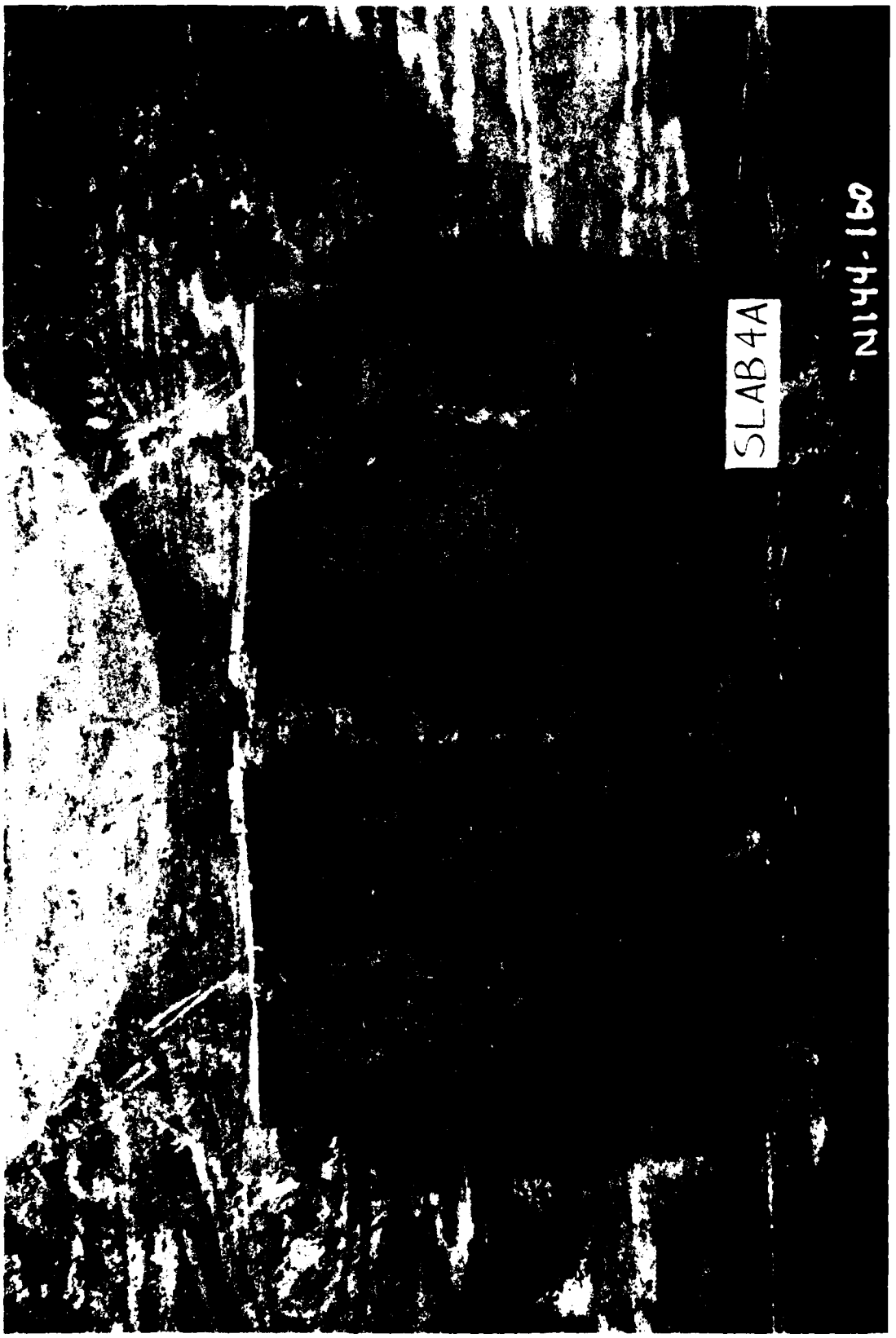
SLAB 4A
N144-169

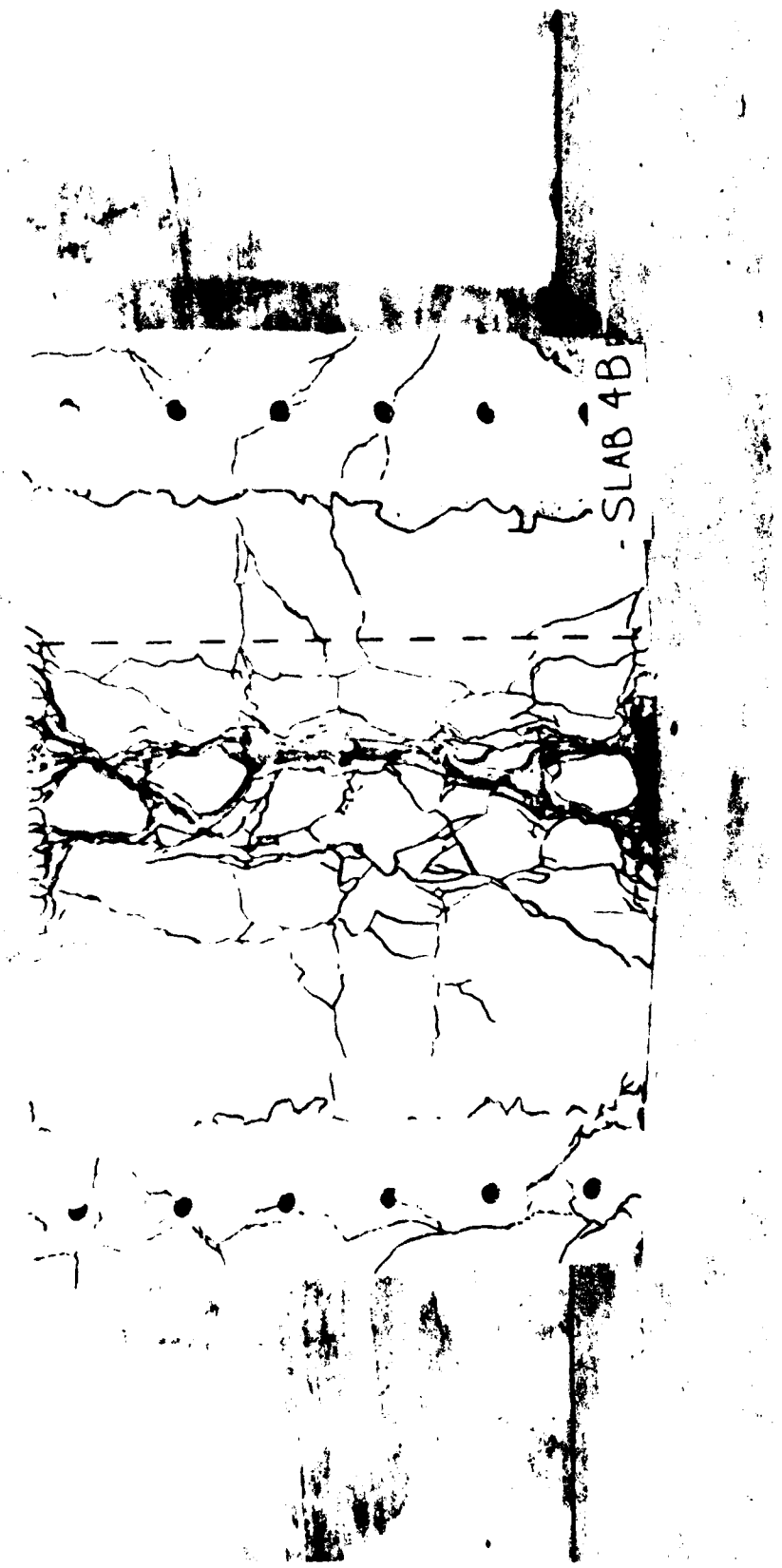
SLAB 4B

SLAB 4B

SLAB 5

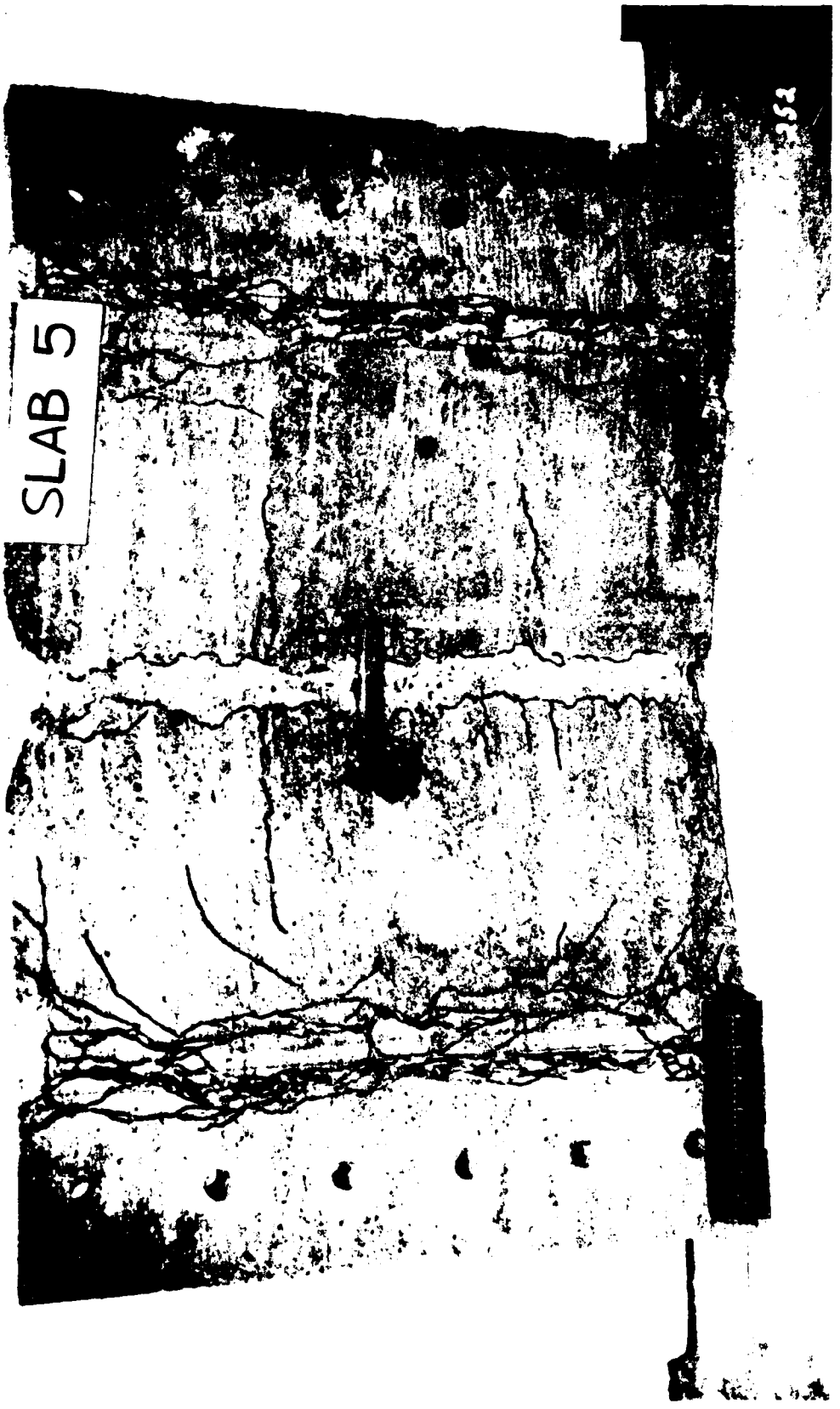
SLAB 5

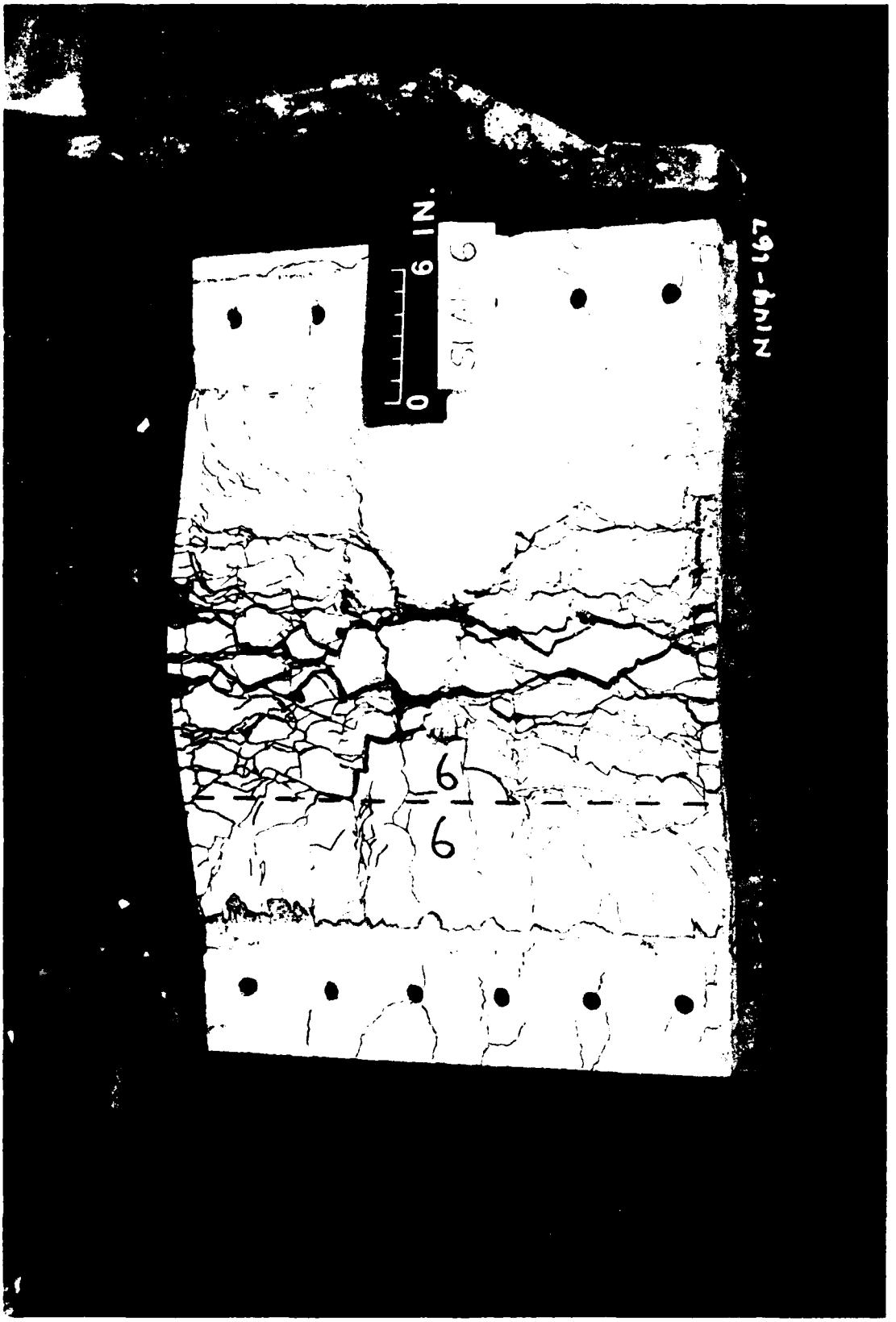
0
6 IN.
6
6


N1N4-169

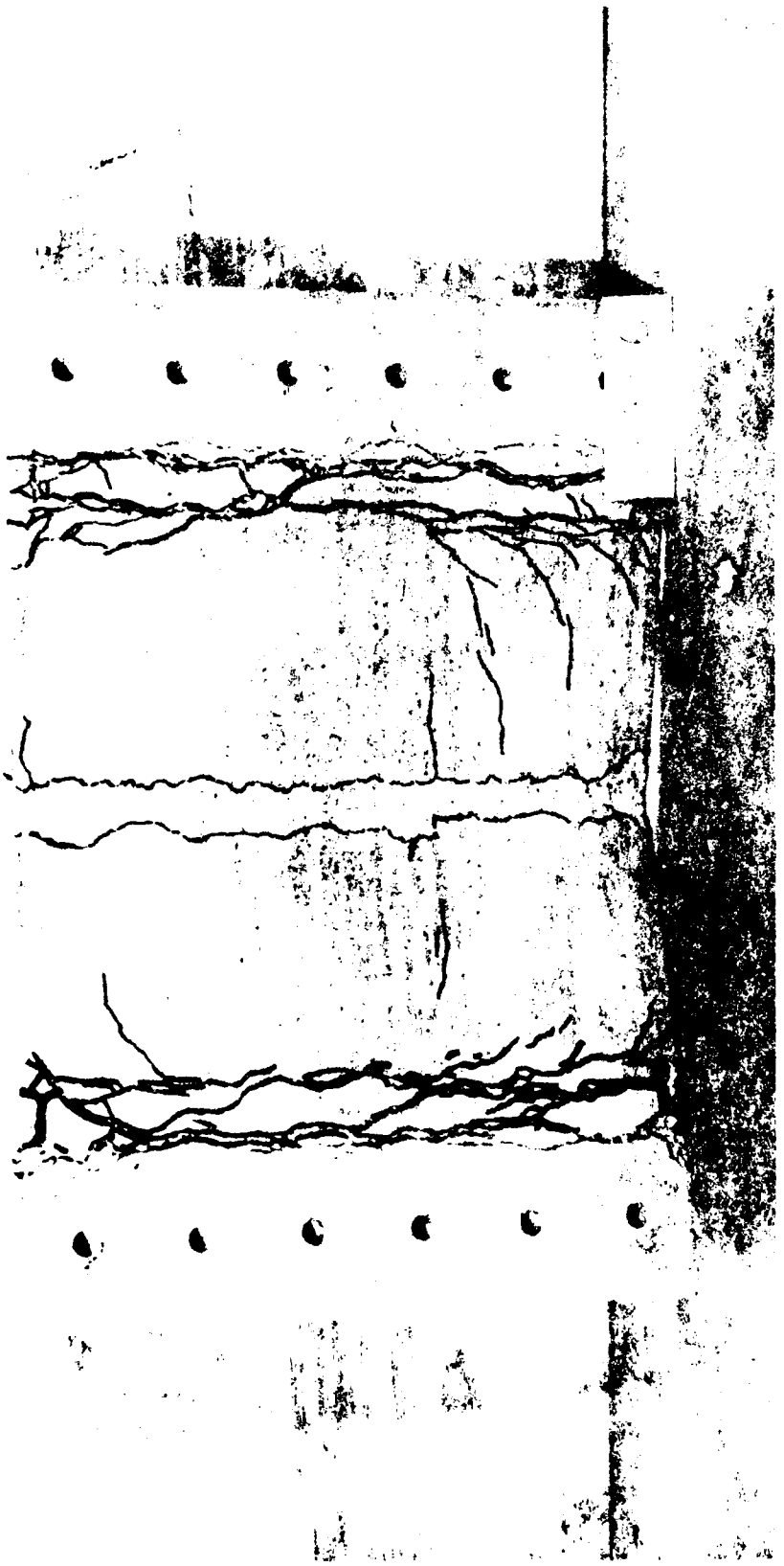

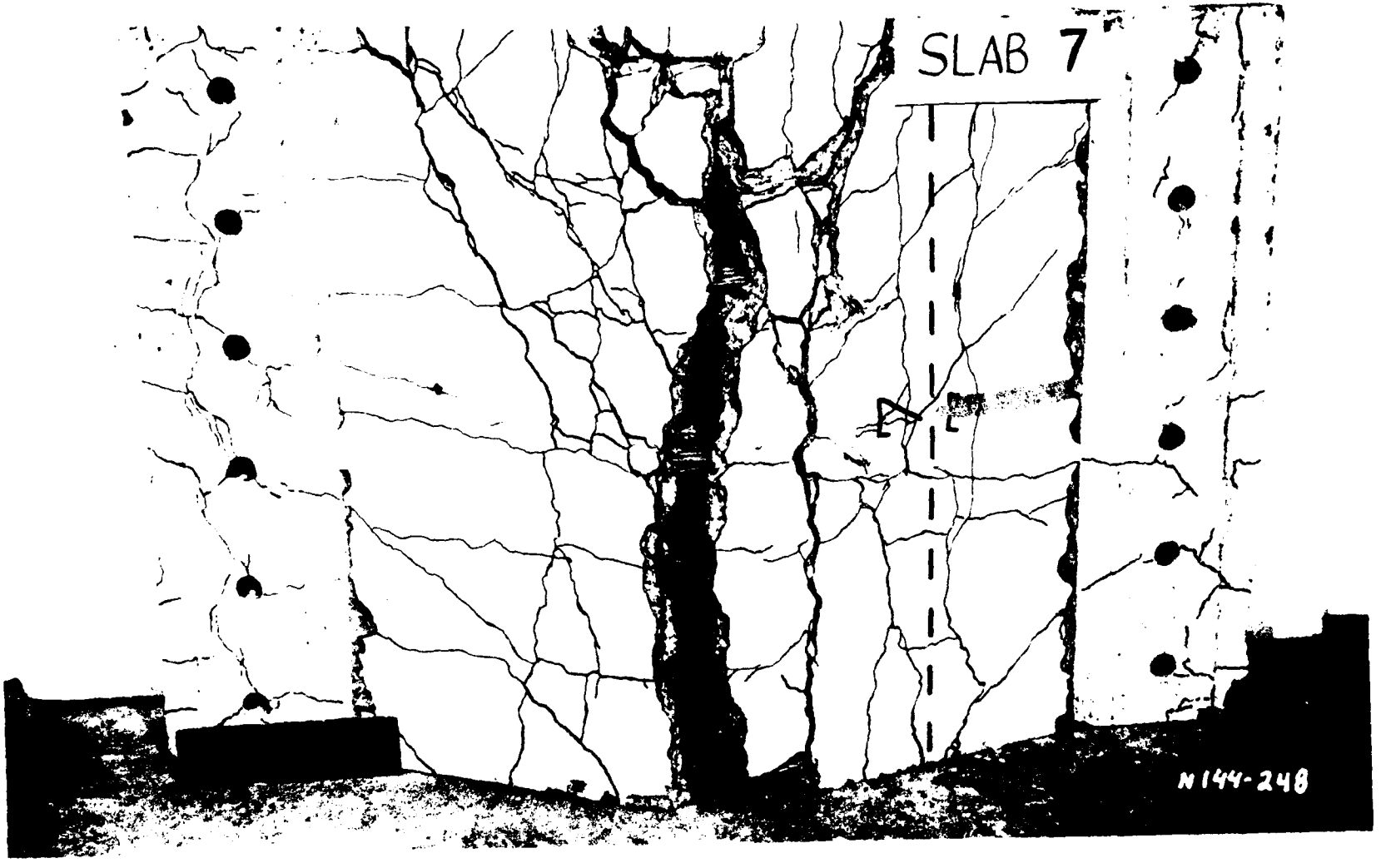
SLAB 7
N144-248

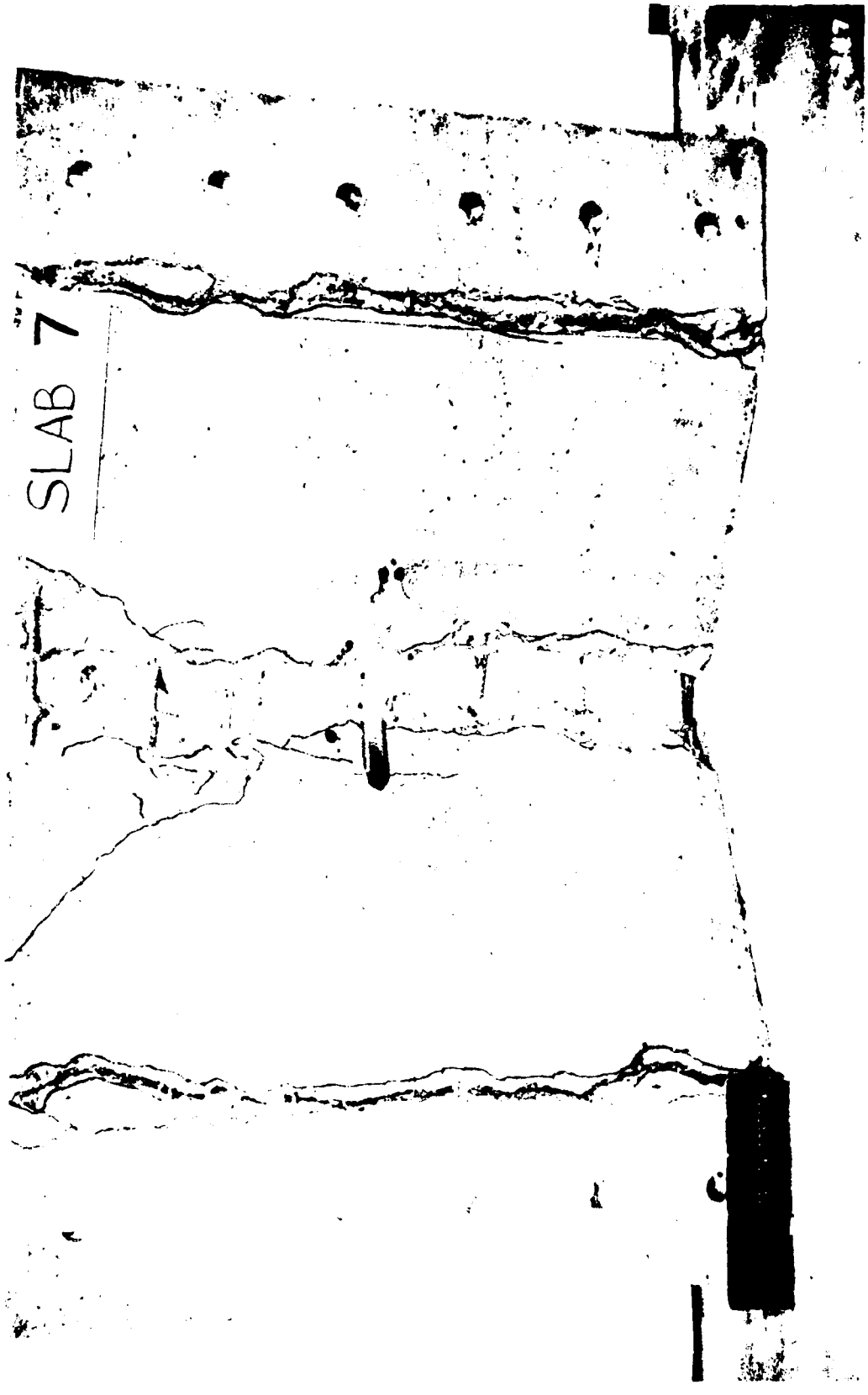
SLAB 7

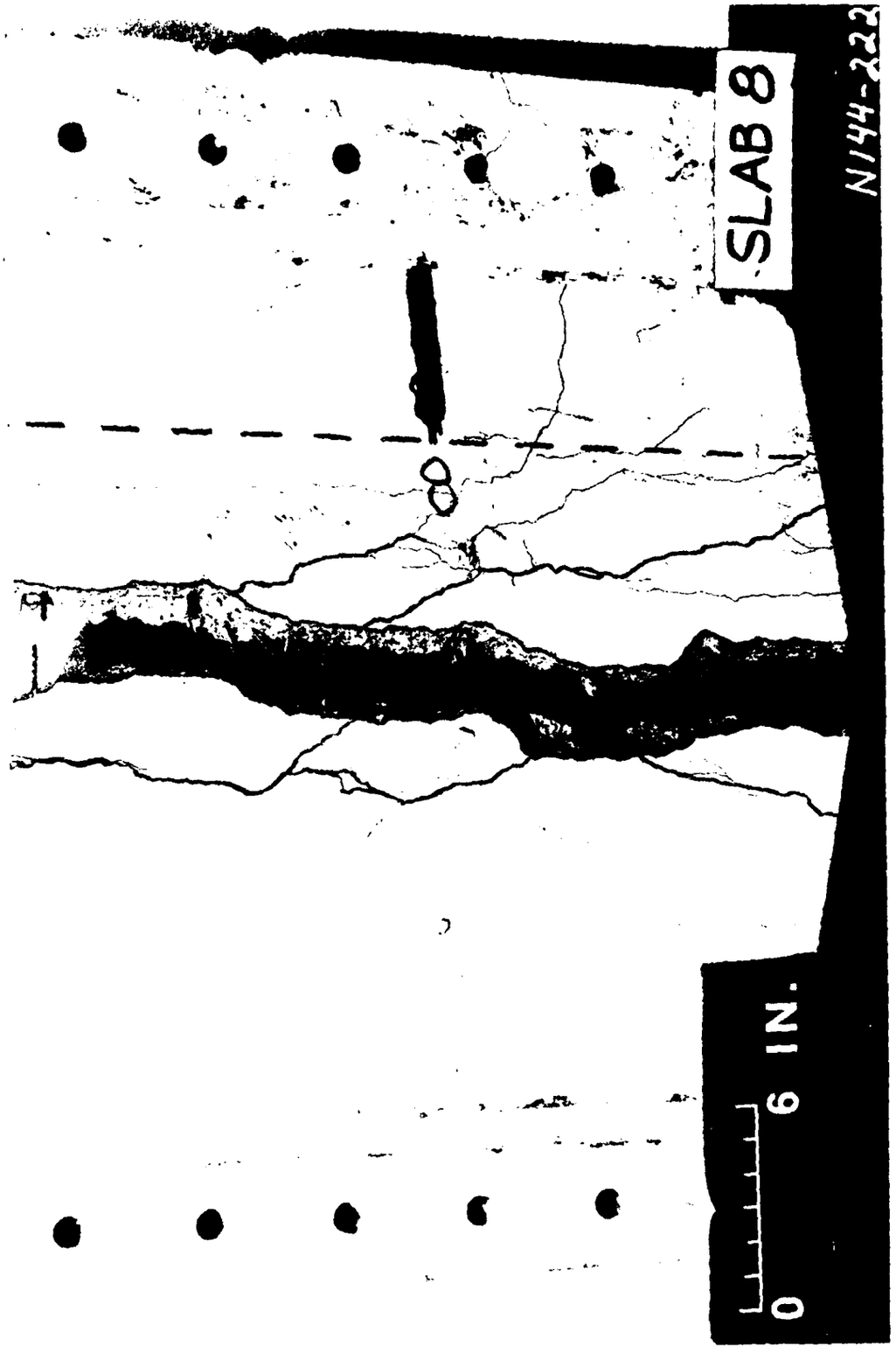
SLAB 8
N144-222
0
6 IN.

SLAB 8
0
6 IN.

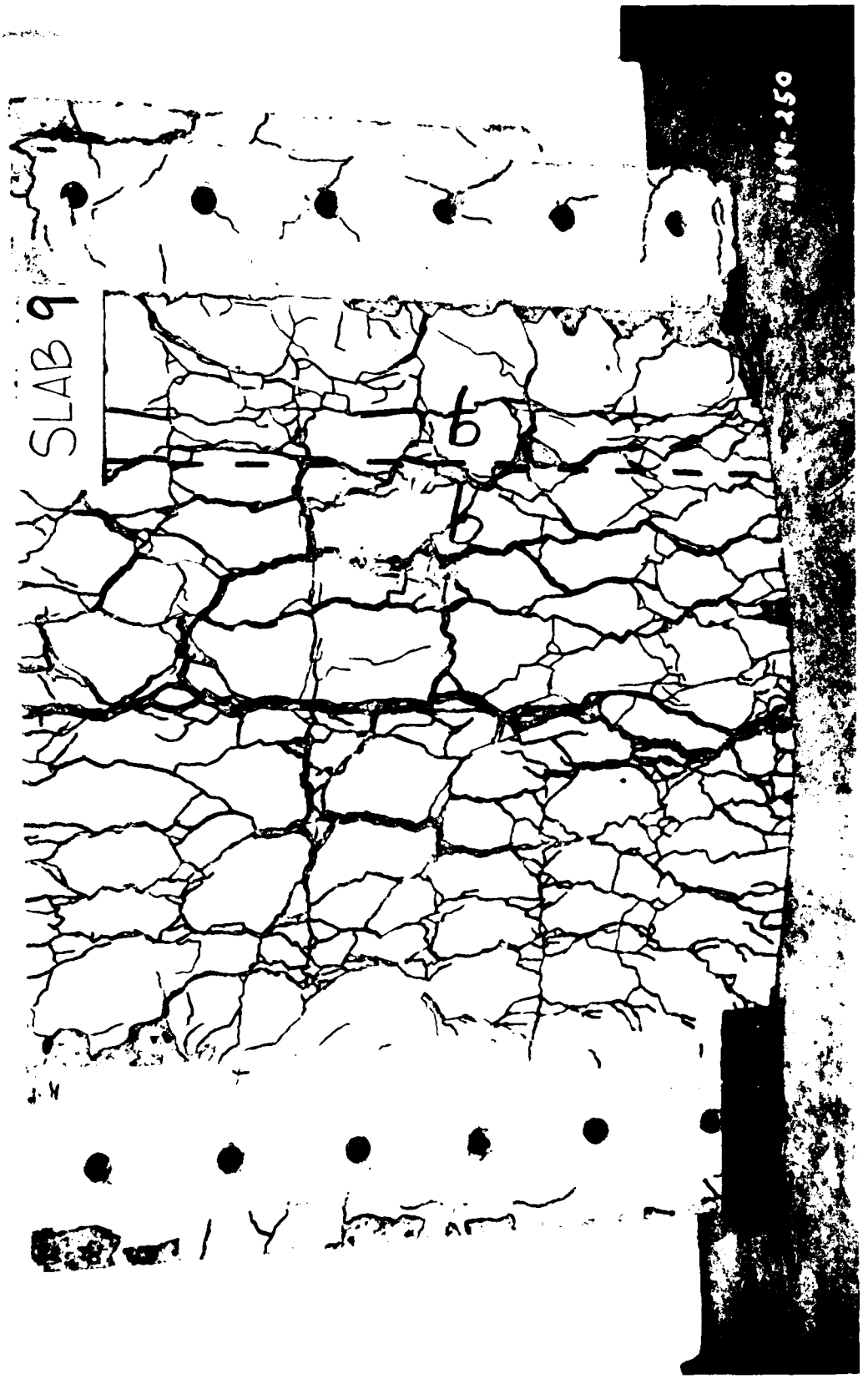
SLAB 9
b
b

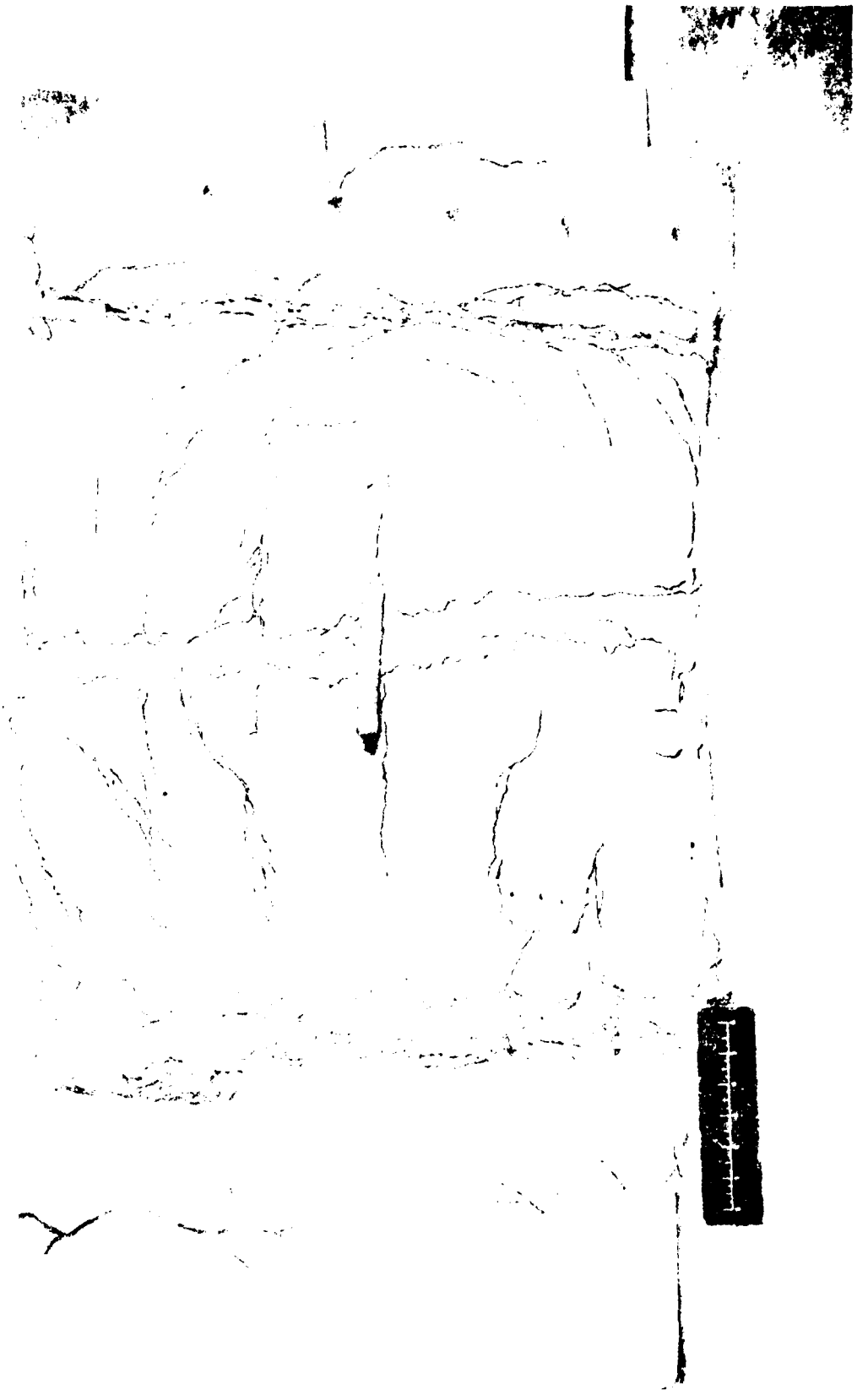

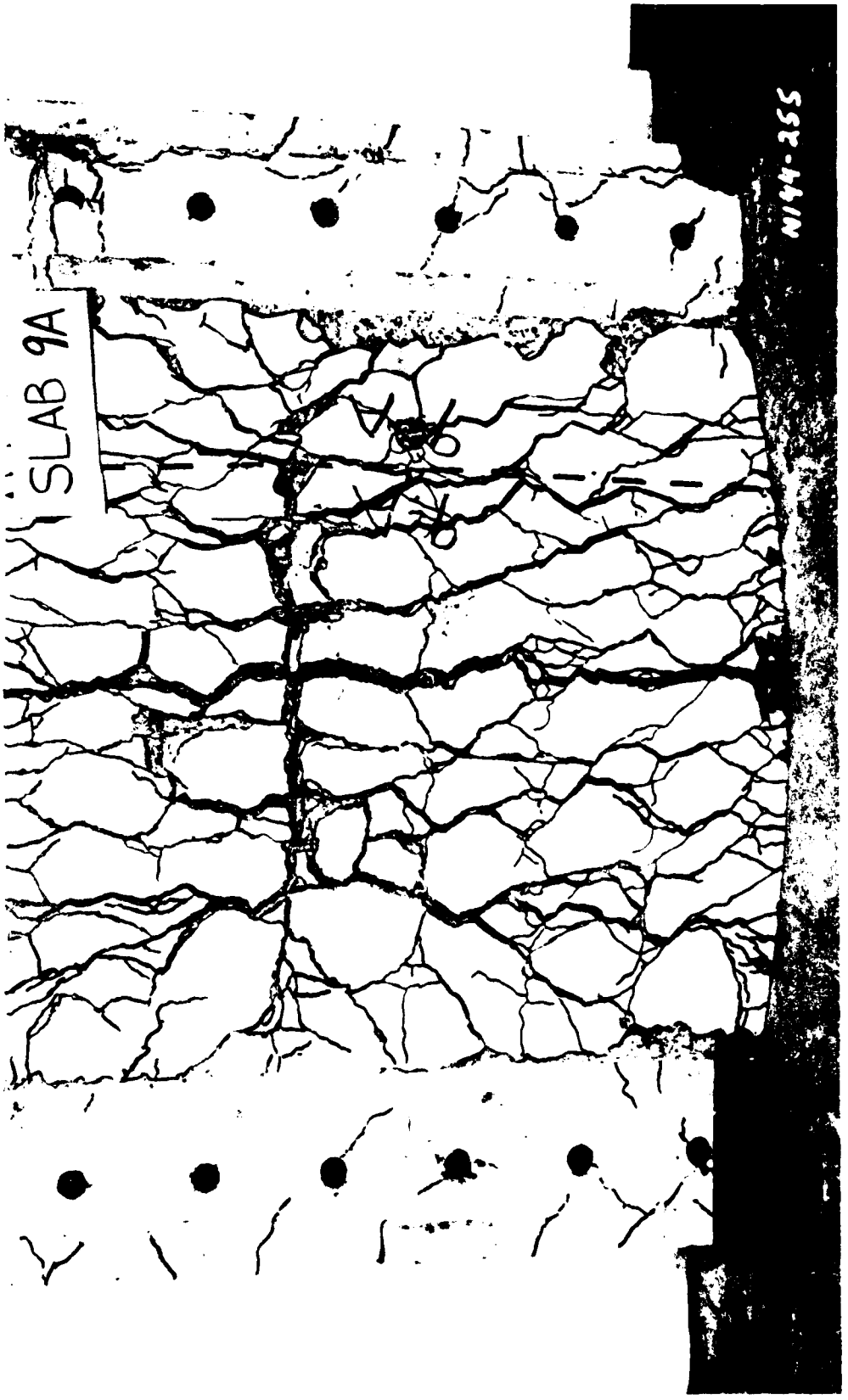
SLAB 9A

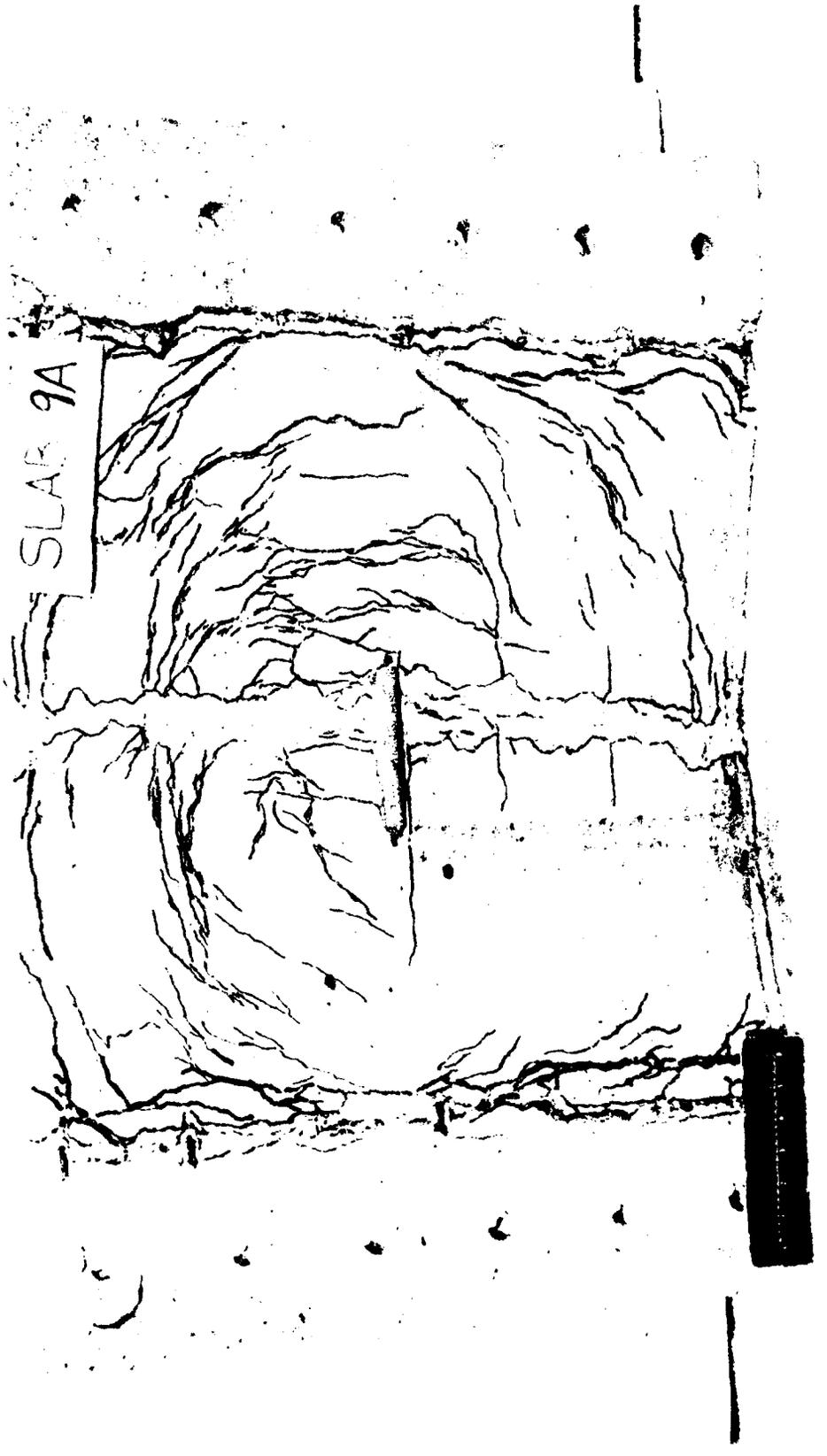
SLAR 9A

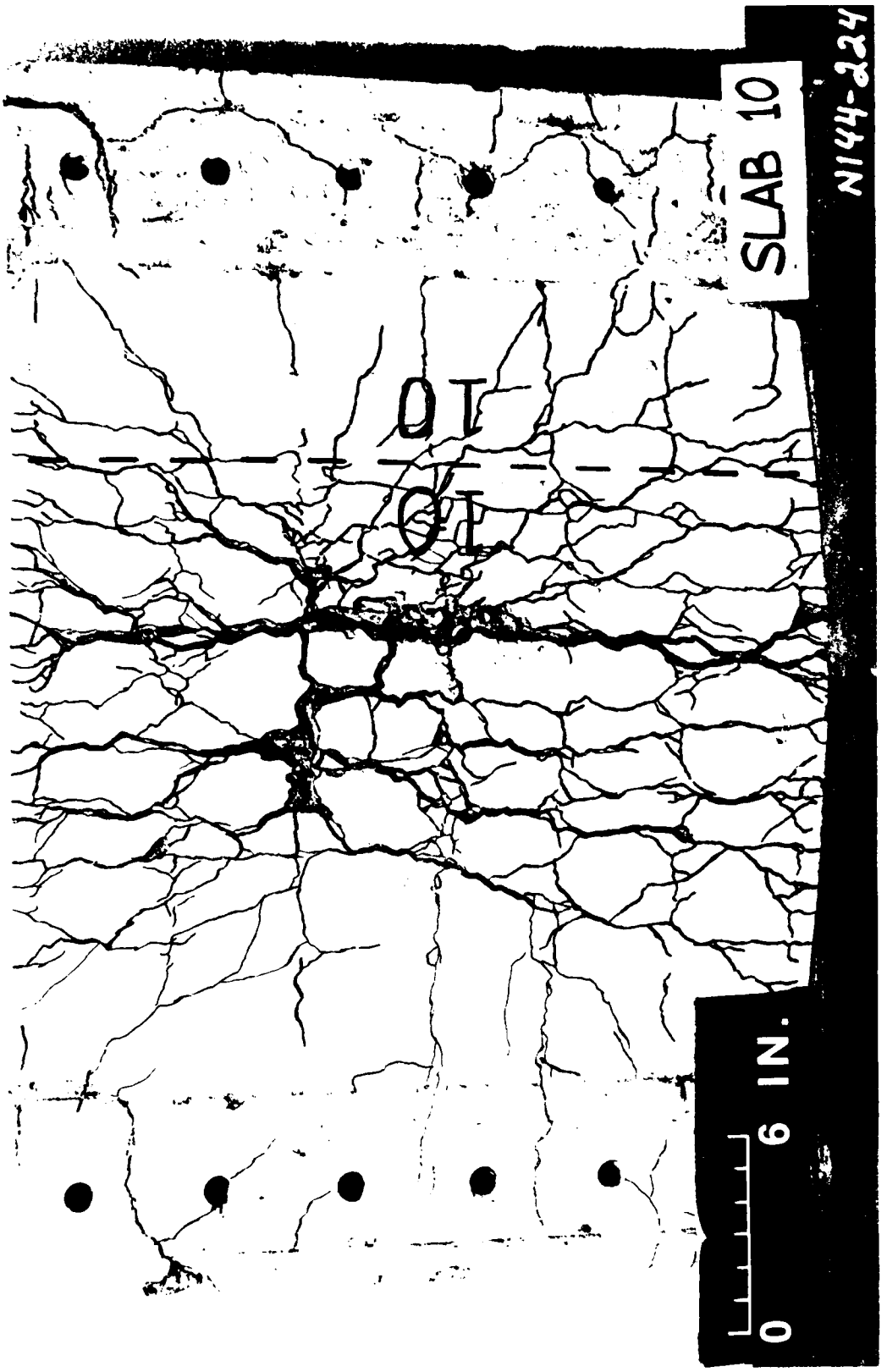
SLAB 10
N14-424
0
6 IN.

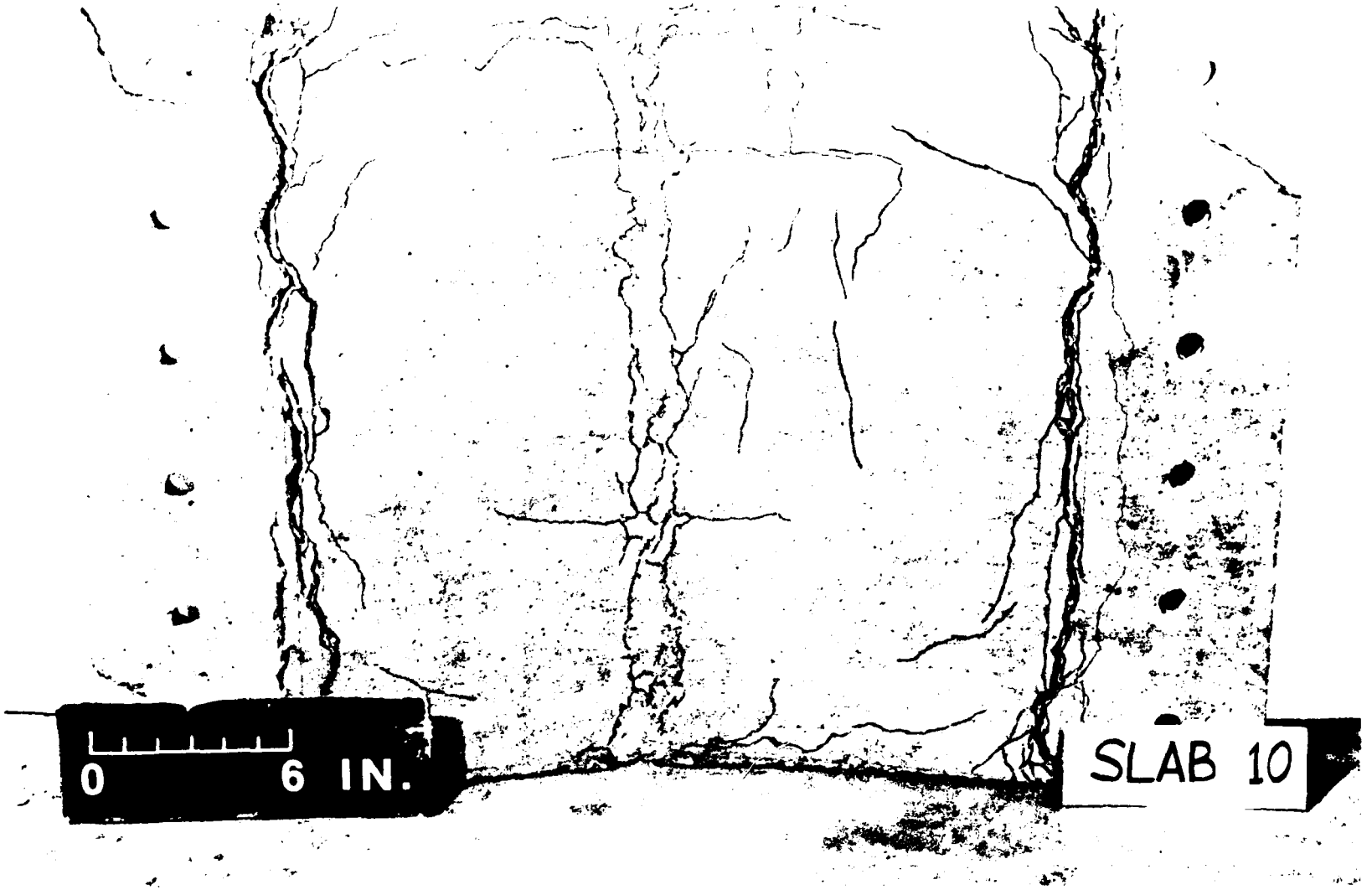
0
6 IN.
SLAB 10

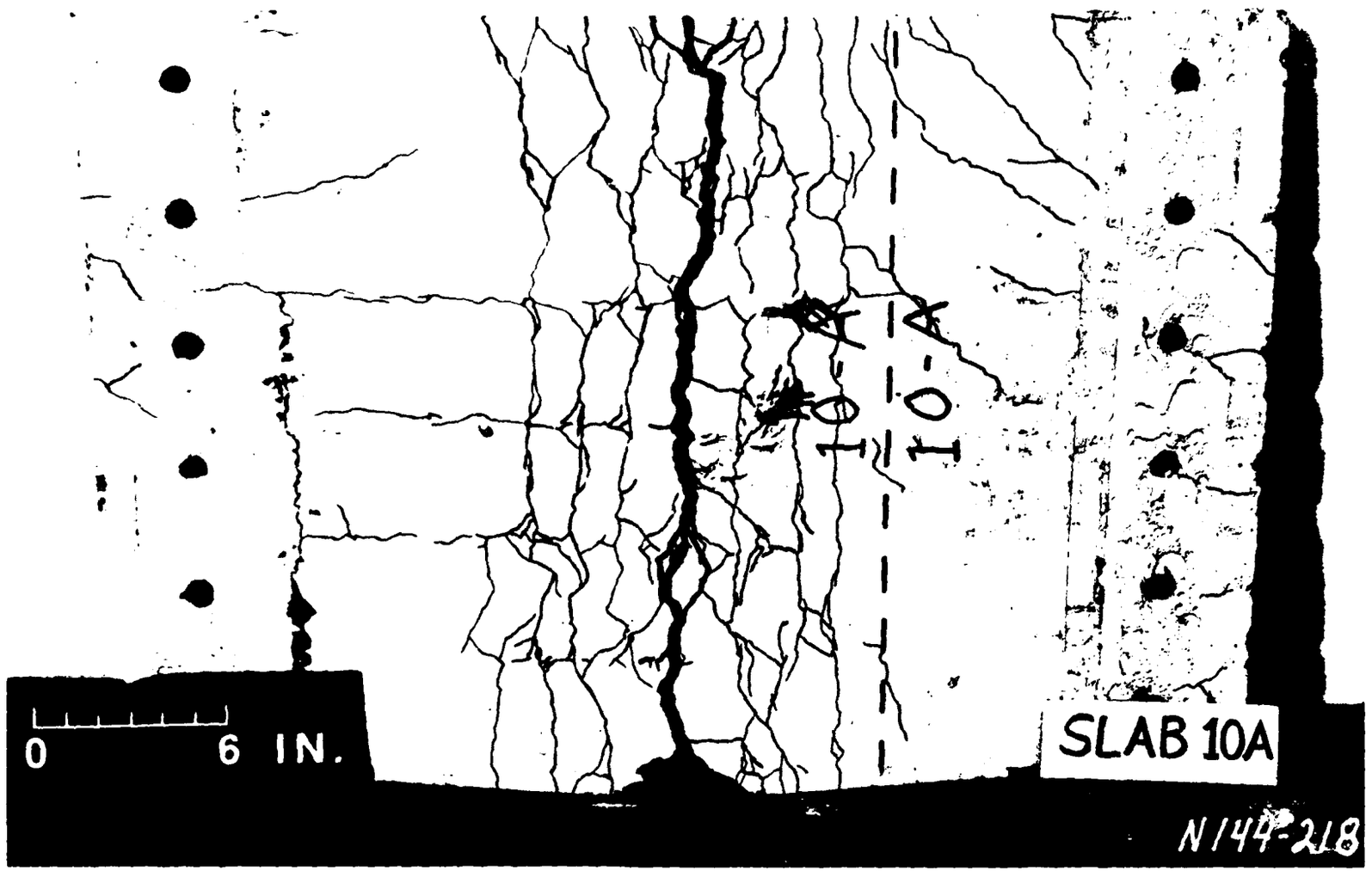
10-4
10-1
0
6 IN.
SLAB 10A
N144-218

SLAB 10A
6 IN.

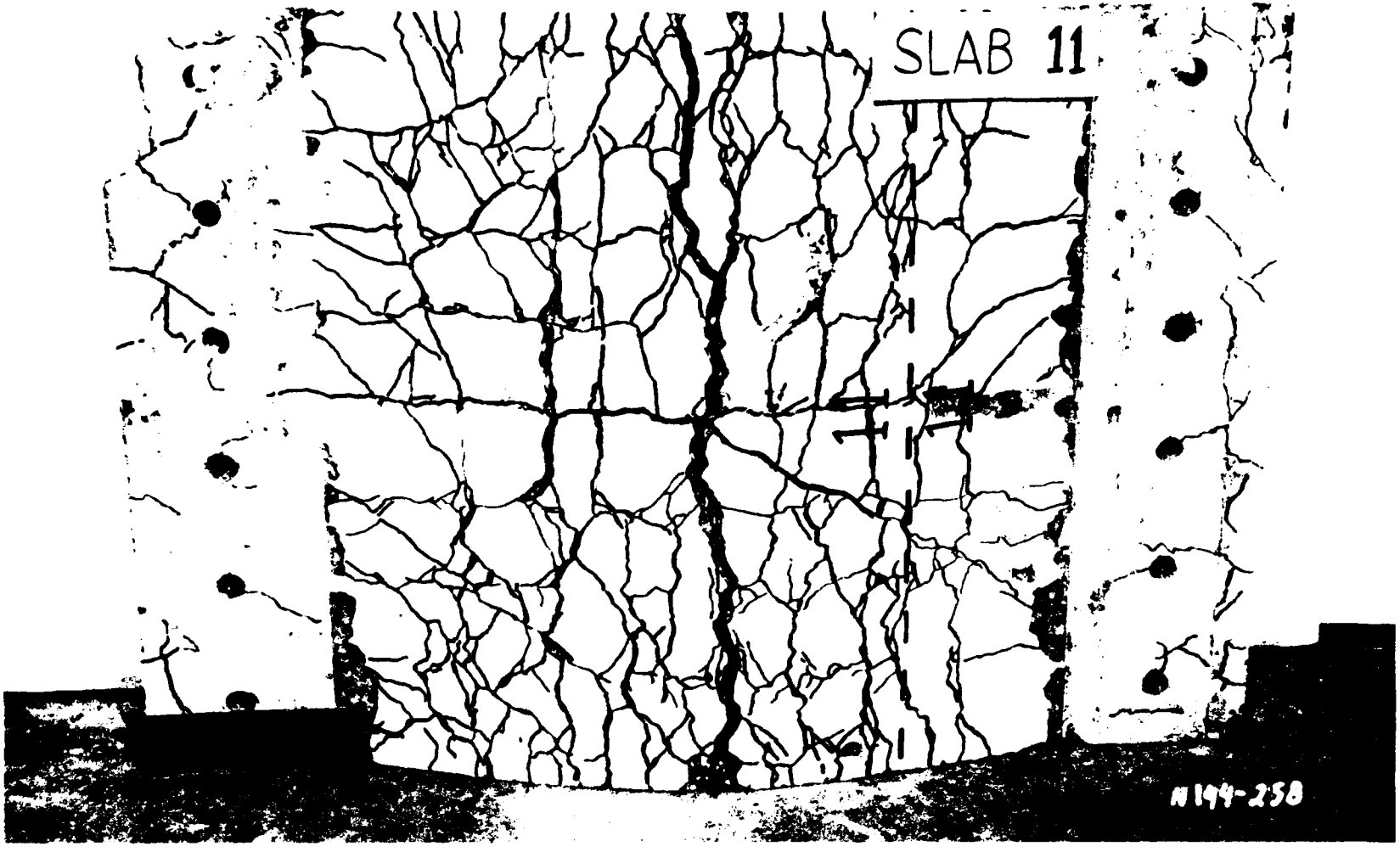
SLAB 11
N199-250

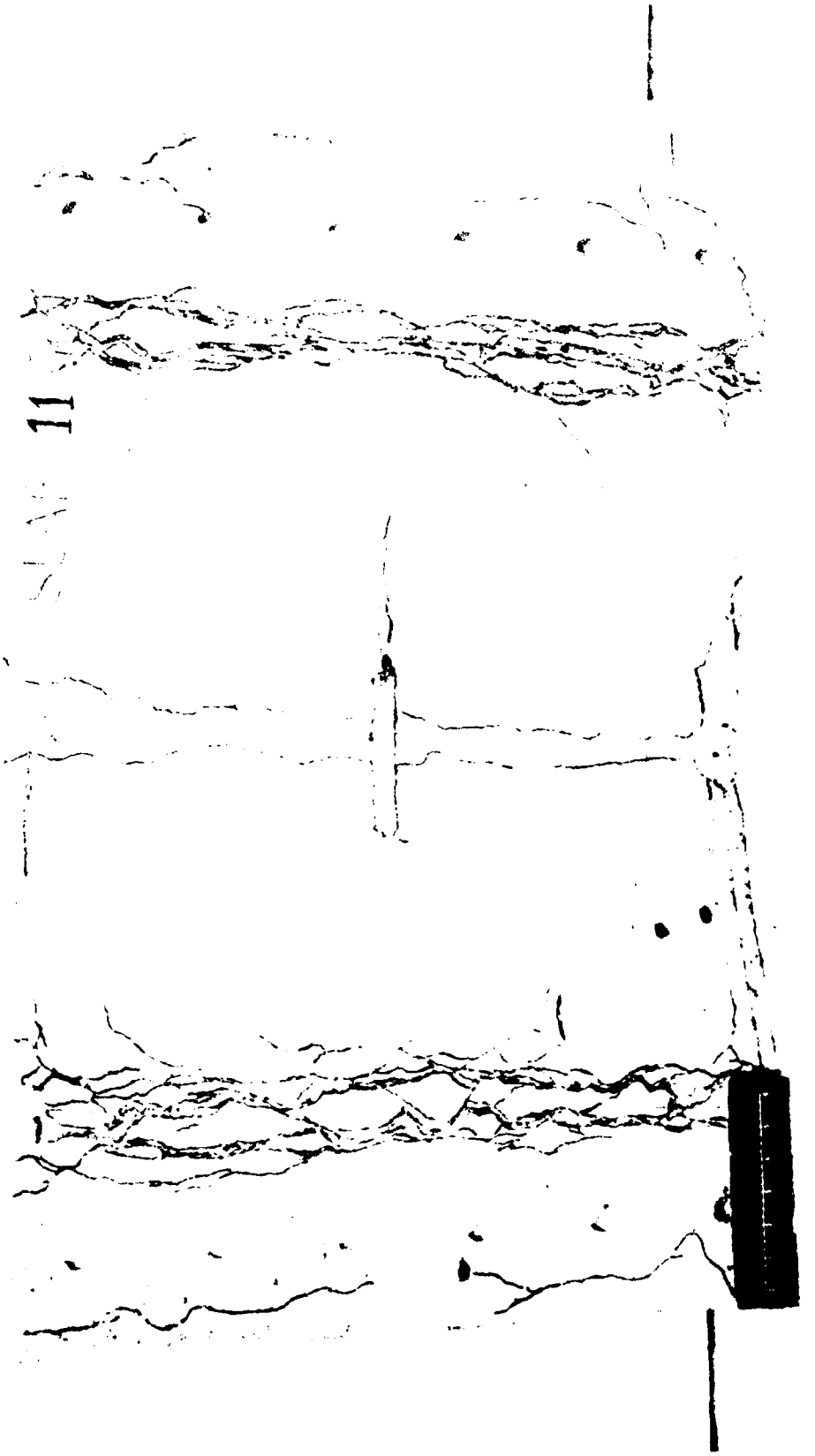

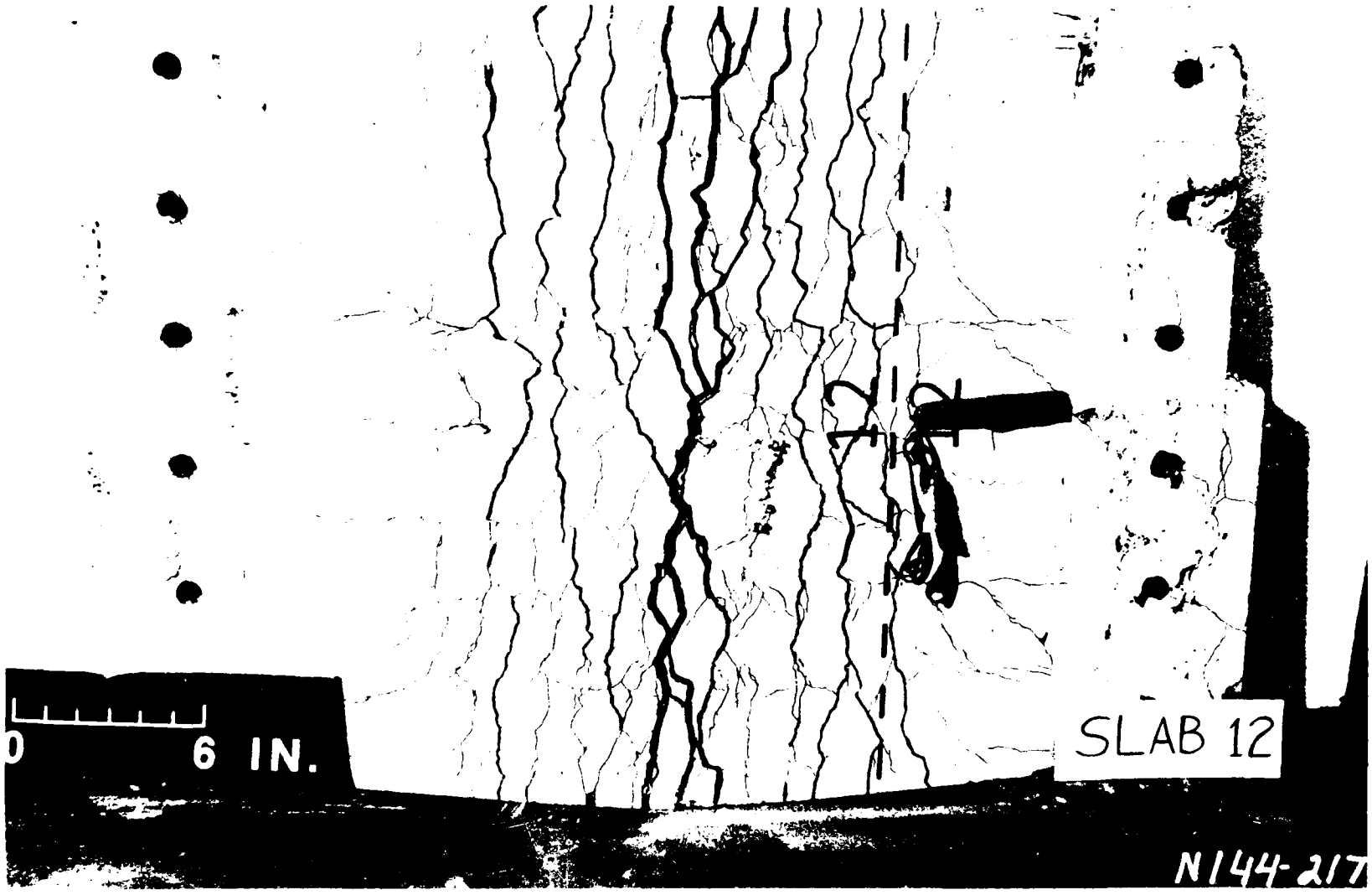
0
6 IN.
SLAB 12
N144-217

SLAB 12
6 IN.

APPENDIX C

EXPERIMENTAL DATA

SLAB RESTRAINT G1

SLAB RESTRAINT G1
D-1

10462 1
09/25/84 R0709

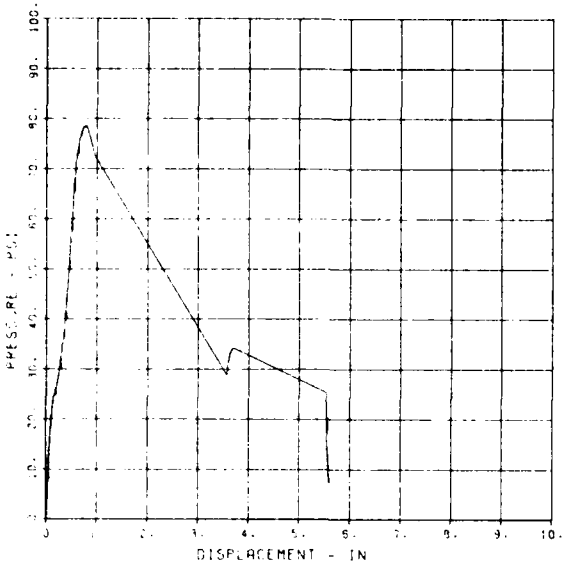

SLAB RESTRAINT G1
D-2

10462 1
09/25/84 R0709

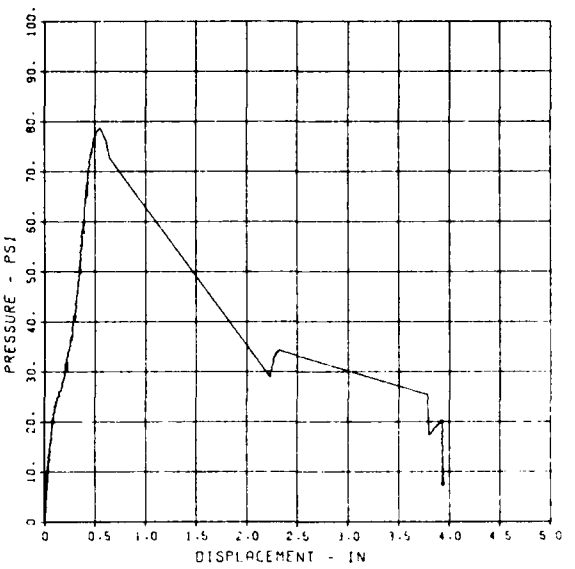

SLAB RESTRAINT G1
D-3

10462 1
09/25/84 R0709

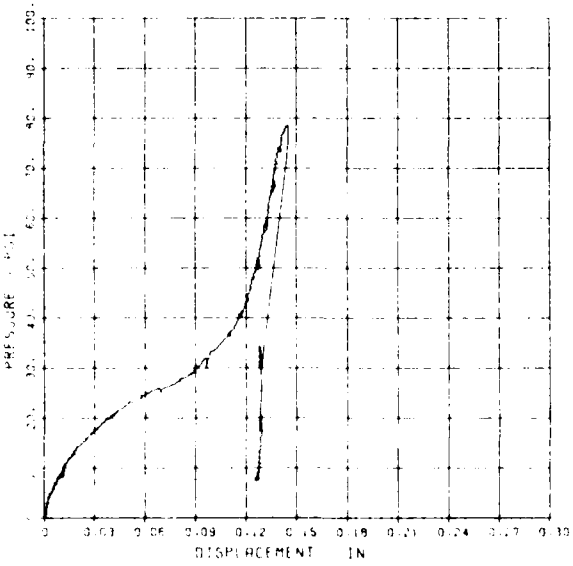

SLAB RESTRAINT G1
D-4

10462 1
09/25/84 R0709

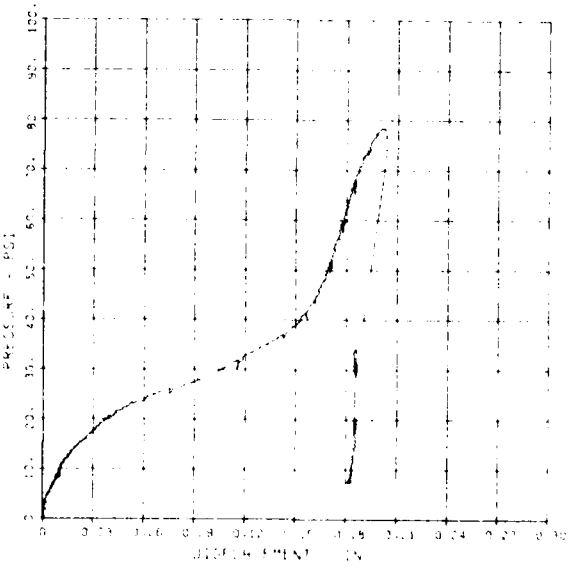

SLAB RESTRAINT 01
LW-1

10462 1
09/25/84 R0709

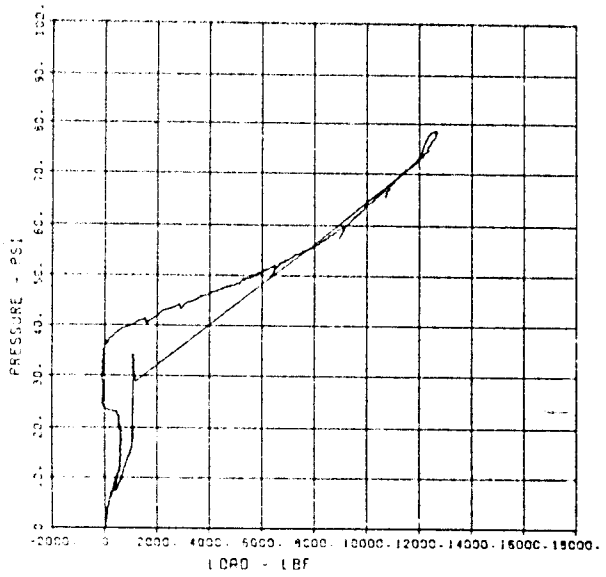

SLAB RESTRAINT 01
LW-2

10462 1
09/25/84 R0709

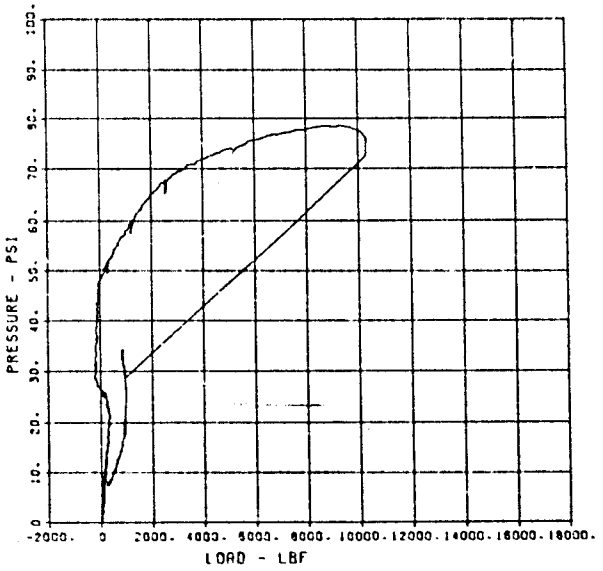

SLAB RESTRAINT G1
LW-3

10462 1
09/25/84 R0709

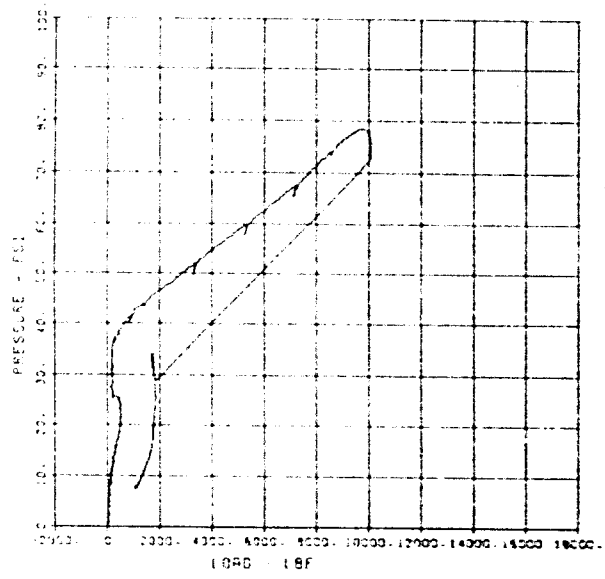

SLAB RESTRAINT G1
LW-4

10462 1
09/25/84 R0709

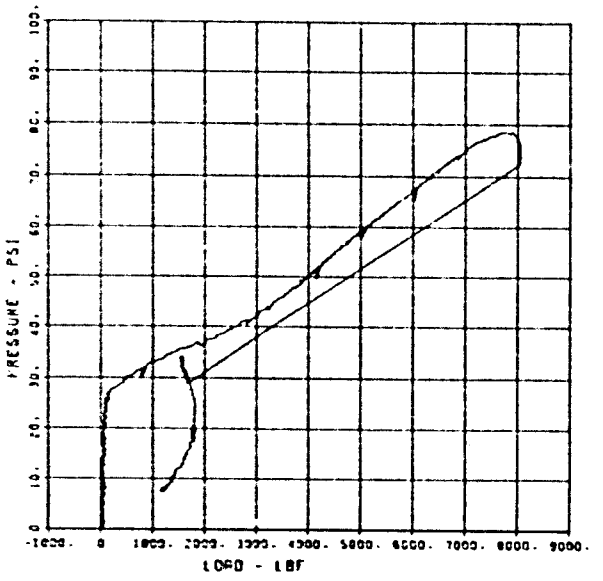

SLAB RESTRAINT GI
LW-5

10462 1
09/25/84 R0709

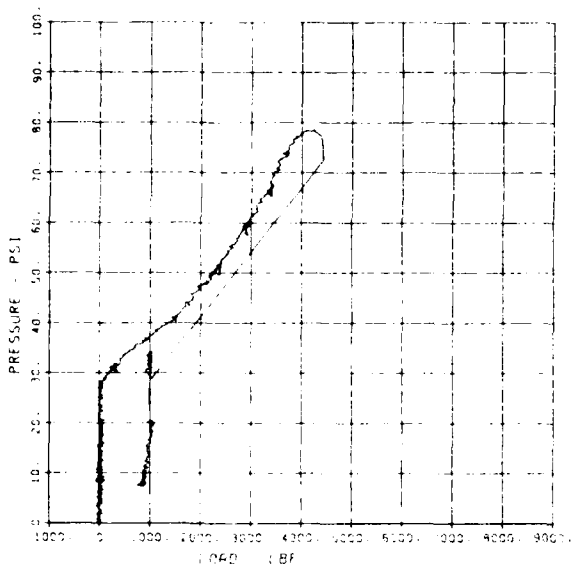

SLAB RESTRAINT GI
LW-6

10462 1
09/25/84 R0709

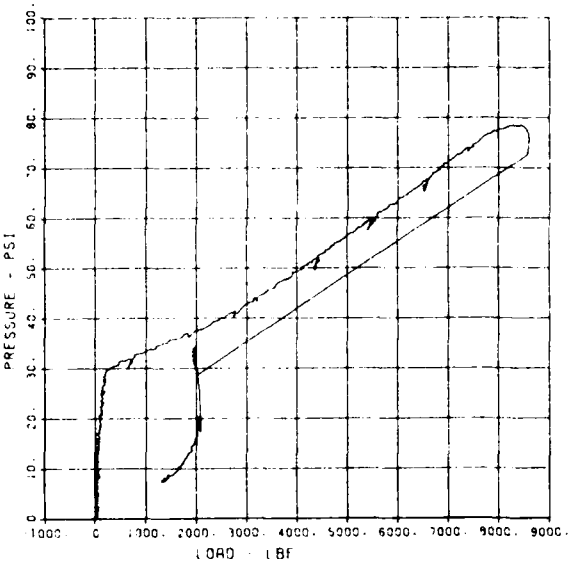

SLAB RESTRAINT GI
LW-7

10462 1
09/25/84 R0709

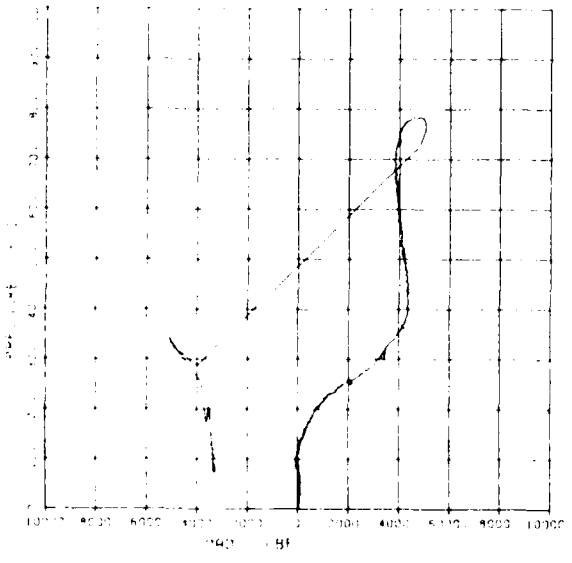

SLAB RESTRAINT GI
LW-8

10462 1
09/25/84 R0709

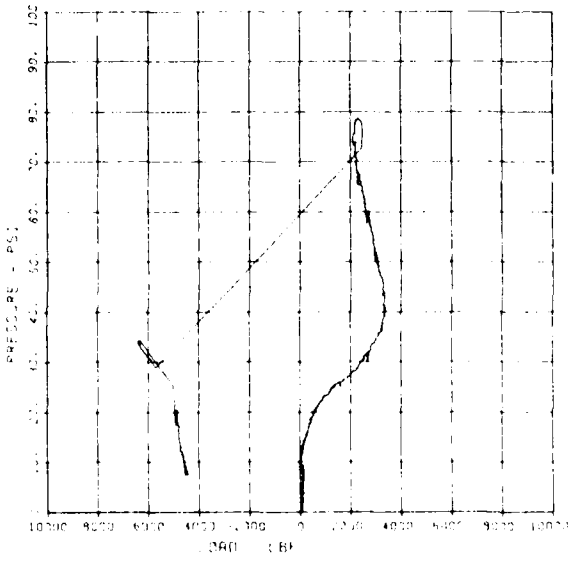

SLAB RESTRAINT G1
LW-9

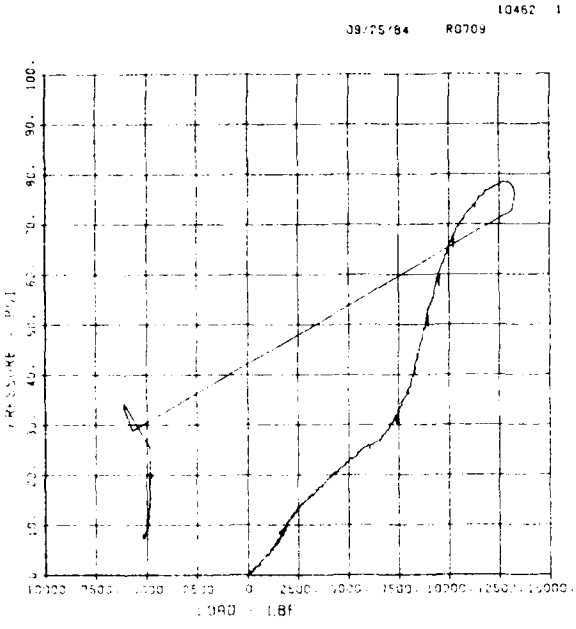

SLAB RESTRAINT G1
LW-10

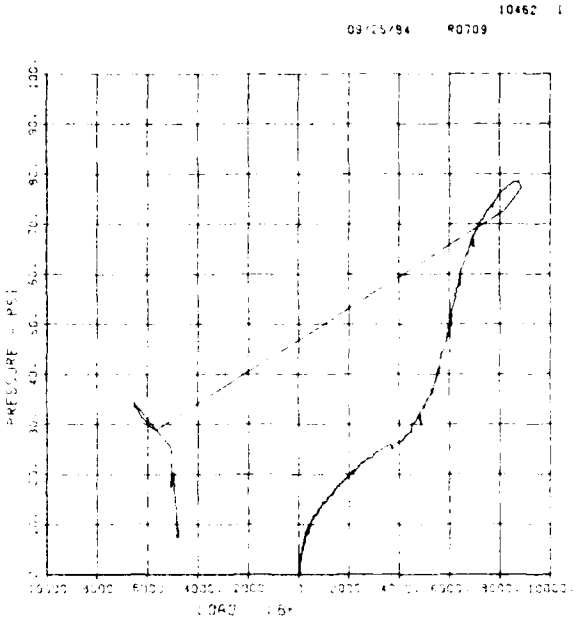

SLAB RESTRAINT G1
LW-11

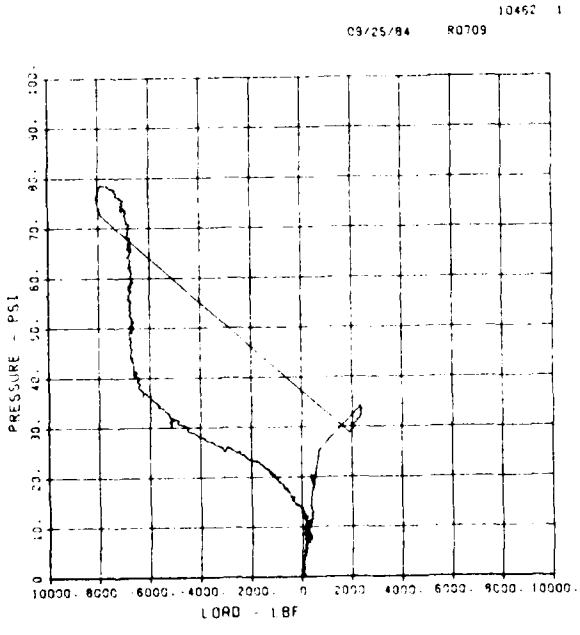

SLAB RESTRAINT G1
LW-13

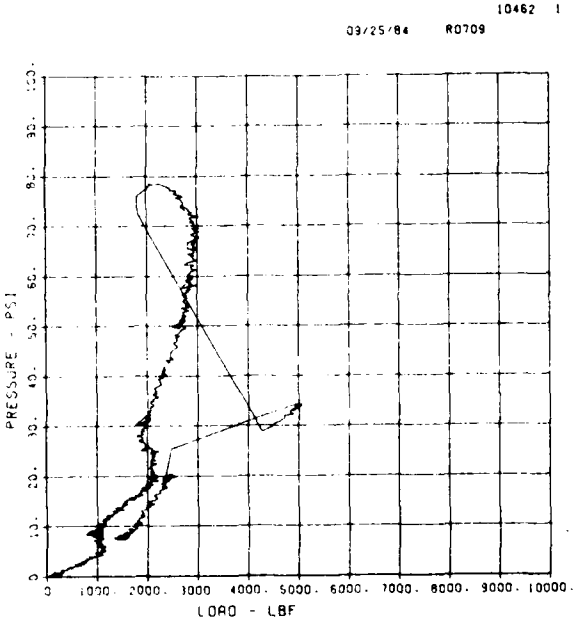

SLAB RESTRAINT G1
LW-14

10462 1
09/25/84 R0709

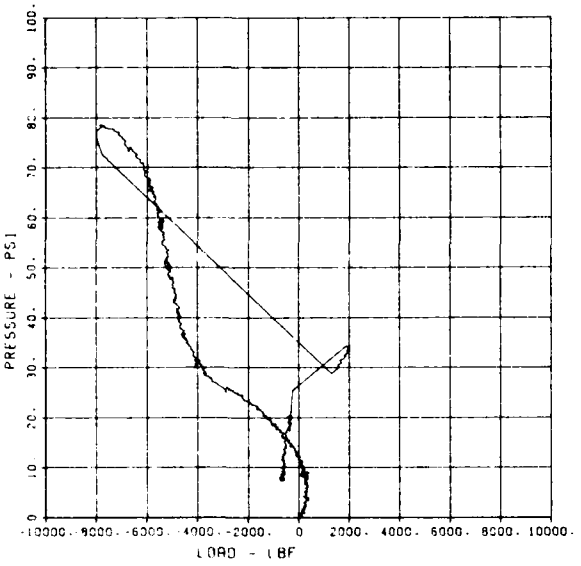

SLAB RESTRAINT G1
LW-15

10462 1
09/25/84 R0709

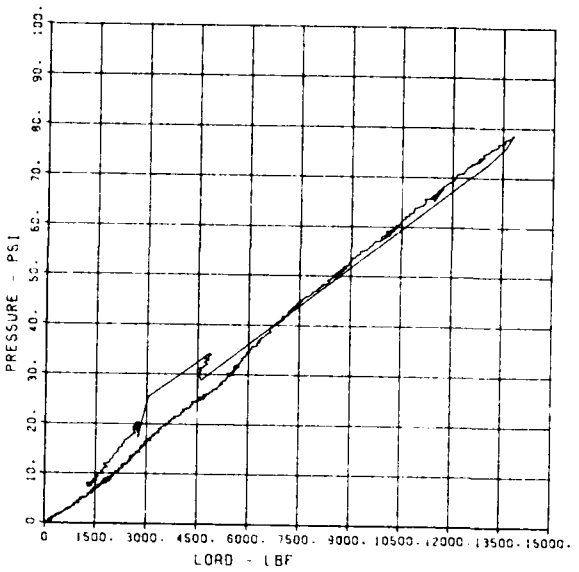

SLAB RESTRAINT G1
ST-1

10462 1
09/25/84 R0709

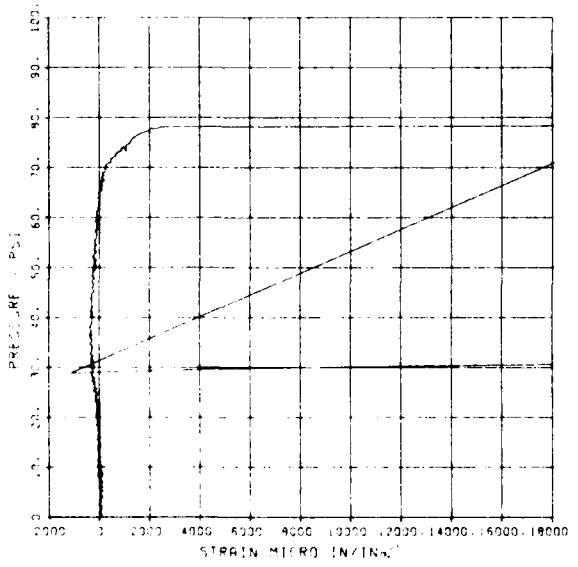

SLAB RESTRAINT G1
ST-2

10462 1
09/25/84 R0709

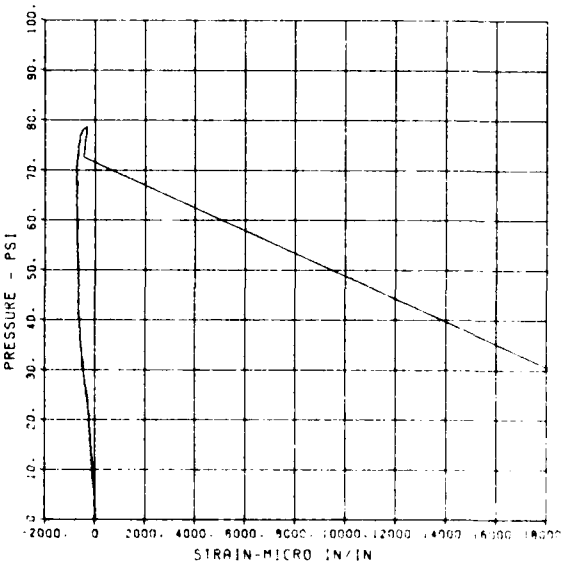

SLAB RESTRAINT G1
ST-3

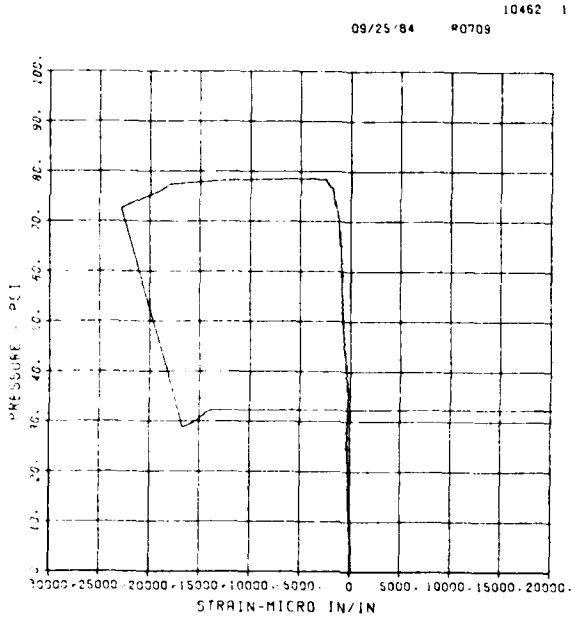

SLAB RESTRAINT G1
SB-1A

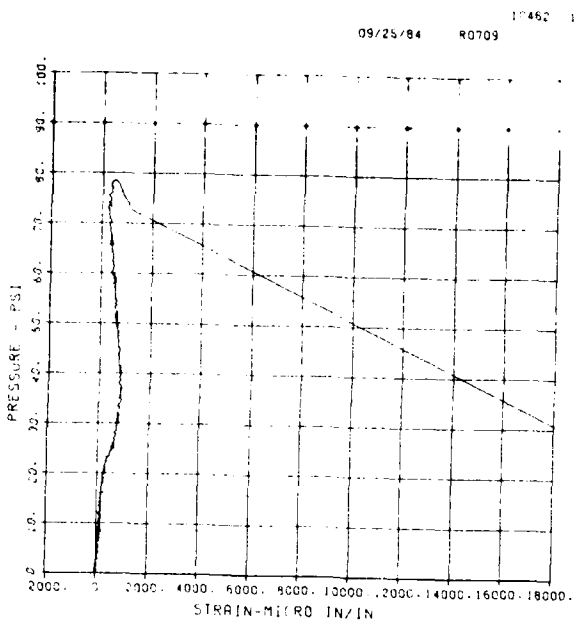

SLAB RESTRAINT G1
SB-2

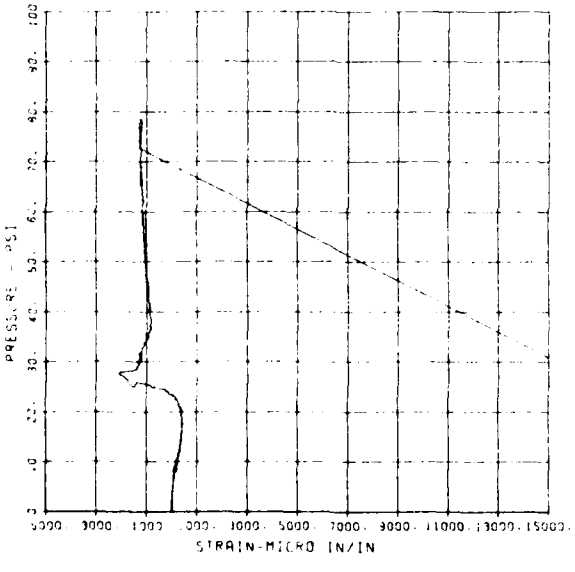

SLAB RESTRAINT G1
SB-3

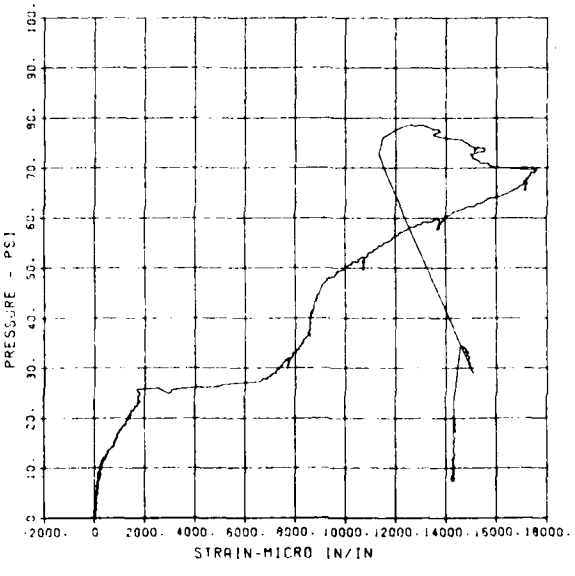

SLAB RESTRAINT G1
ST-1

10462 1
09/25/84 R0709

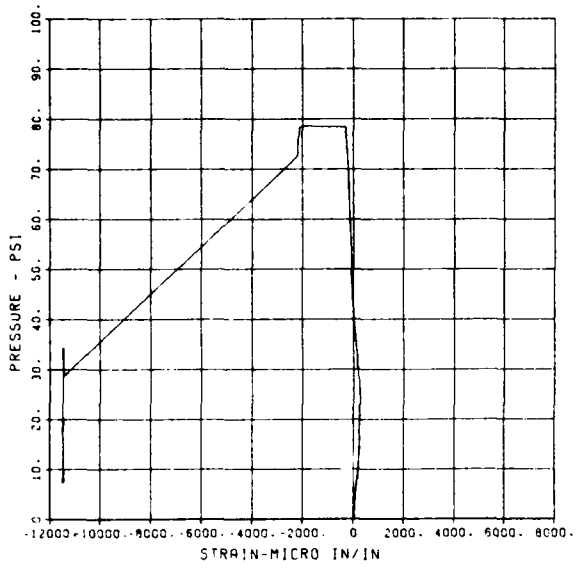

SLAB RESTRAINT G1
CB-3

10462 1
09/25/84 R0709

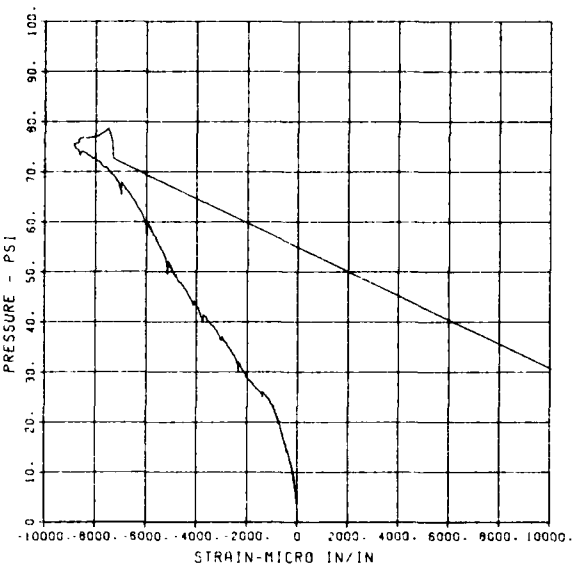

SLAB RESTRAINT G1
CB-390

10462 1
09/25/84 R0709

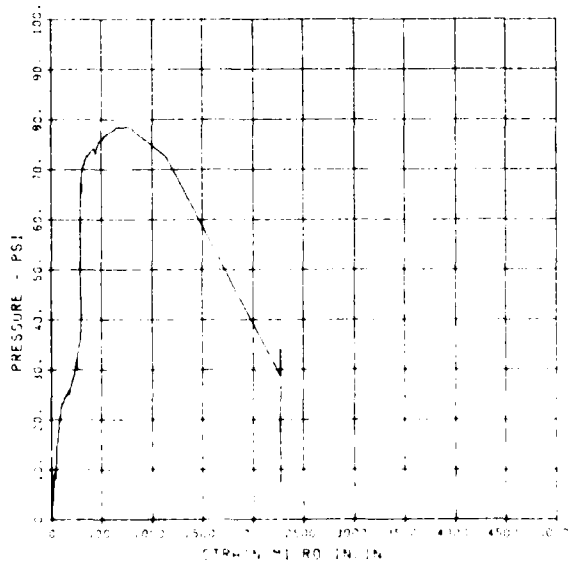

SLAB RESTRAINT G1
ST-1A

10462 1
09/25/84 R0709

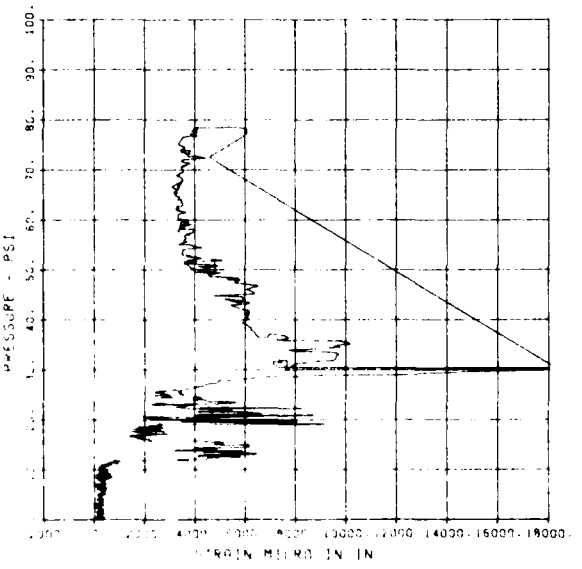

SLAB RESTRAINT G2

SLAB RESTRAINT G2
O-1

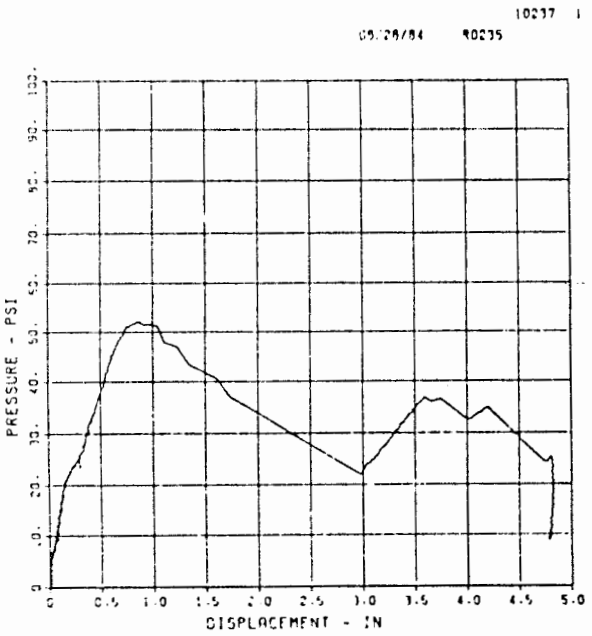

SLAB RESTRAINT G2
O-3

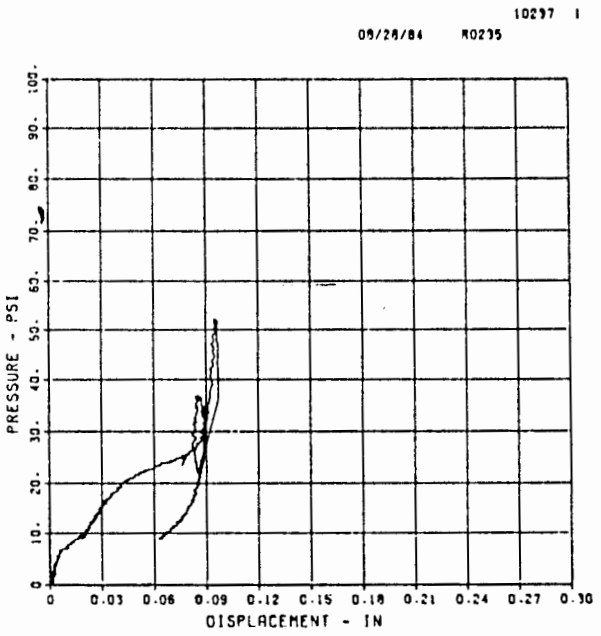

SLAB RESTRAINT G2
O-4

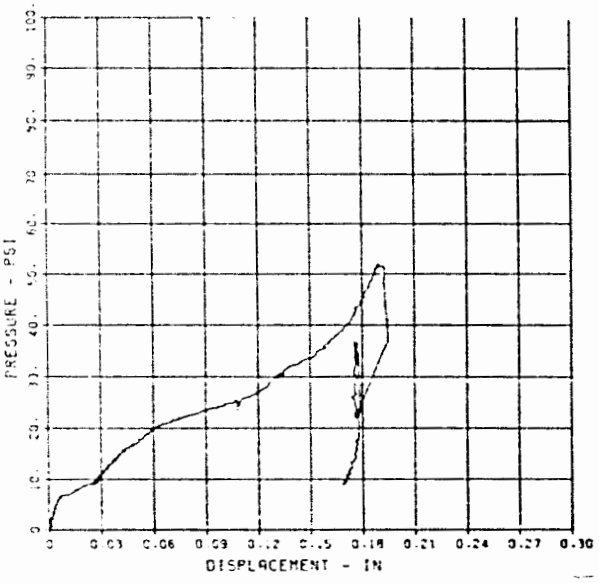

SLAB RESTRAINT G2
LW-1

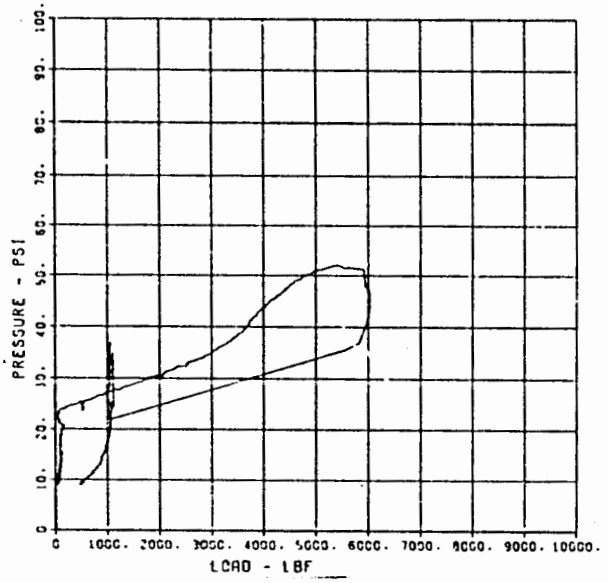

SLAB RESTRAINT C2
LW-2

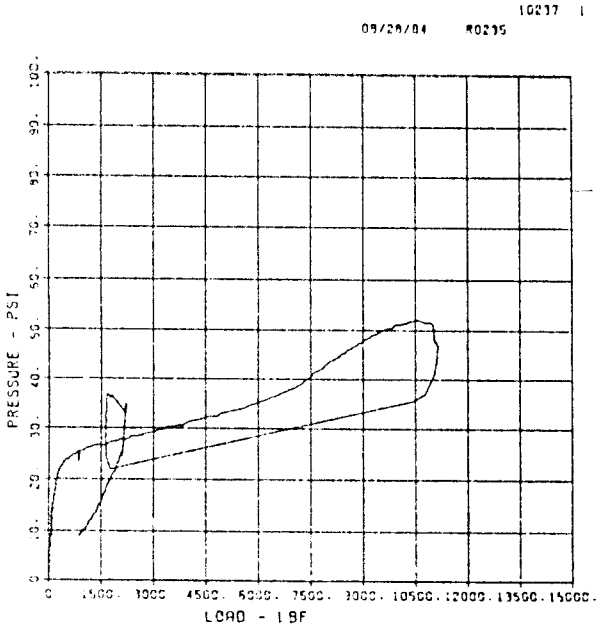

SLAB RESTRAINT C2
LW-3

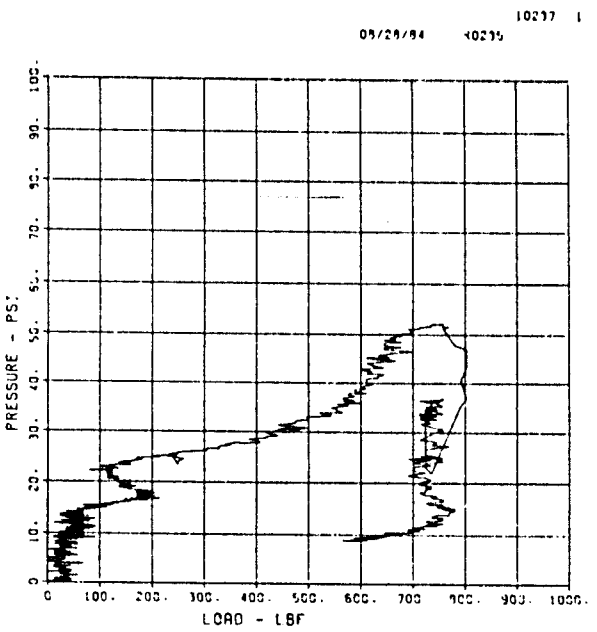

SLAB RESTRAINT C2
LW-4

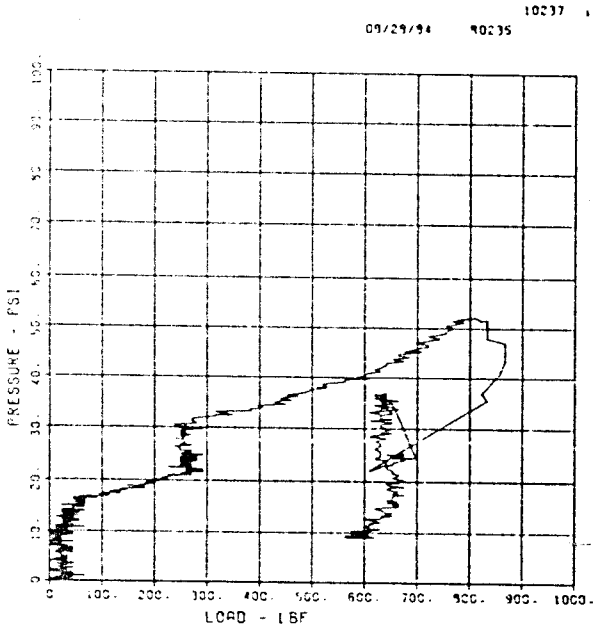

SLAB RESTRAINT C2
LW-5

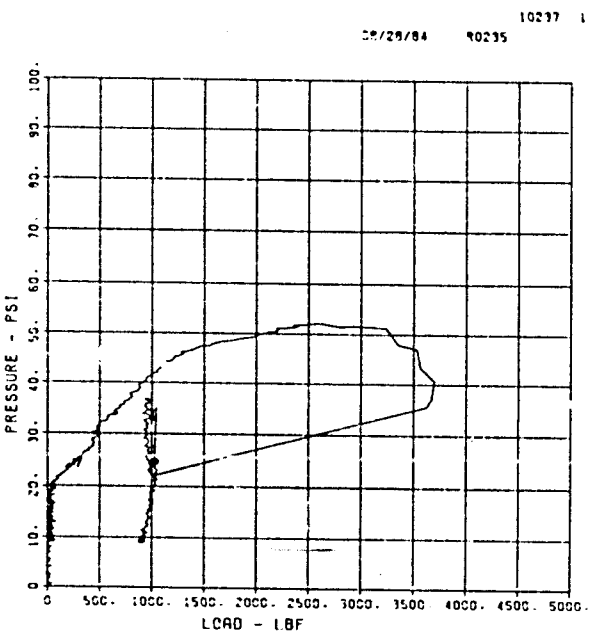

SLAB RESTRAINT G2
LW-6

10237 1
09/28/84 80235

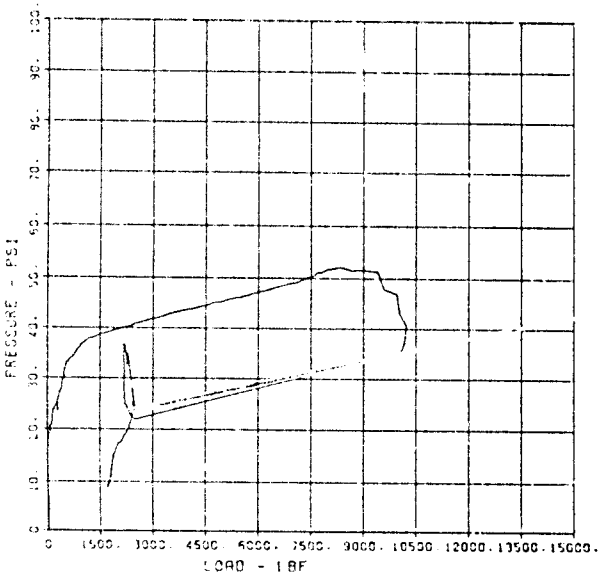

SLAB RESTRAINT G2
LW-7

10237 1
09/28/84 80235

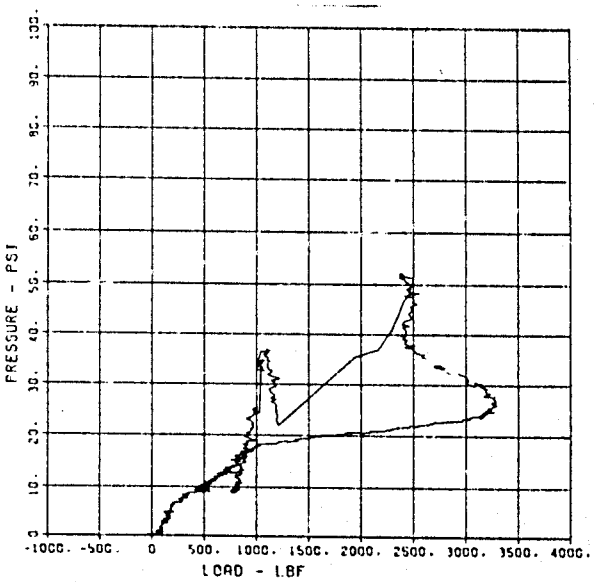

SLAB RESTRAINT G2
LW-8

10237 1
09/28/84 80235

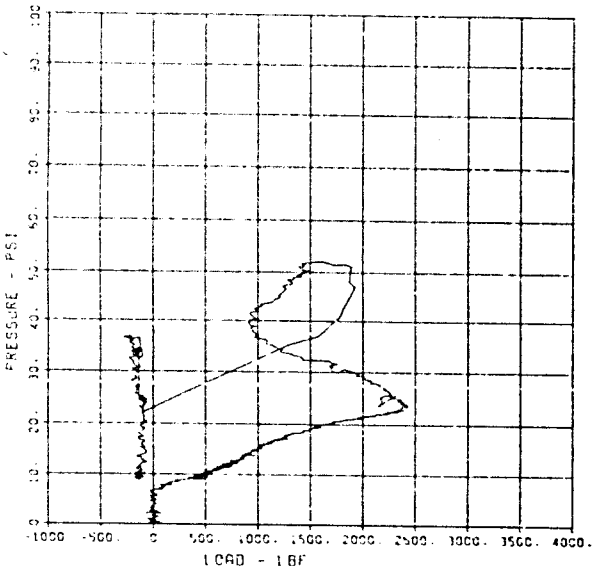

SLAB RESTRAINT G2
LW-9

10237 1
09/28/84 80235

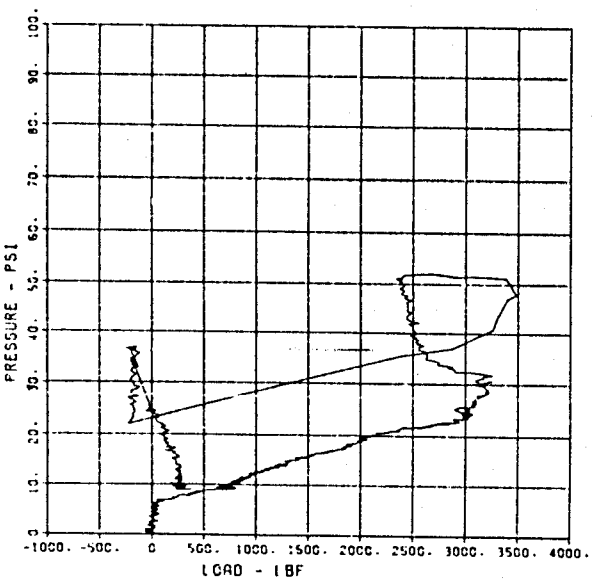

SLAB RESTRAINT G2
GW-10

10237
09/28/94 80235

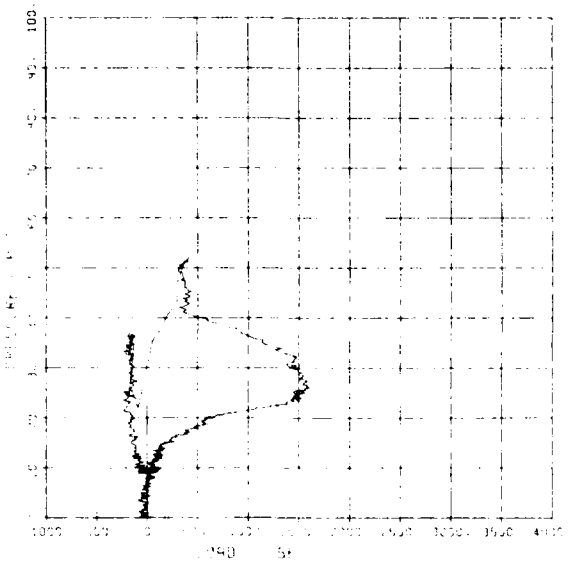

SLAB RESTRAINT G2
GW-11

10237
09/28/94 80235

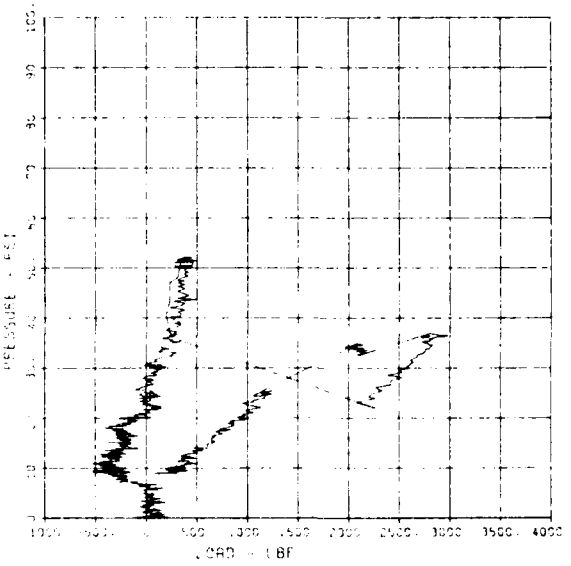

SLAB RESTRAINT G2
GW-12

10237
09/28/94 80235

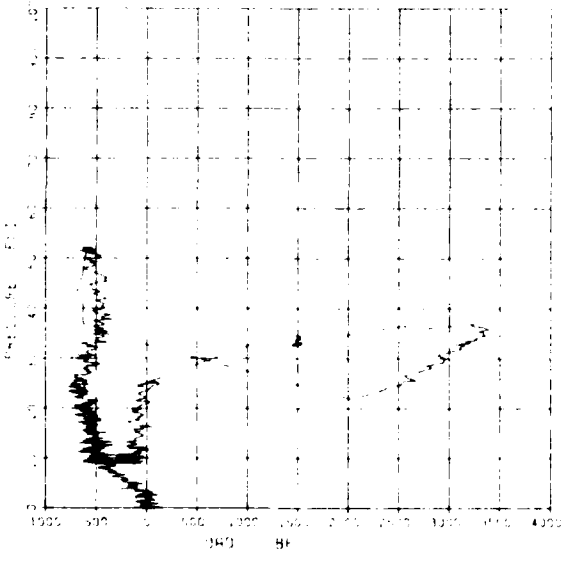

SLAB RESTRAINT G2
GW-13

10237
09/28/94 80235

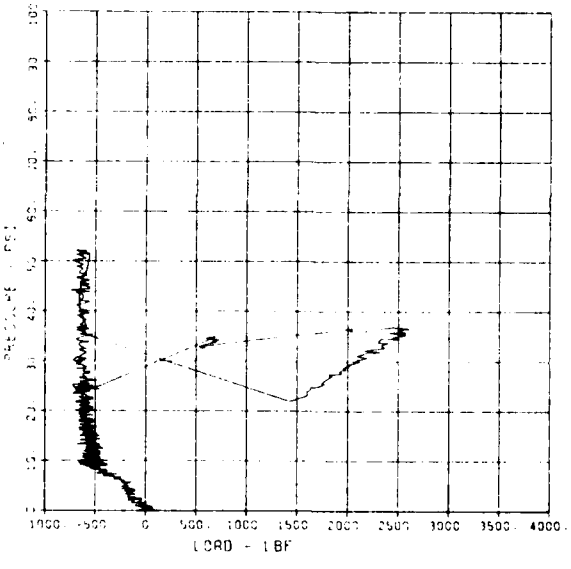

SLAB RESTRAINT 02
LW-14

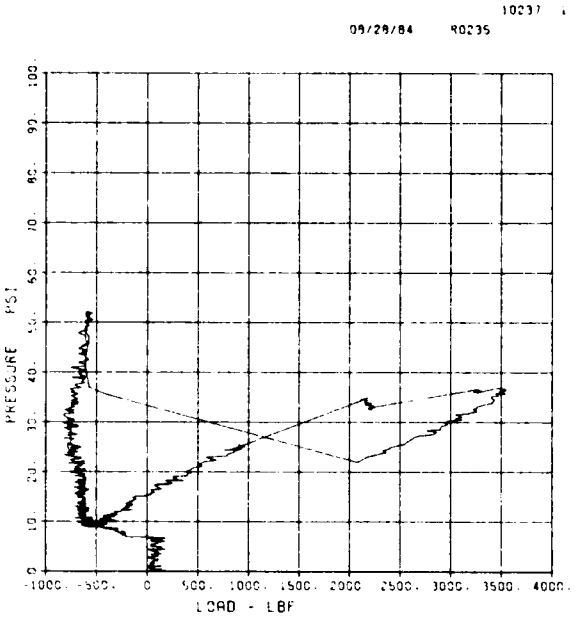

SLAB RESTRAINT 02
LW-15

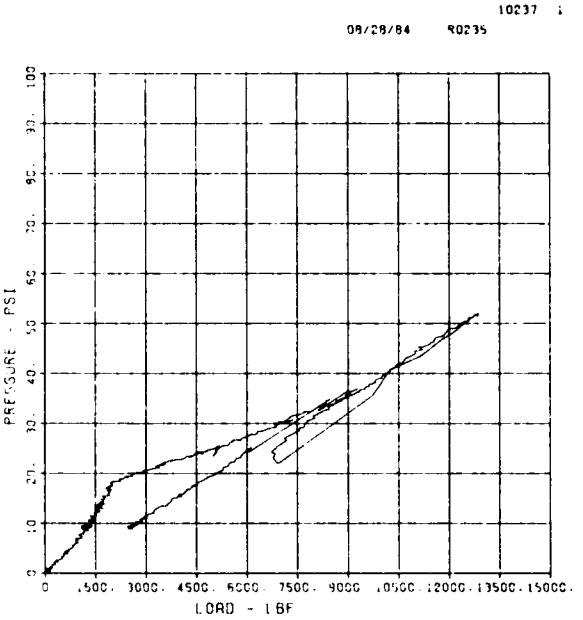

SLAB RESTRAINT 02
LW-16

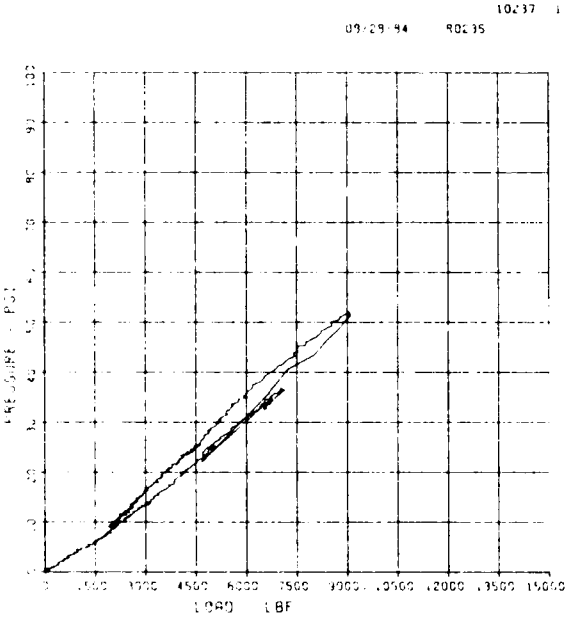

SLAB RESTRAINT 02
ST-1

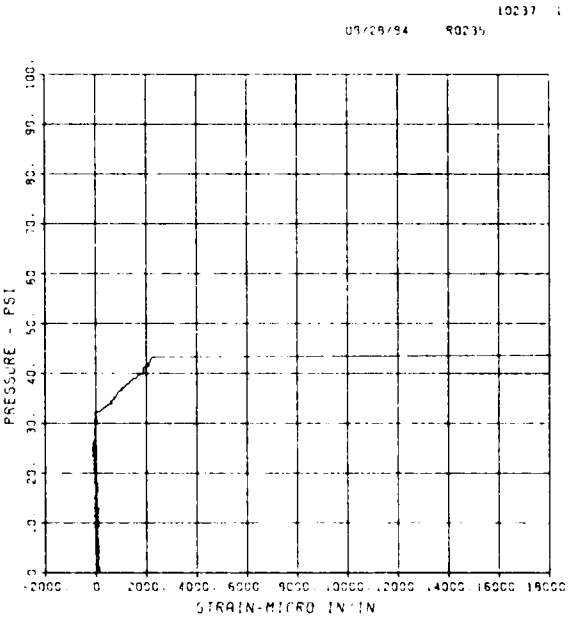

SLAB RESTRAINT G2
ST-2

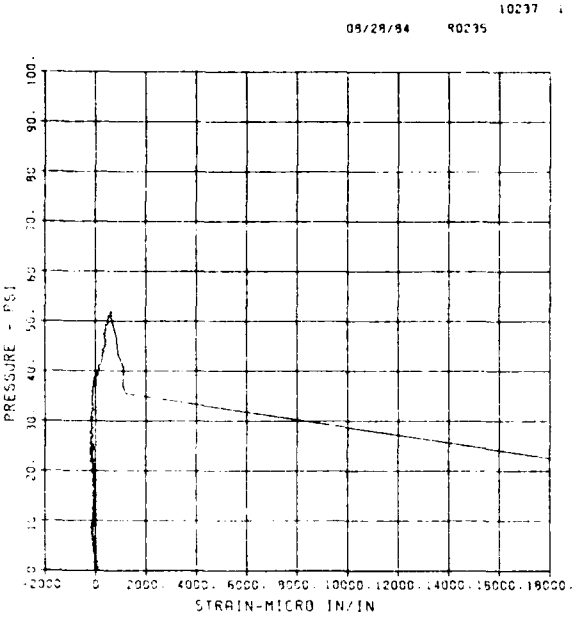

SLAB RESTRAINT G2
ST-3

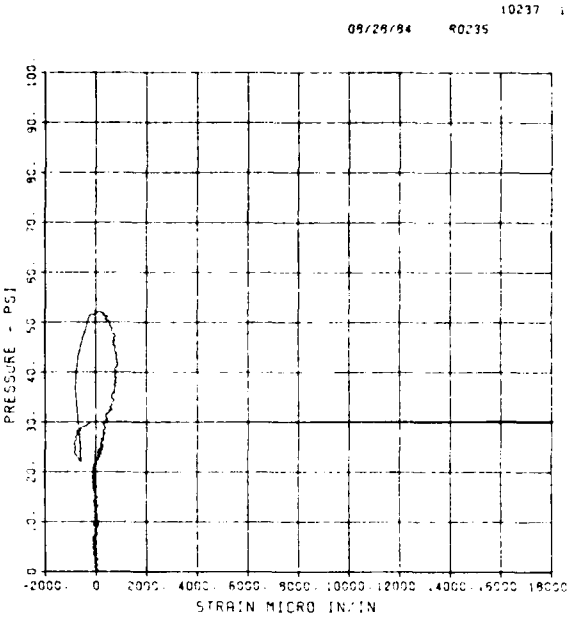

SLAB RESTRAINT G2
SB-1

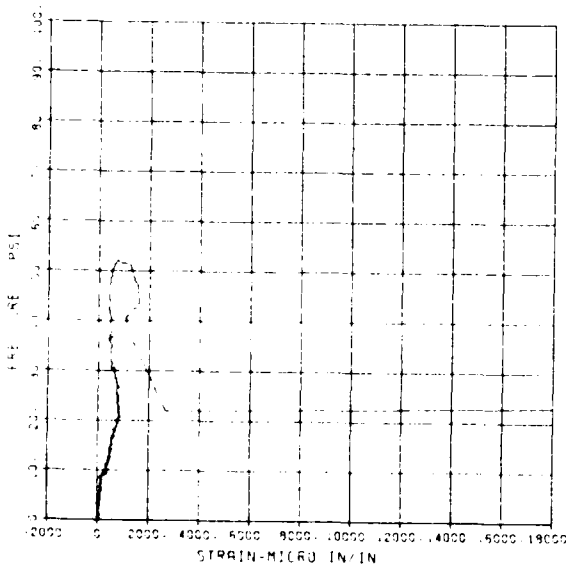

SLAB RESTRAINT G2
SB-2

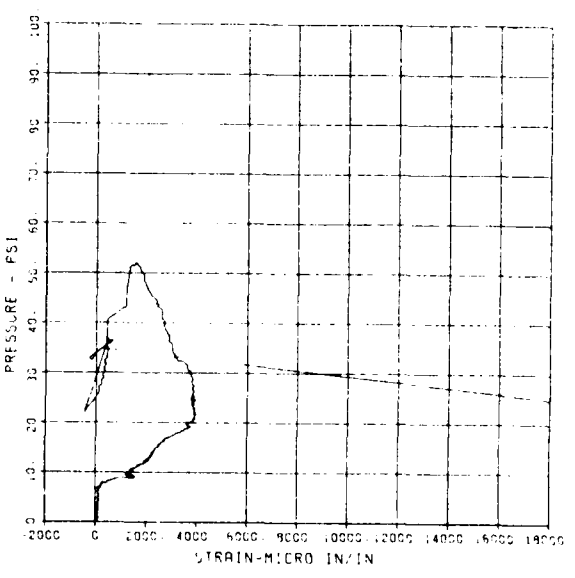

SLAB RESTRAINT G2
SB-3

10237 1

09/29/94 90235

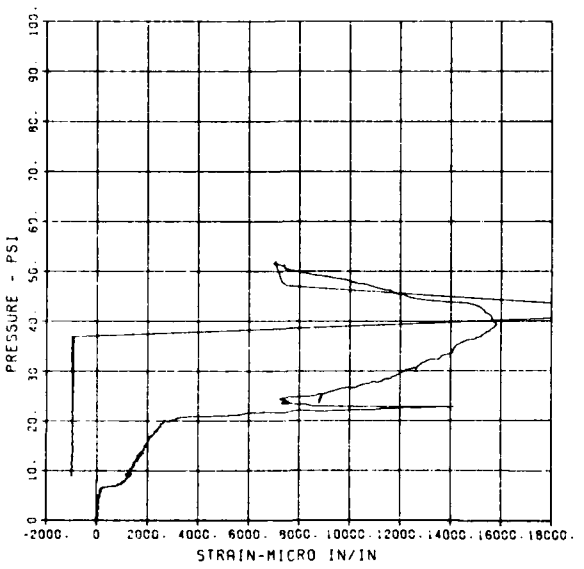

SLAB RESTRAINT G3

SLAB RESTRAINT G3
D-1

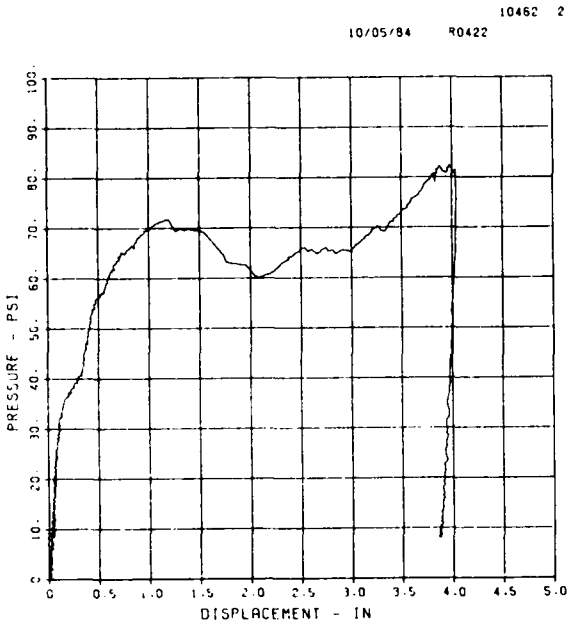

SLAB RESTRAINT G3
D-2

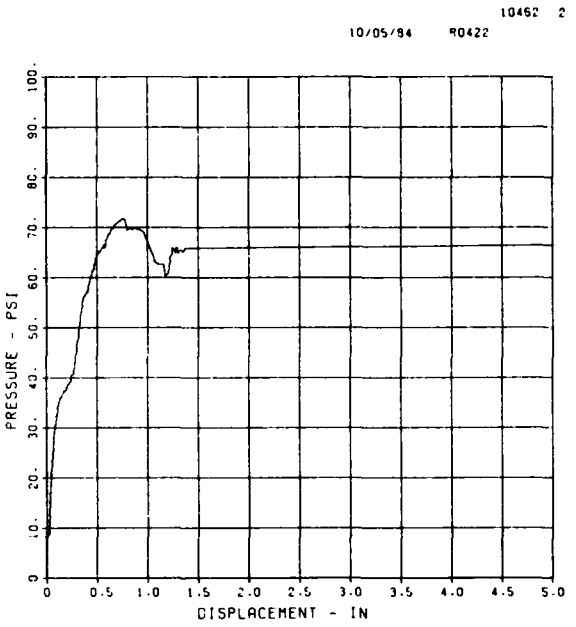

SLAB RESTRAINT G3
D-3

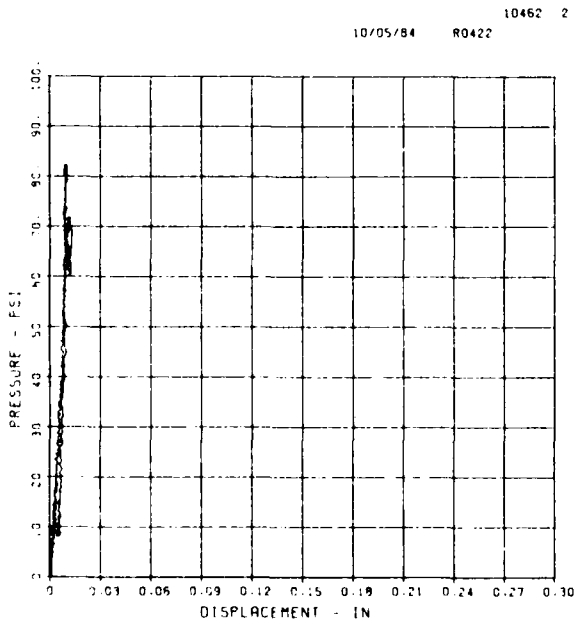

SLAB RESTRAINT G3
D-4

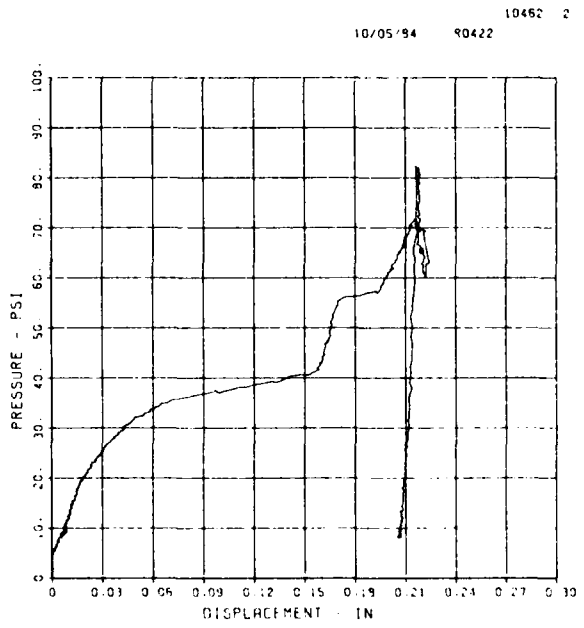

SLAB RESTRAINT G3
LW-1

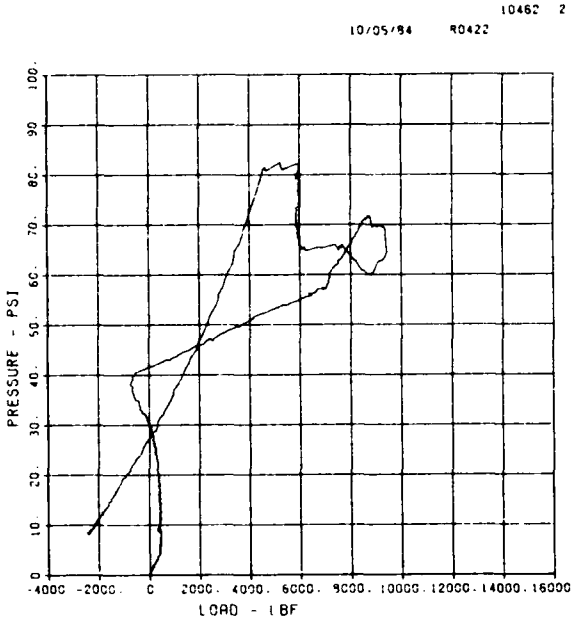

SLAB RESTRAINT G3
LW-2

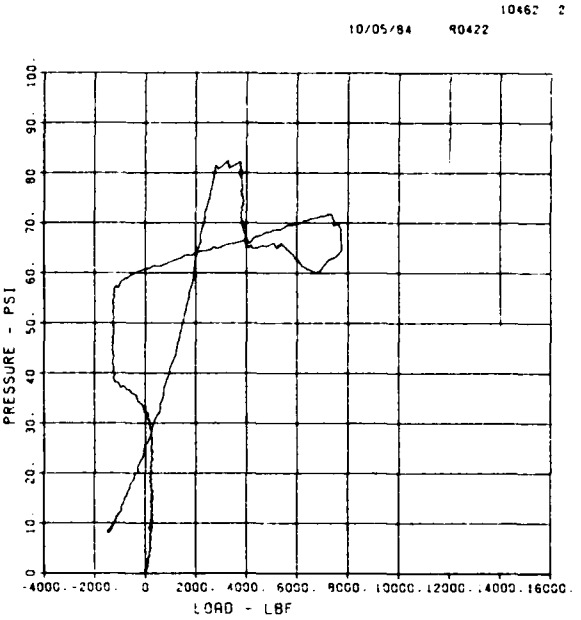

SLAB RESTRAINT G3
LW-3

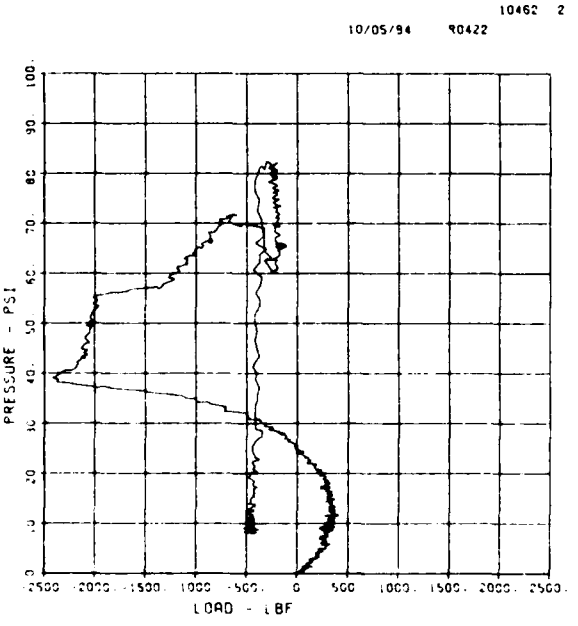

SLAB RESTRAINT G3
LW-4

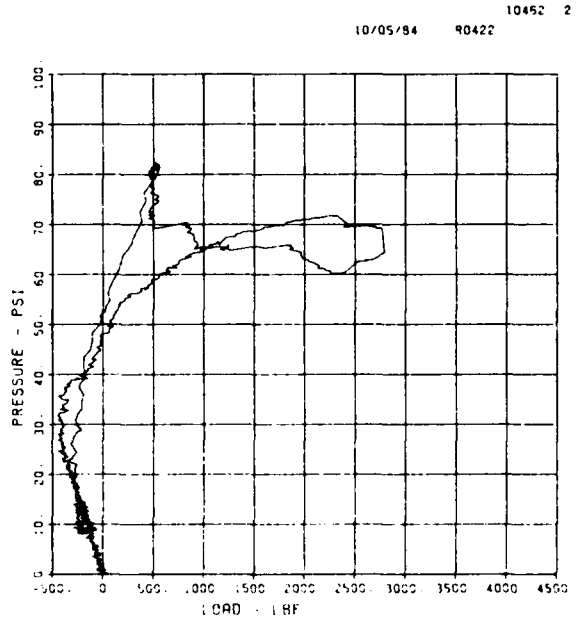

SLAB RESTRAINT G3
LW-6

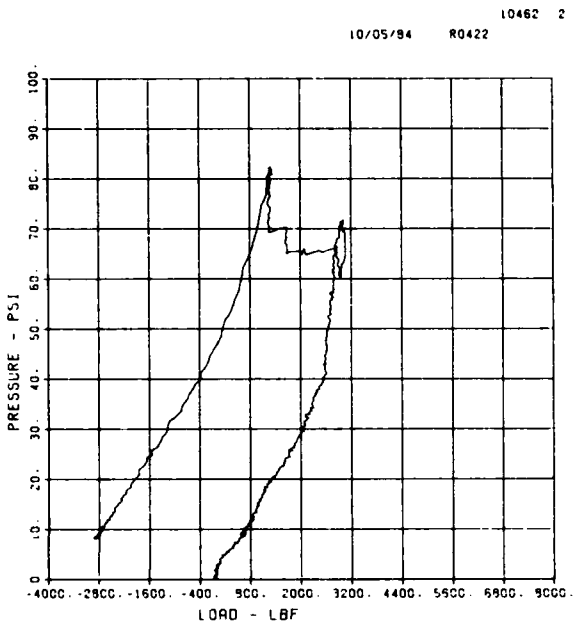

SLAB RESTRAINT G3
LW-5

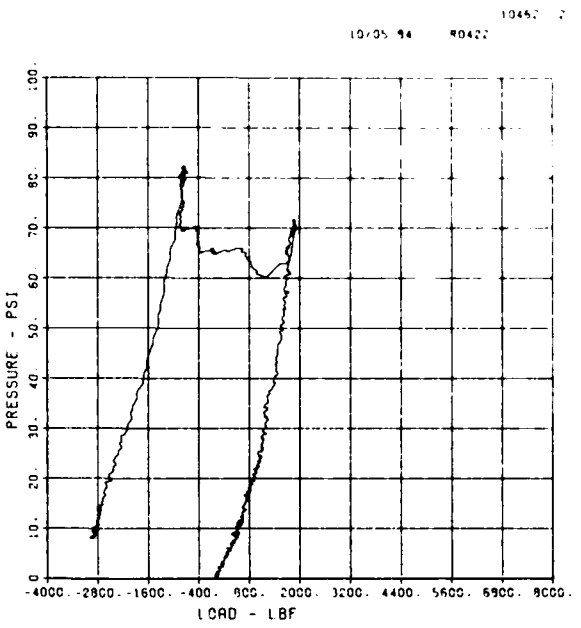

SLAB RESTRAINT G3
LW-7

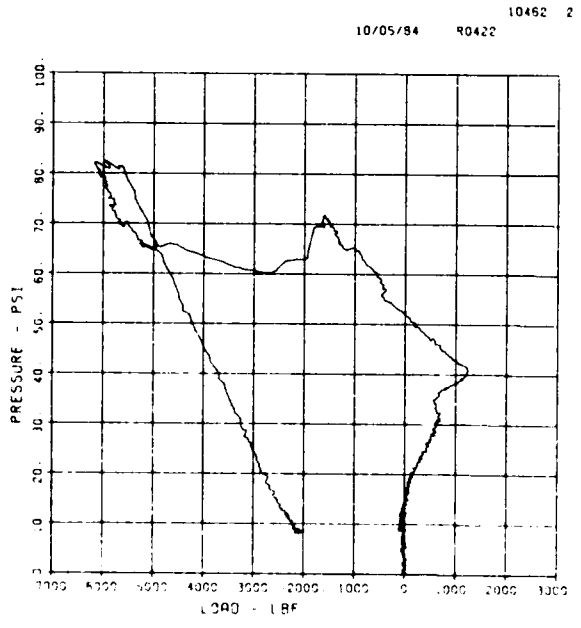

SLAB RESTRAINT G3
LW-8

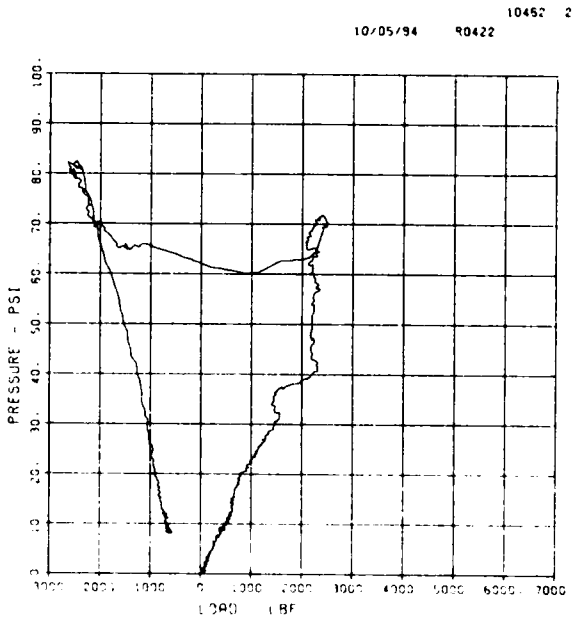

S B RESTRAINT G3
LW-9

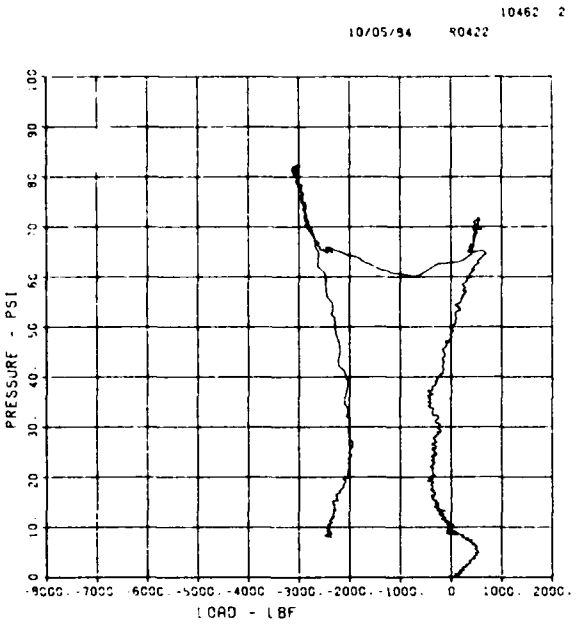

SLAB RESTRAINT G3
LW-10

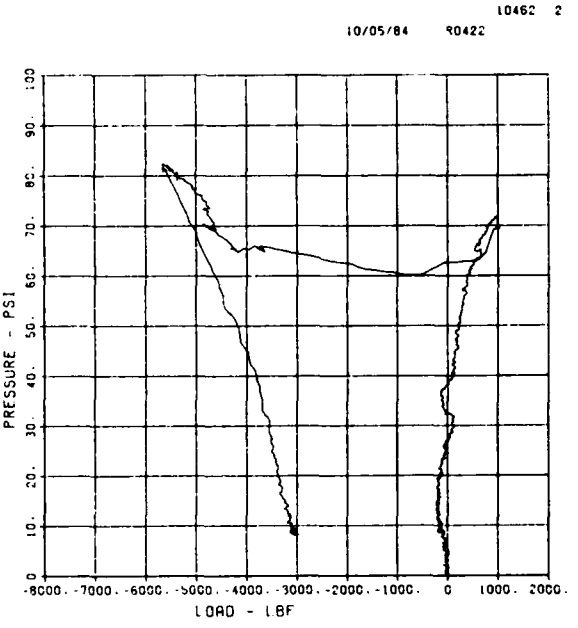

SLAB RESTRAINT G3
LW-11

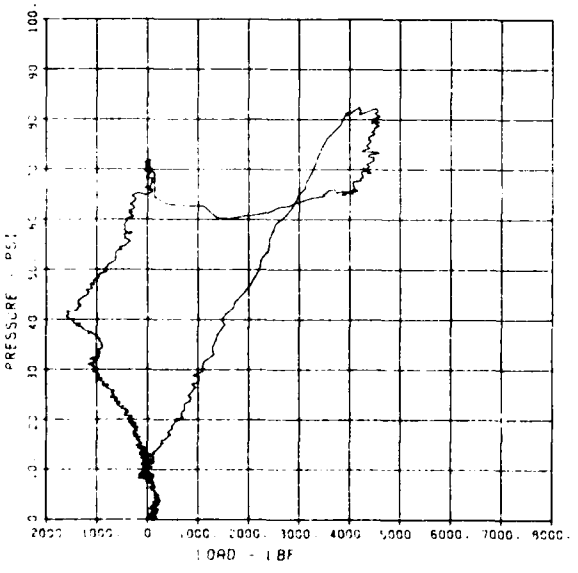

SLAB RESTRAINT G3
LW-13

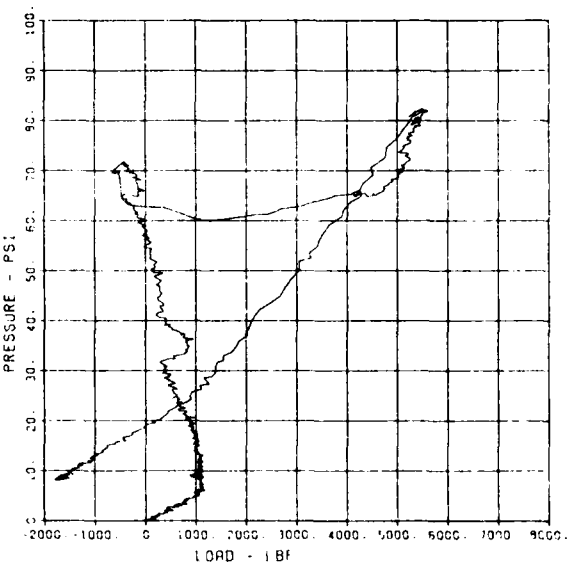

SLAB RESTRAINT G3
LW-14

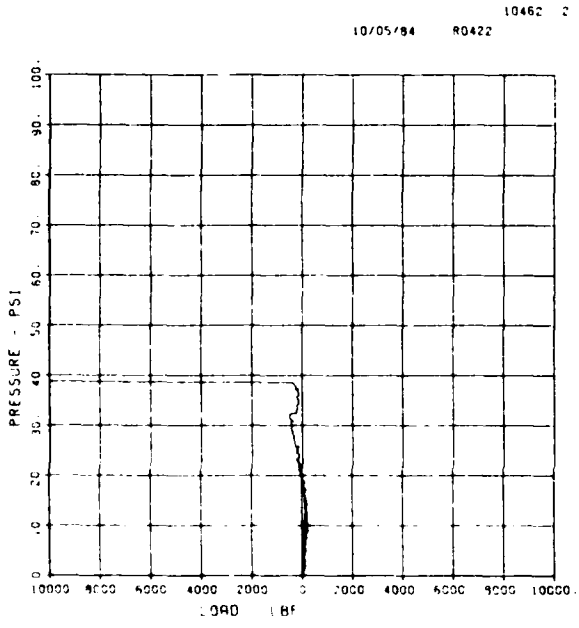

SLAB RESTRAINT G3
LW-15

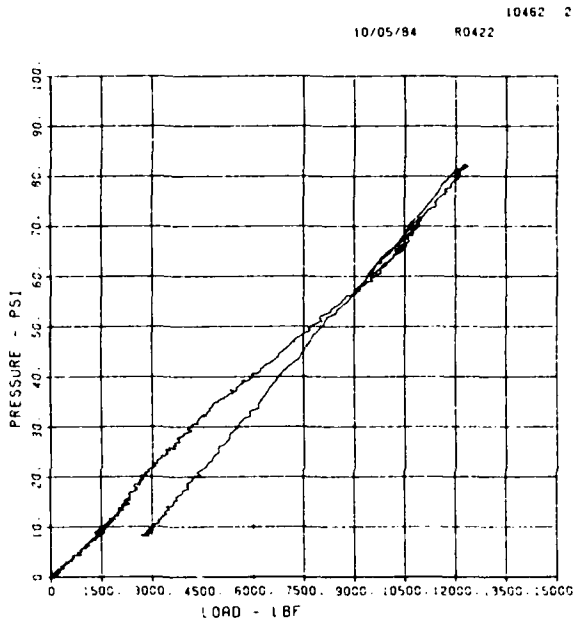

SLAB RESTRAINT G3
ST-1

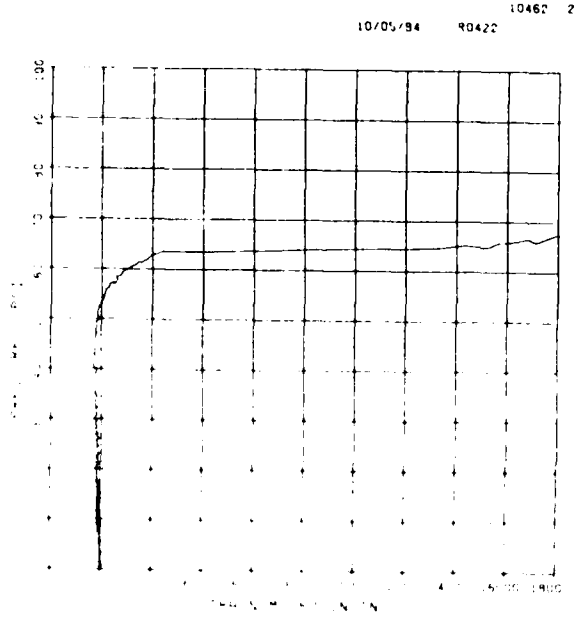

SLAB RESTRAINT G3
ST-2

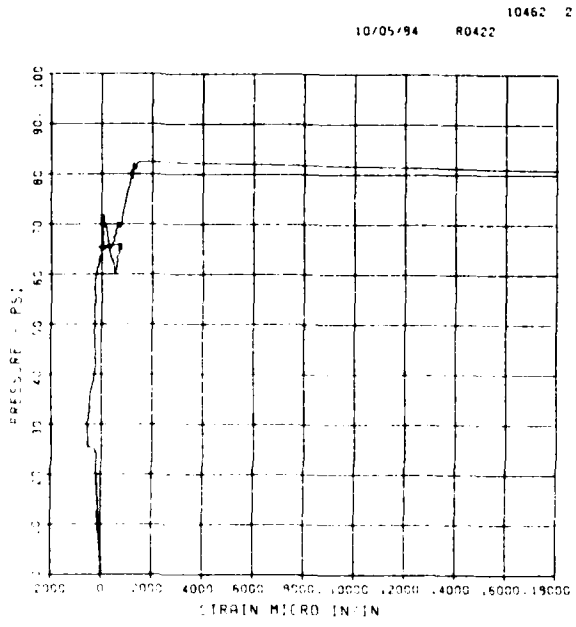

SLAB RESTRAINT G3
ST-3

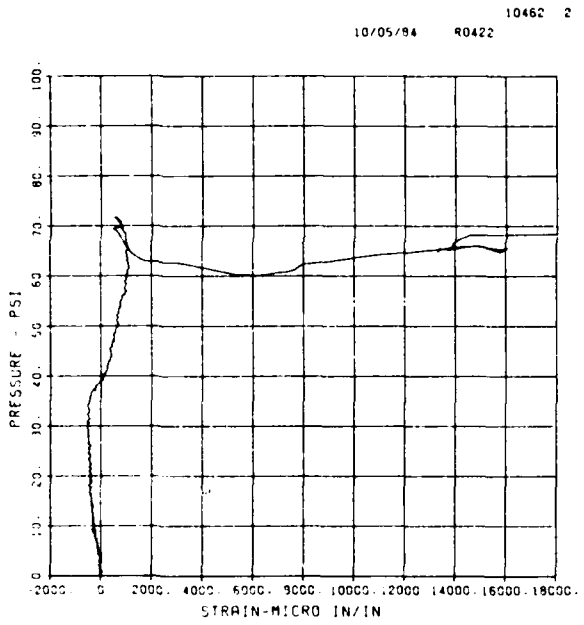

SLAB RESTRAINT G3
SB-1

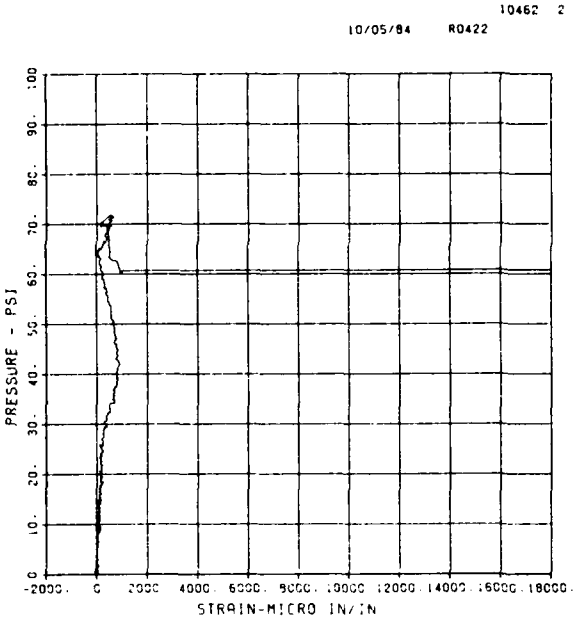

SLAB RESTRAINT G3
SB-2

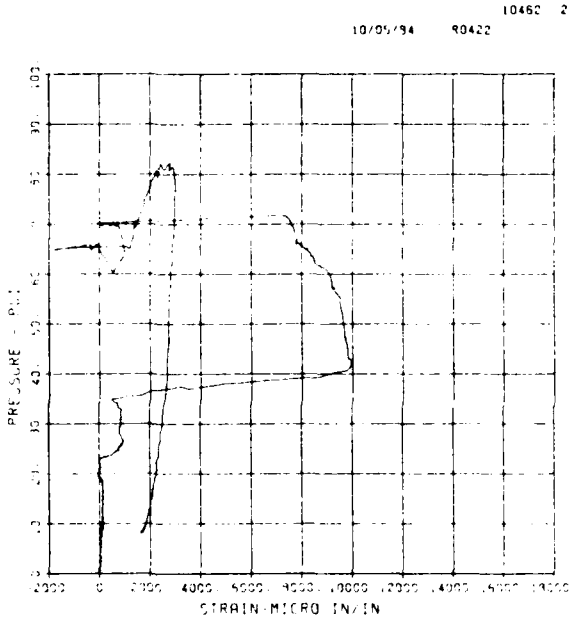

SLAB RESTRAINT G3
SB-3

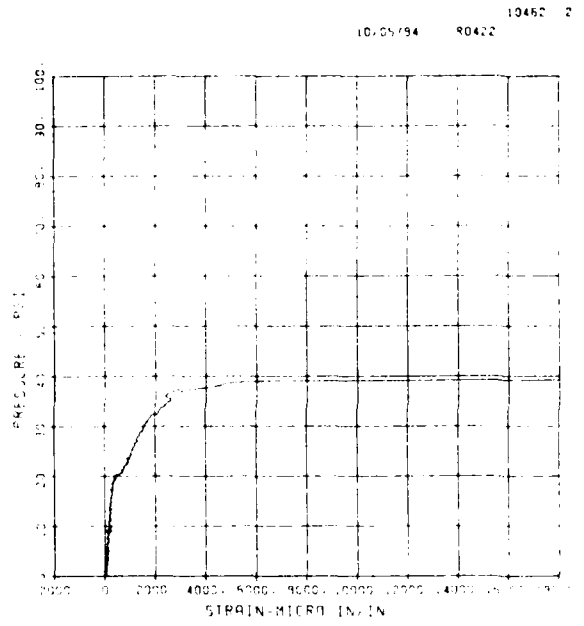

SLAB RESTRAINT 03
ST-1

10462 2
10/05/84 R0422

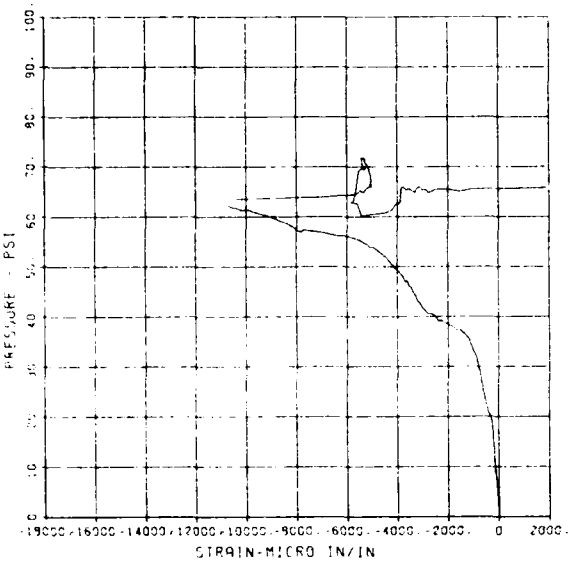

SLAB RESTRAINT 03
CB-390

10462 2
10/05/84 R0422

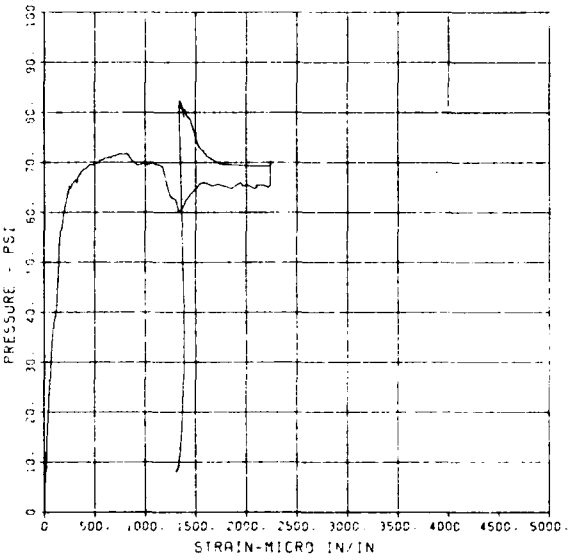

SLAB RESTRAINT 03
CB-3

10462 2
10/05/84 R0422

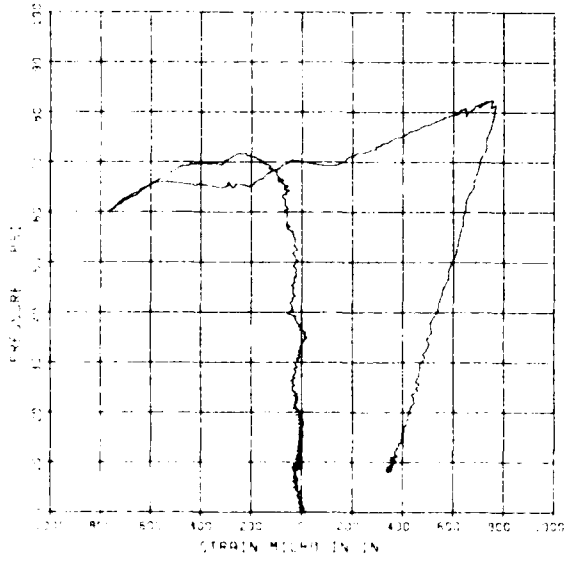

SLAB RESTRAINT 03
ST-19

10462 2
10/05/84 R0422

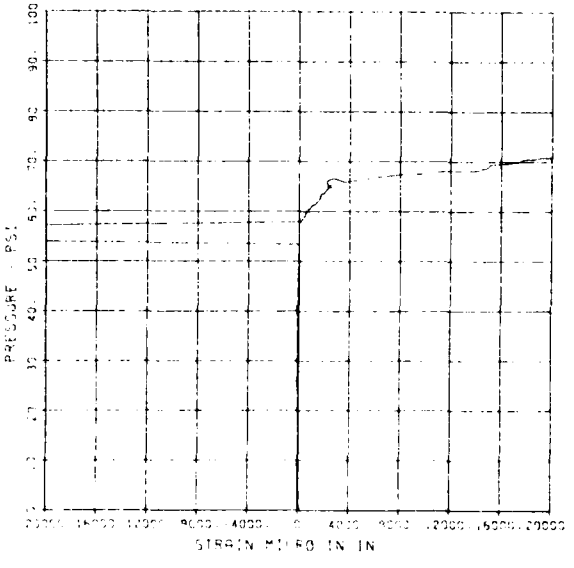

SLAB RESTRAINT G4

SLAB RESTRAINT C4
D-1

7350

09/23/94 80163

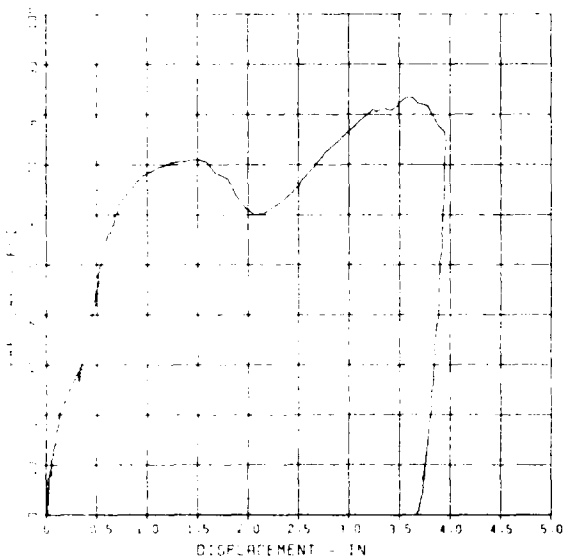

SLAB RESTRAINT C4
D-2

7350

09/23/94 80163

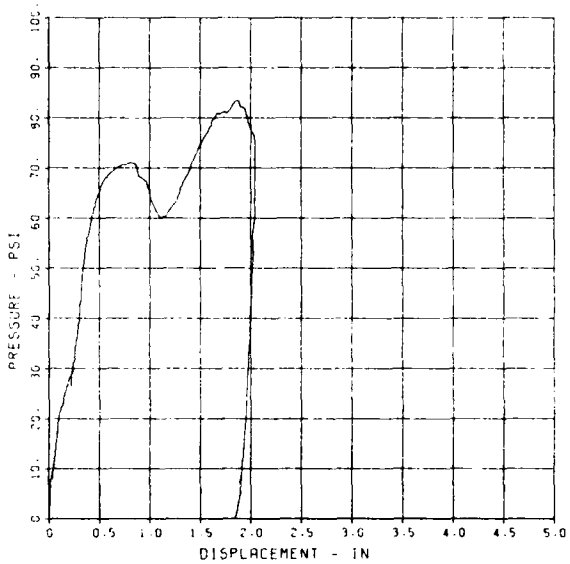

SLAB RESTRAINT C4
D-3

7350

09/23/94 80163

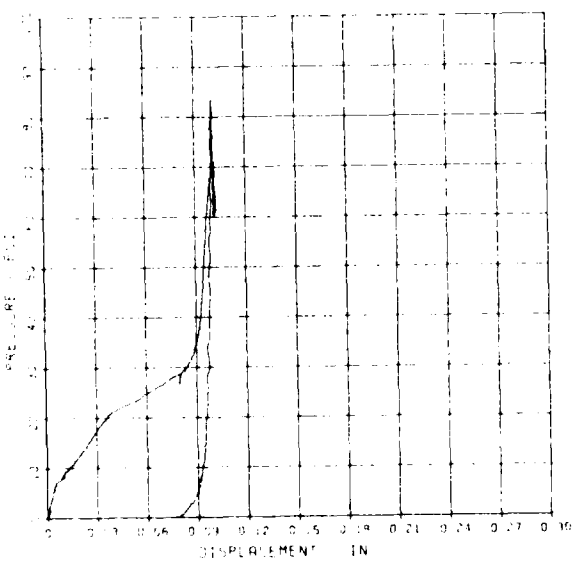

SLAB RESTRAINT C4
D-4

7350

09/23/94 80163

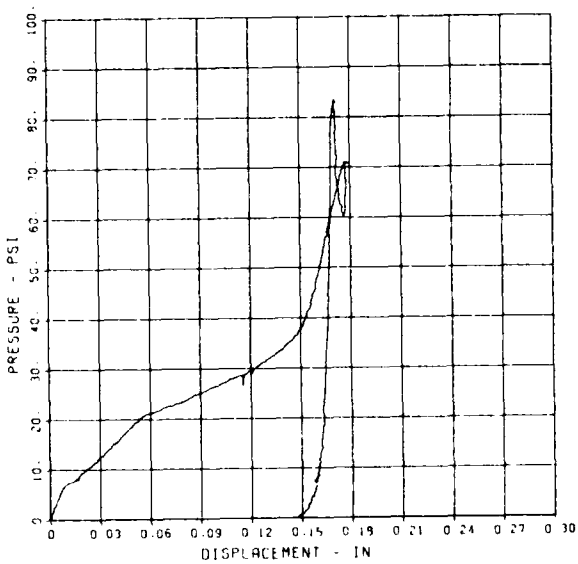

SLAB RESTRAINT C4
LW-1

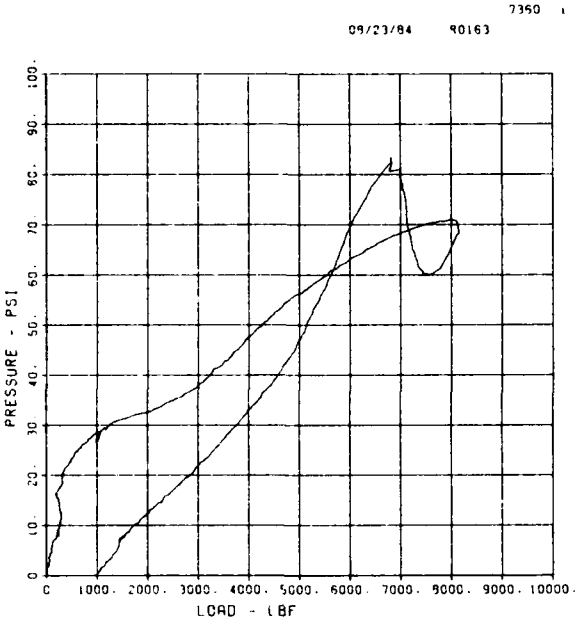

SLAB RESTRAINT C4
LW-2

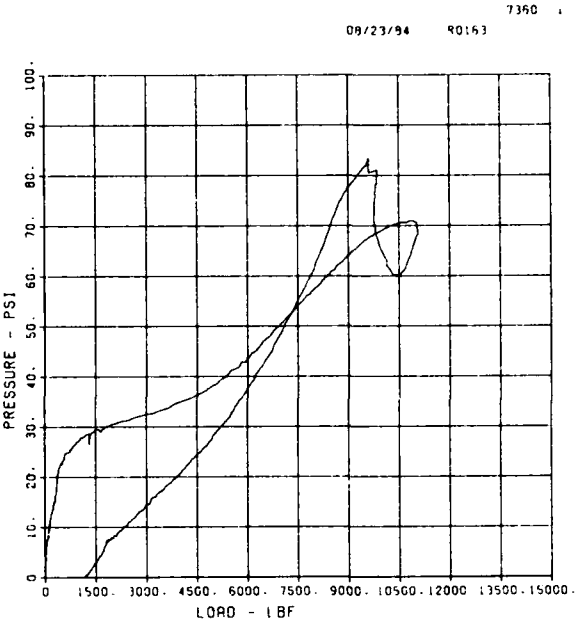

SLAB RESTRAINT C4
LW-3

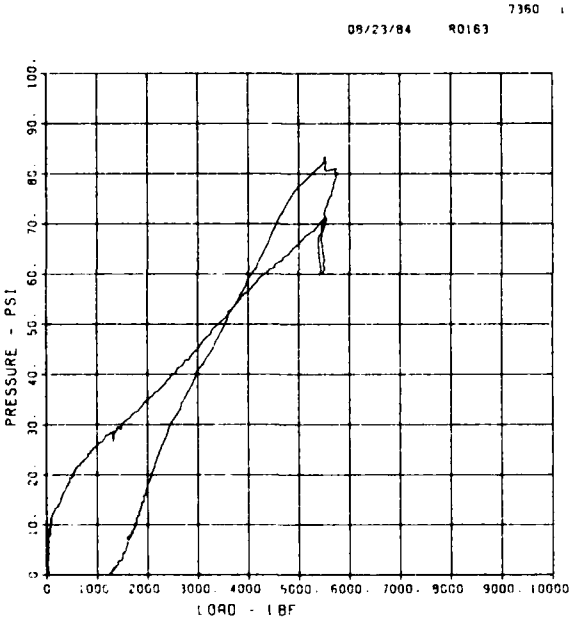

SLAB RESTRAINT C4
LW-4

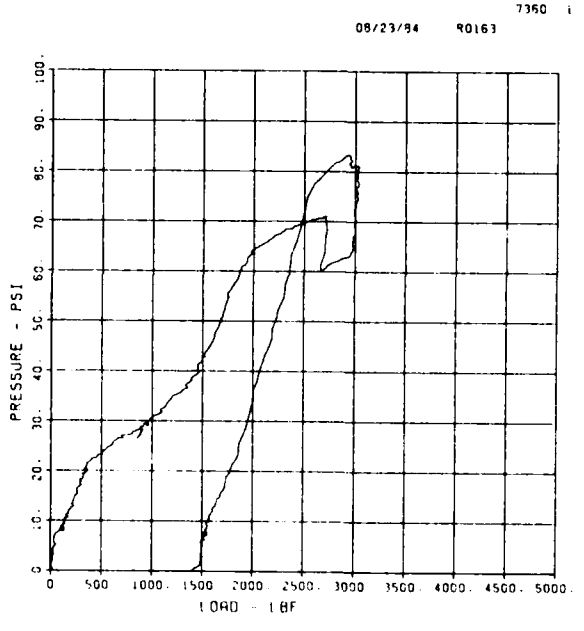

SLAB RESTRAINT C4
LW-5

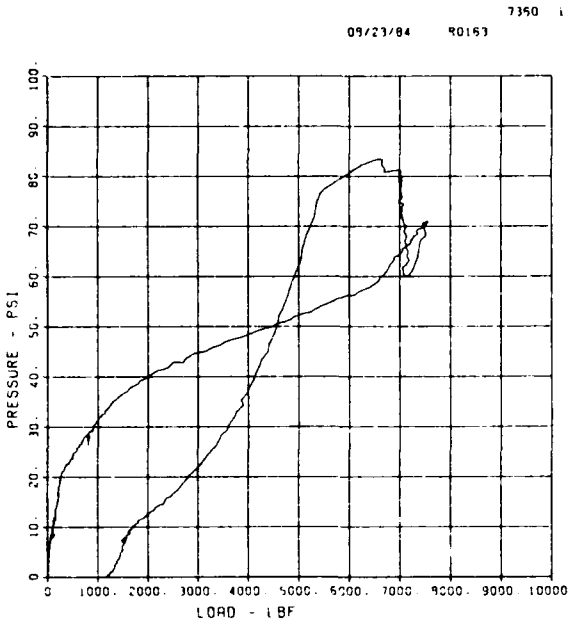

SLAB RESTRAINT C4
LW-6

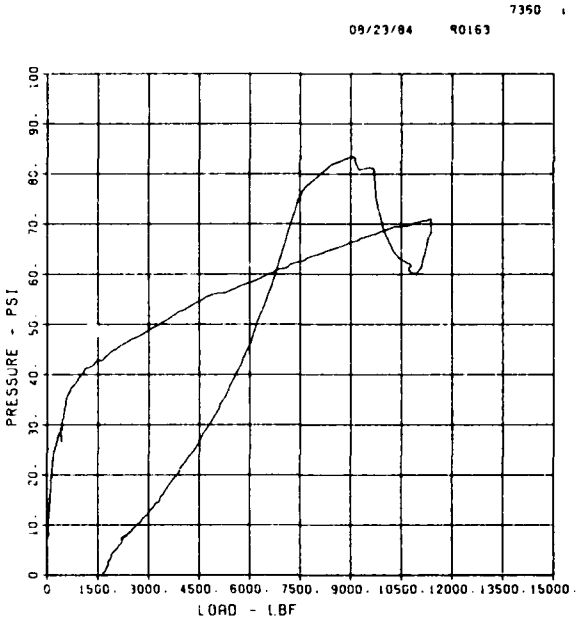

SLAB RESTRAINT C4
LW-7

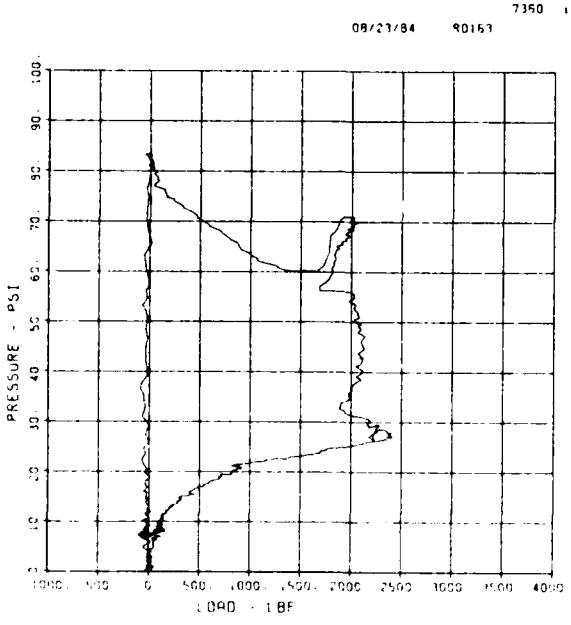

SLAB RESTRAINT C4
LW-8

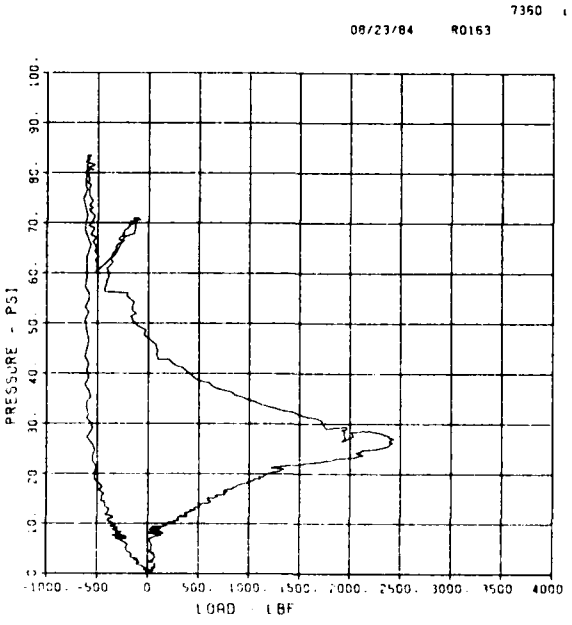

SLAB RESTRAINT C4
LW-9

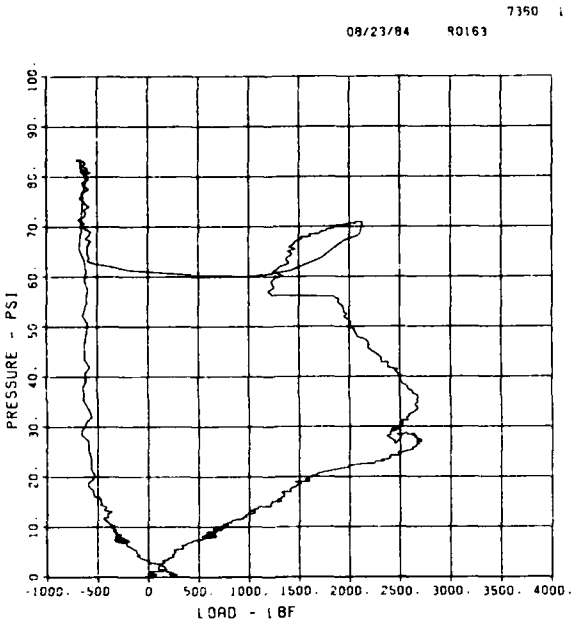

SLAB RESTRAINT C4
LW-11

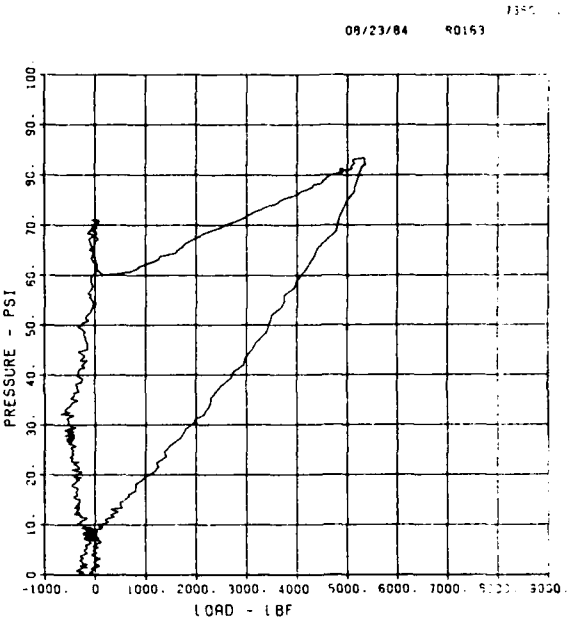

SLAB RESTRAINT C4
LW-12

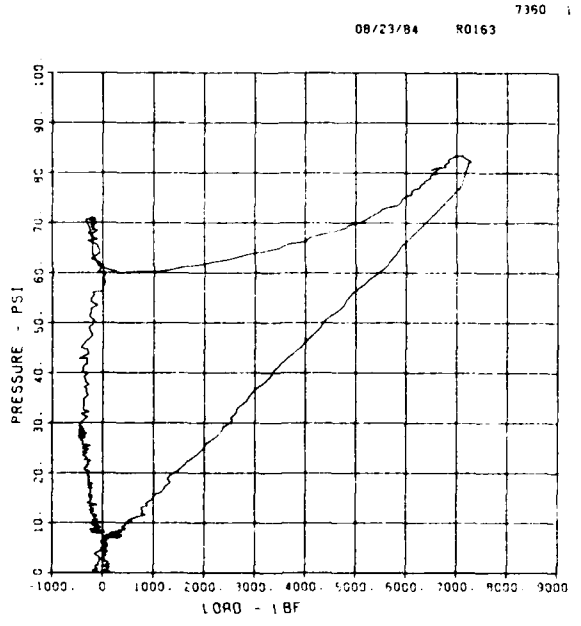

SLAB RESTRAINT C4
LW-13

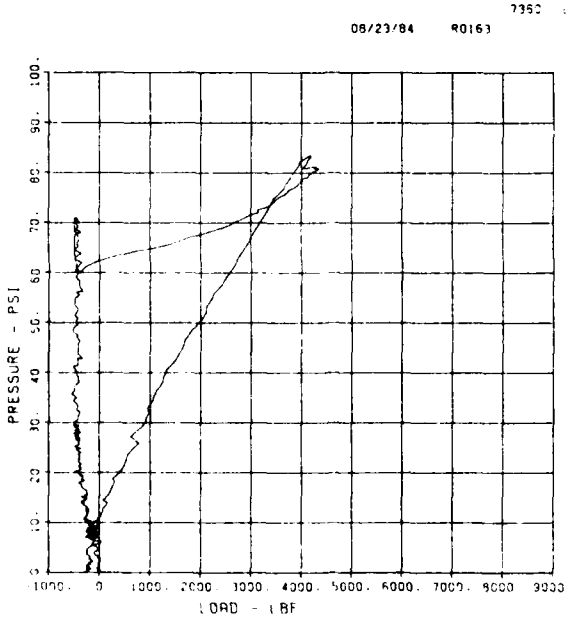

SLAB RESTRAINT G4
LW-15

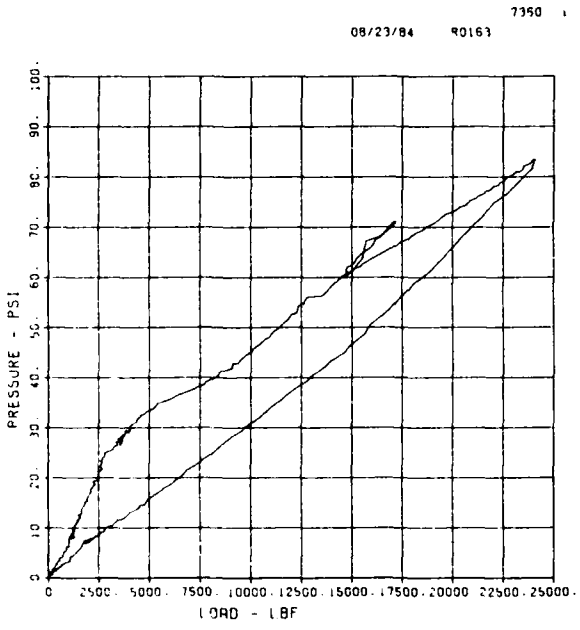

SLAB RESTRAINT G4
ST-1

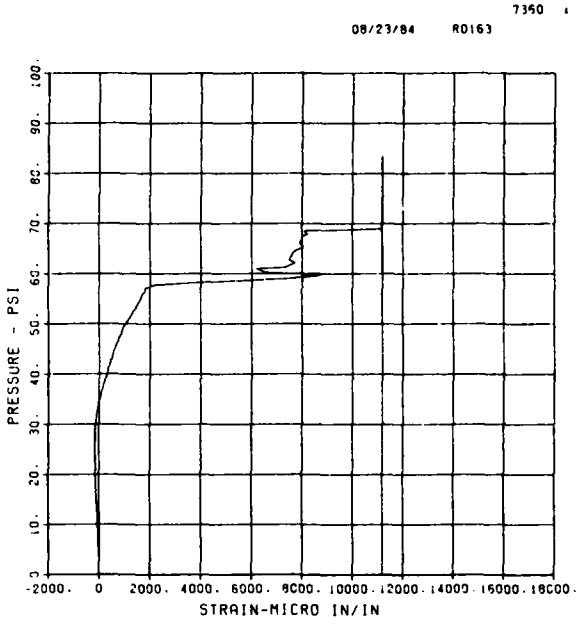

SLAB RESTRAINT G4
ST-2

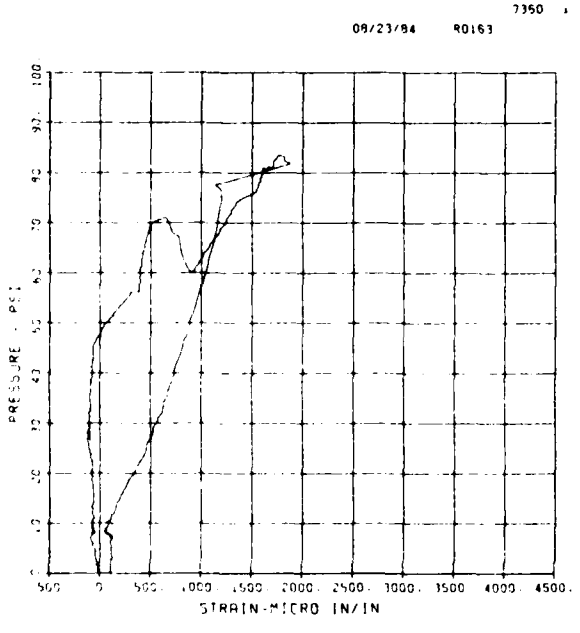

SLAB RESTRAINT G4
ST-3

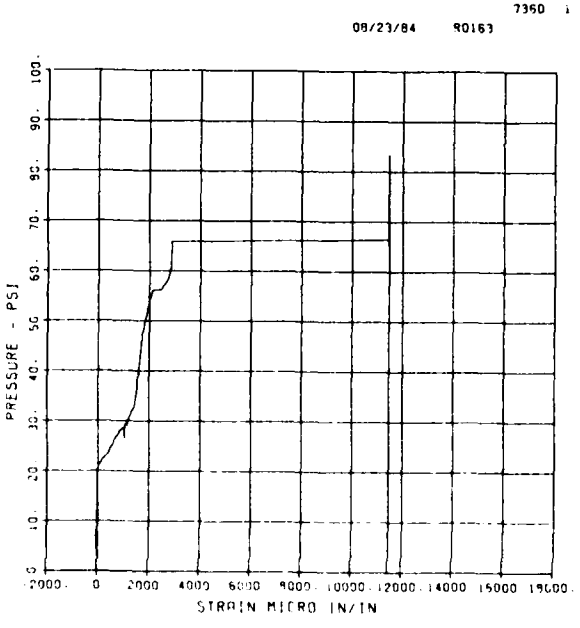

SLAB RESTRAINT C4
SB-1

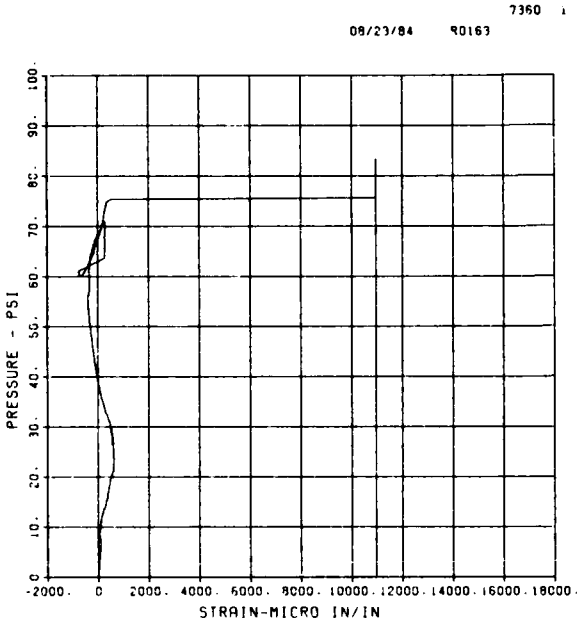

SLAB RESTRAINT C4
SB-2

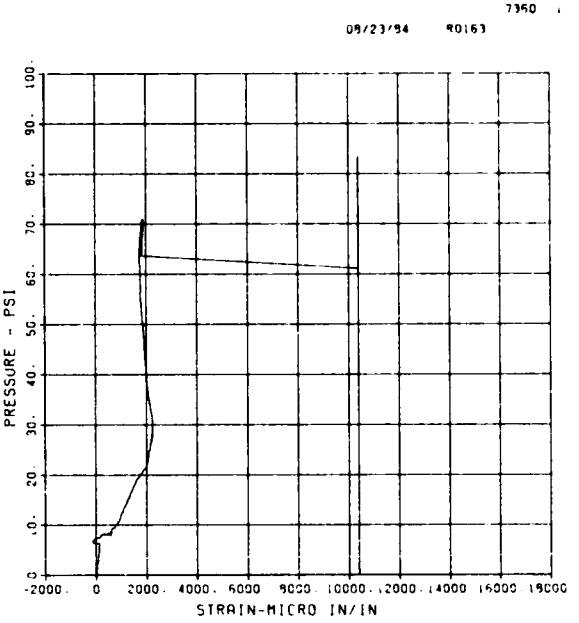

SLAB RESTRAINT C4
SB-3

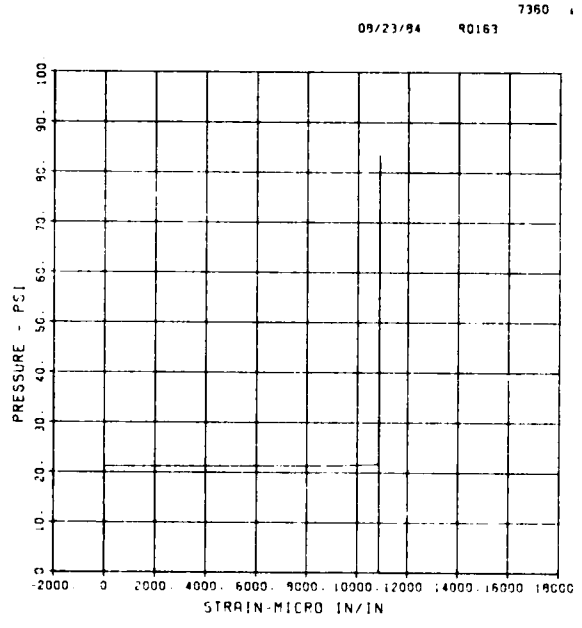

SLAB RESTRAINT C4
D-3-S

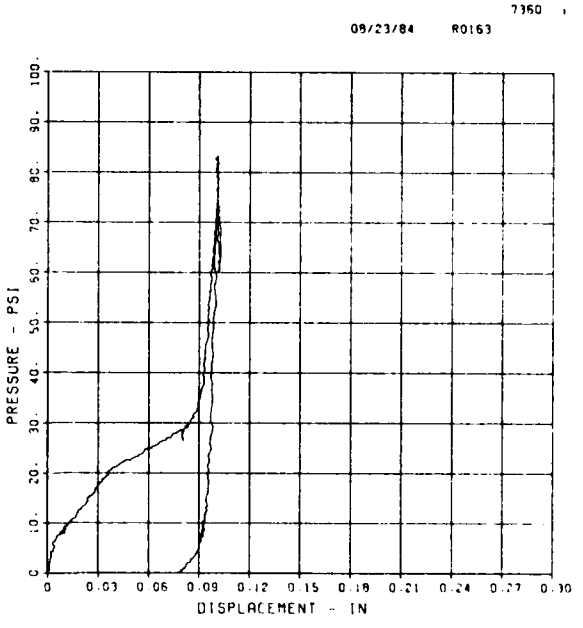

SLAB RESTRAINT G4
D-4-S

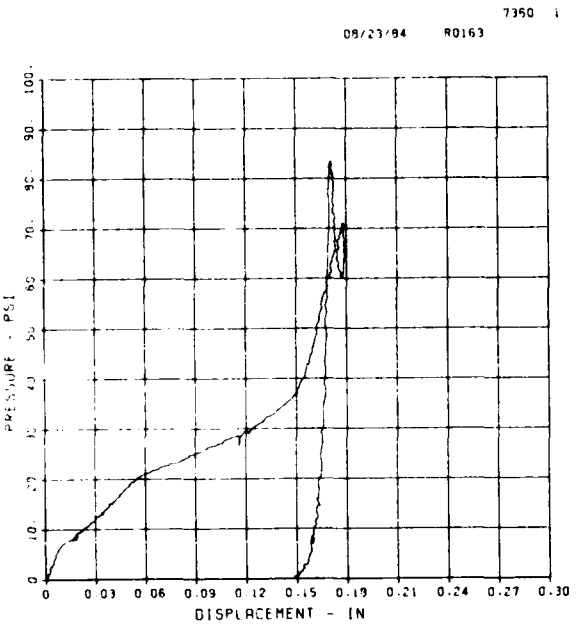

SLAB RESTRAINT G4
ST-1-S

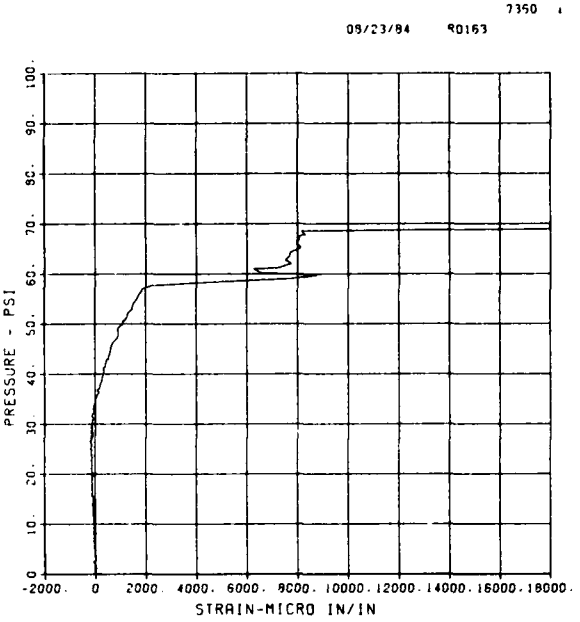

SLAB RESTRAINT G4
ST-3-S

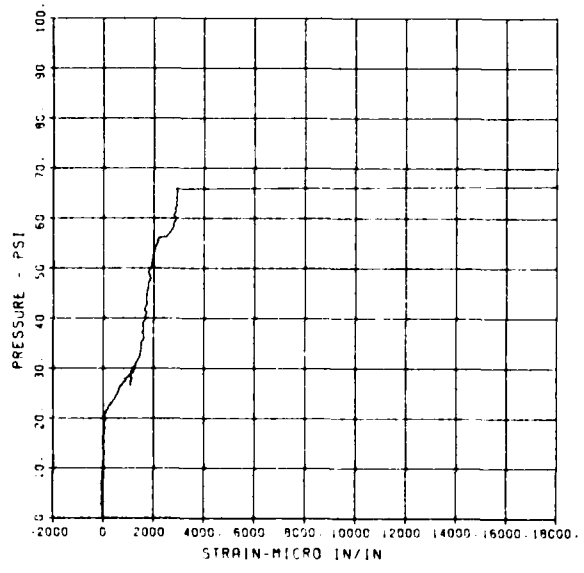

SLAB RESTRAINT G4
SB-1-S

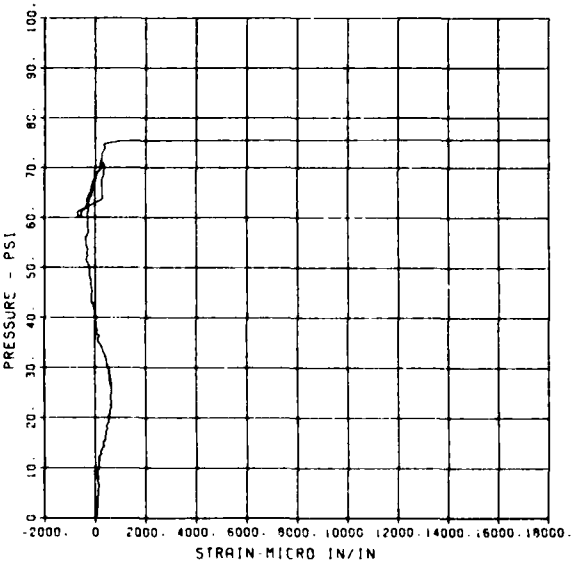

SLAB RESTRAINT G4
SB-3-S

7360 1
08/23/84 90163

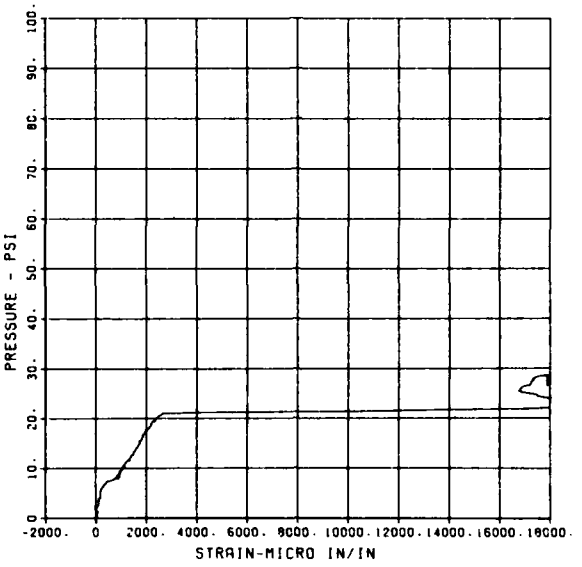

SLAB RESTRAINT G4A

SLAB RESTRAINT C4A
D-1

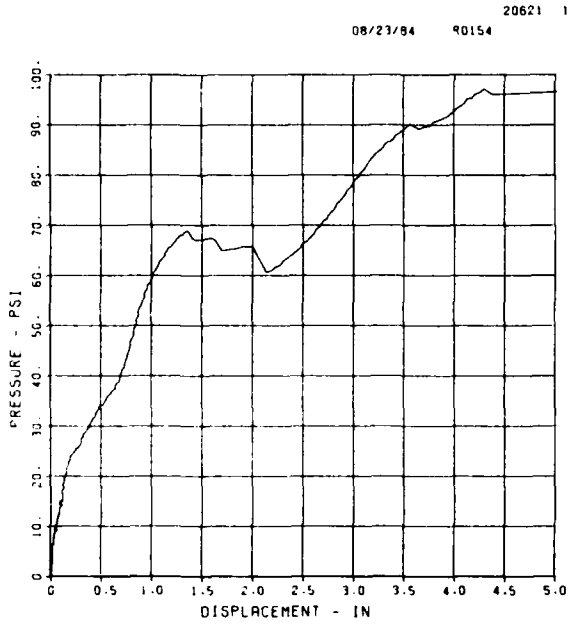

SLAB RESTRAINT C4A
D-2

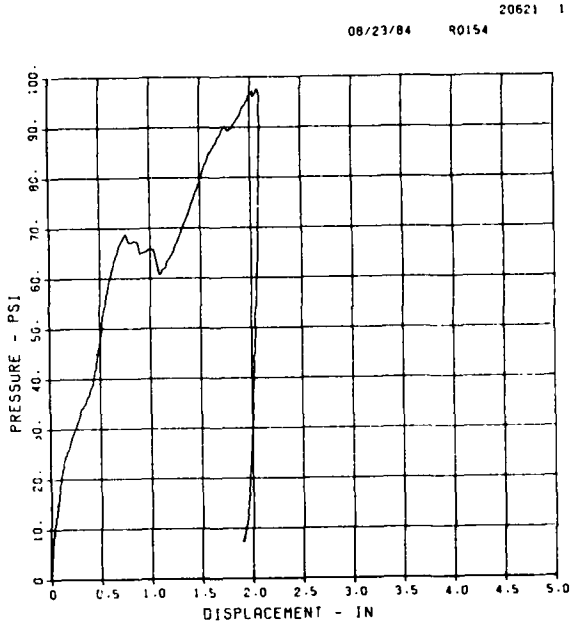

SLAB RESTRAINT C4A
D-3

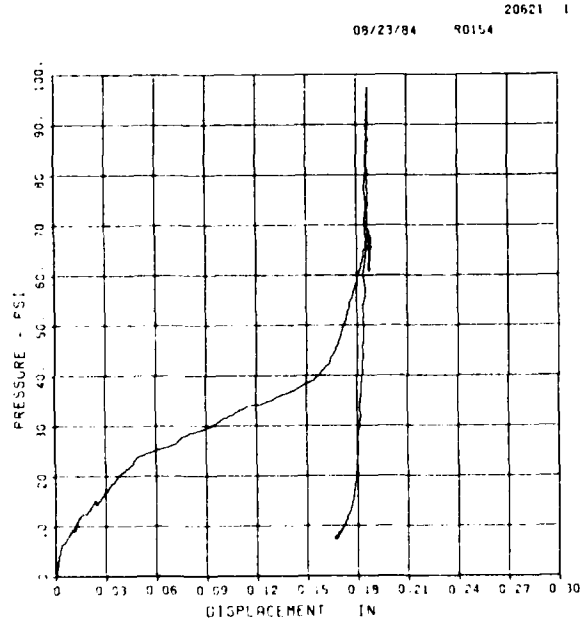

SLAB RESTRAINT C4A
D-4

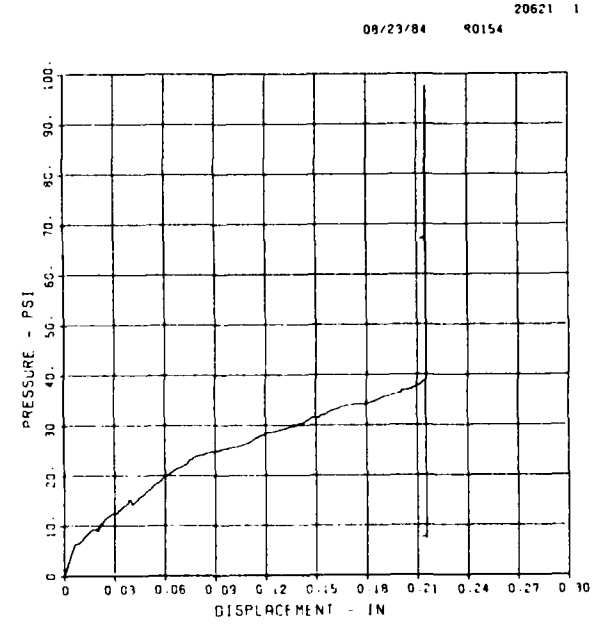

SLAB RESTRAINT C4A
LW-1

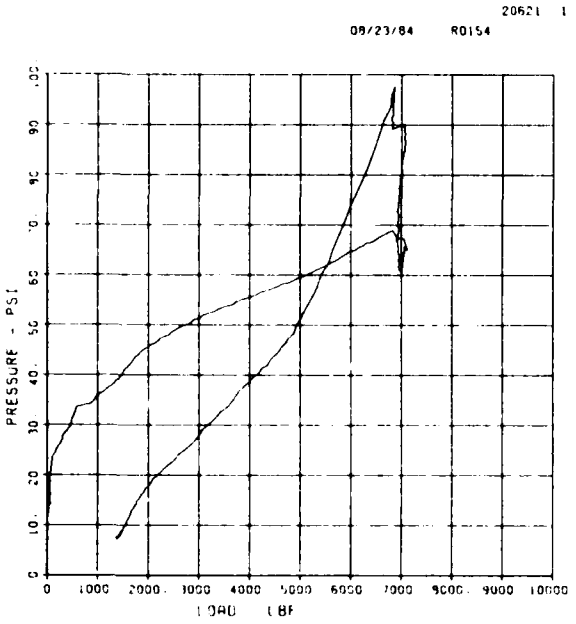

SLAB RESTRAINT C4A
LW-2

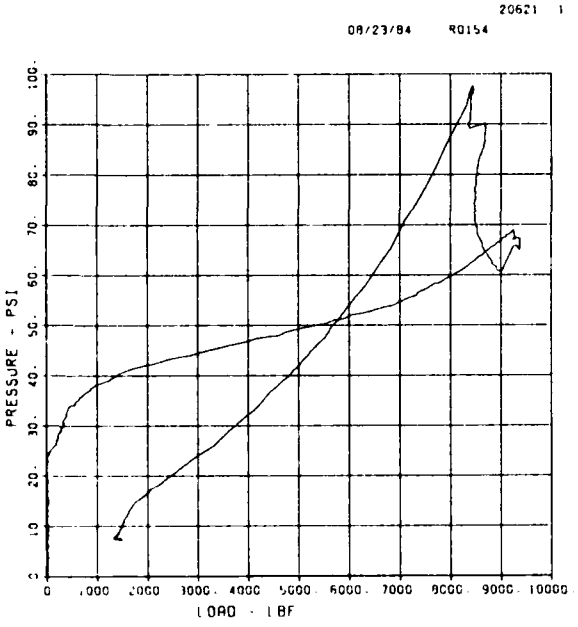

SLAB RESTRAINT C4A
LW-3

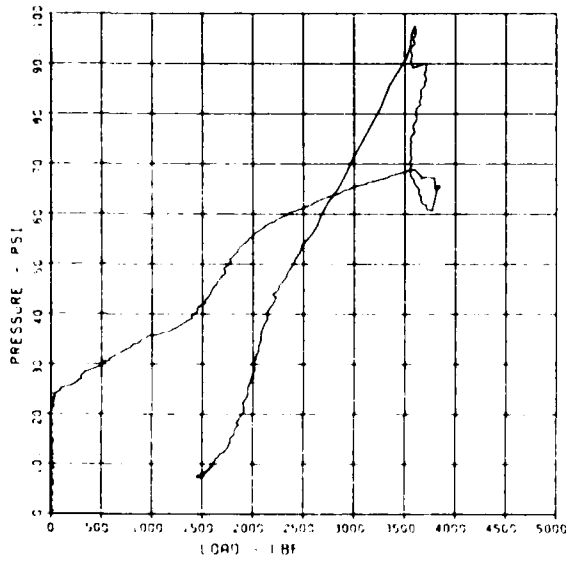

SLAB RESTRAINT C4A
LW-4

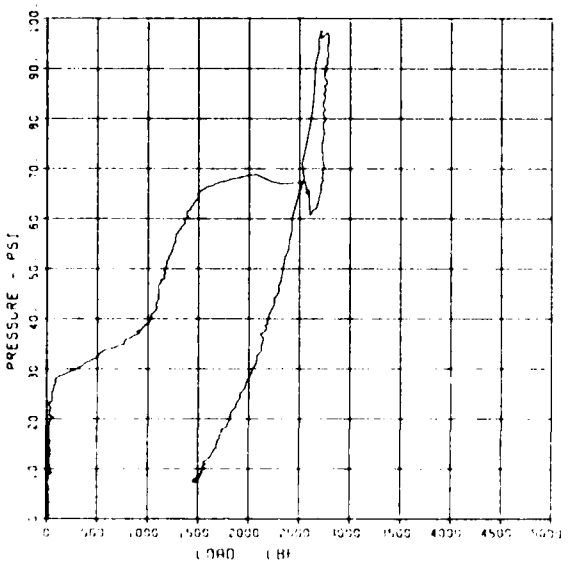

SLAB RESTRAINT G4A
LW-5

20621 1
08/23/84 R0154

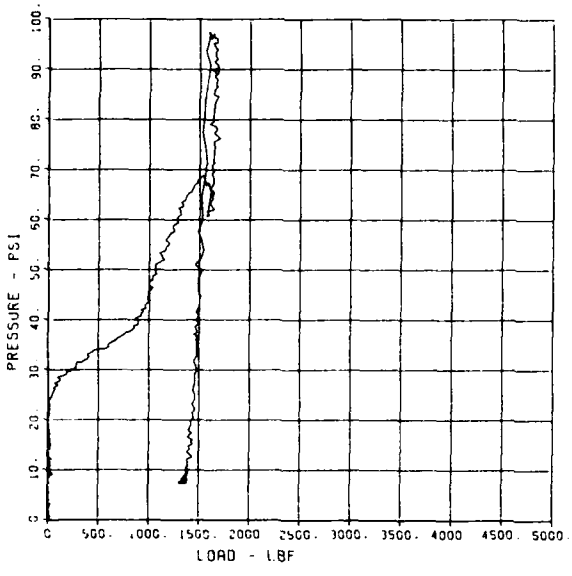

SLAB RESTRAINT G4A
LW-6

20621 1
08/23/84 R0154

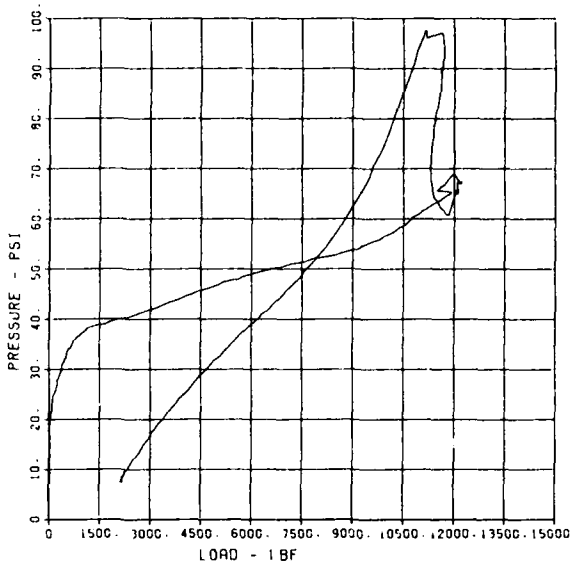

SLAB RESTRAINT G4A
LW-7

20621 1
08/23/84 R0154

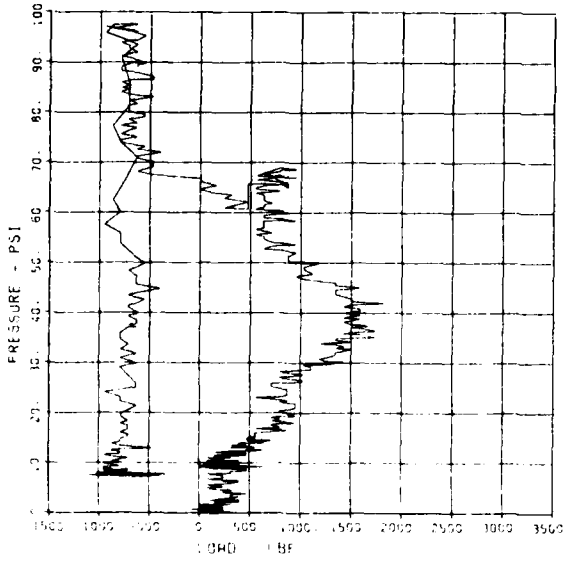

SLAB RESTRAINT G4A
LW-11

20621 1
09/23/84 R0154

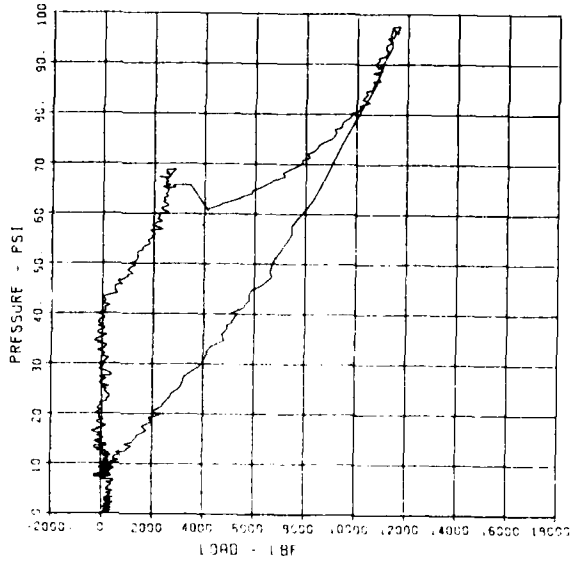

SLAB RESTRAINT G49
ST-1

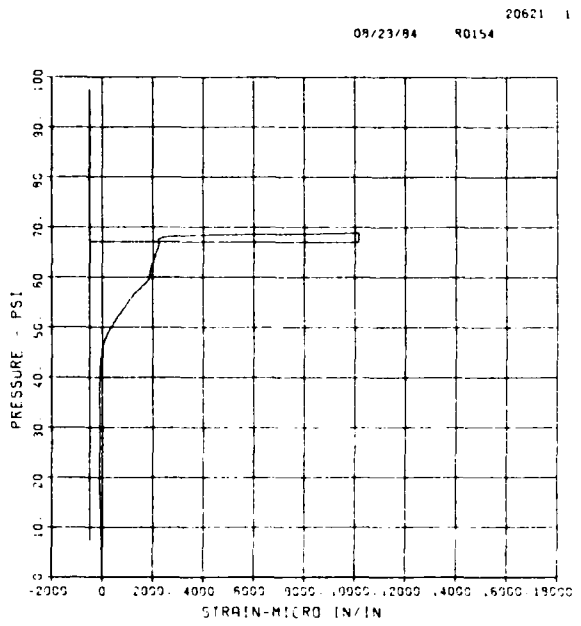

SLAB RESTRAINT G49
ST-2

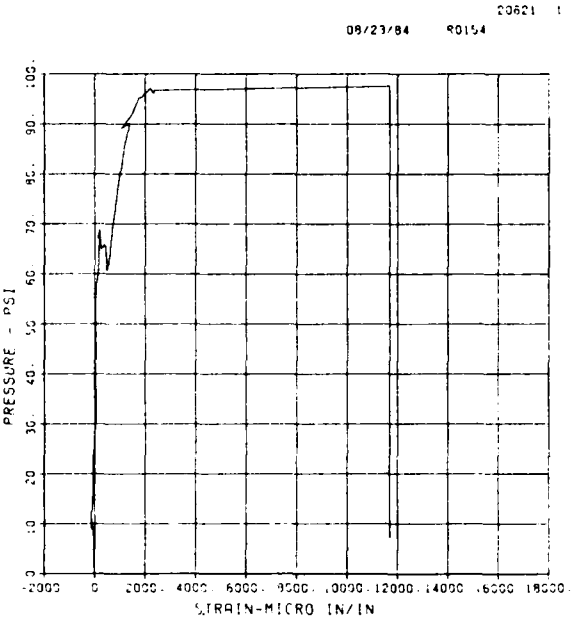

SLAB RESTRAINT G49
ST-3

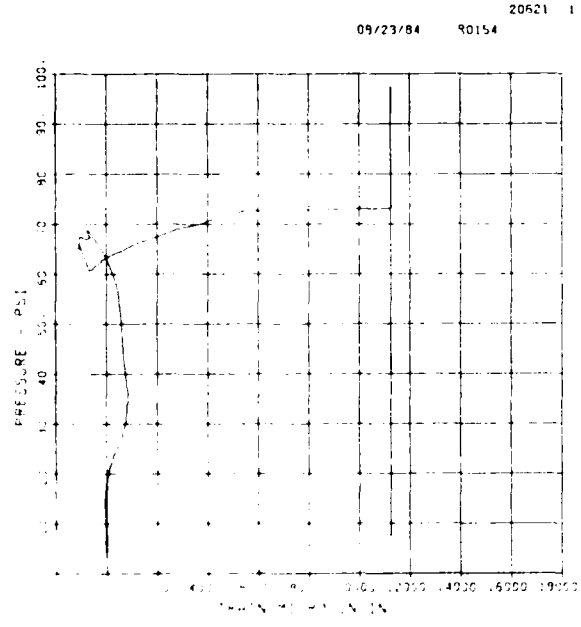

SLAB RESTRAINT G49
SB-1

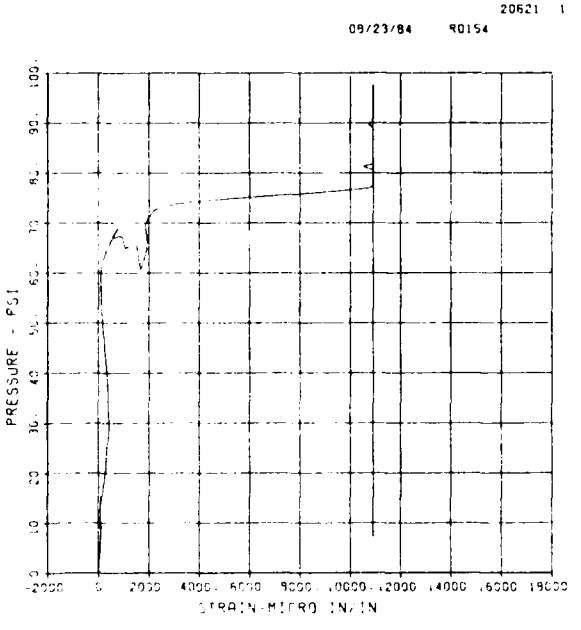

SLAB RESTRAINT C4A
SB-2

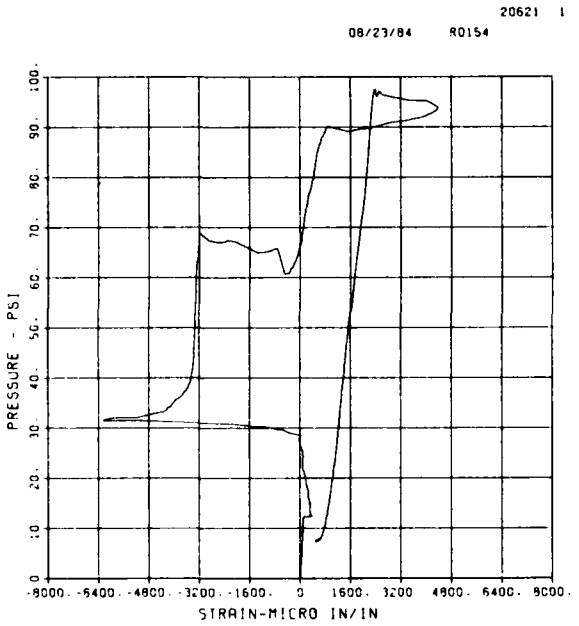

SLAB RESTRAINT C4A
SB-3

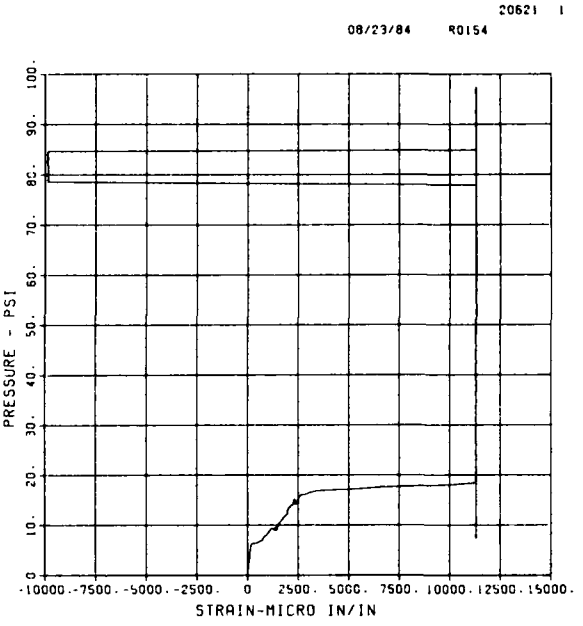

SLAB RESTRAINT C4A
D-3-S

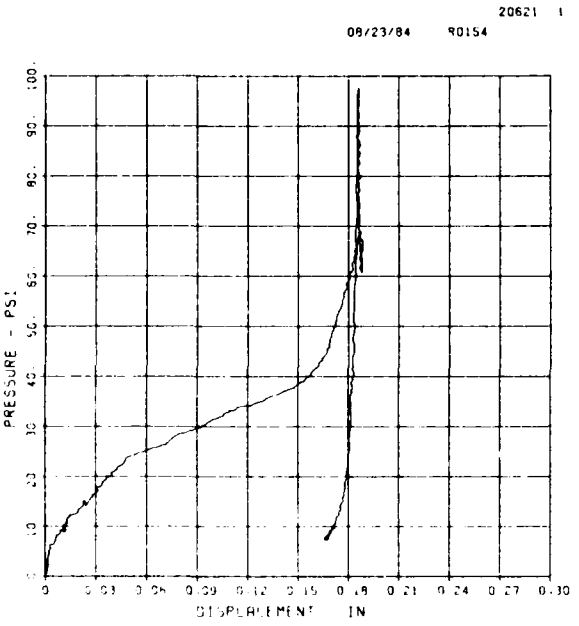

SLAB RESTRAINT C4A
D-4-S

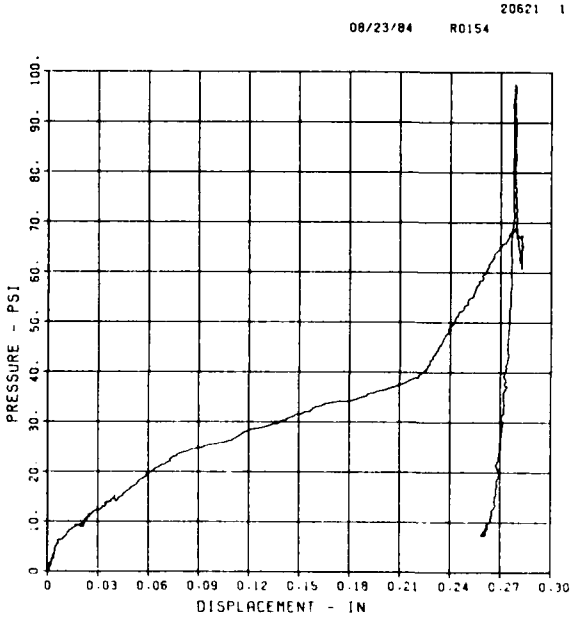

SLAB RESTRAINT G4A
ST-1-S

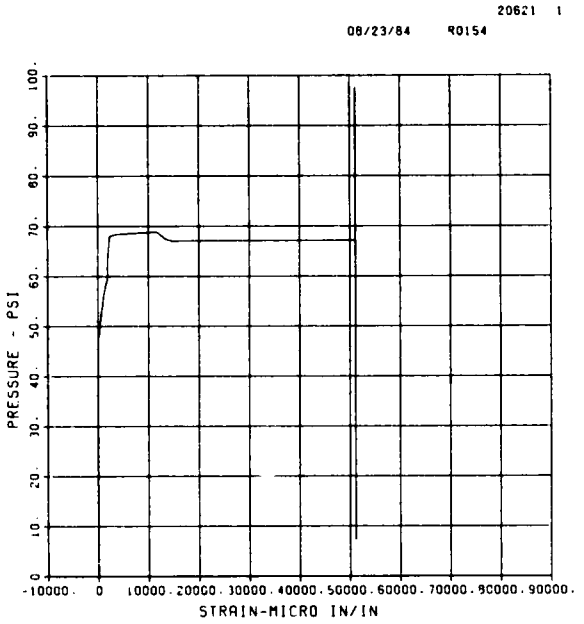

SLAB RESTRAINT G4A
ST-3-S

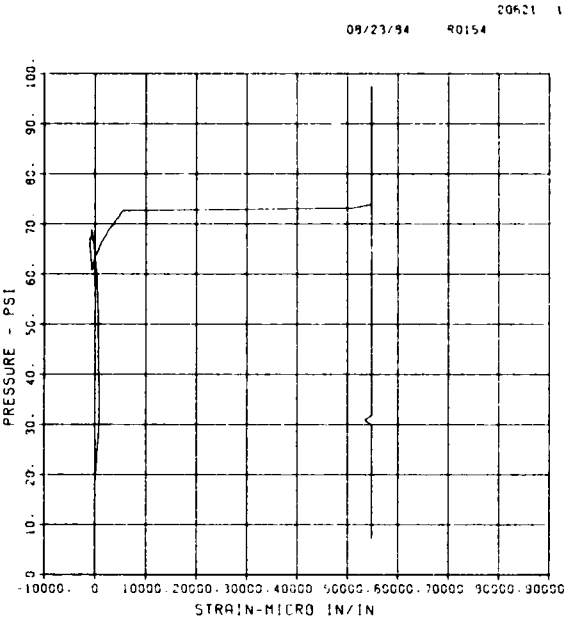

SLAB RESTRAINT G4A
SB-1-S

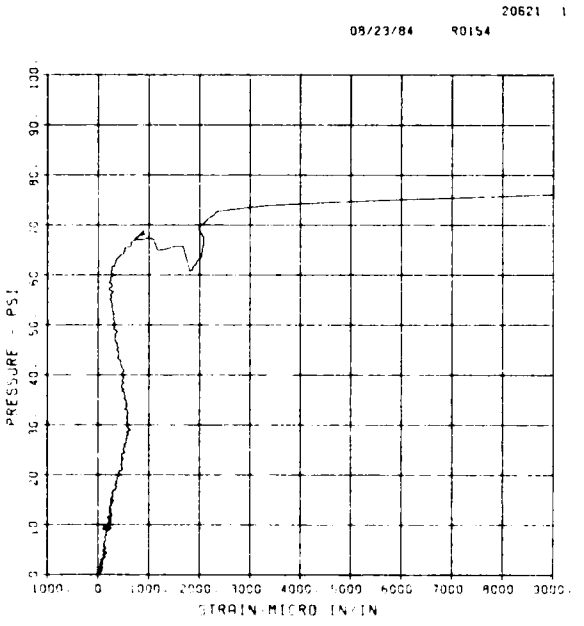

SLAB RESTRAINT G4A
SB-3-S

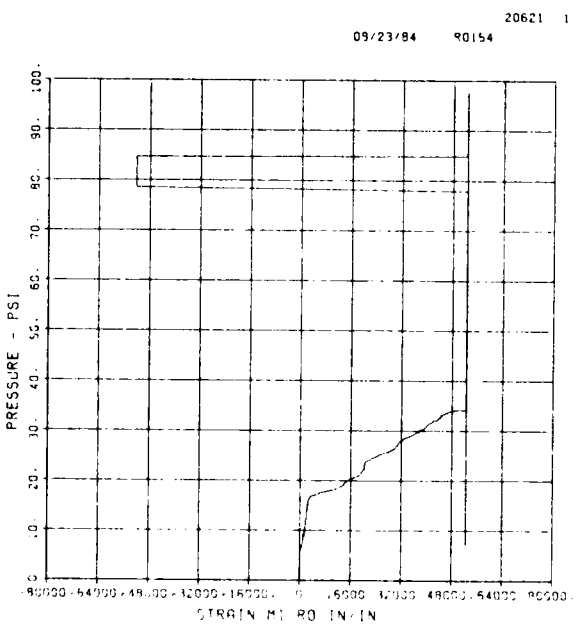

SLAB RESTRAINT G4B

SLAB RESTRAINT C4B
C-1

6918 1
08/23/94 R0159

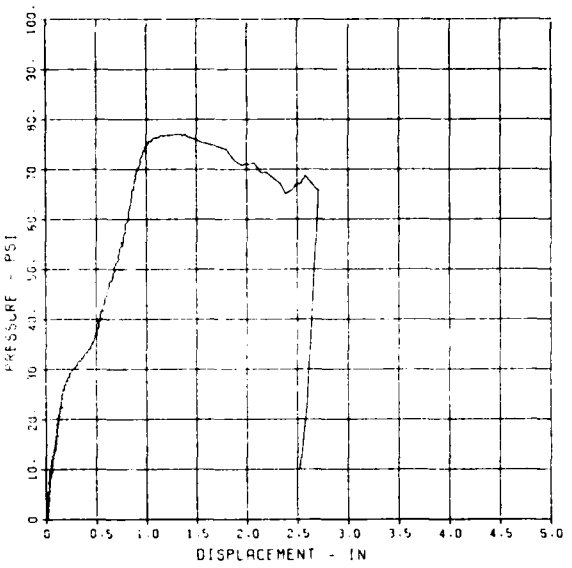

SLAB RESTRAINT C4B
C-2

6918 1
08/23/94 R0159

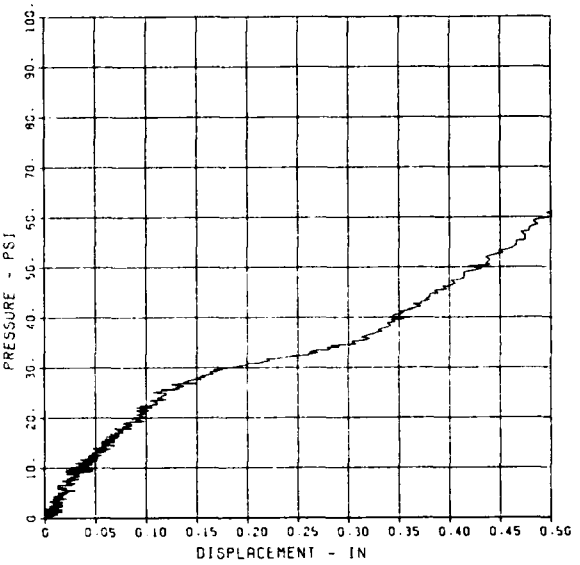

SLAB RESTRAINT C4B
C-3

6918 1
08/23/84 R0159

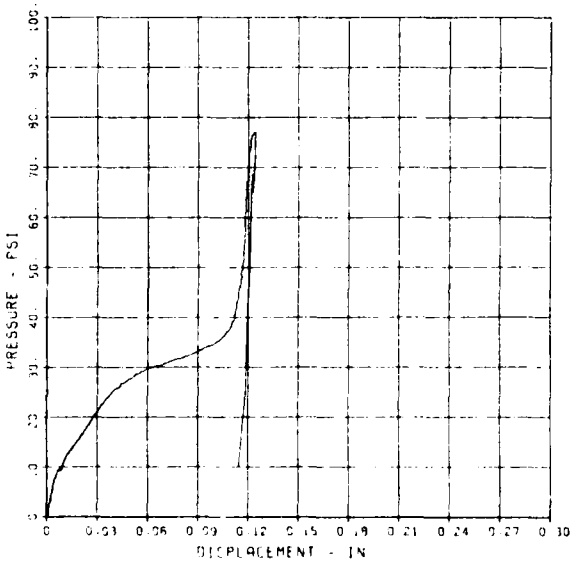

SLAB RESTRAINT C4B
C-4

6918 1
08/23/84 R0159

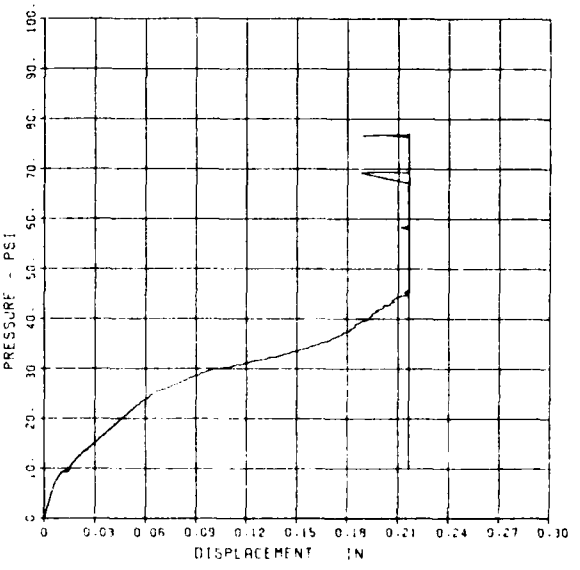

SLAB RESTRAINT G4B
LW-1

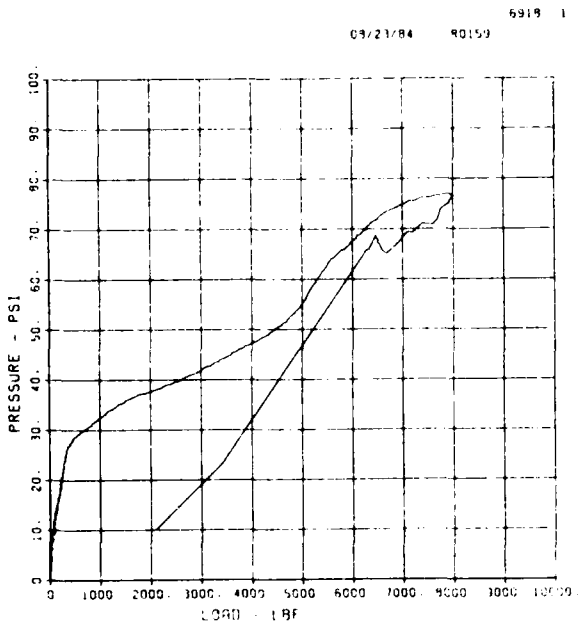

SLAB RESTRAINT G4B
LW-2

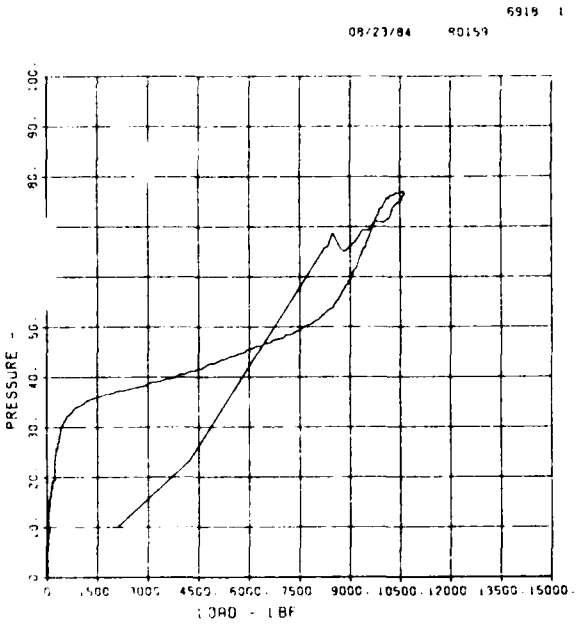

SLAB RESTRAINT G4B
LW-3

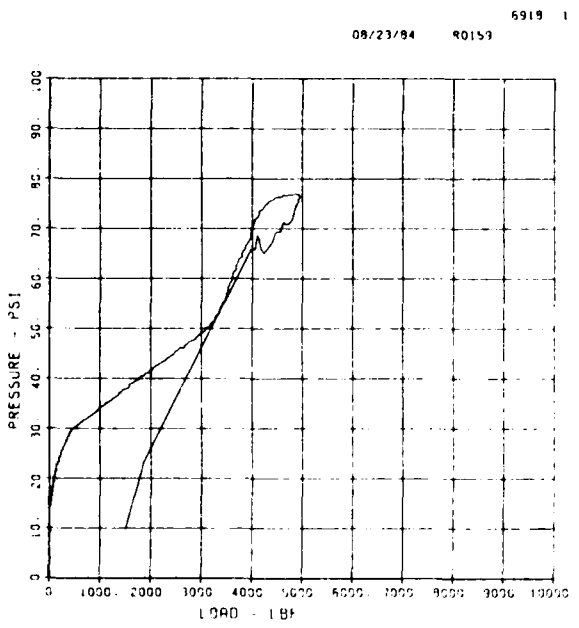

SLAB RESTRAINT G4B
LW-4

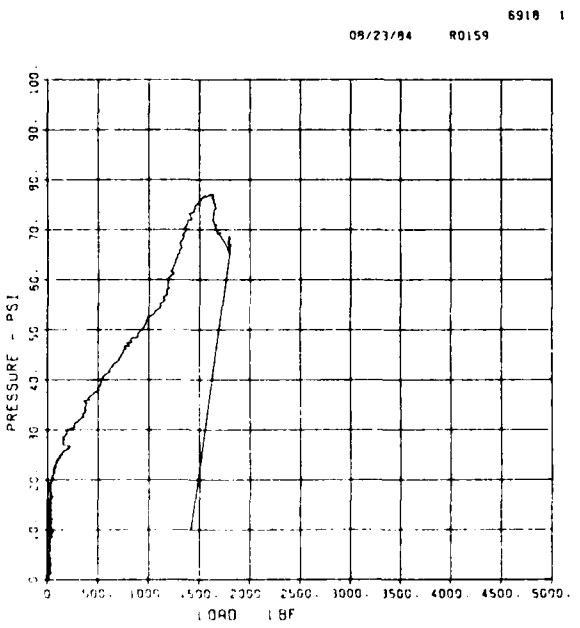

SLAB RESTRAINT C4B
LW-5

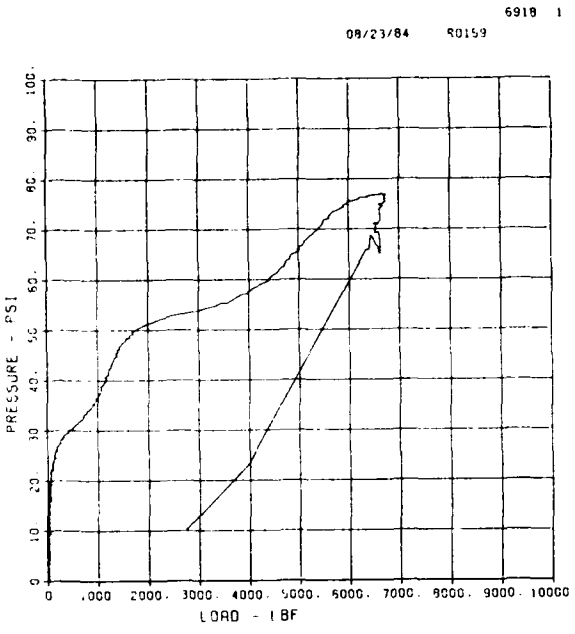

SLAB RESTRAINT C4B
LW-6

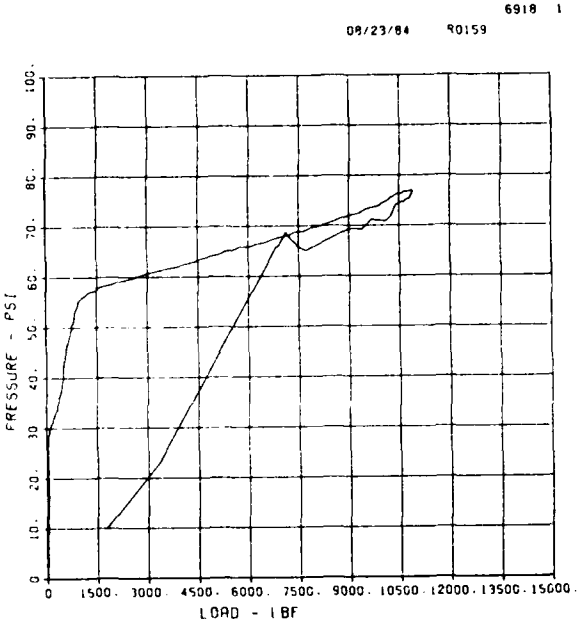

SLAB RESTRAINT C4B
LW-7

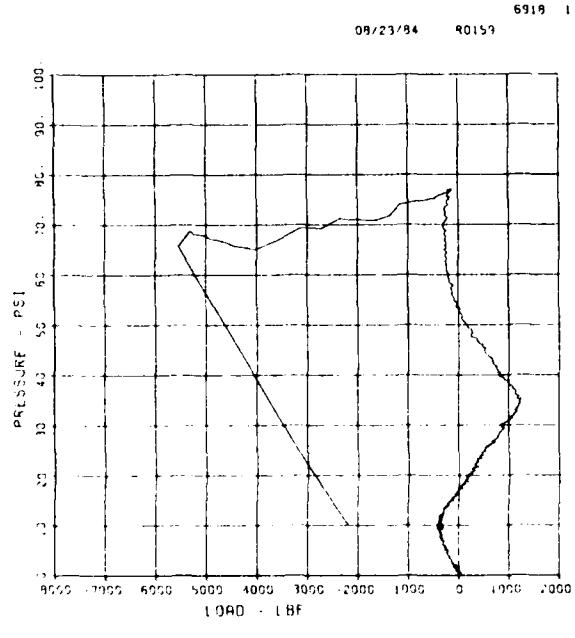

SLAB RESTRAINT C4B
LW-8

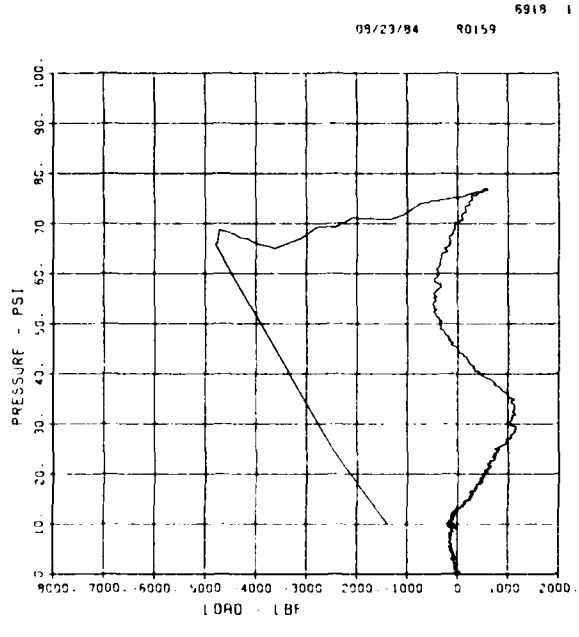

SLAB RESTRAINT G4B
LW-9

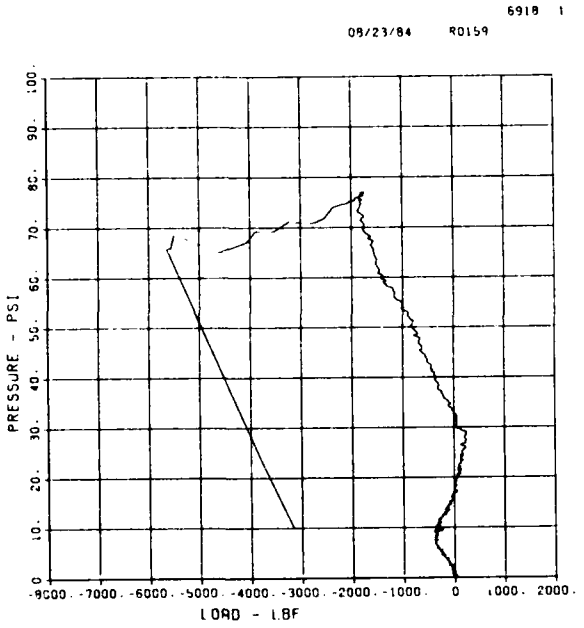

SLAB RESTRAINT G4B
LW-11

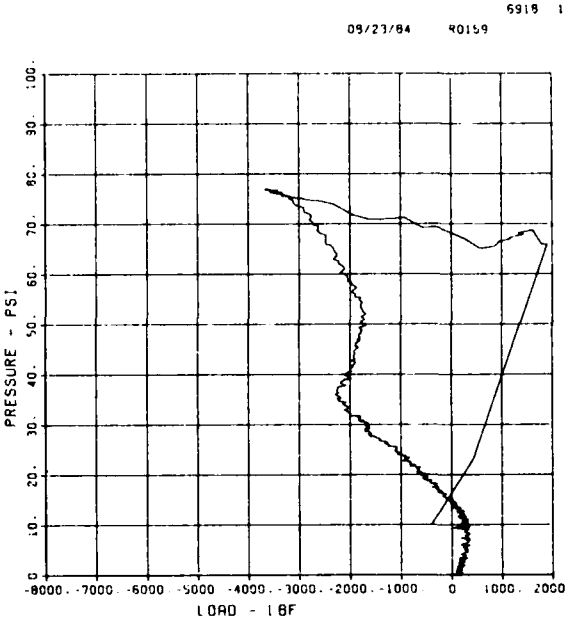

SLAB RESTRAINT G4B
LW-12

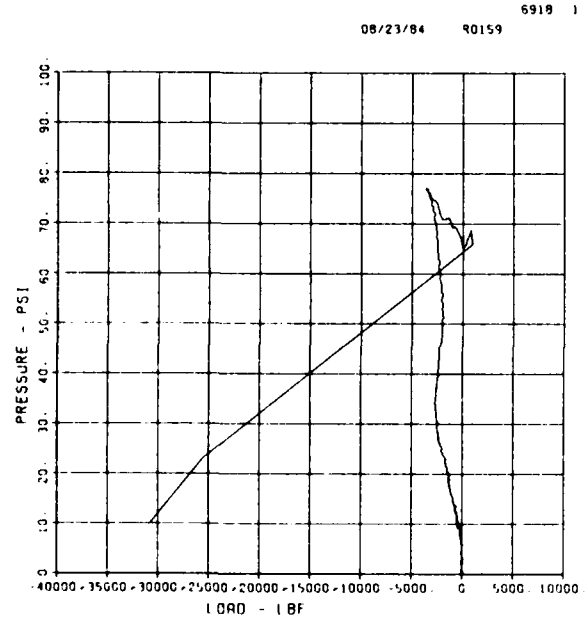

SLAB RESTRAINT G4B
LW-13

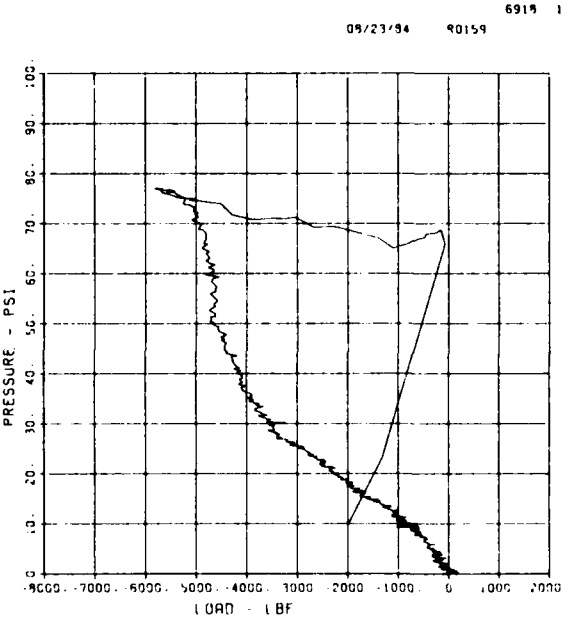

SLAB RESTRAINT G4B
ST-1

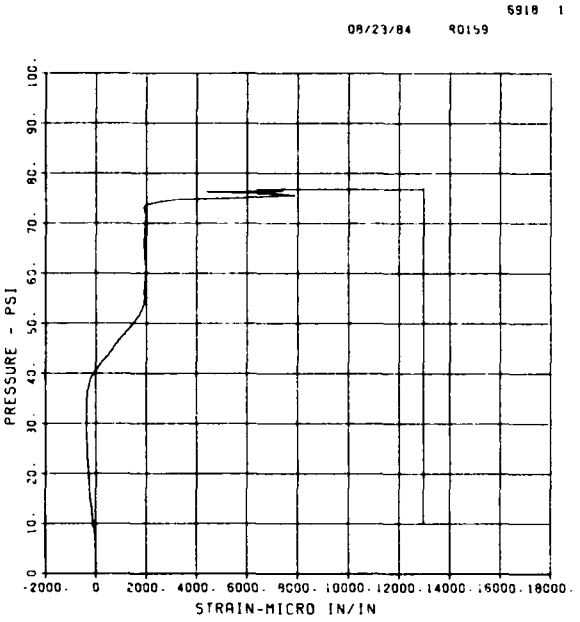

SLAB RESTRAINT G4B
ST-2

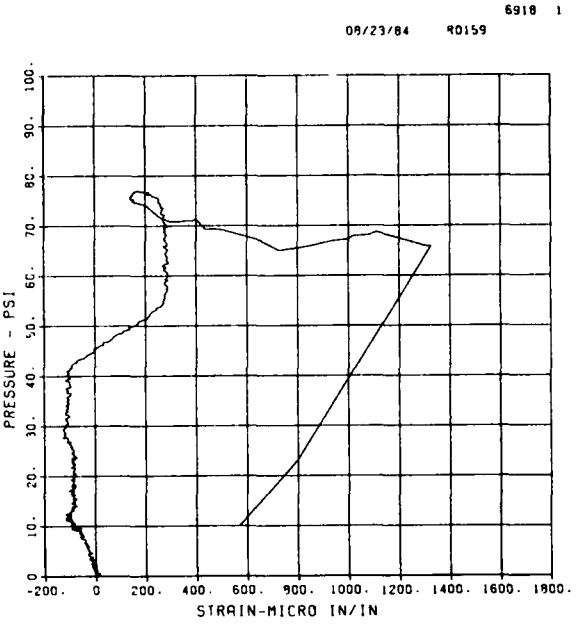

SLAB RESTRAINT G4B
ST-3

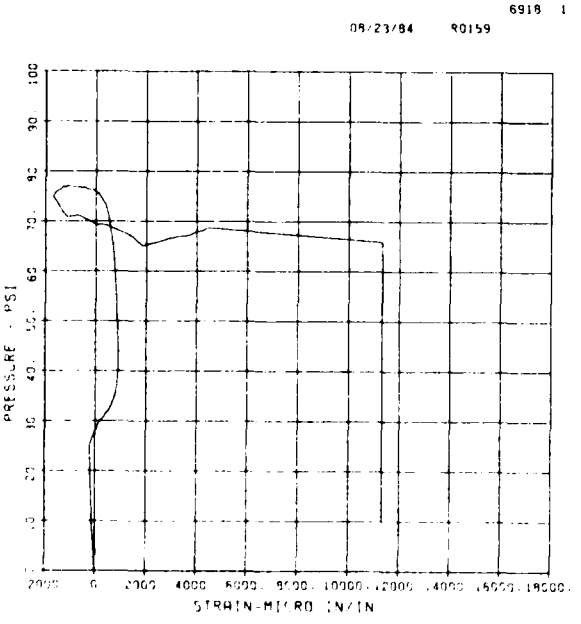

SLAB RESTRAINT G4B
SB-1

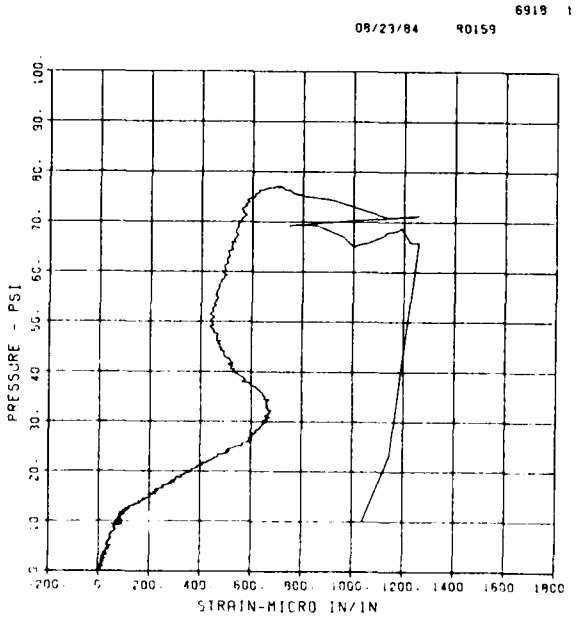

SLAB RESTRAINT G4B
SB-2

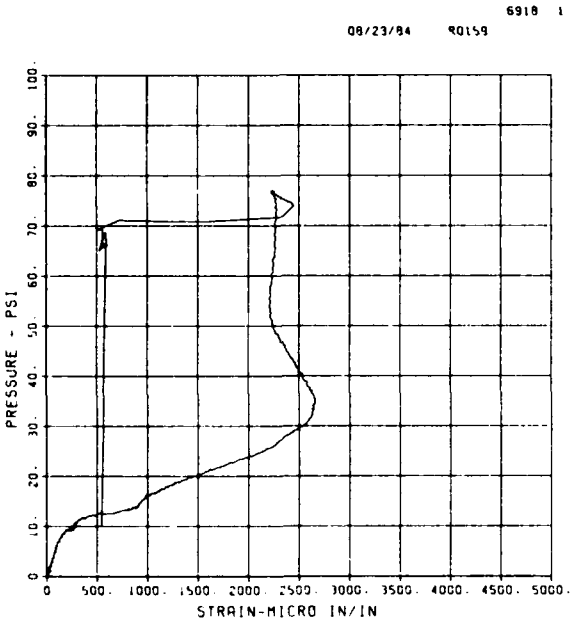

SLAB RESTRAINT G4B
SB-3

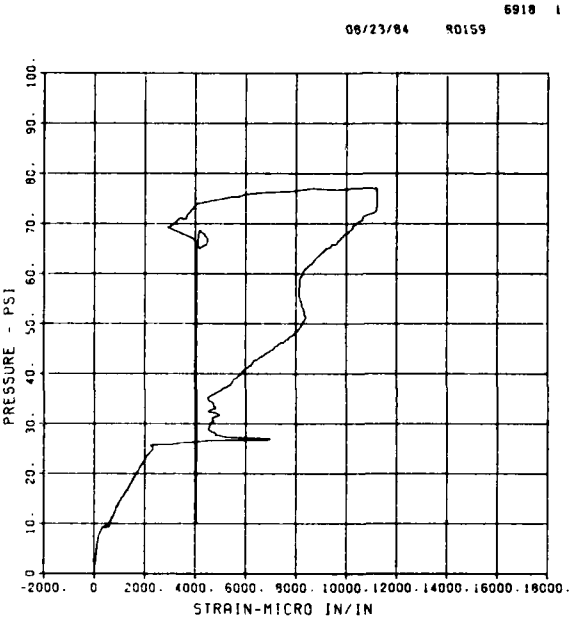

SLAB RESTRAINT G4B
D-3-S

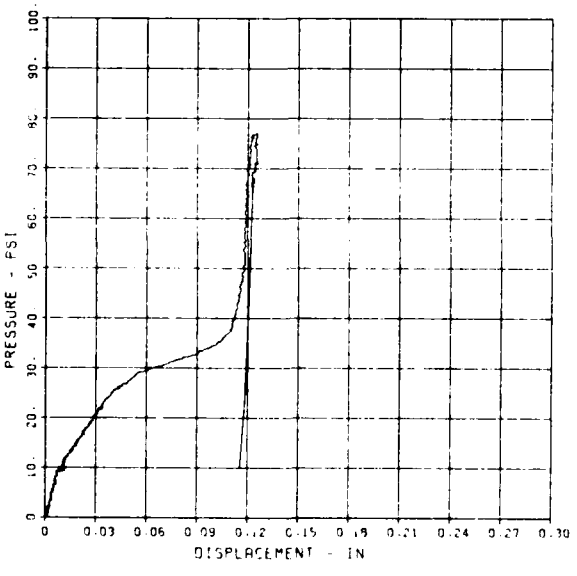

SLAB RESTRAINT G4B
D-4-S

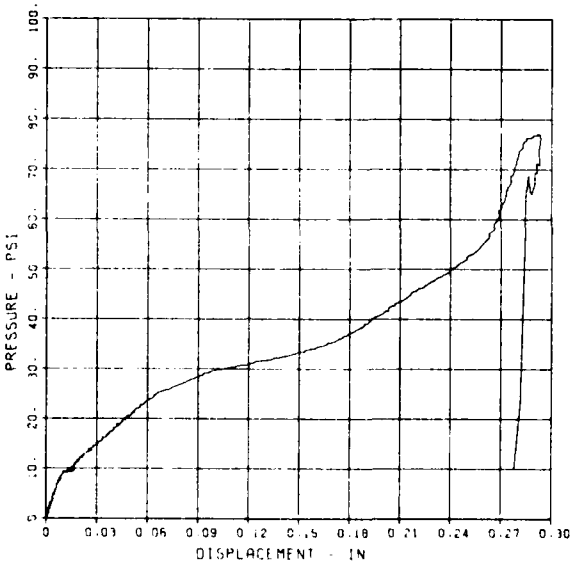

SLAB RESTRAINT C4B
ST-1-S

6918 1
09/23/84 R0159

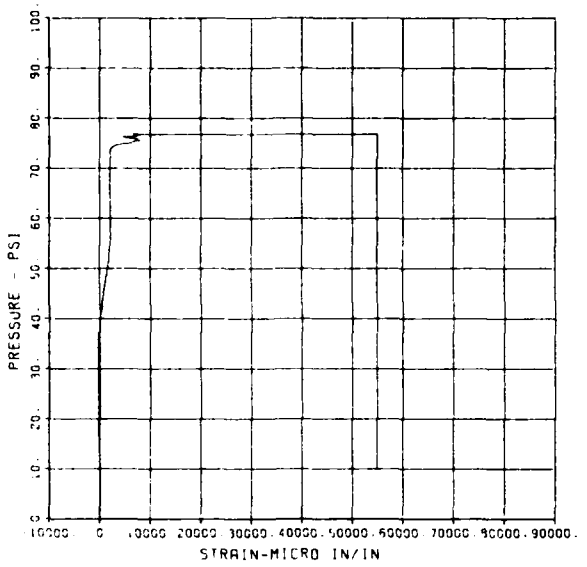

SLAB RESTRAINT C4B
ST-3-S

6918 1
09/23/84 R0159

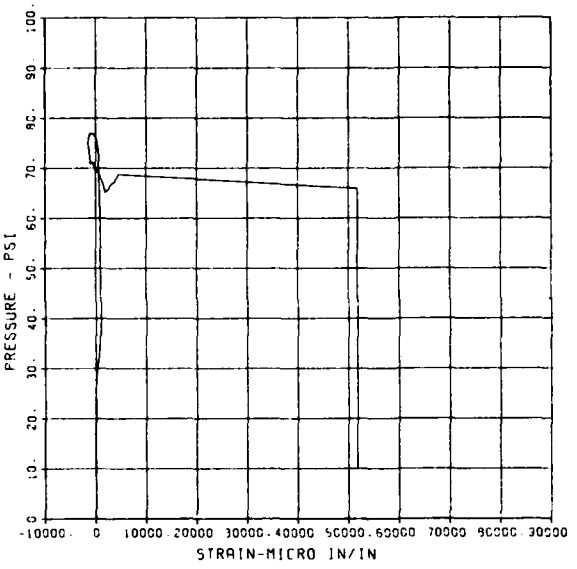

SLAB RESTRAINT C4B
SB-1-S

6919 1
09/23/84 R0159

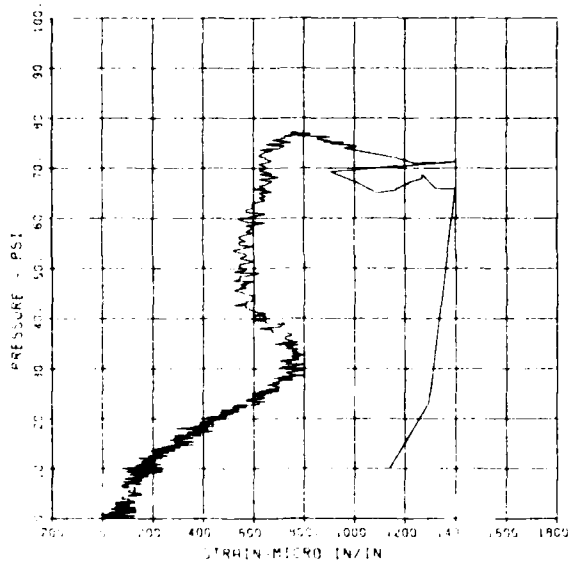

SLAB RESTRAINT C4B
SB-3-S

6919 1
09/23/84 R0159

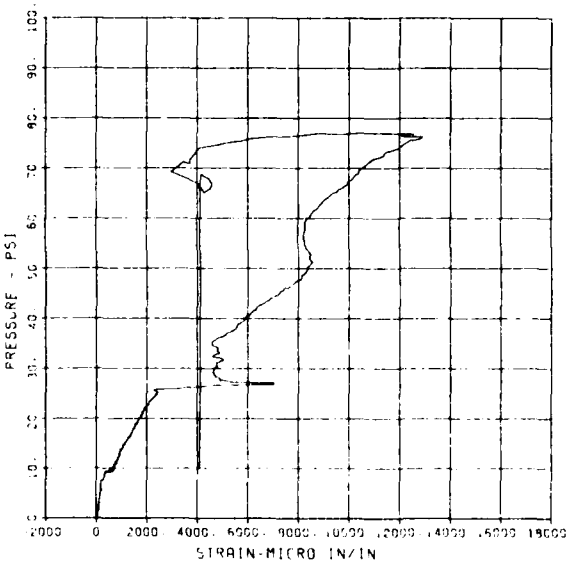

SLAB RESTRAINT G5

SLAB RESTRAINT G5
G-1

19305
10/09/84 R0435

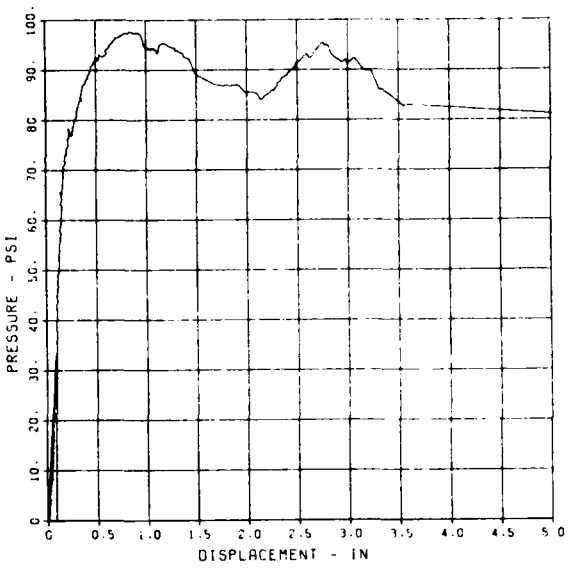

SLAB RESTRAINT G5
G-2

19305
10/09/84 R0435

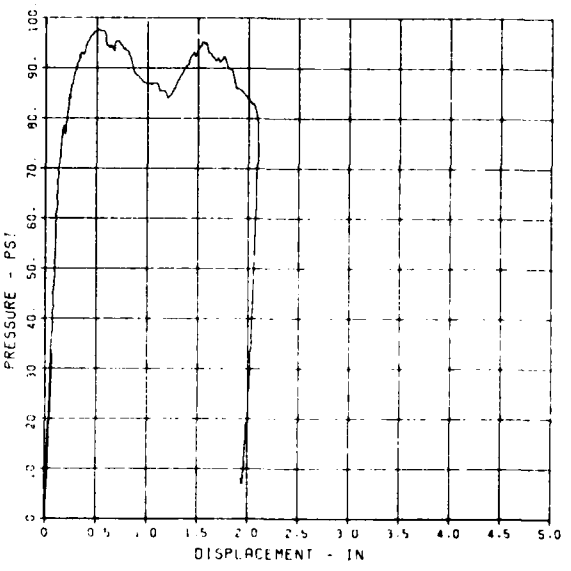

SLAB RESTRAINT G5
G-3

19305
10/09/84 R0435

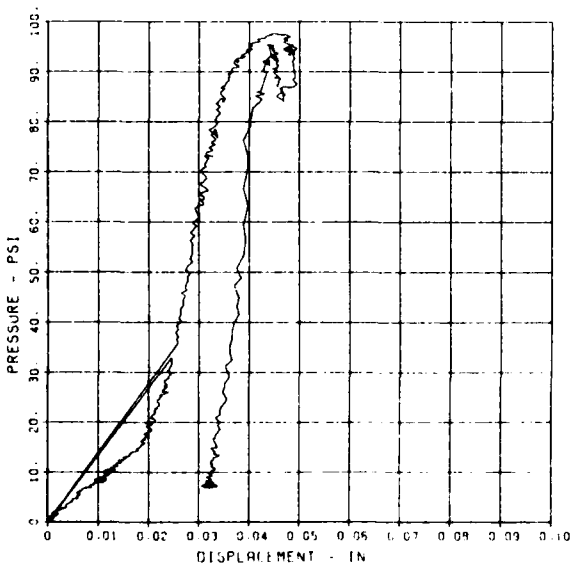

SLAB RESTRAINT G5
G-4

19305
10/09/84 R0435

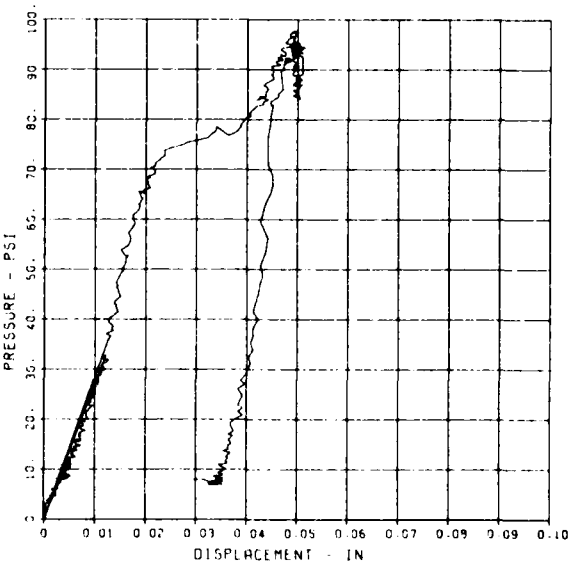

SLAB RESTRAINT G5
LW-1

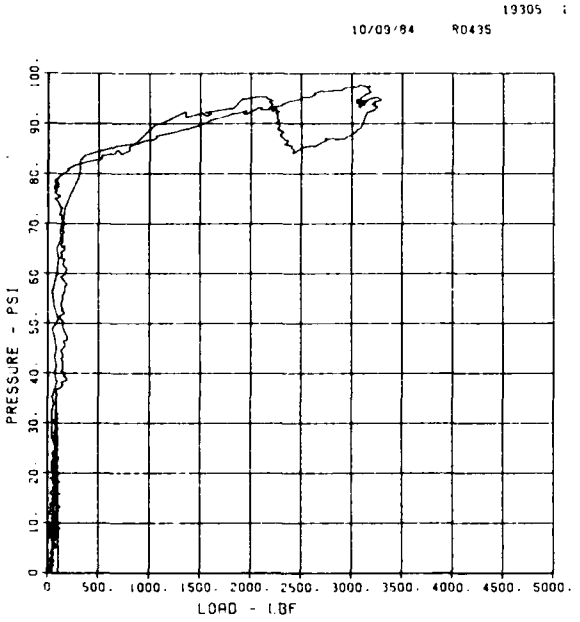

SLAB RESTRAINT G5
LW-2

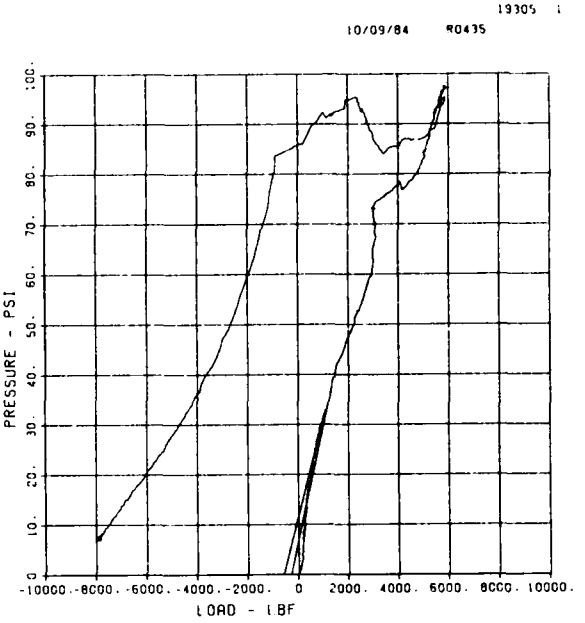

SLAB RESTRAINT G5
LW-3

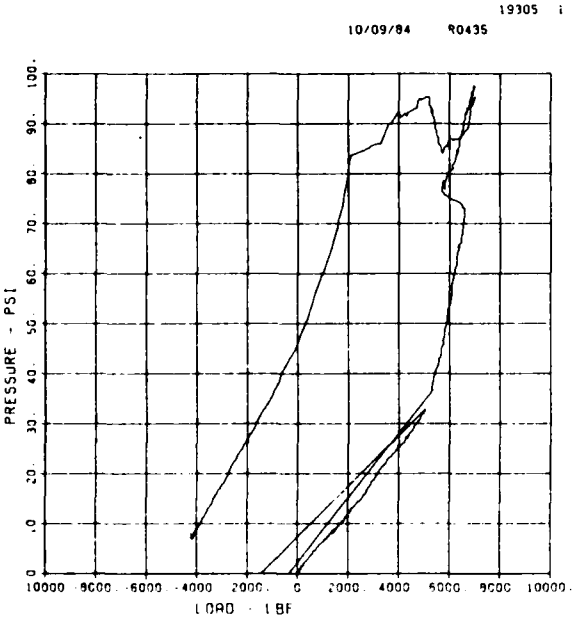

SLAB RESTRAINT G5
LW-4

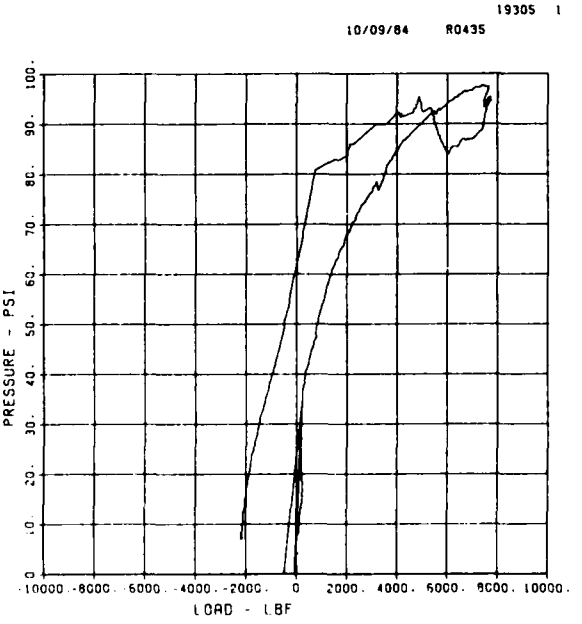

SLAB RESTRAINT GS
LW-5

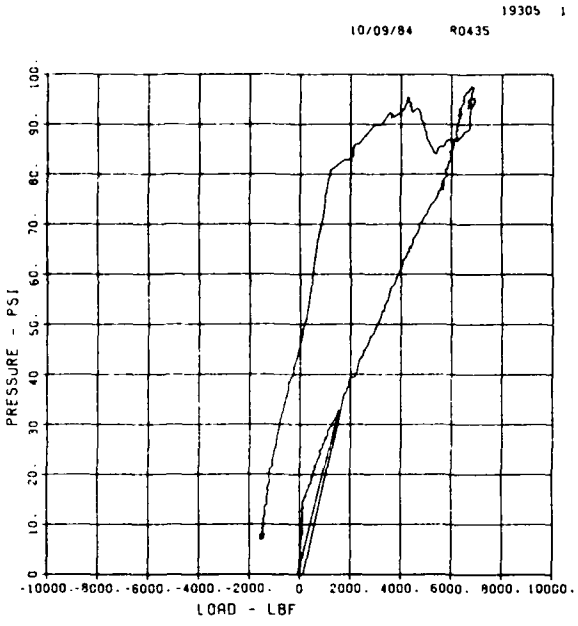

SLAB RESTRAINT GS
LW-6

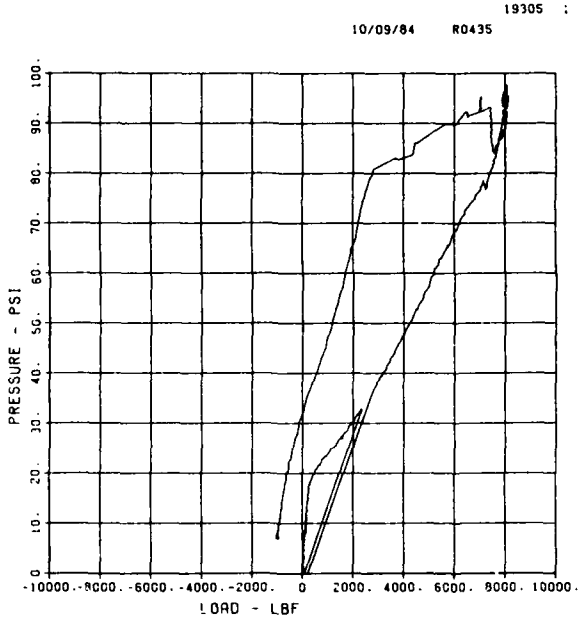

SLAB RESTRAINT GS
LW-7

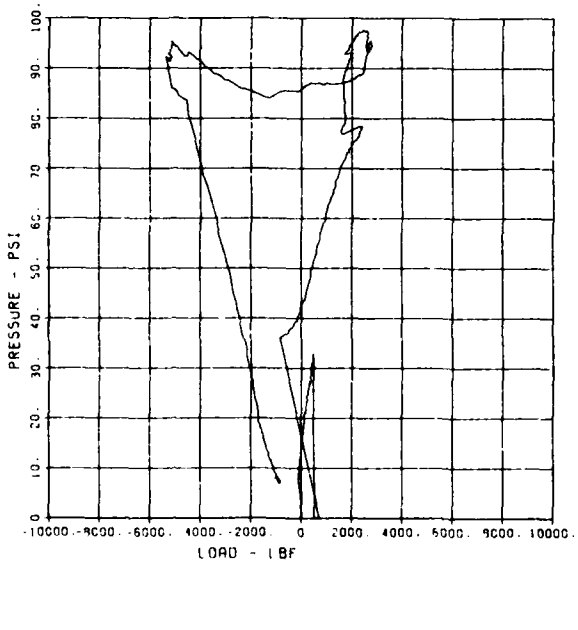

SLAB RESTRAINT GS
LW-8

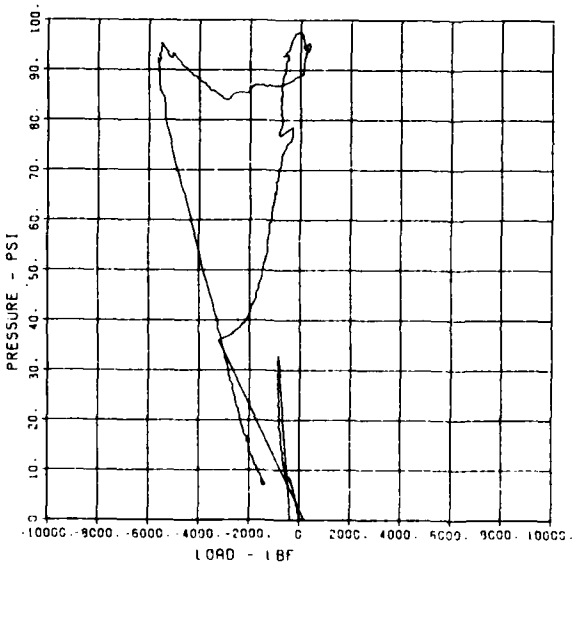

SLAB RESTRAINT G5
LW-9

19305
10/09/84 R0435

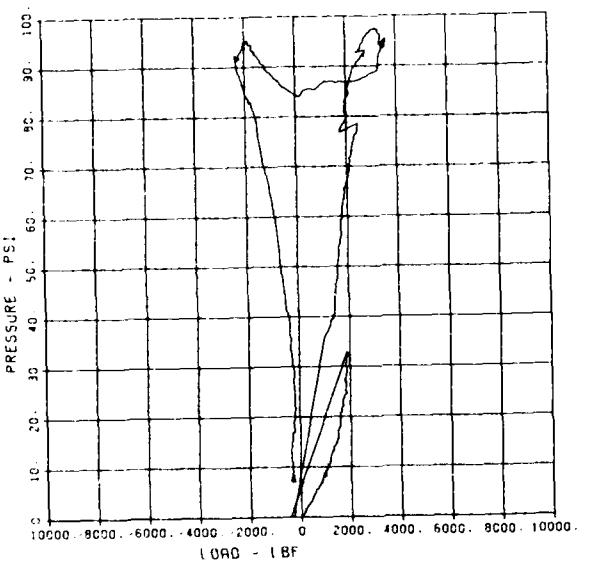

SLAB RESTRAINT G5
LW-10

19305
10/09/84 R0435

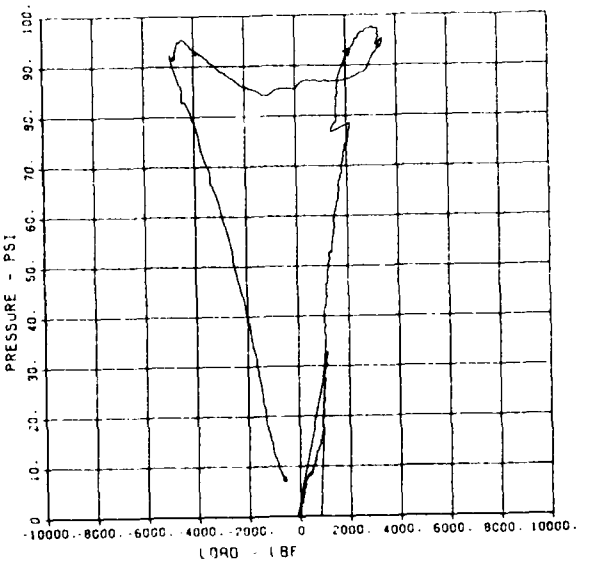

SLAB RESTRAINT G5
LW-11

19305
10/09/84 R0435

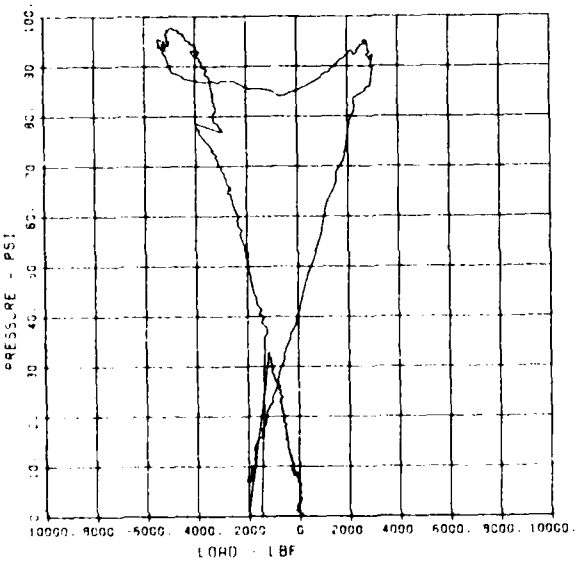

SLAB RESTRAINT G5
LW-13

19305
10/09/84 R0435

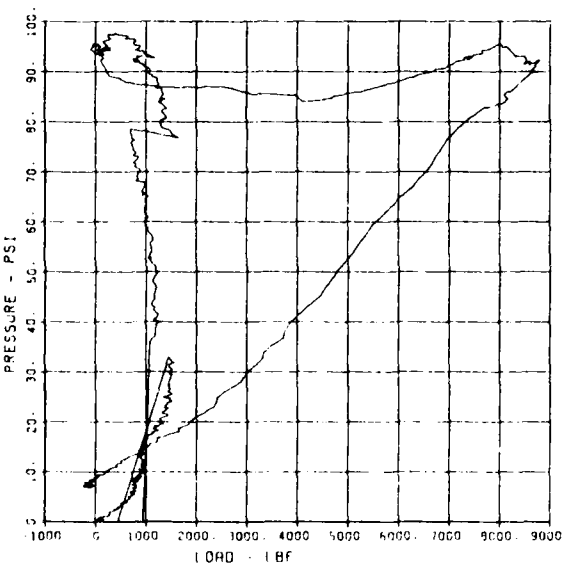

SLAB RESTRAINT GS
LW-14

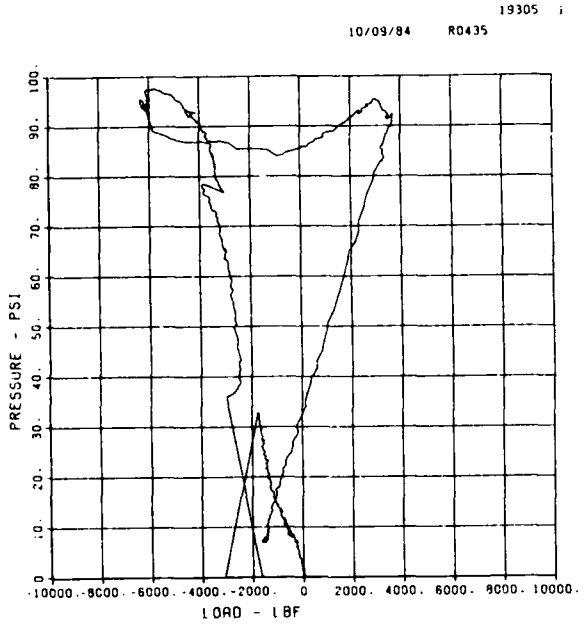

SLAB RESTRAINT GS
LW-15

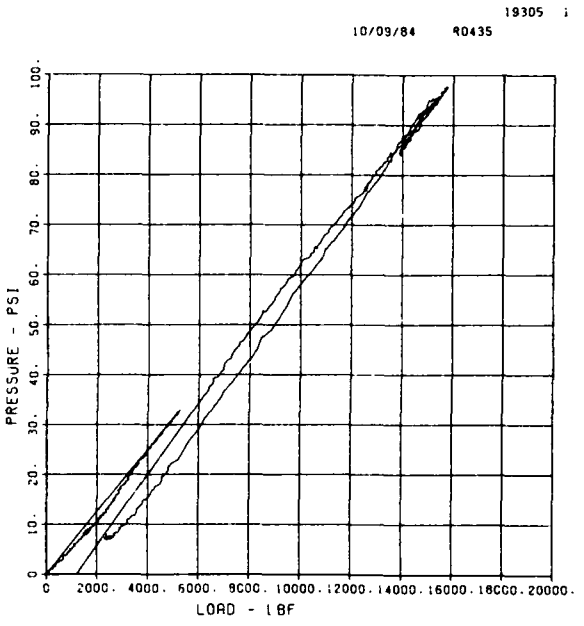

SLAB RESTRAINT GS
ST-1

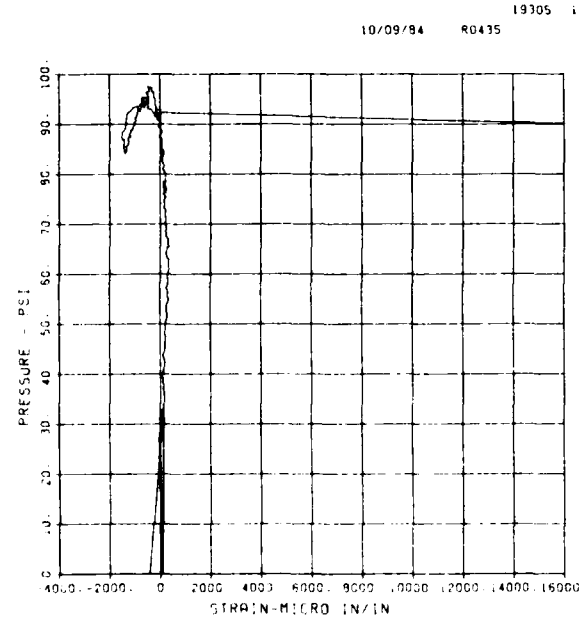

SLAB RESTRAINT GS
ST-2

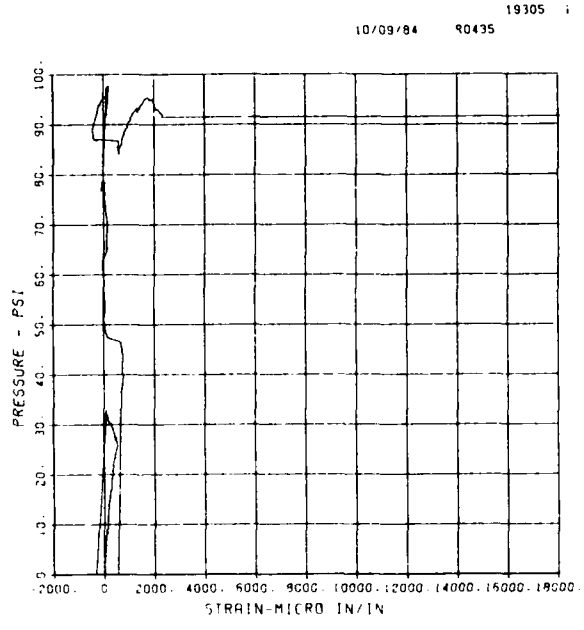

SLAB RESTRAINT G5
ST-3

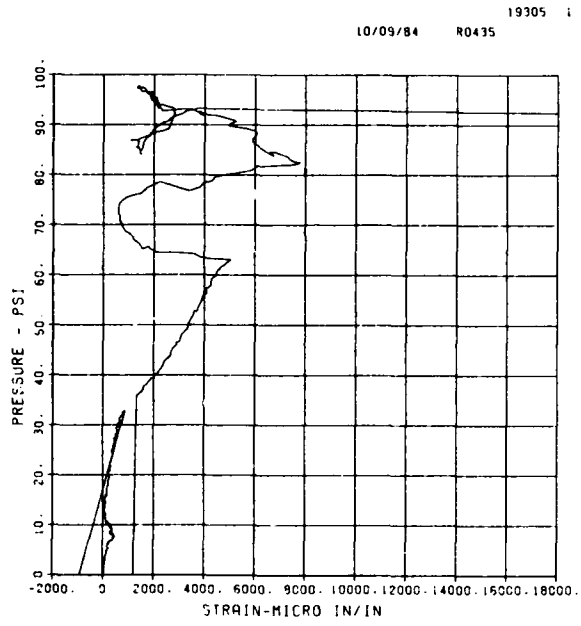

SLAB RESTRAINT G5
SB-1

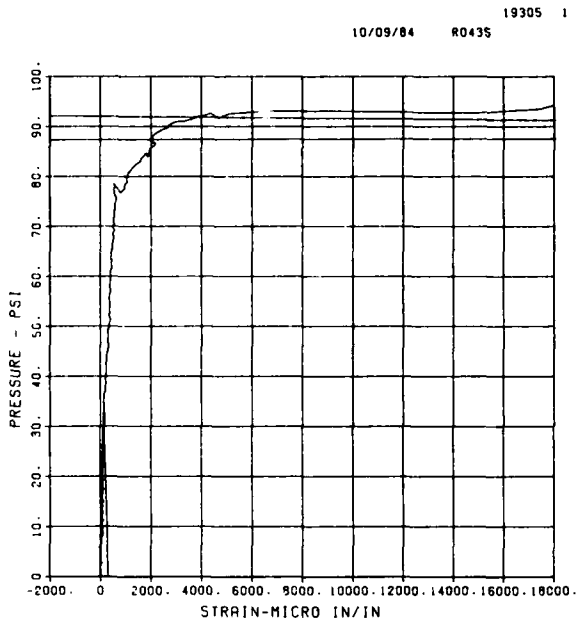

SLAB RESTRAINT G5
SB-2

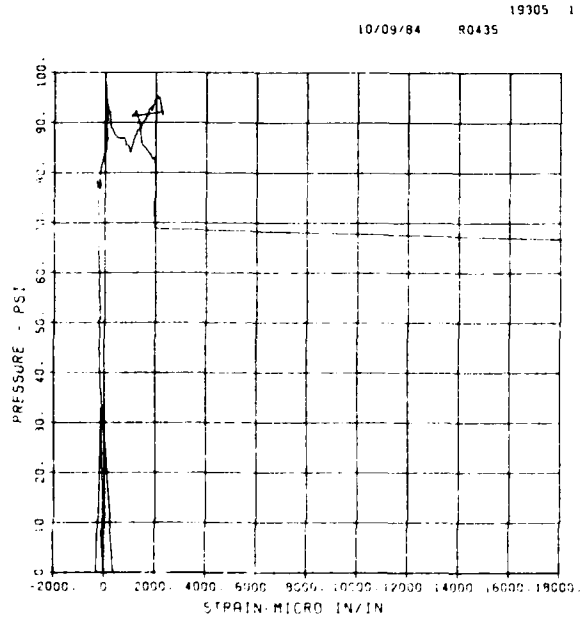

SLAB RESTRAINT G5
SB-3

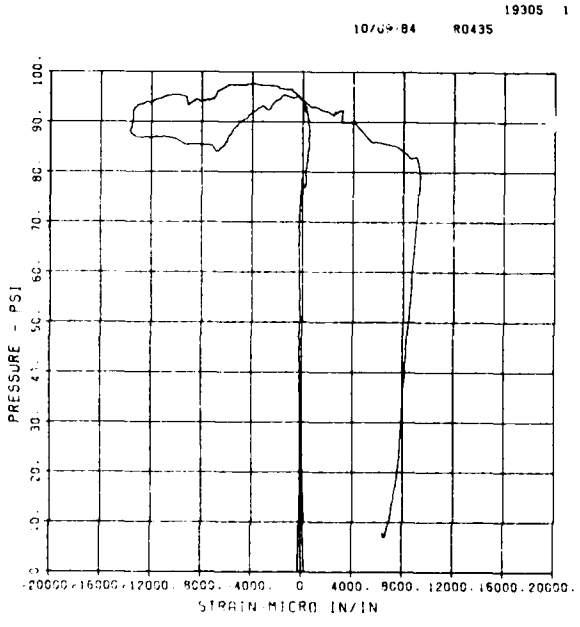

SLAB RESTRAINT G5
CT-1

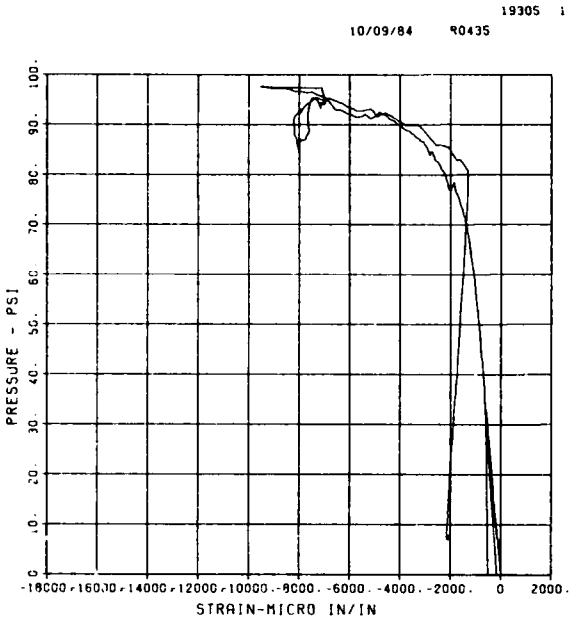

SLAB RESTRAINT G5
CB-3

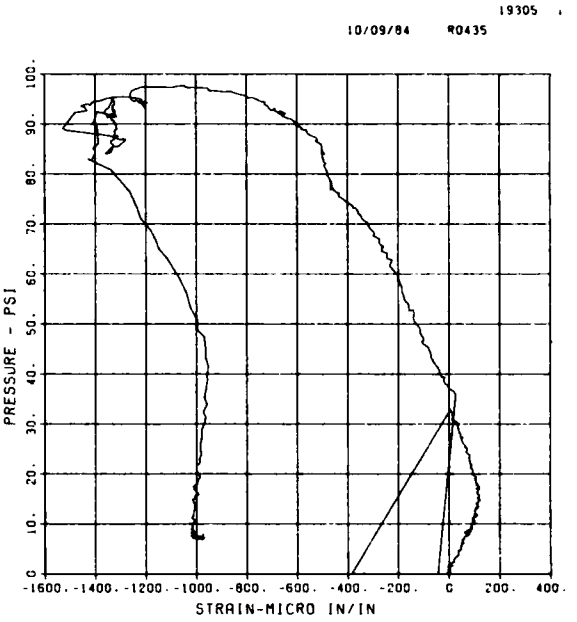

SLAB RESTRAINT G5
CB-390

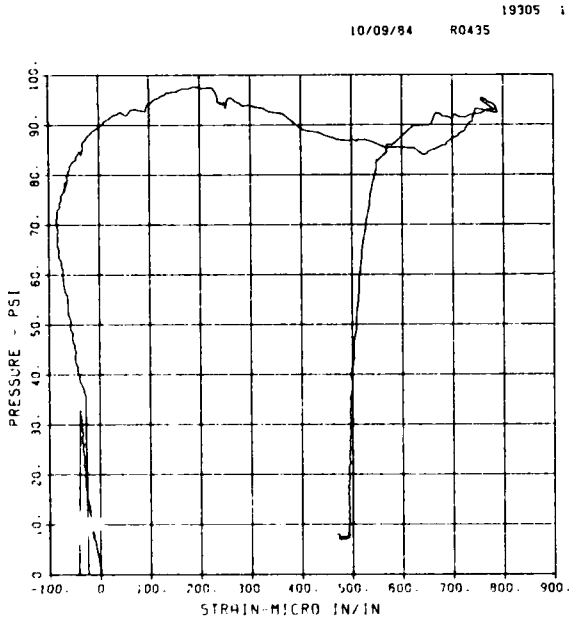

SLAB RESTRAINT G5
ST-1A

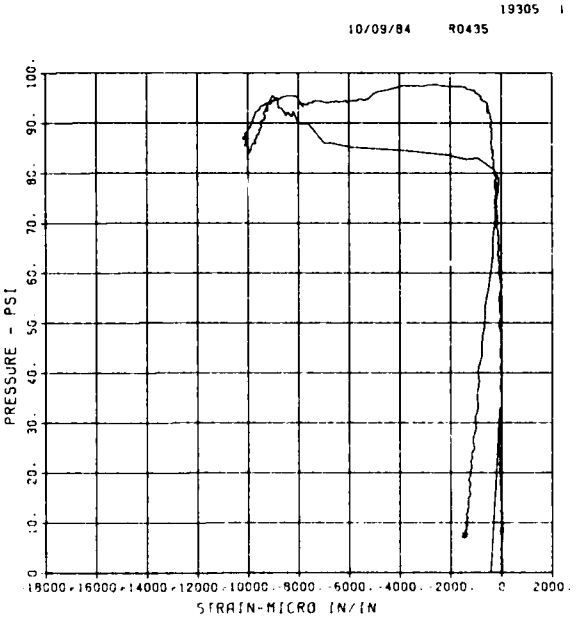

SLAB RESTRAINT G6

SLAB RESTRAINT C6
C-1

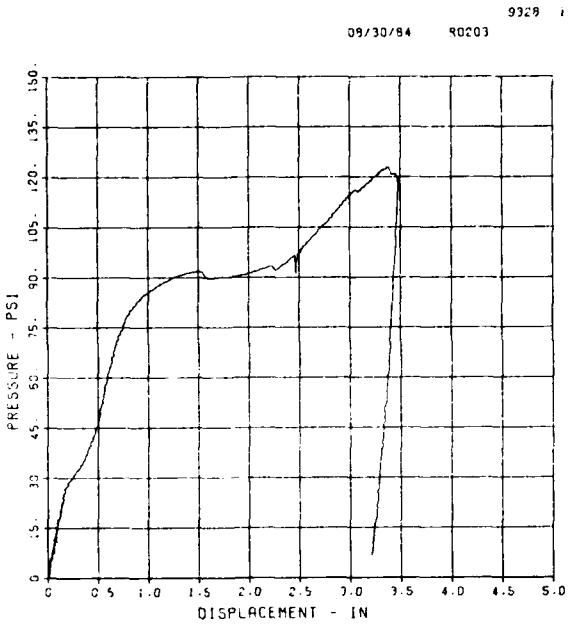

SLAB RESTRAINT C6
C-2

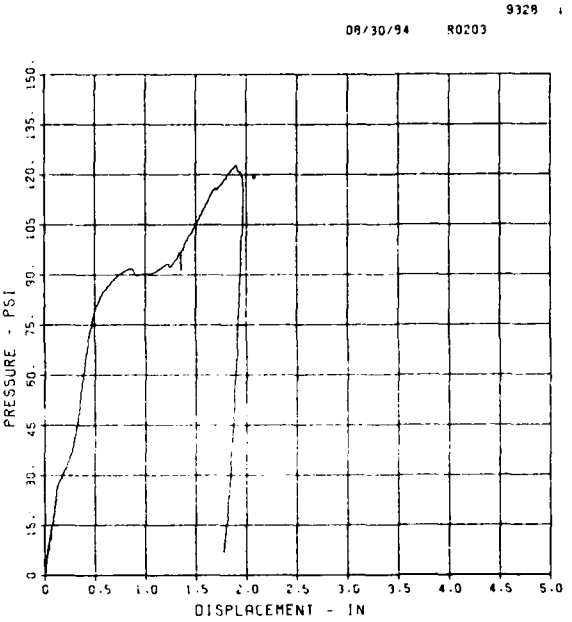

SLAB RESTRAINT C6
C-3

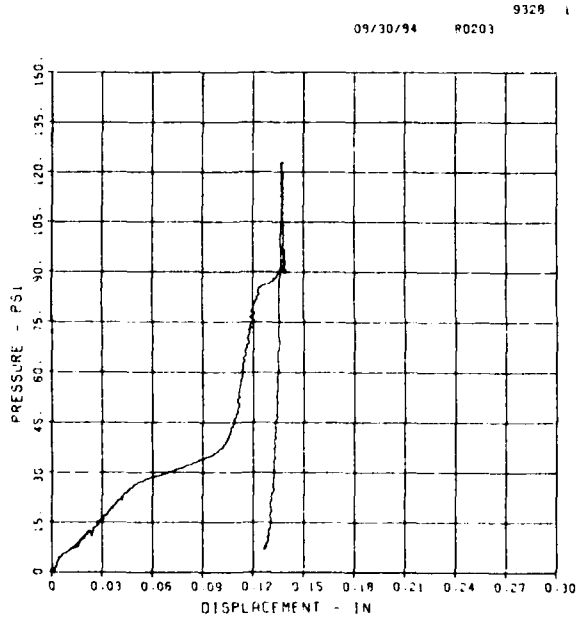

SLAB RESTRAINT C6
C-4

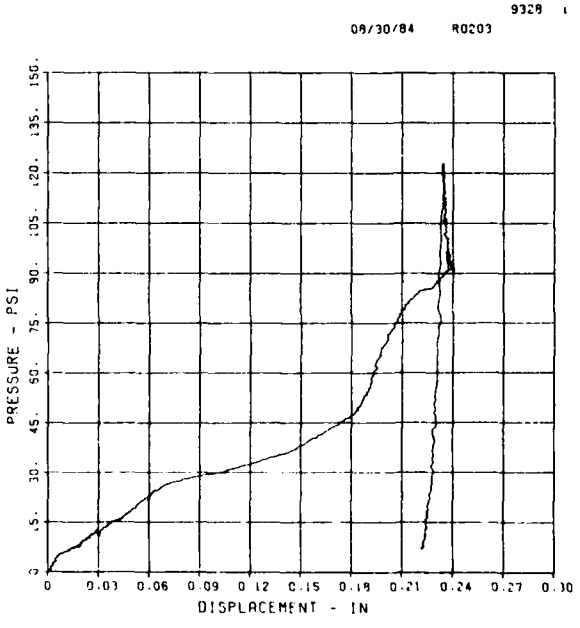

SLAB RESTRAINT C6
LW-1

9328
09/30/84 R0203

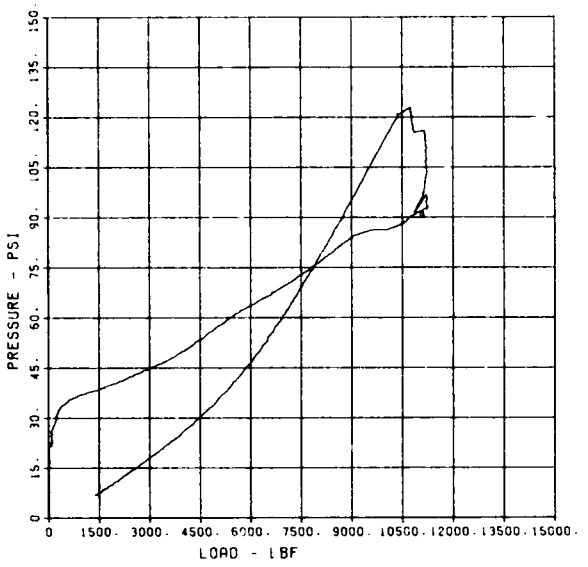

SLAB RESTRAINT C6
LW-2

9328
09/30/84 R0203

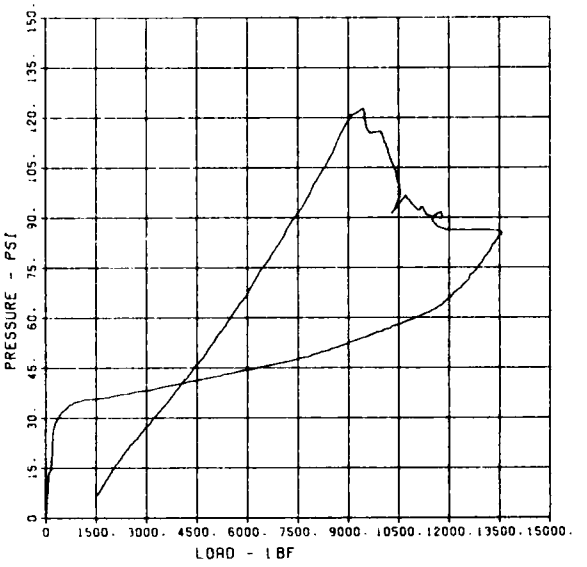

SLAB RESTRAINT C6
LW-3

9328
09/30/84 R0203

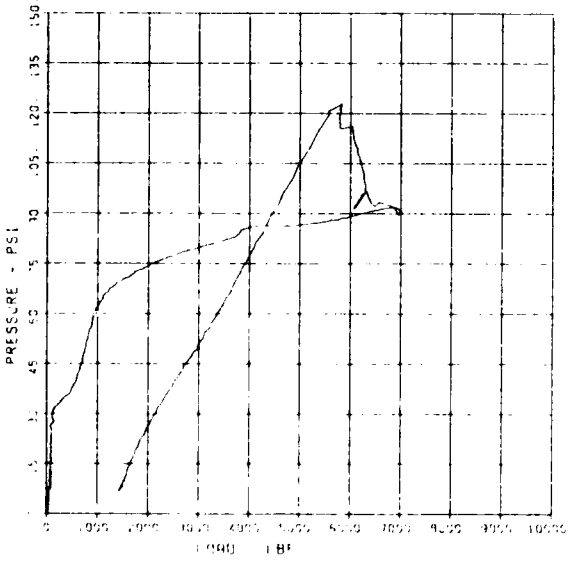

SLAB RESTRAINT C6
LW-4

9328
09/30/84 R0203

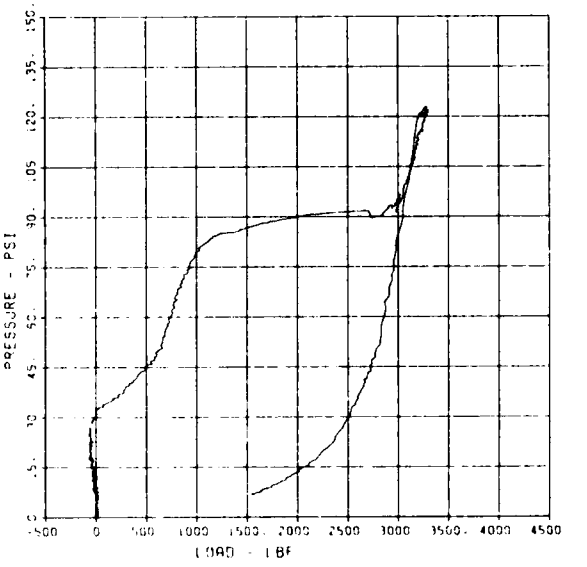

SLAB RESTRAINT 06
LW-5

9328
09/30/84 R0203

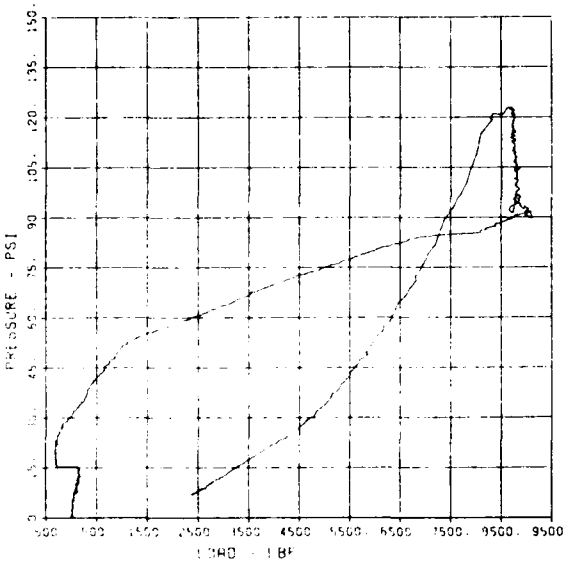

SLAB RESTRAINT 06
LW-6

9328
09/30/84 R0203

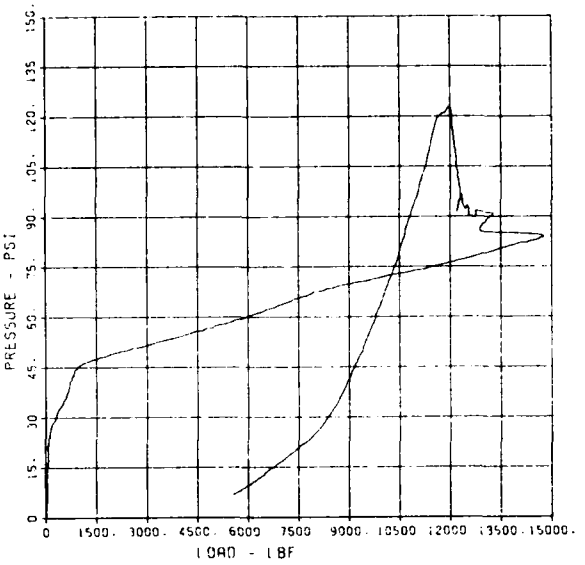

SLAB RESTRAINT 06
LW-7

9328
09/30/84 R0203

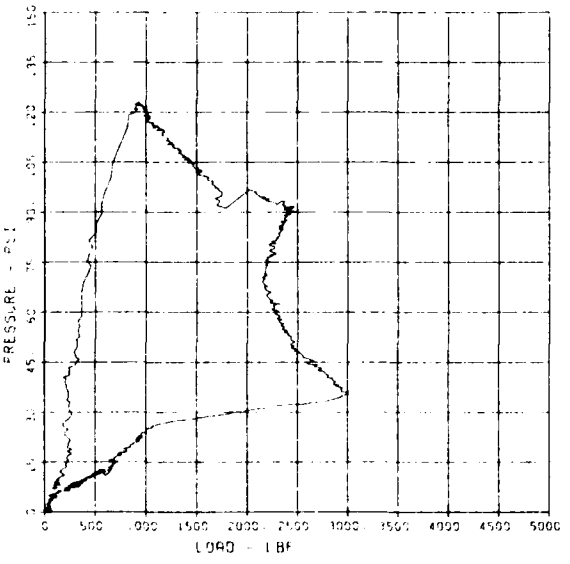

SLAB RESTRAINT 06
LW-8

9328
09/30/84 R0203

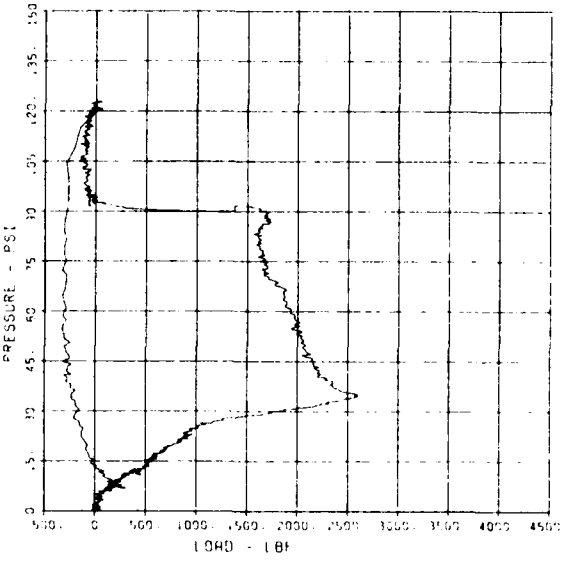

SLAB RESTRAINT G6
LW-9

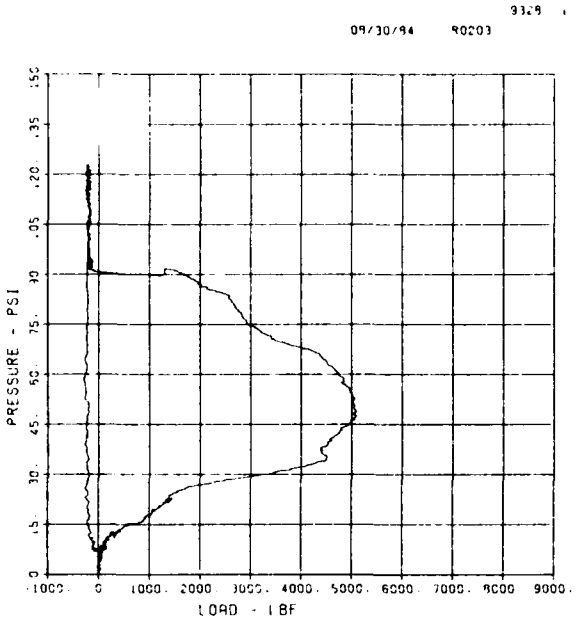

SLAB RESTRAINT G6
LW-10

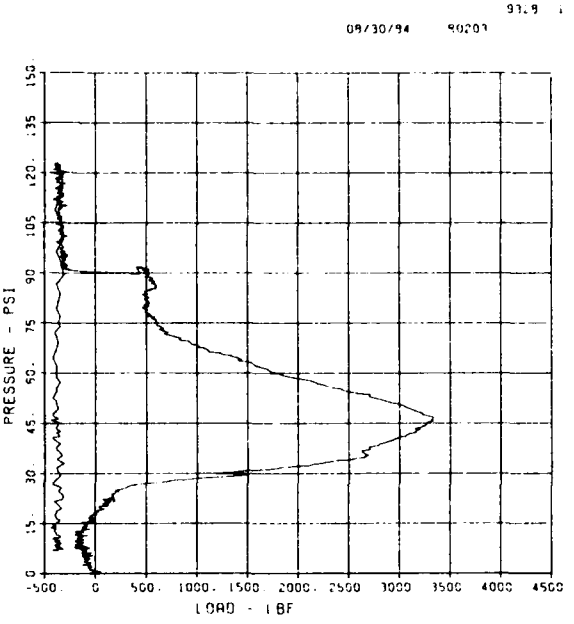

SLAB RESTRAINT G6
LW-11

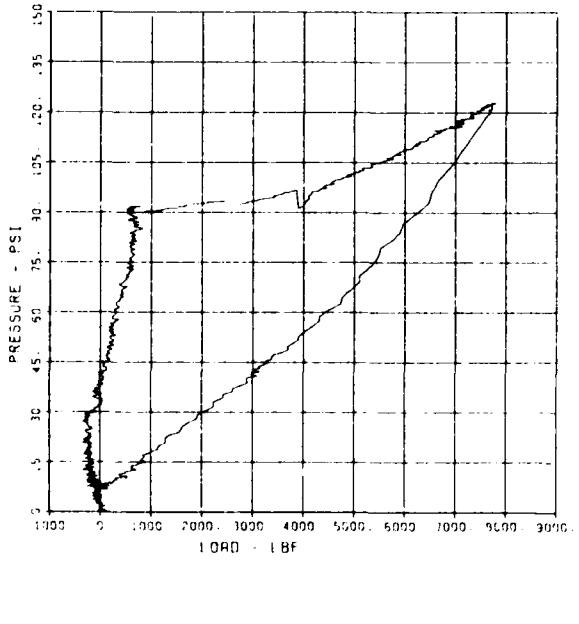

SLAB RESTRAINT G6
LW-12

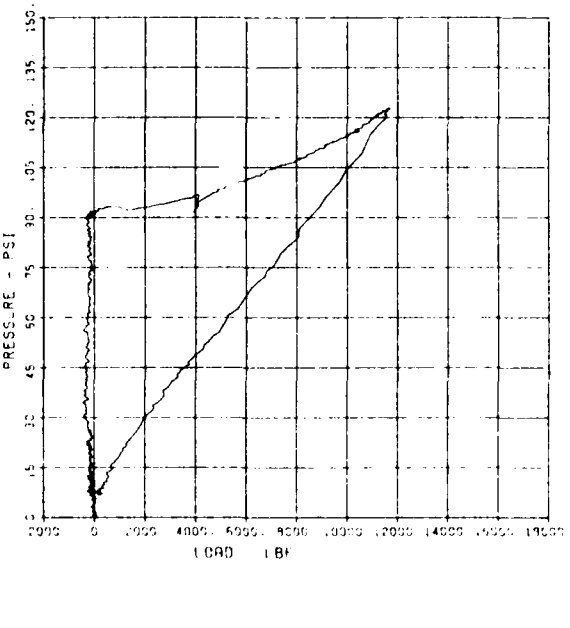

SLAB RESTRAINT 06
LW-13

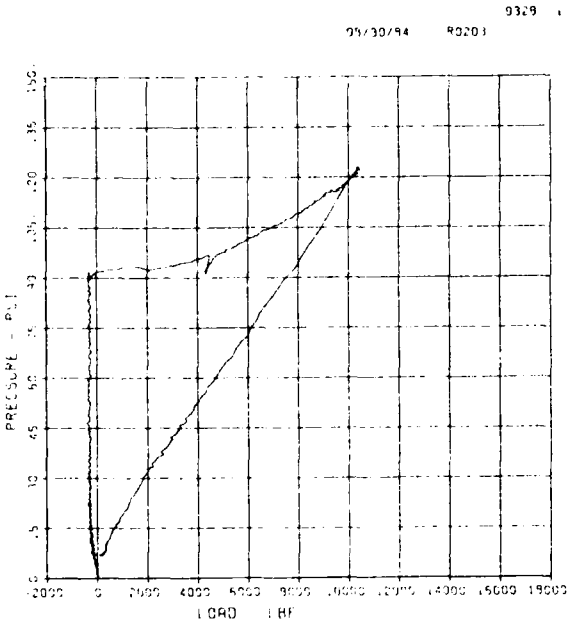

SLAB RESTRAINT 06
LW-14

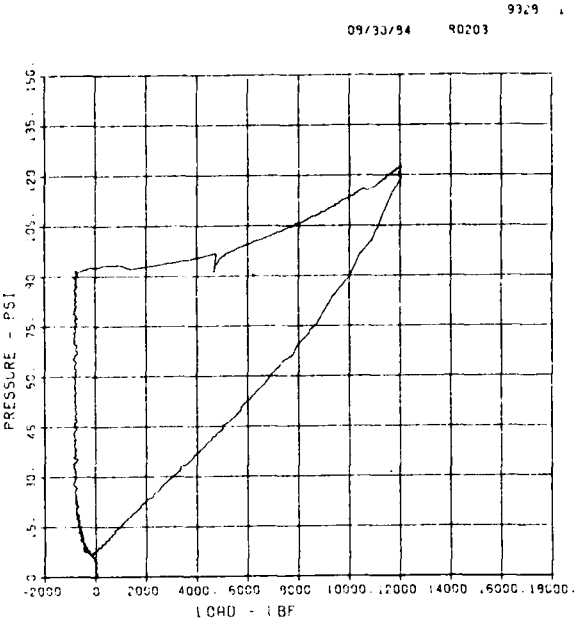

SLAB RESTRAINT 06
LW-15

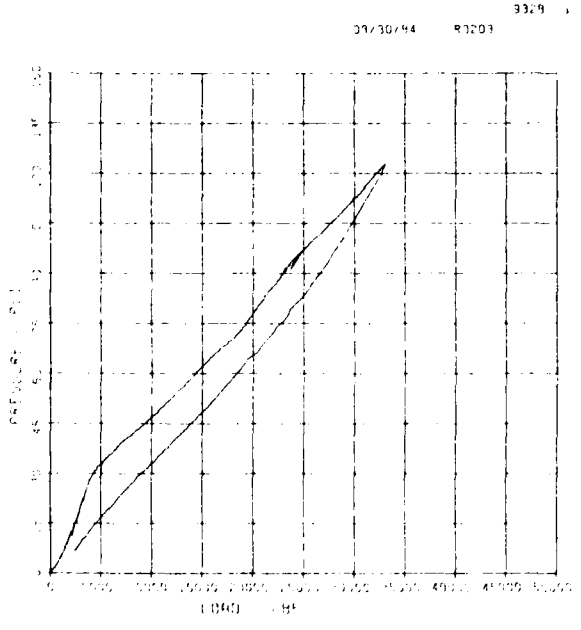

SLAB RESTRAINT 06
LW-16

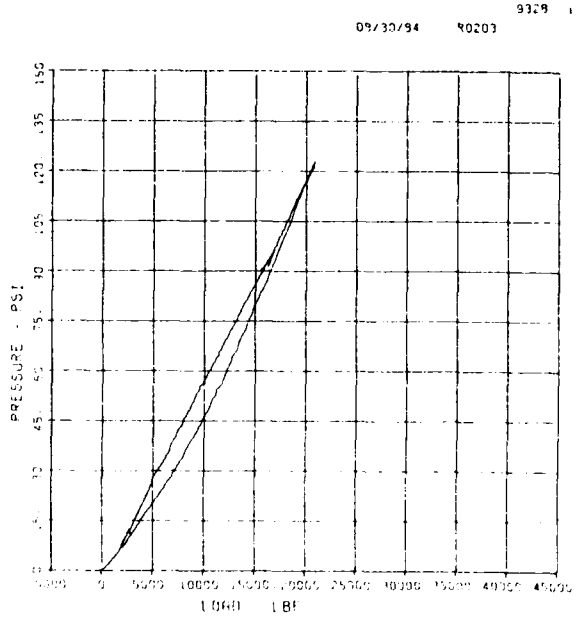

SLAB RESTRAINT G6
ST-1

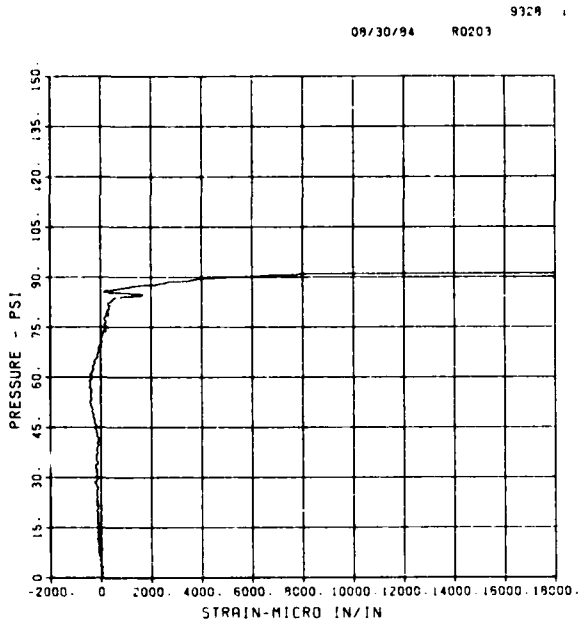

SLAB RESTRAINT G6
ST-2

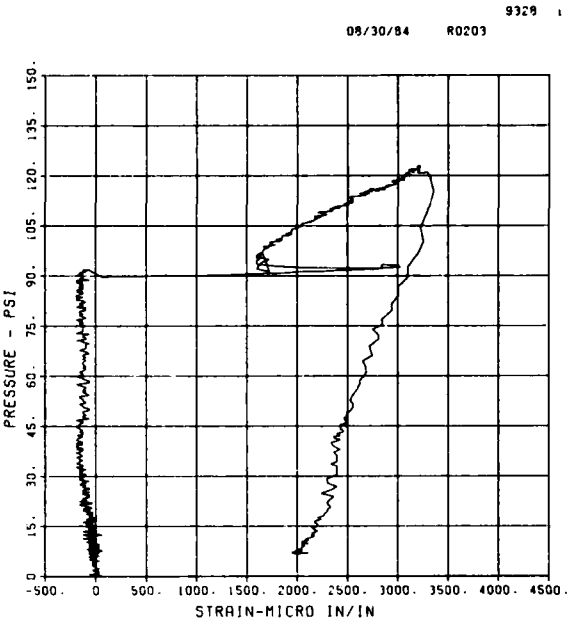

SLAB RESTRAINT G6
ST-3

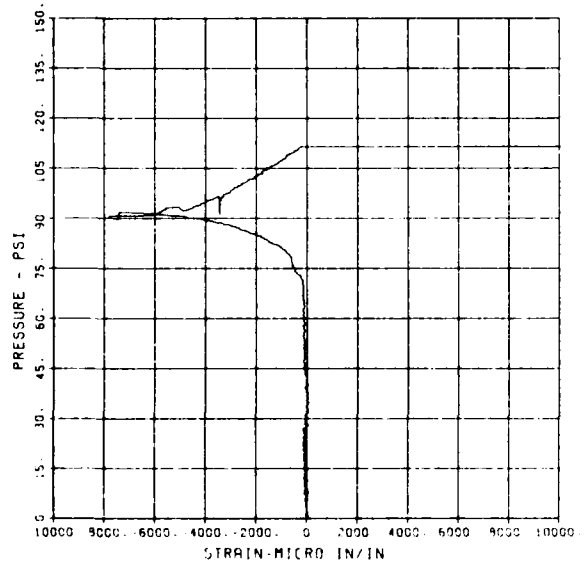

SLAB RESTRAINT G6
SB-1

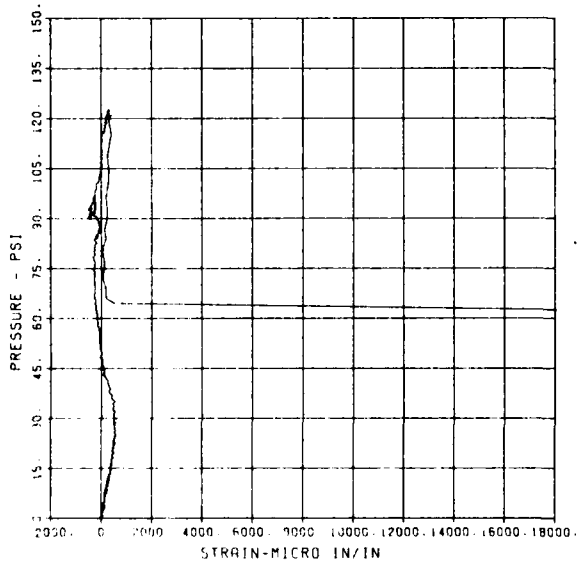

SLAB RESTRAINT G6
SB-2

9328 1
08/30/84 R0213

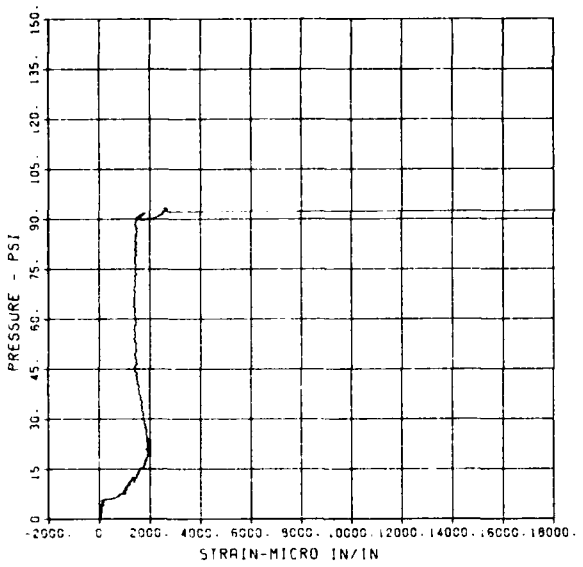

SLAB RESTRAINT G6
SB-3

9328 1
09/31/84 R0217

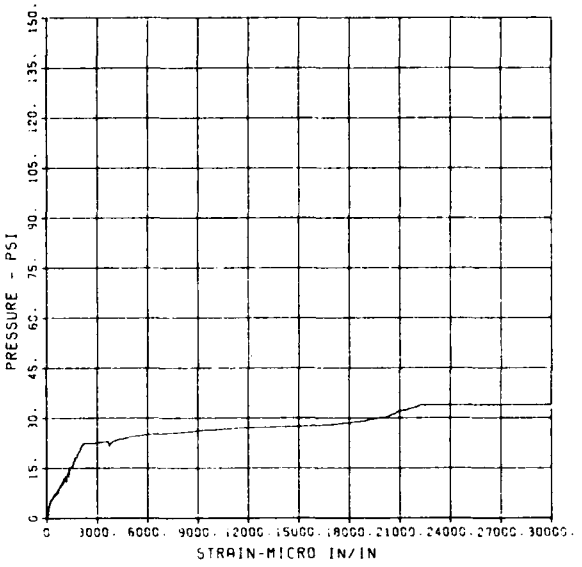

SLAB RESTRAINT G7

SLAB RESTRAINT G7
D-1

11976 1
10/10/84 R0448

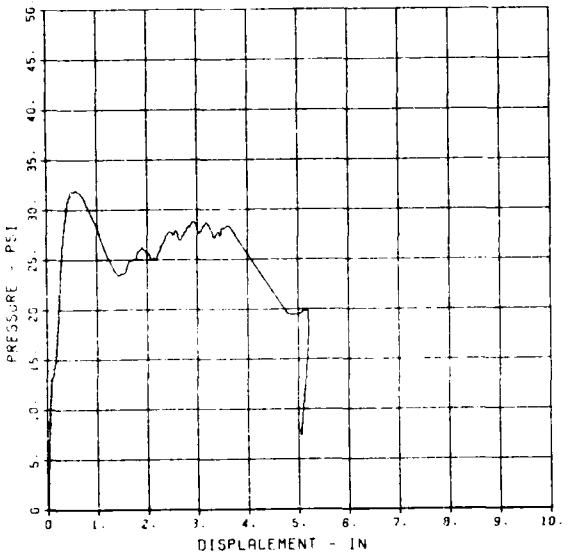

SLAB RESTRAINT G7
D-2

11976 1
10/10/84 R0448

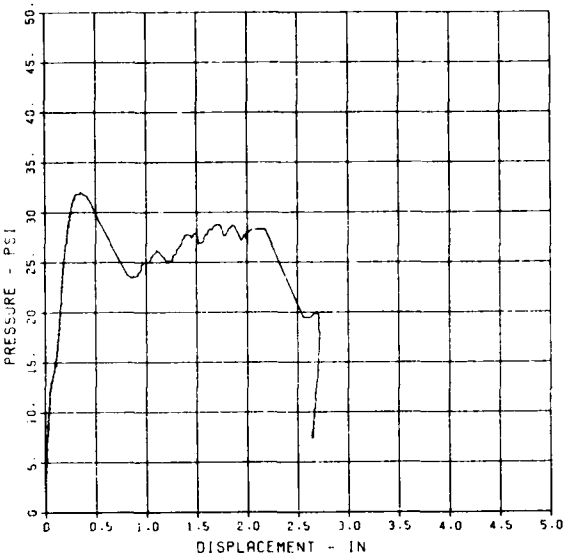

SLAB RESTRAINT G7
D-3

11976 1
10/10/84 R0448

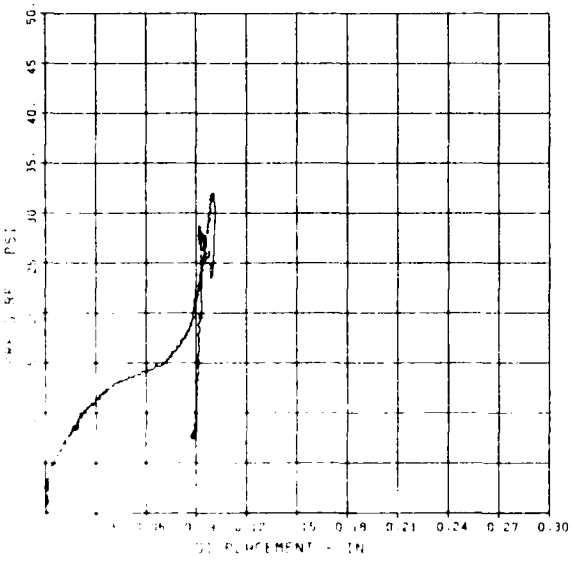

SLAB RESTRAINT G7
D-4

11976 1
10/10/84 R0448

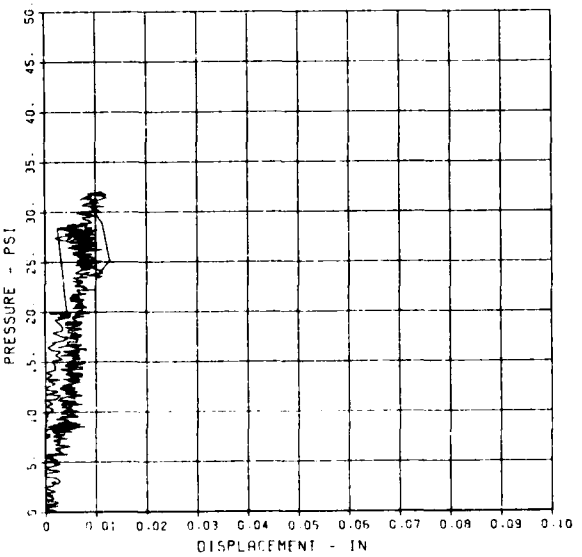

SLAB RESTRAINT G7
LW-2

11975 1
10/10/84 80448

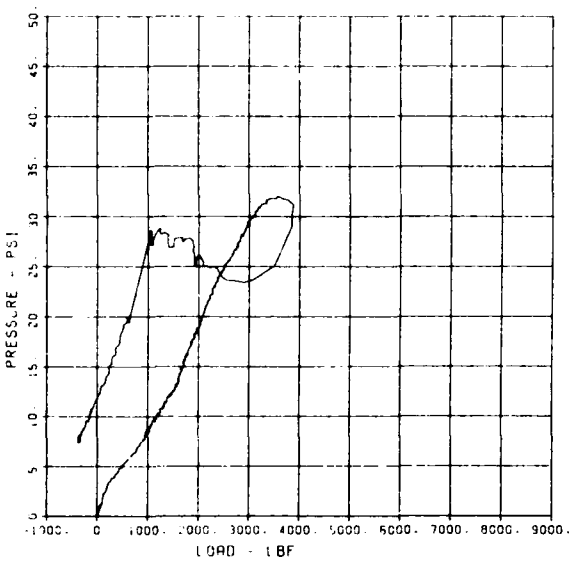

SLAB RESTRAINT G7
LW-3

11976 1
10/10/84 80448

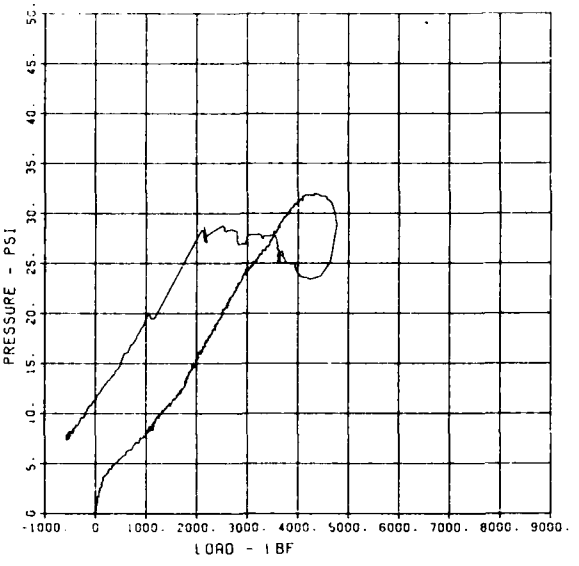

SLAB RESTRAINT G7
LW-6

11976 1
10/10/84 80448

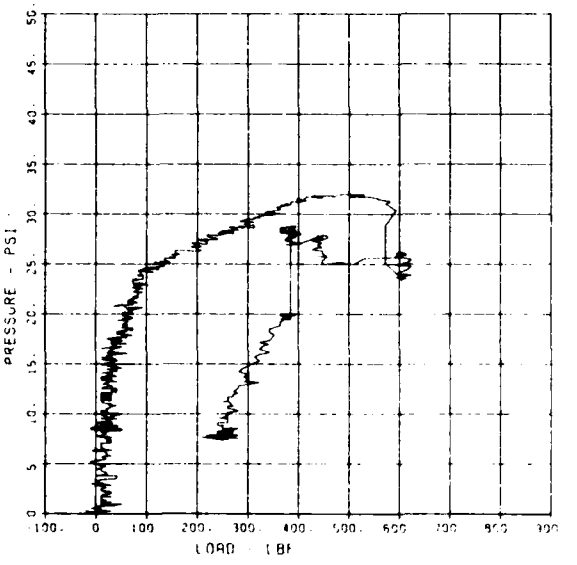

SLAB RESTRAINT G7
LW-7

11976 1
10/10/84 80448

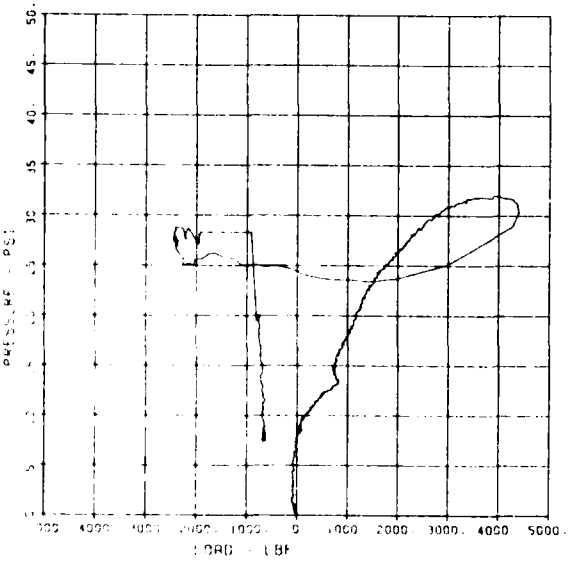

SLAB RESTRAINT G7
LW-8

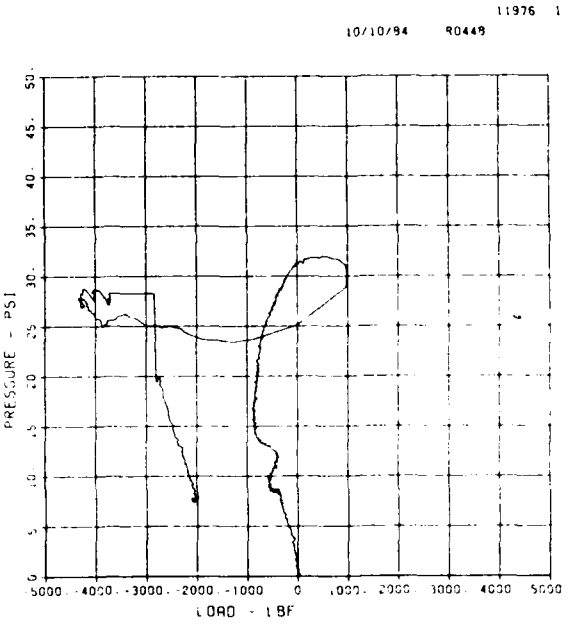

SLAB RESTRAINT G7
LW-9

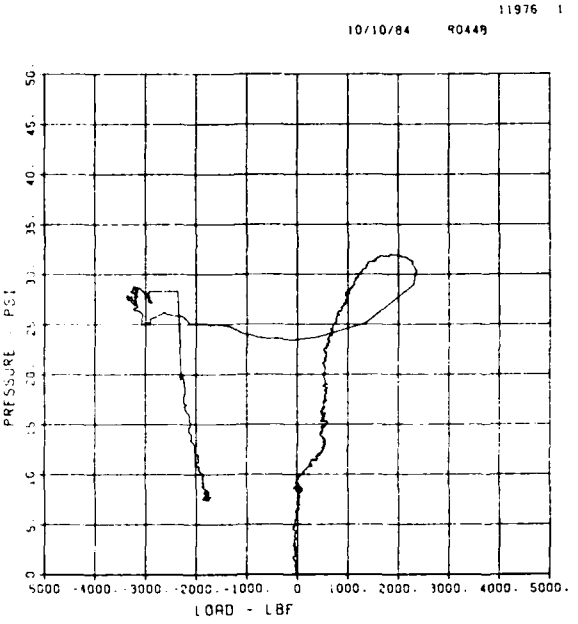

SLAB RESTRAINT G7
LW-10

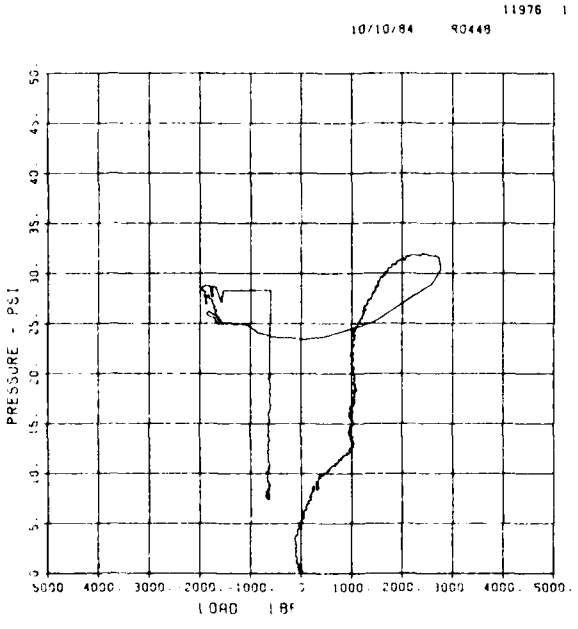

SLAB RESTRAINT G7
LW-11

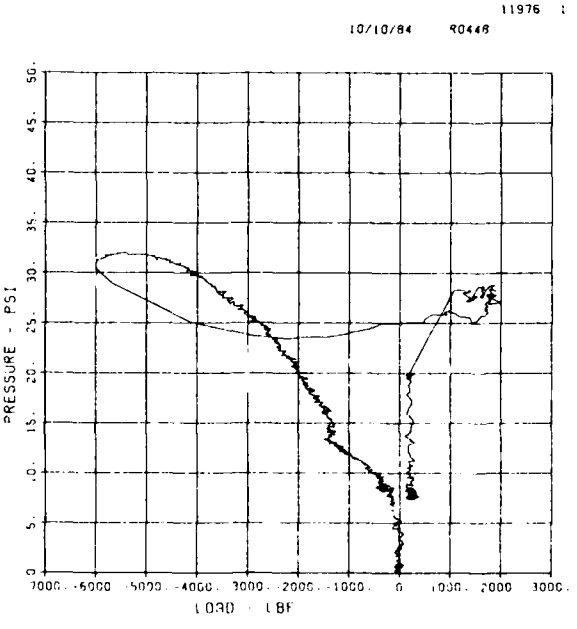

SLAB RESTRAINT G7
LW-13

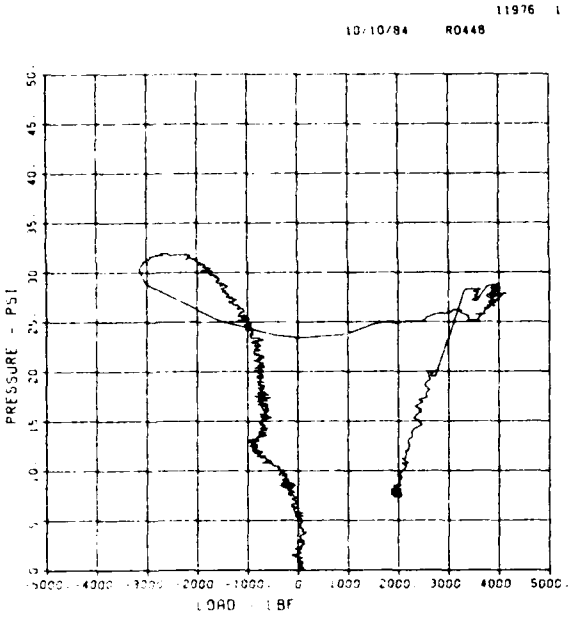

SLAB RESTRAINT G7
LW-14

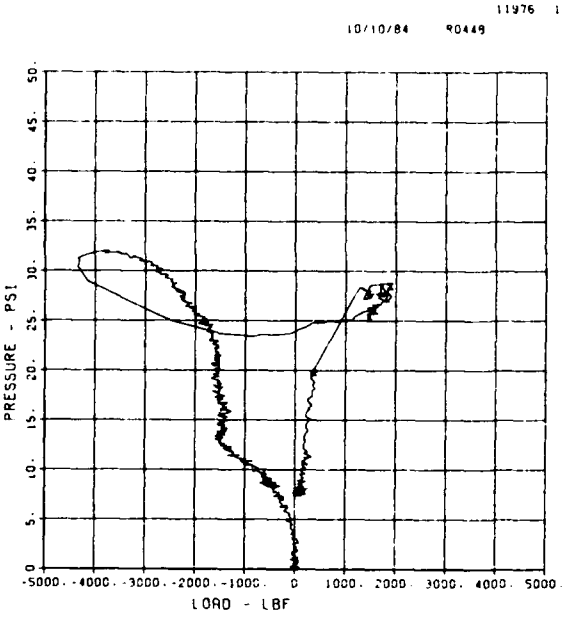

SLAB RESTRAINT G7
LW-15

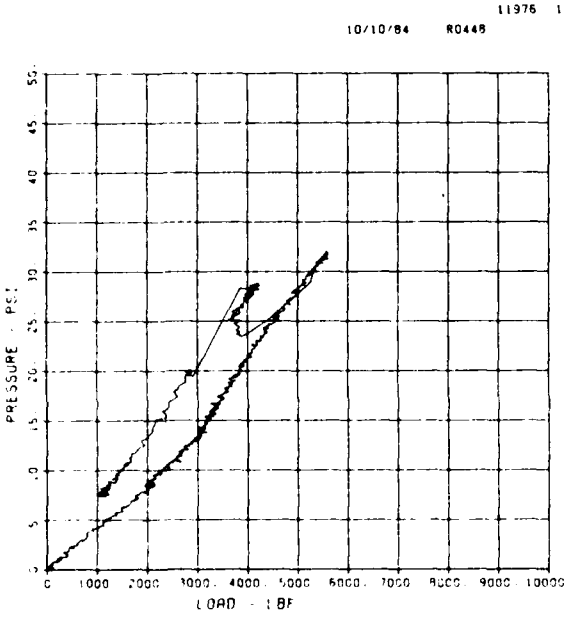

SLAB RESTRAINT G7
ST-1

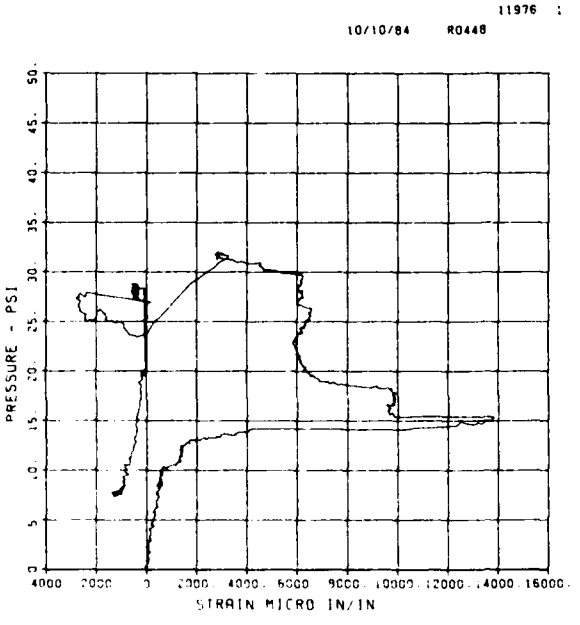

SLAB RESTRAINT G7
ST-2

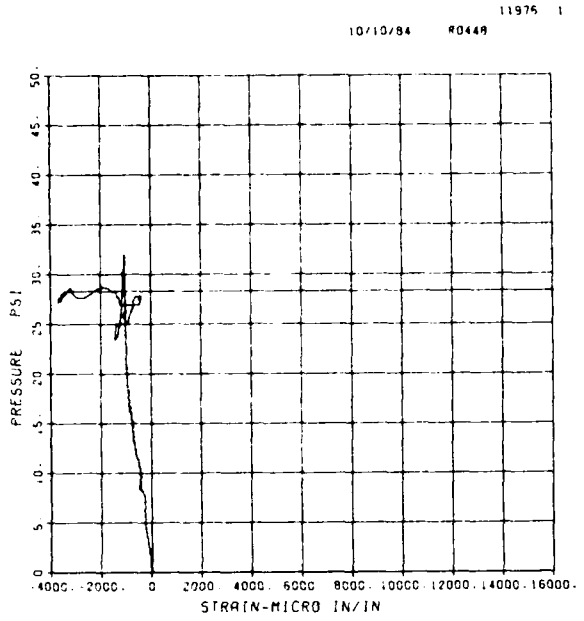

SLAB RESTRAINT G7
ST-3

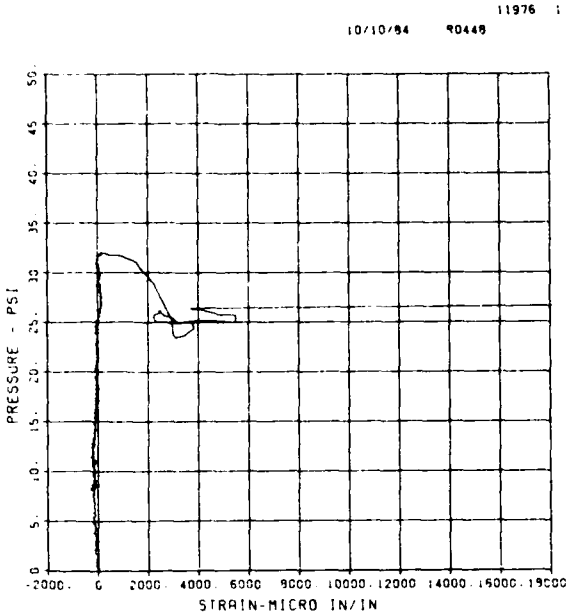

SLAB RESTRAINT G7
SB-1

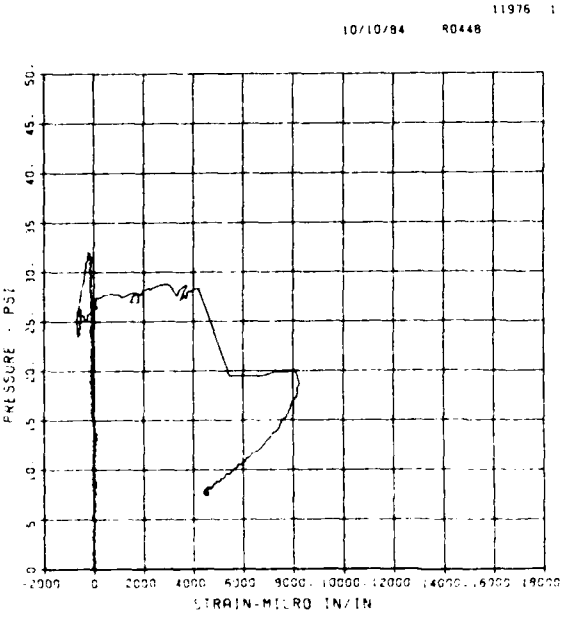

SLAB RESTRAINT G7
SB-2

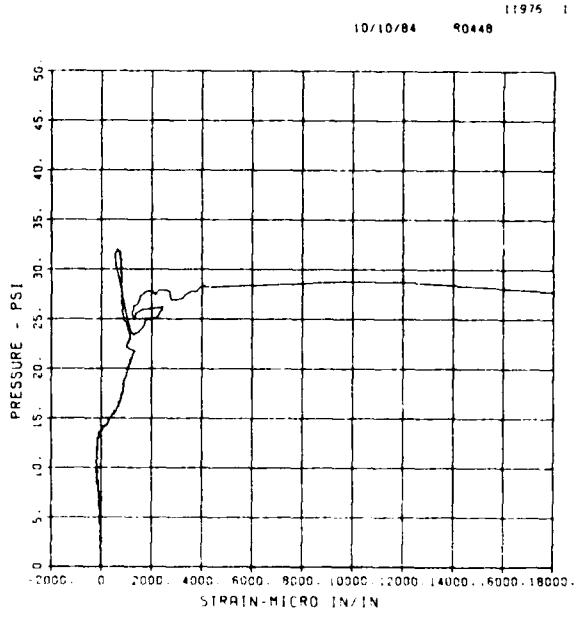

SLAB RESTRAINT G7
SB-3

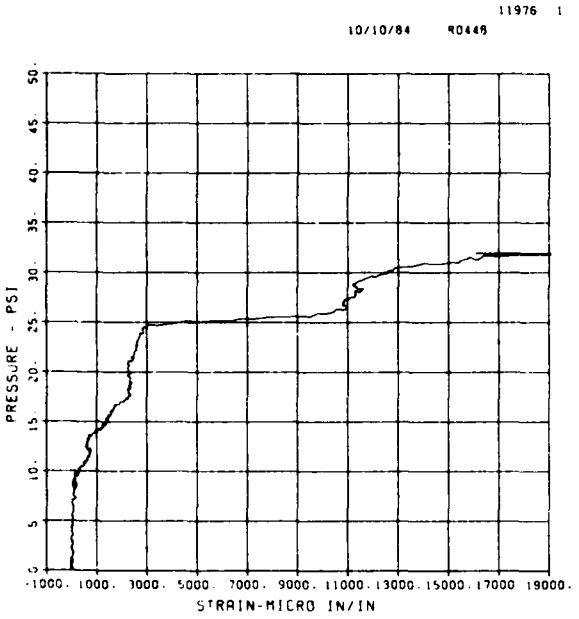

SLAB RESTRAINT G7
ST-1A

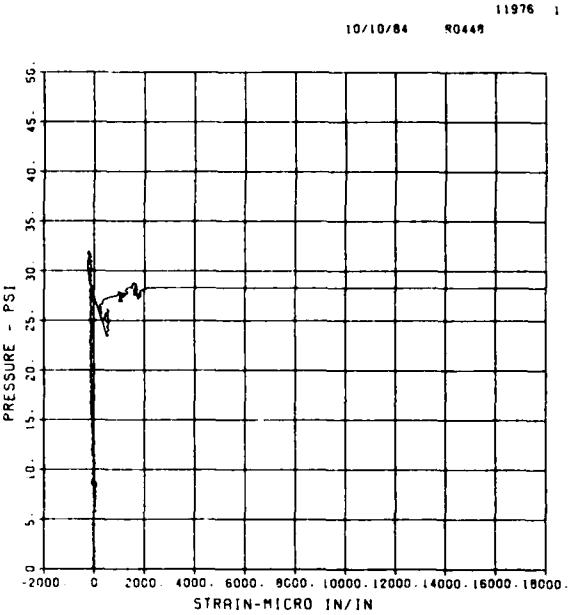

SLAB RESTRAINT G7
ST-3A

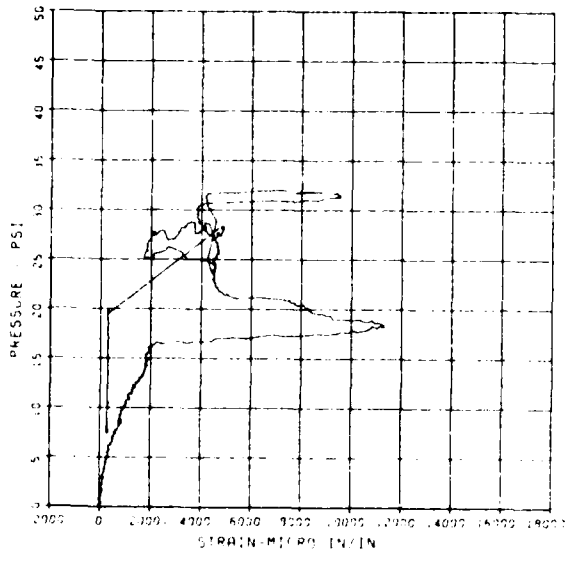

SLAB RESTRAINT G7
CT-1

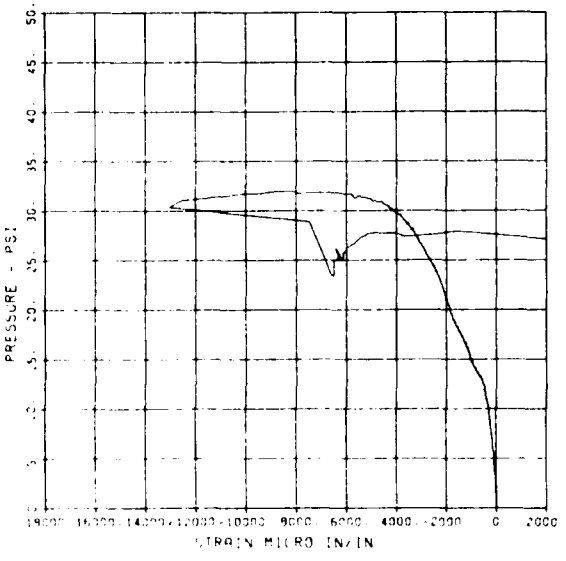

SLAB RESTRAINT G7
CB-3

11976 1
10/10/84 80448

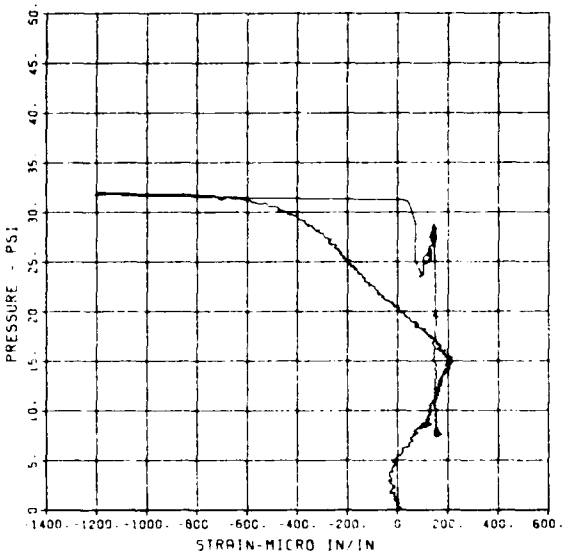

SLAB RESTRAINT G7
SB-3A

11976 1
10/10/84 80448

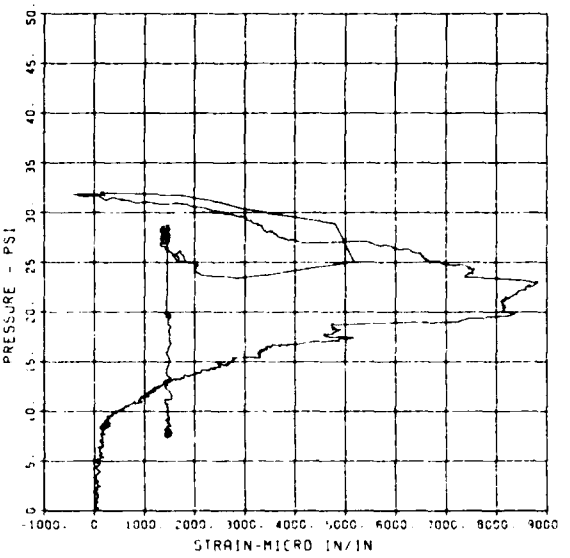

SLAB RESTRAINT G8

SLAB RESTRAINT 08
D-1

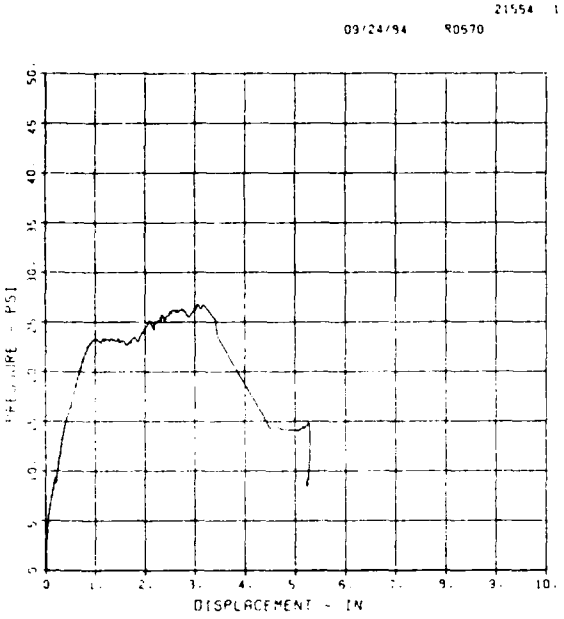

SLAB RESTRAINT 08
D-2

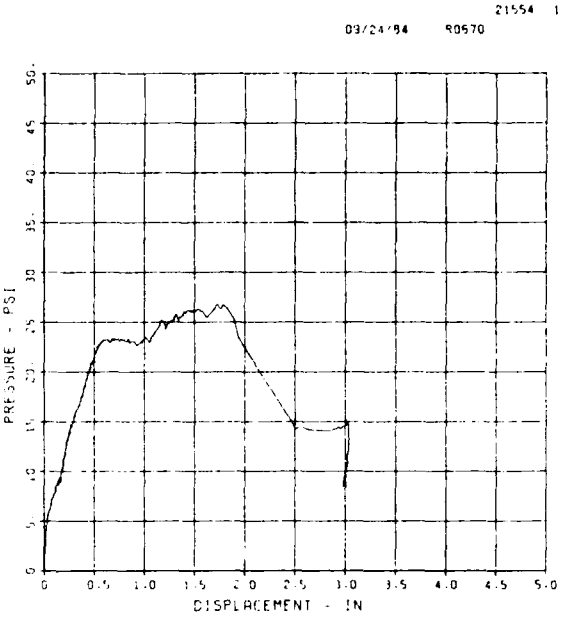

SLAB RESTRAINT 08
D-3

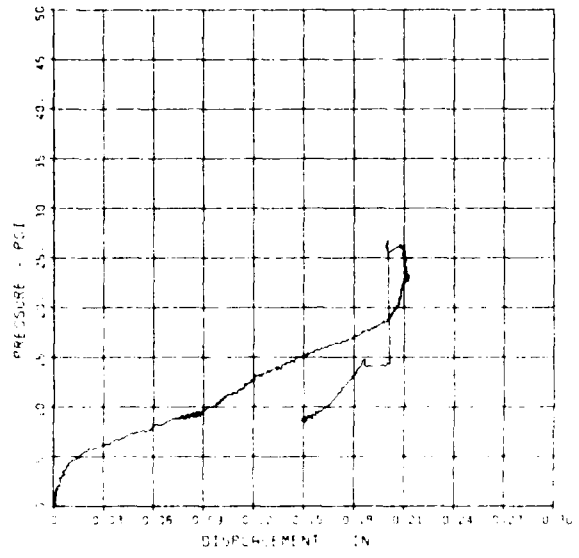

SLAB RESTRAINT 08
D-4

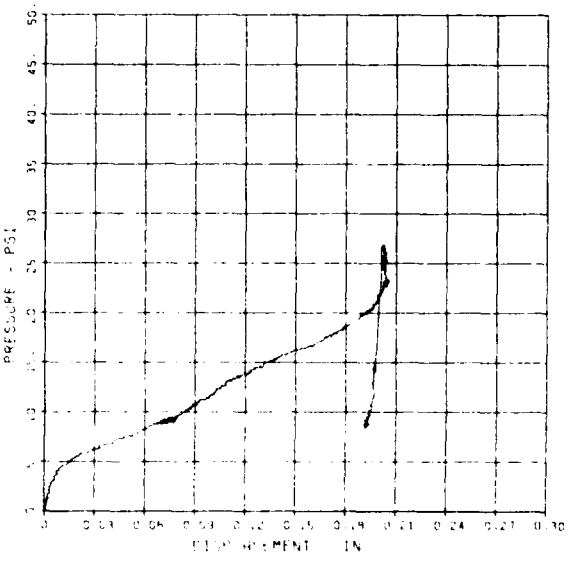

SLAB RESTRAINT GB
LW-2

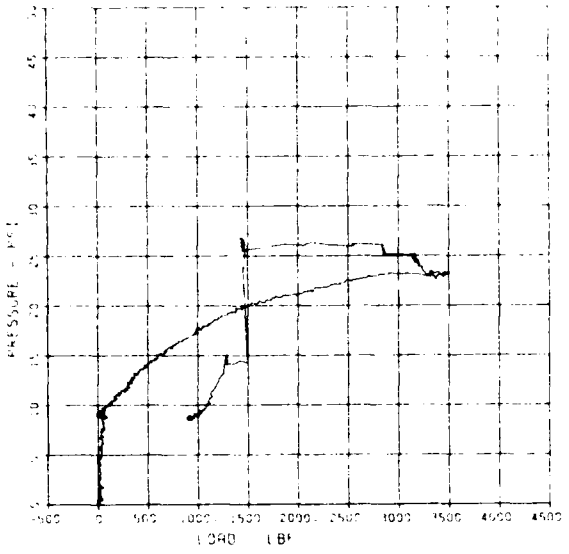

SLAB RESTRAINT GB
LW-3

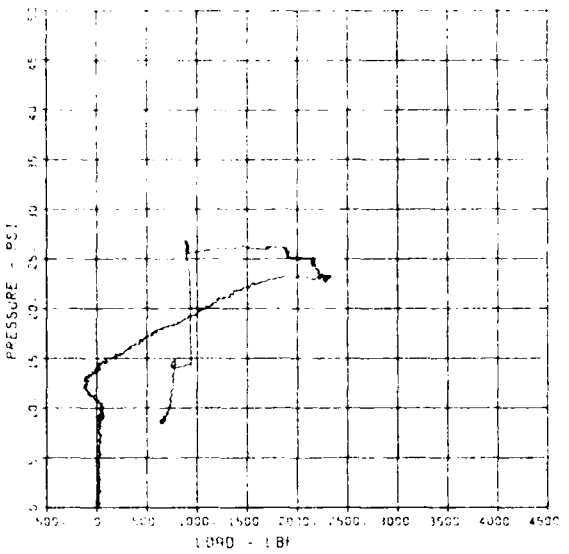

SLAB RESTRAINT GB
LW-4

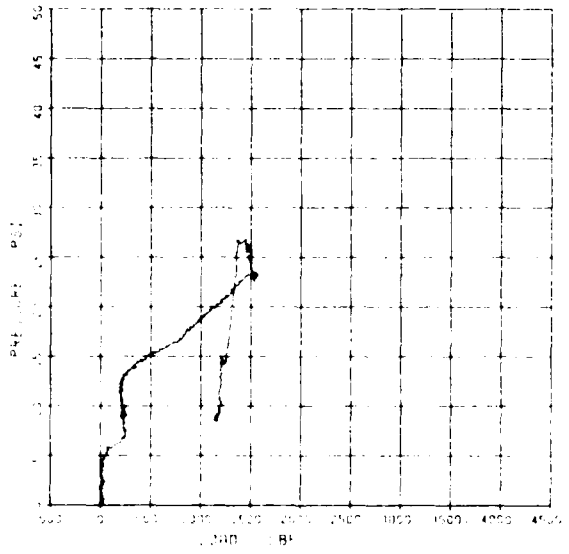

SLAB RESTRAINT GB
LW-5

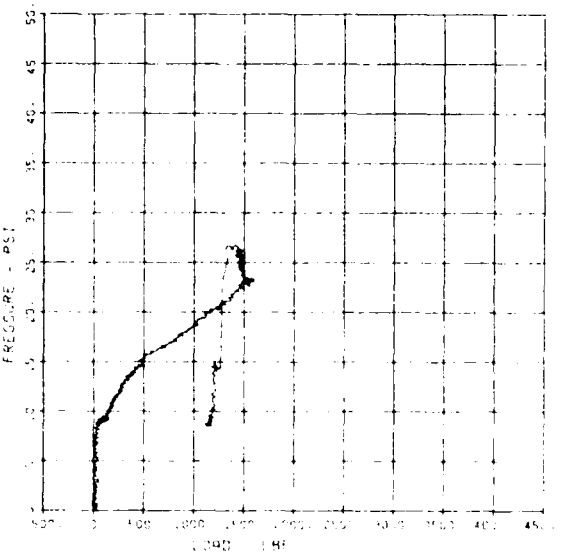

SLAB RESTRAINT 08
LW-6

21554 1
09/24/94 R0670

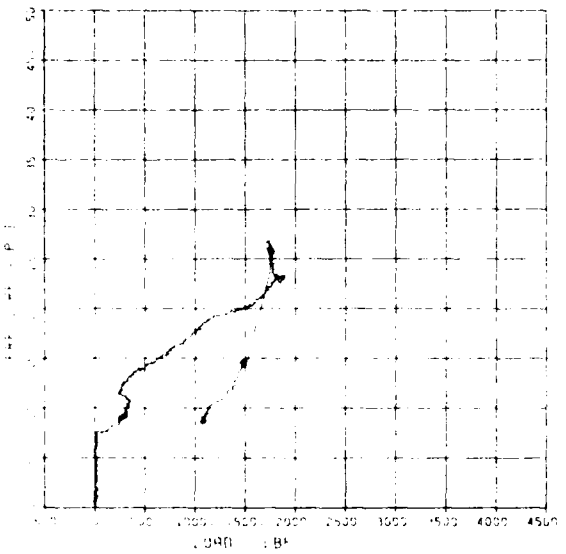

SLAB RESTRAINT 08
LW-7

21554 1
09/24/94 R0670

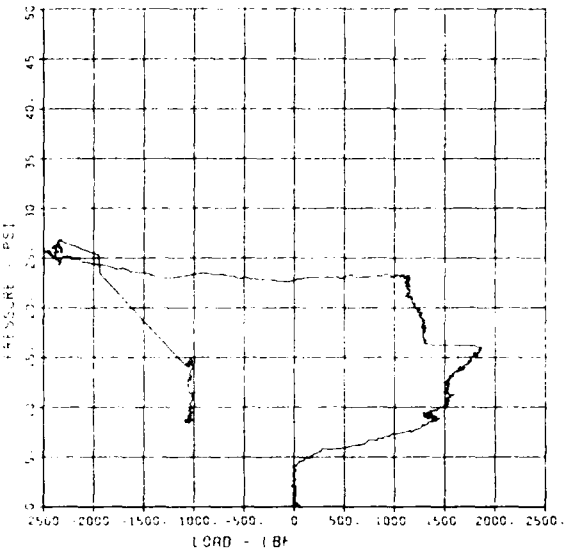

SLAB RESTRAINT 08
LW-8

21554 1
09/24/94 R0670

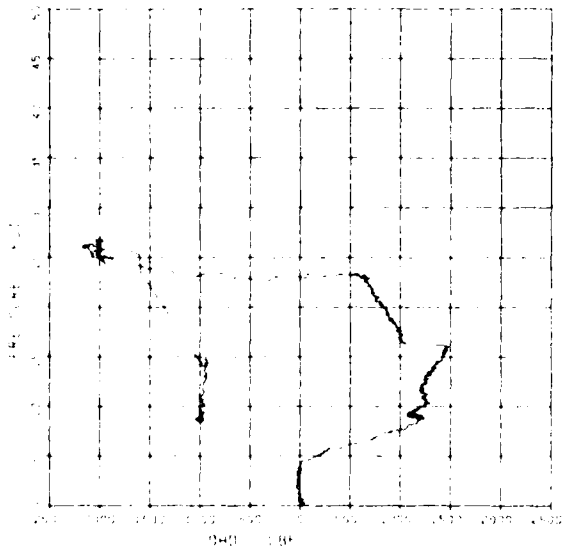

SLAB RESTRAINT 08
LW-9

21554 1
09/24/94 R0670

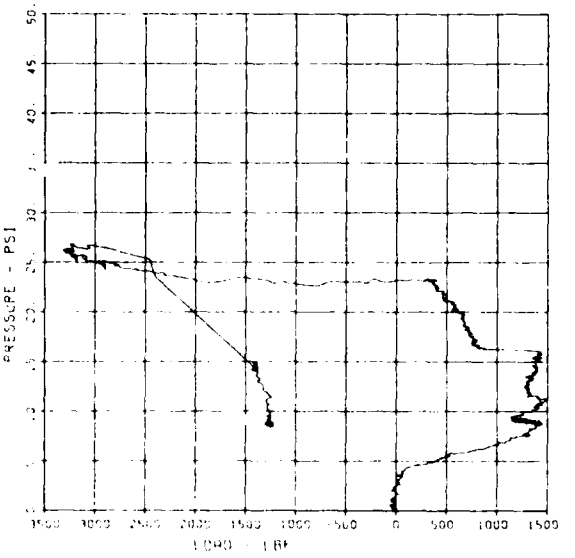

SLAB RESTRAINT GB
LW 10

21554 1
09/24/94 80670

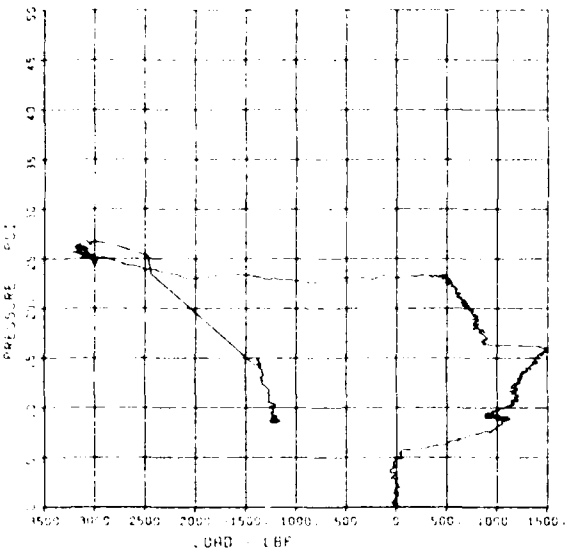

SLAB RESTRAINT GB
LW 11

21554 1
09/24/94 80670

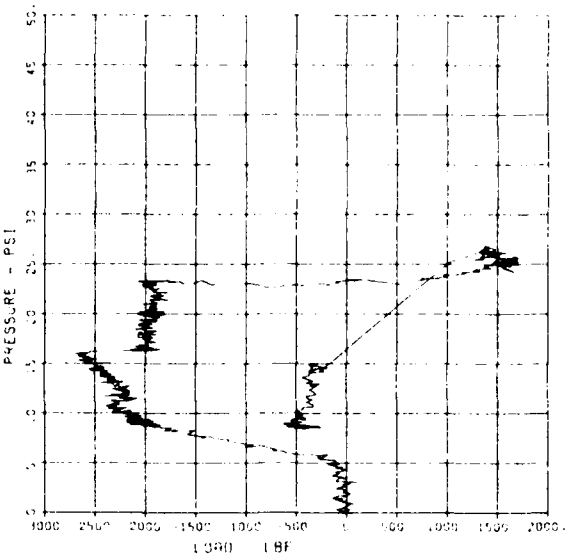

SLAB RESTRAINT GB
LW-12

21554 1
09/24/94 80670

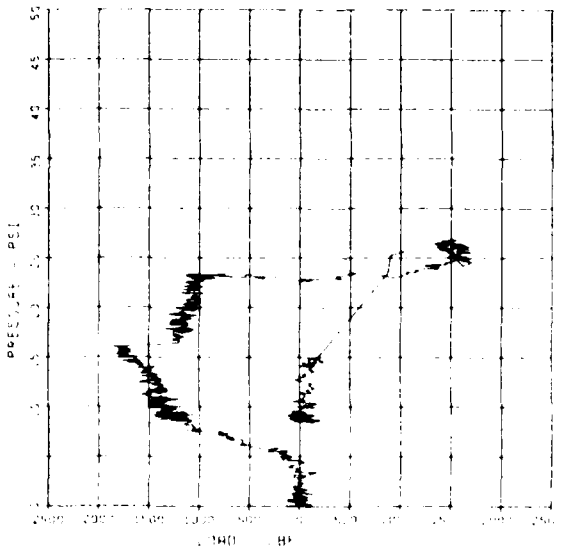

SLAB RESTRAINT GB
LW 13

21554 1
09/24/94 80670

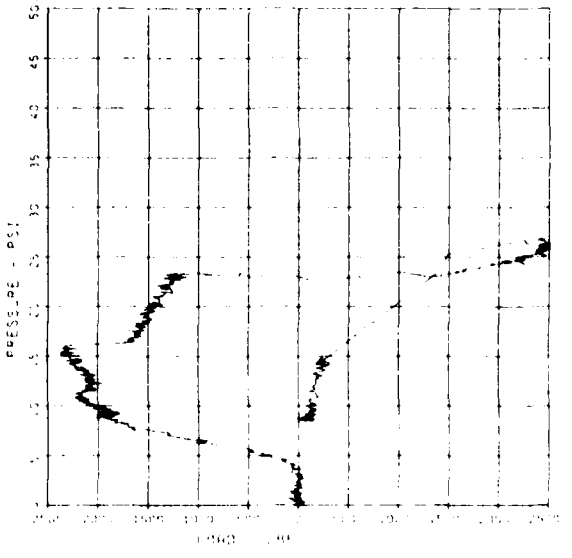

SLAB RESTRAINT 08
LW-14

21554 1
09/24/94 R0670

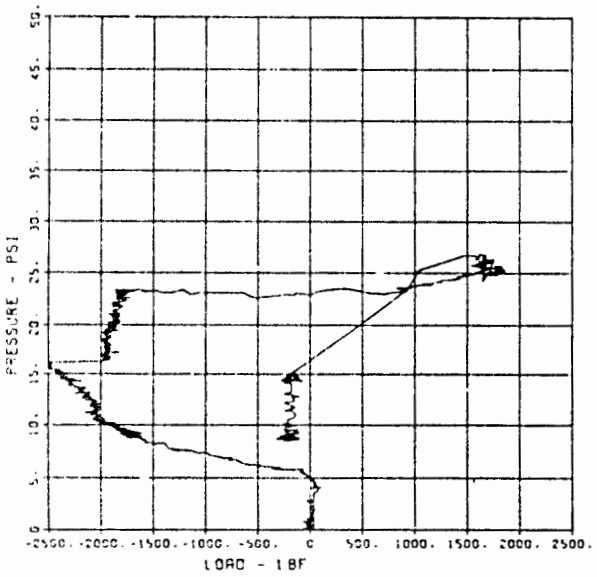

SLAB RESTRAINT 08
LW-15

21554 1
09/24/94 R0670

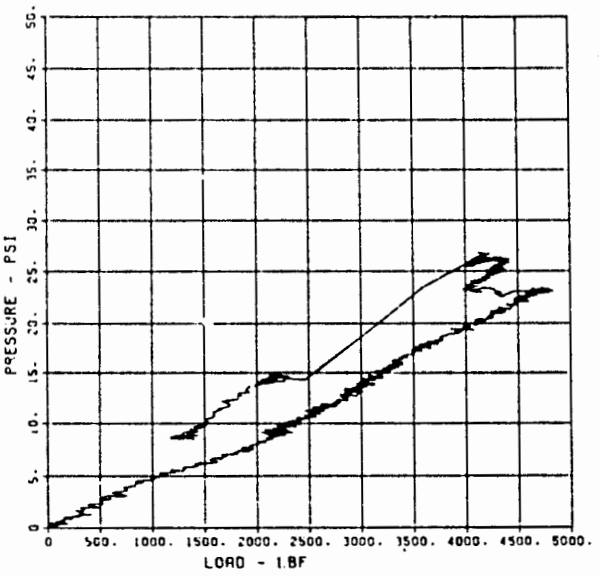

SLAB RESTRAINT 08
LW-16

21554 1
09/24/94 R0670

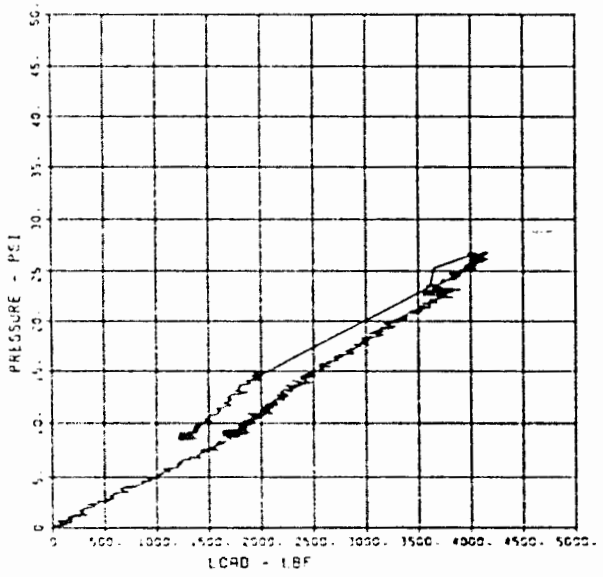

SLAB RESTRAINT 08
ST-1

21554 1
09/24/94 R0670

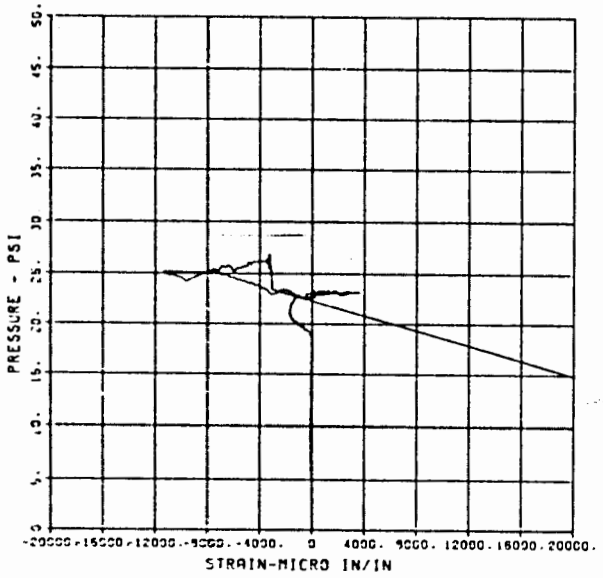

SLAB RESTRAINT 08
ST-2

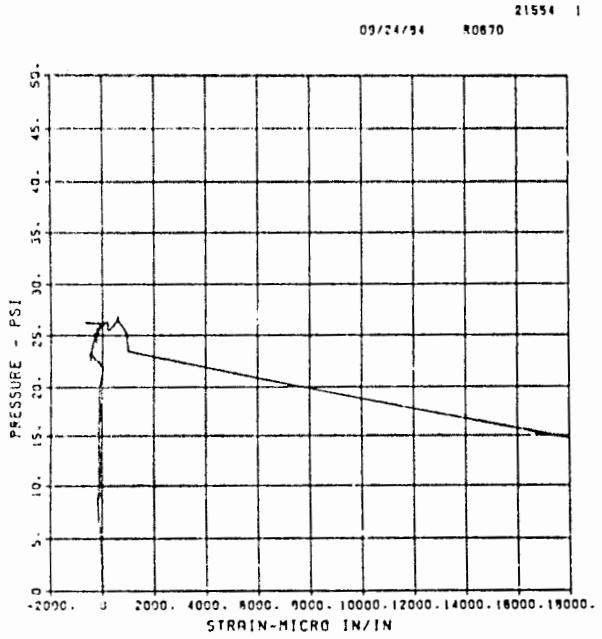

SLAB RESTRAINT 08
ST-3

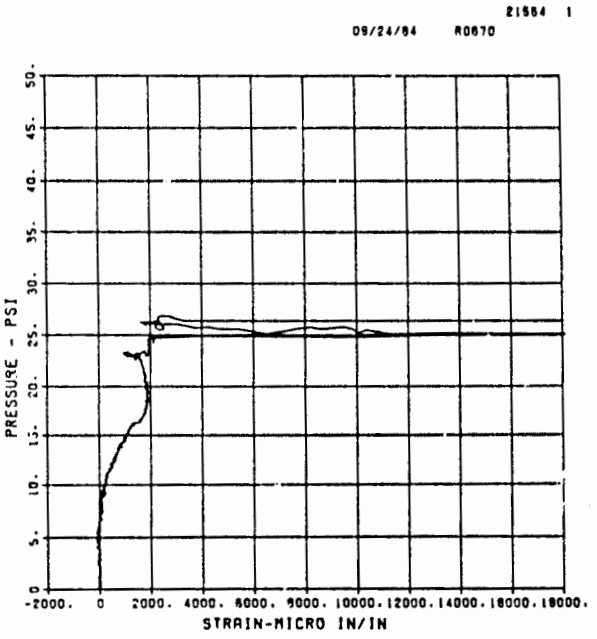

SLAB RESTRAINT 08
SB-1

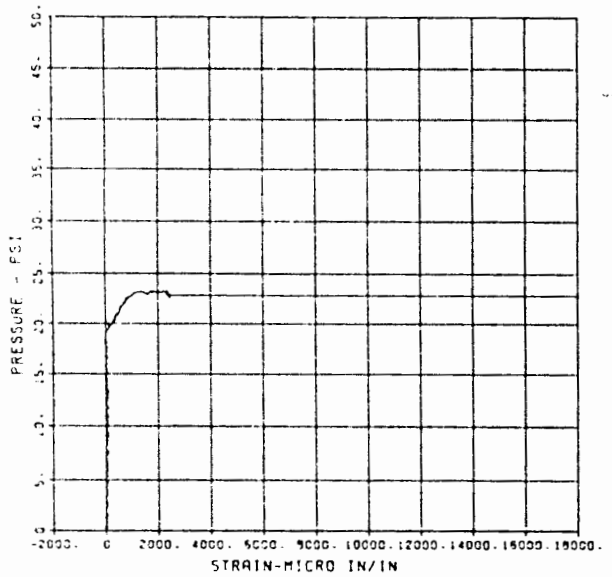

SLAB RESTRAINT 08
SB-2

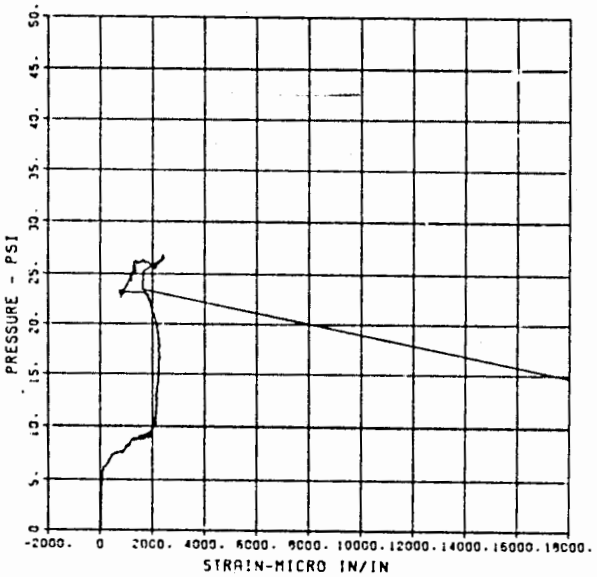

SLAB RESTRAINT CB
SB-3

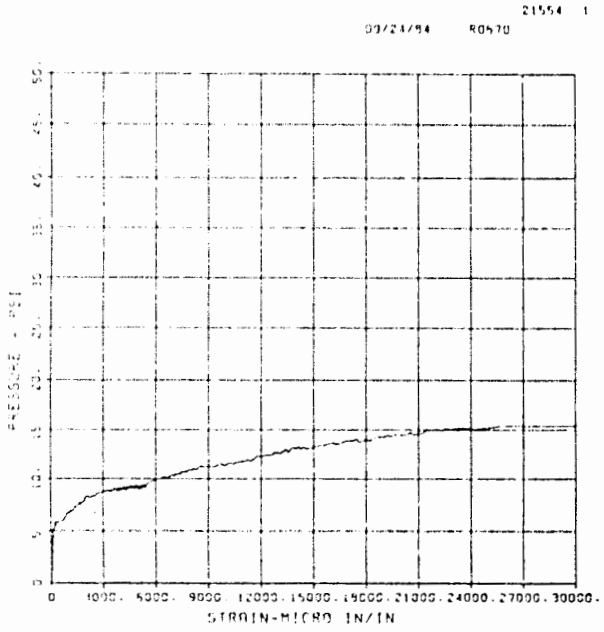

SLAB RESTRAINT CB
CB-3

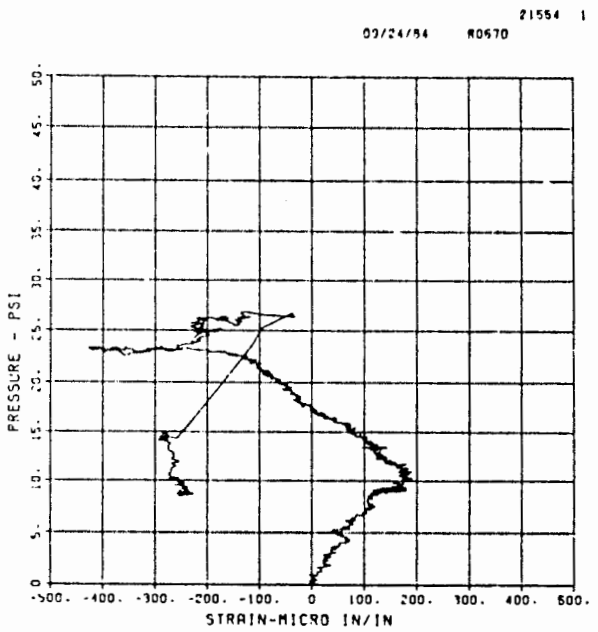

SLAB RESTRAINT CB
CT-1

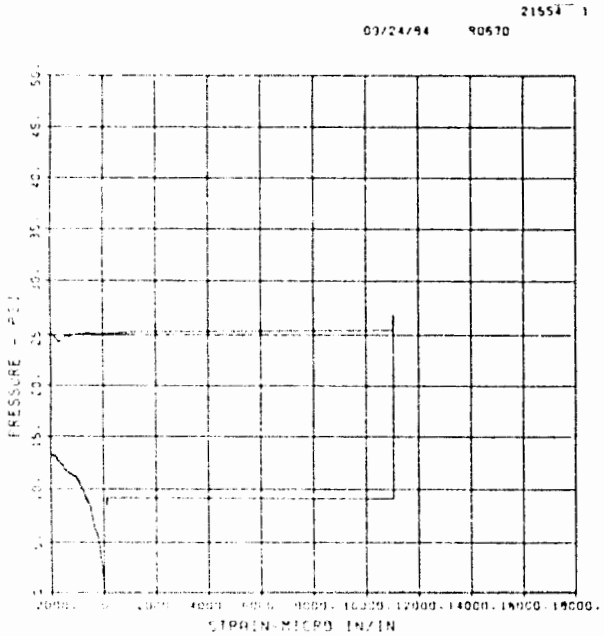

SLAB RESTRAINT CB
CT-190

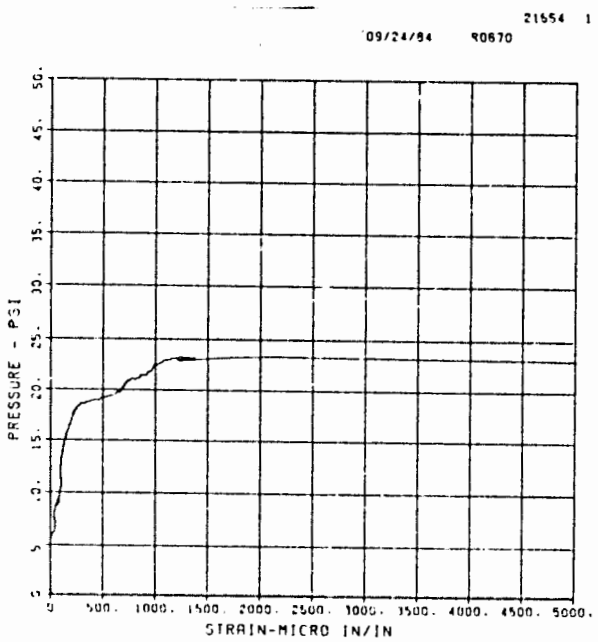

SLAB RESTRAINT G9

SLAB RESTRAINT C9
D-1

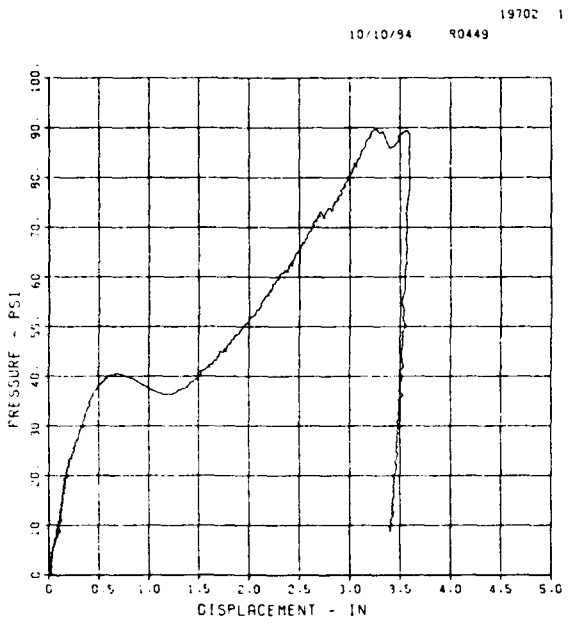

SLAB RESTRAINT C9
D-2

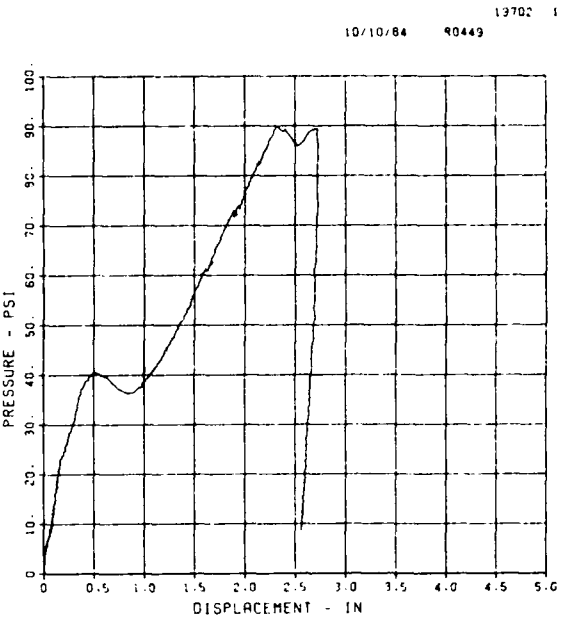

SLAB RESTRAINT C9
D-3

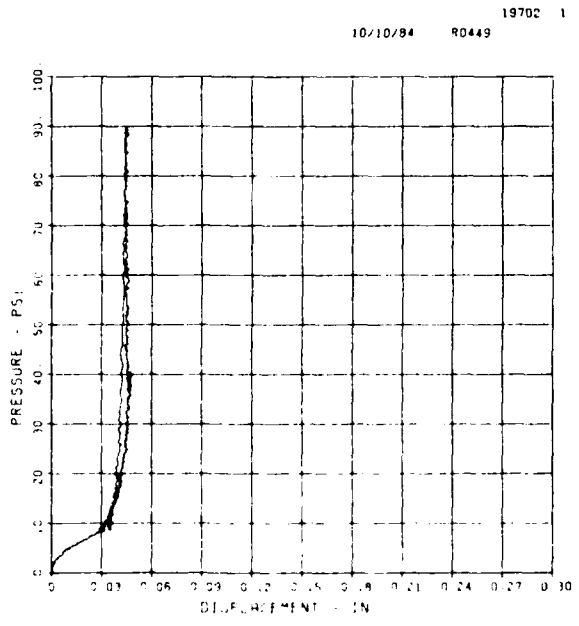

SLAB RESTRAINT C9
D-4

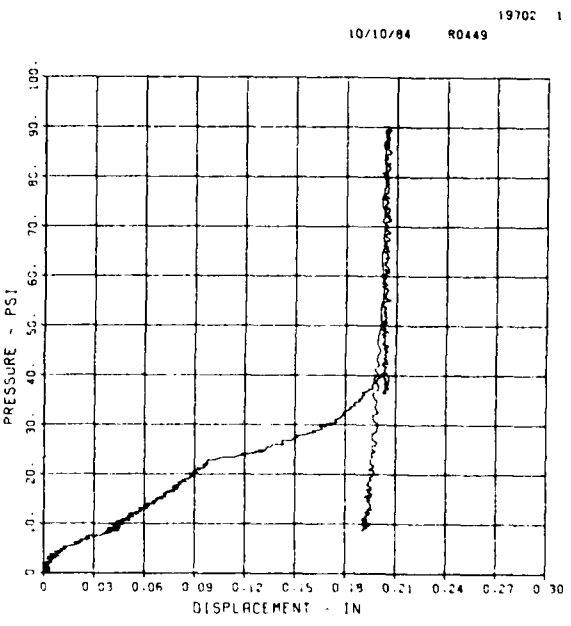

SLAB RESTRAINT G9
LW-1

19702 1
10/10/84 R0449

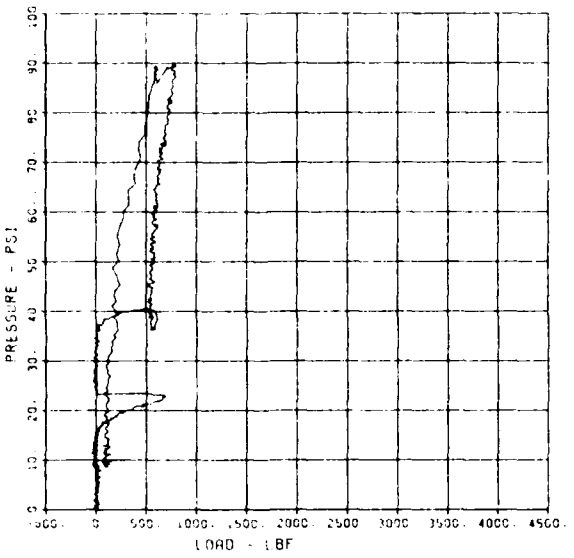

SLAB RESTRAINT G9
LW-2

19702 1
10/10/84 R0443

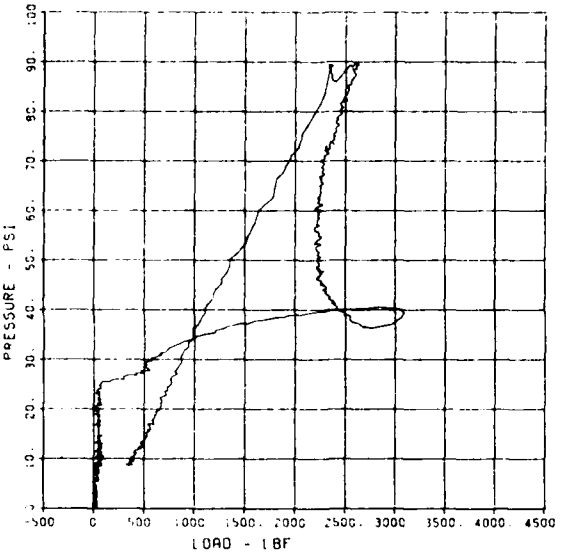

SLAB RESTRAINT G9
LW-3

19702 1
10/10/84 R0449

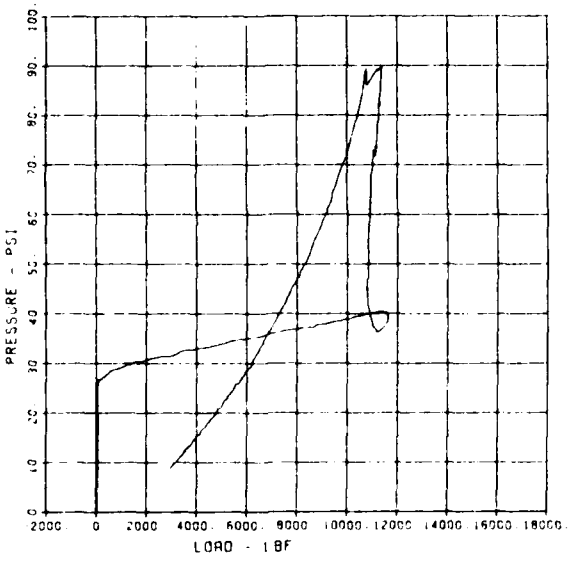

SLAB RESTRAINT G9
LW-4

19702 1
10/10/84 R0449

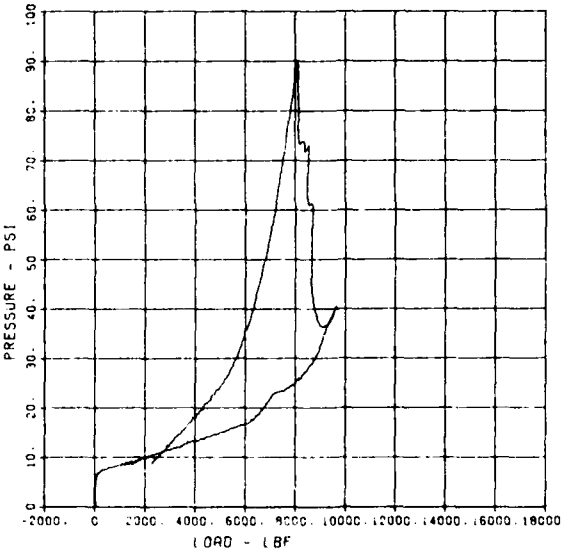

SLAB RESTRAINT G9
LW-5

19702 1
10/10/84 R0449

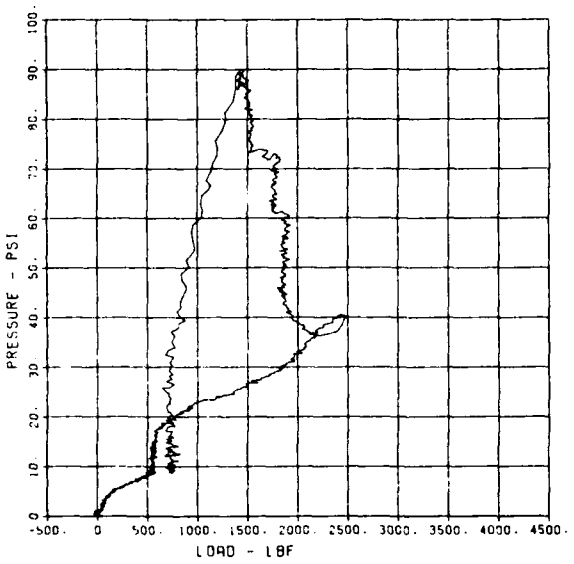

SLAB RESTRAINT G9
LW-6

19702 1
10/10/84 R0449

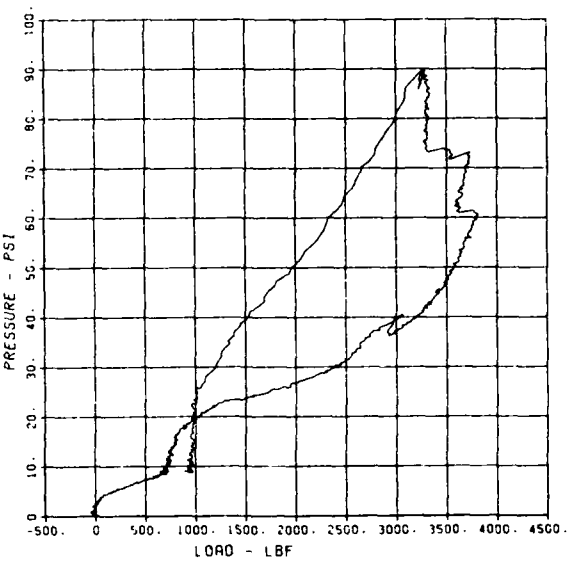

SLAB RESTRAINT G9
LW-7

19702 1
10/10/84 R0449

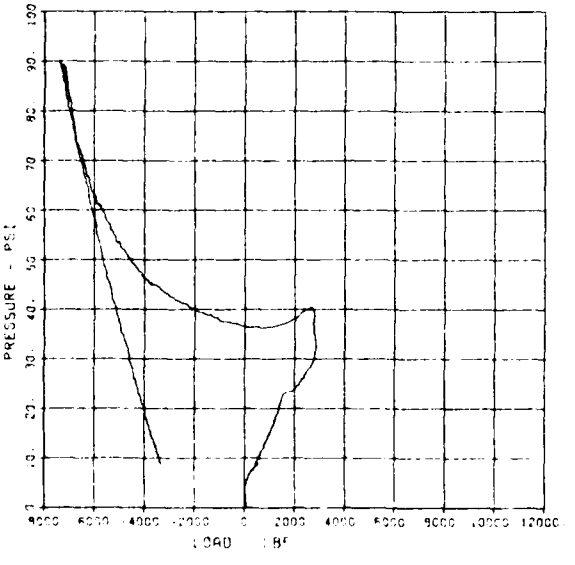

SLAB RESTRAINT G9
LW-8

19702 1
10/10/84 R0449

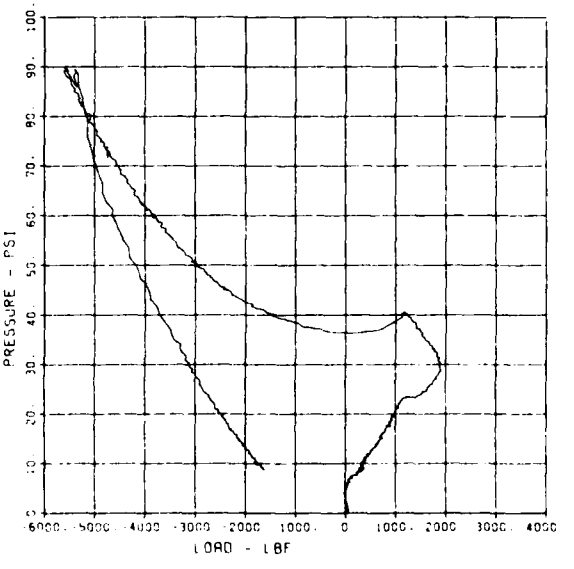

SLAB RESTRAINT 09
LW-9

19702 1
10/10/84 R0449

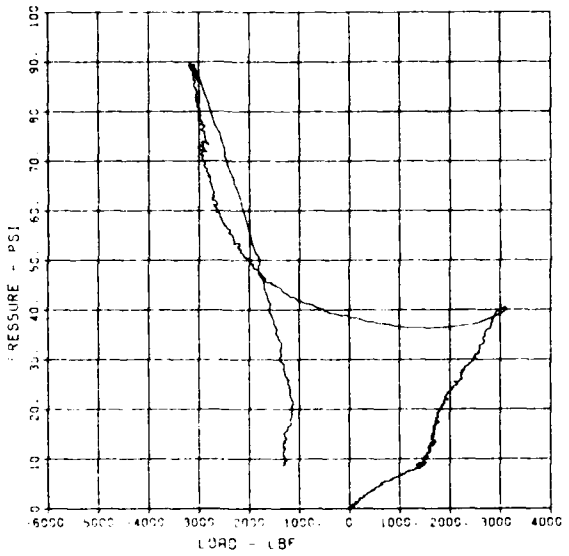

SLAB RESTRAINT 09
LW-10

19702 1
10/10/84 R0449

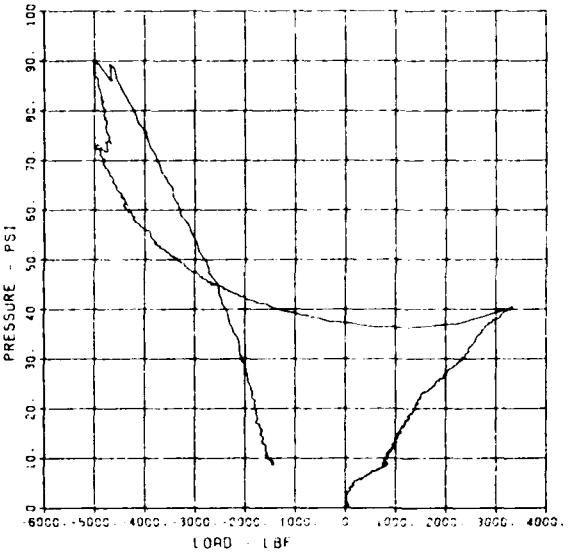

SLAB RESTRAINT 09
LW-11

19702 1
10/10/84 R0449

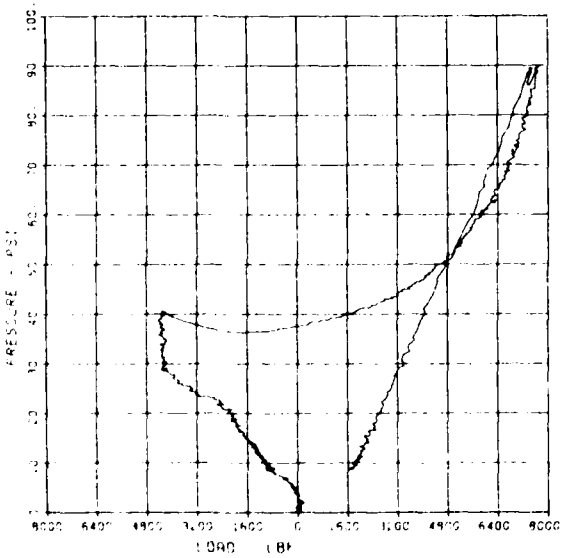

SLAB RESTRAINT 09
LW-13

19702 1
10/10/84 R0449

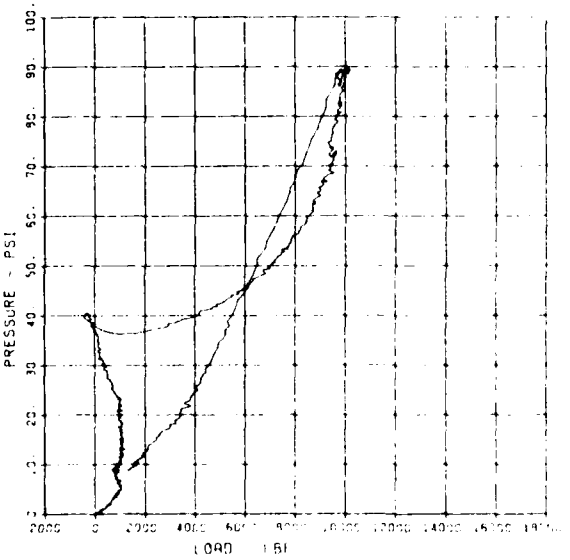

SLAB RESTRAINT 09
LW-14

19702 1
10/15/84 R0530

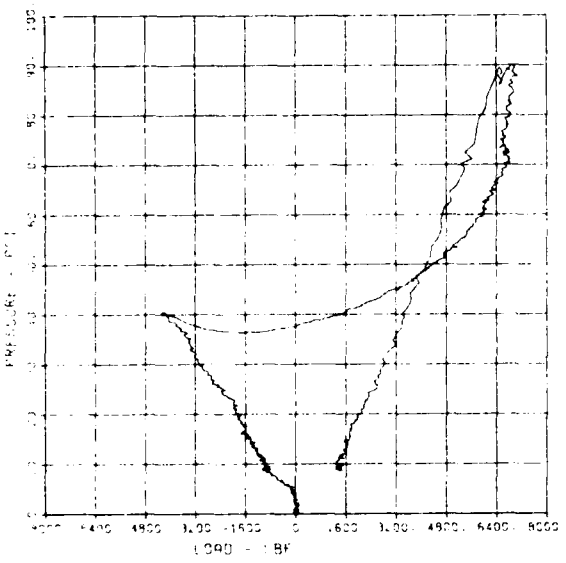

SLAB RESTRAINT 09
LW-15

19702 1
10/10/84 R0449

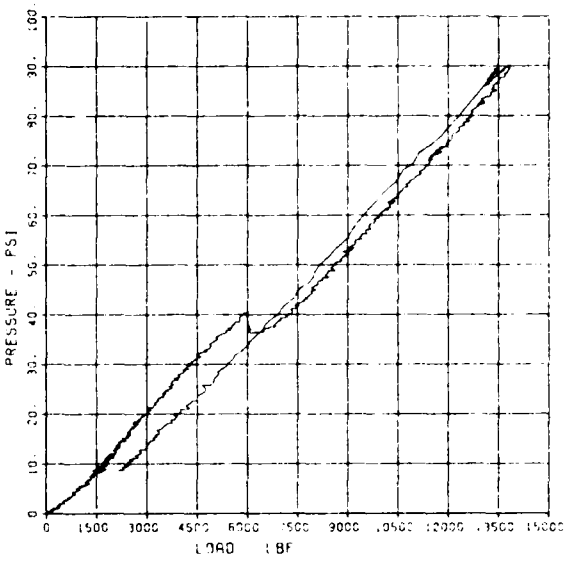

SLAB RESTRAINT 09
ST-1

19702 1
10/10/84 R0449

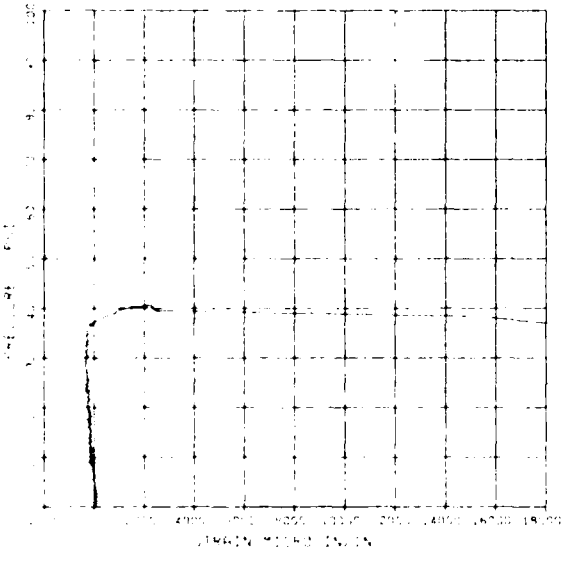

SLAB RESTRAINT 09
ST-2

19702 1
10/10/84 R0449

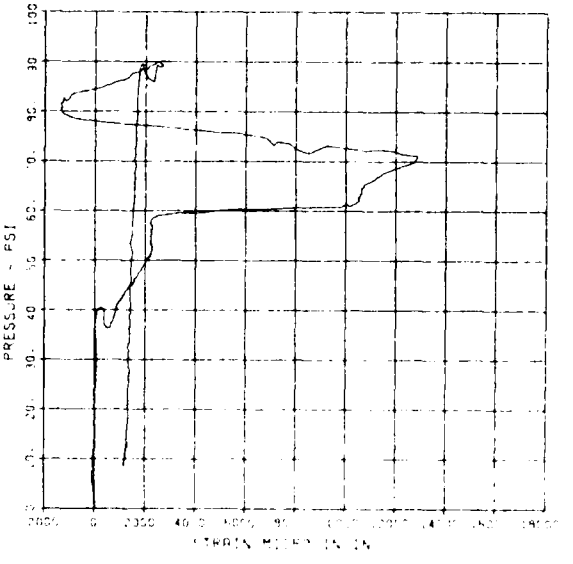

SLAB RESTRAINT 09
ST-3

19702 1
10/10/84 R0443

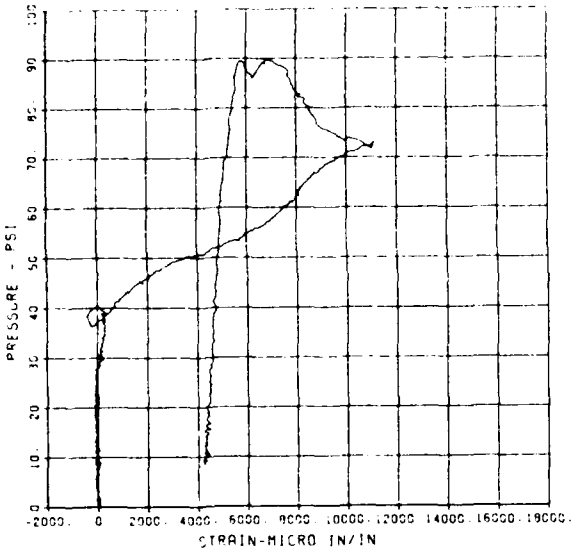

SLAB RESTRAINT 09
SB-1

19702 1
10/10/84 R0443

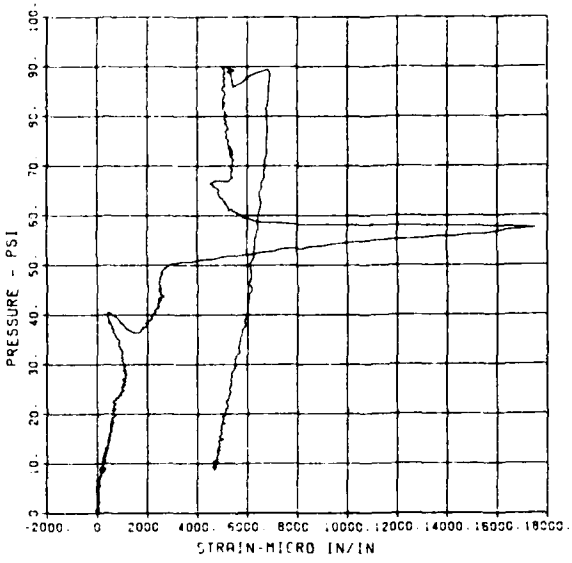

SLAB RESTRAINT 09
SB-2

19702 1
10/10/84 R0449

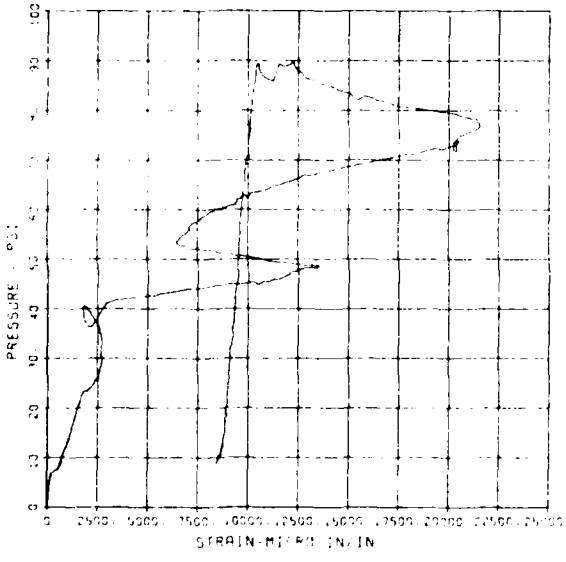

SLAB RESTRAINT 09
SB-3

19702 1
10/10/84 R0449

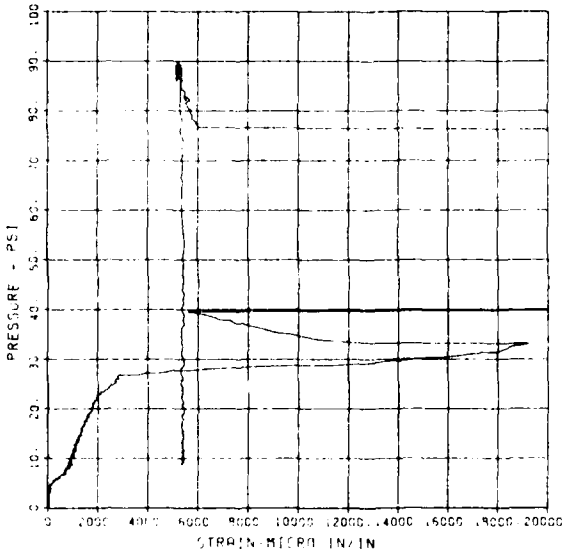

SLAB RESTRAINT 09
CT-1

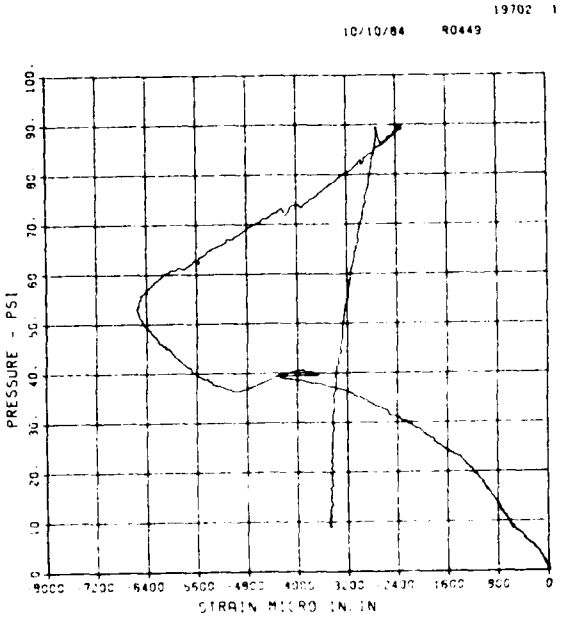

SLAB RESTRAINT 09
CB-3

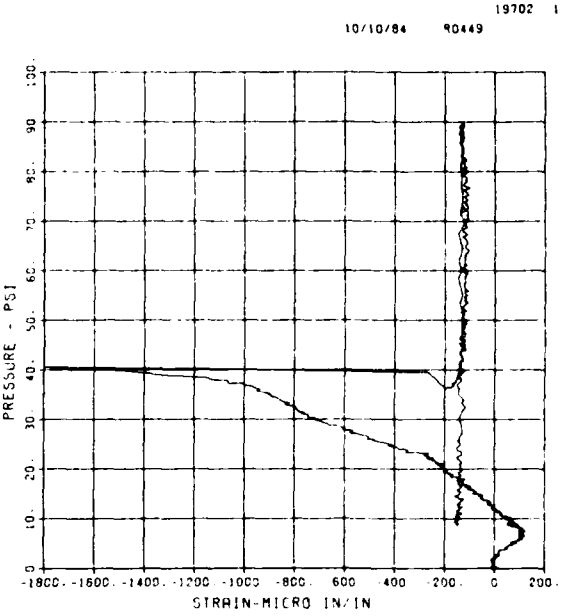

SLAB RESTRAINT 09
ST-1A

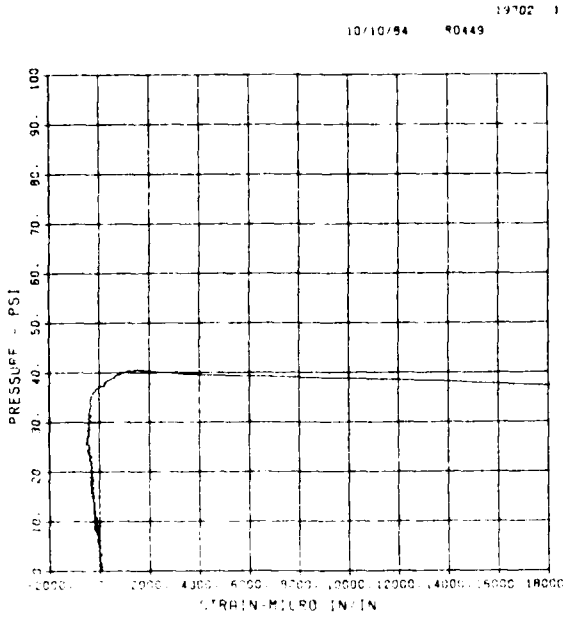

SLAB RESTRAINT 09
SB-1A

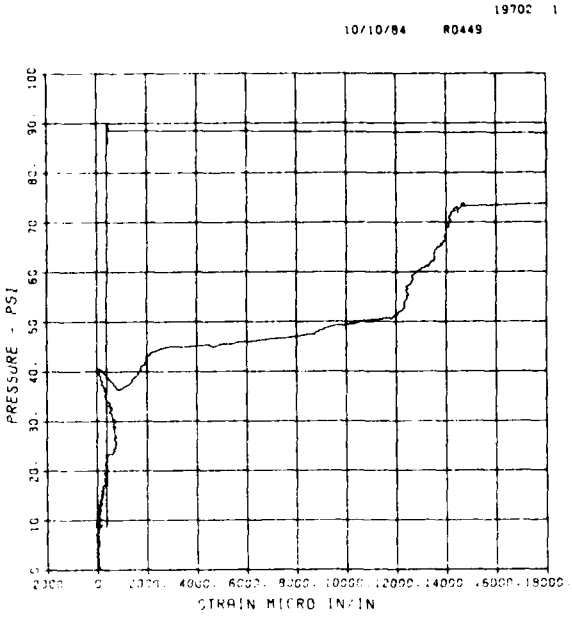

SLAB RESTRAINT 09
ST-3A

19702 1

10/10/84 R0449

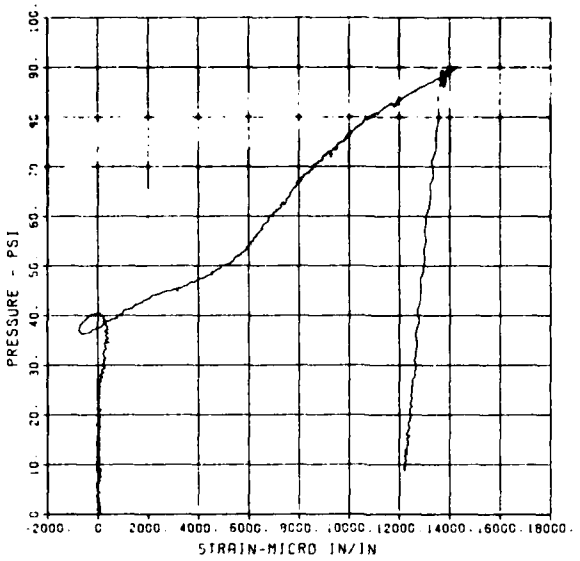

SLAB RESTRAINT G9A

SLAB RESTRAINT G9A
D-1

19305 4
10/09/94 R0435

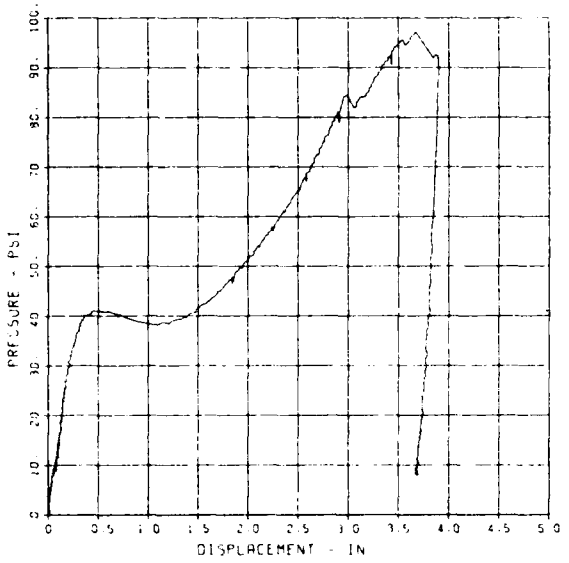

SLAB RESTRAINT G9A
D-2

19305 2
10/09/94 R0435

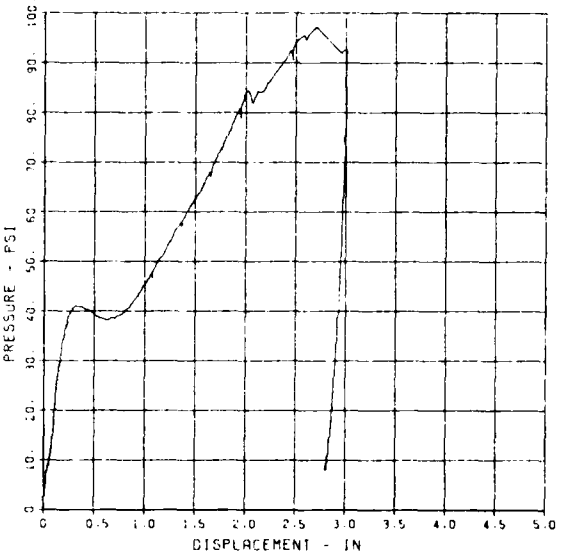

SLAB RESTRAINT G9A
D-3

19305 2
10/09/94 R0435

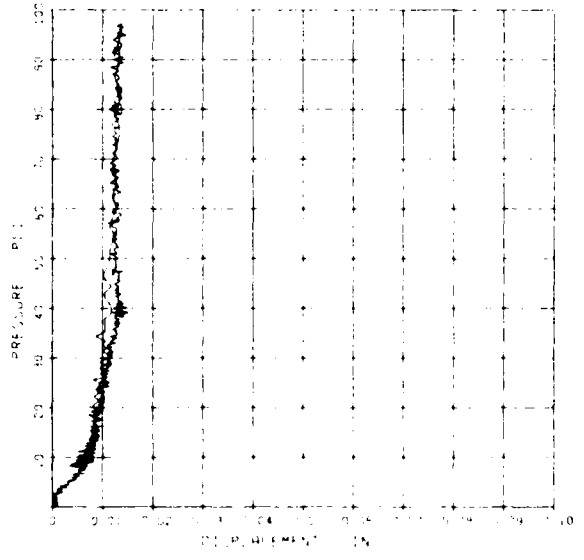

SLAB RESTRAINT G9A
D-4

19305 2
10/09/94 R0435

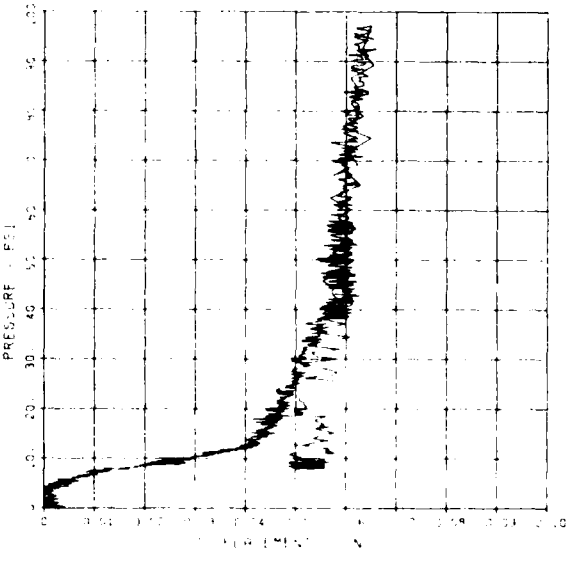

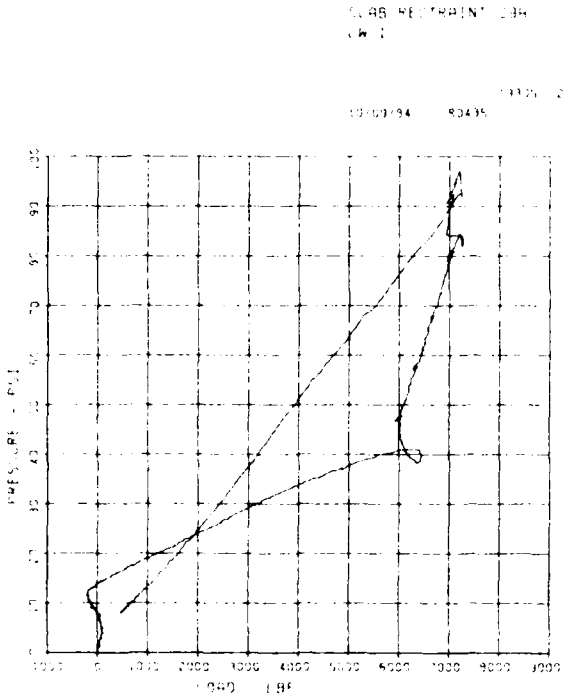
10/09/84 90435
PRESSURE - PSI
LOAD - LBF

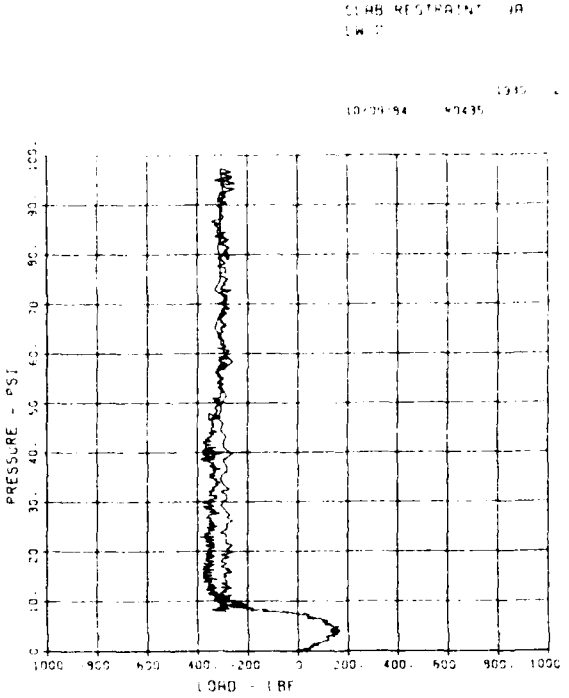
10/09/84 90435
PRESSURE - PSI
LOAD - LBF

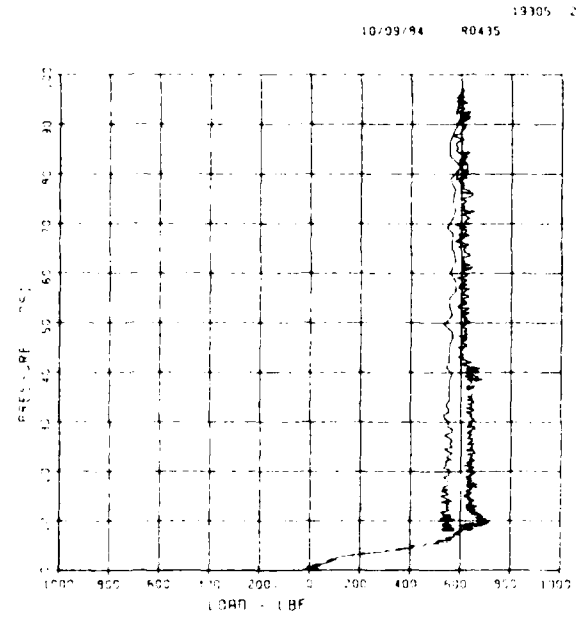
10/09/84 90435
LOAD - LBF

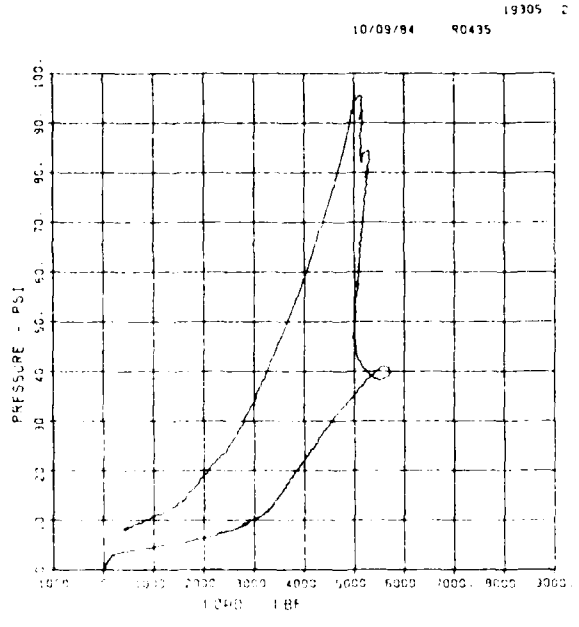
10/09/84 90435
PRESSURE - PSI

SLAB RESTRAINT 09A
LW-5

19305 2
10/09/84 R0435

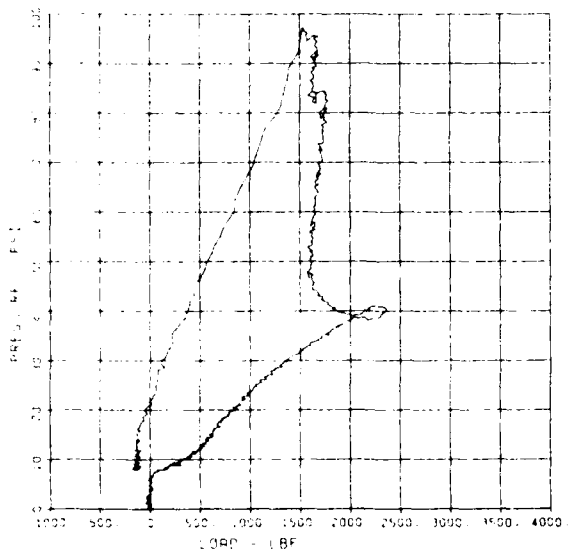

SLAB RESTRAINT 09A
LW-6

19305 2
10/09/84 R0435

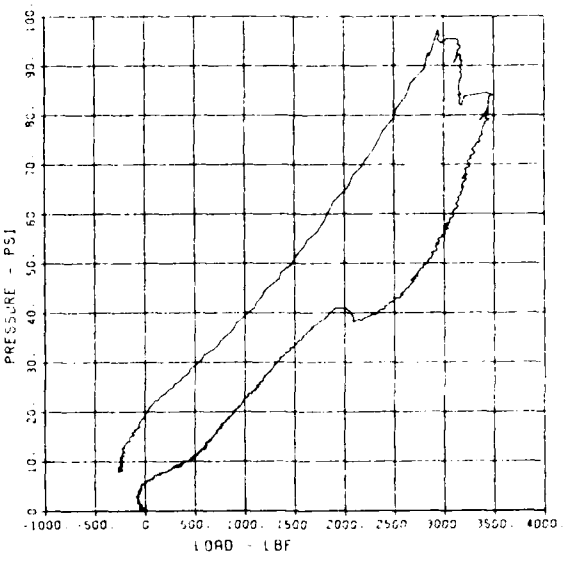

SLAB RESTRAINT 09A
LW-7

19305 2
10/09/84 R0435

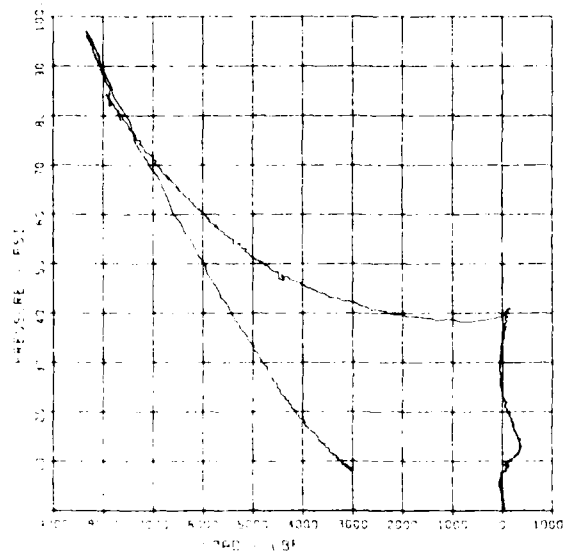

SLAB RESTRAINT 09A
LW-8

19305 2
10/09/84 R0435

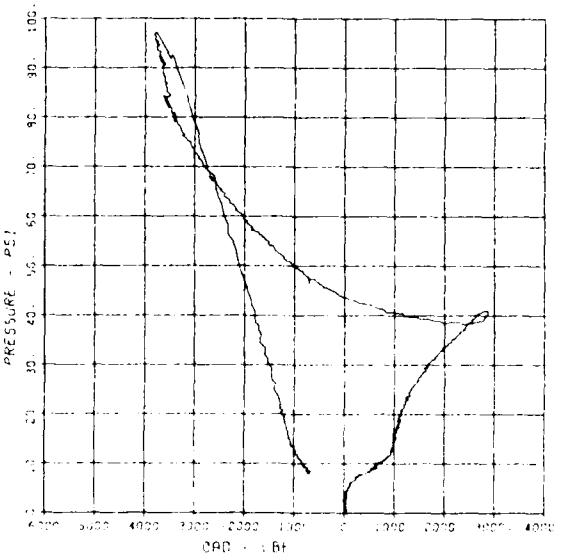

SLAB RESTRAINT 09A
LW-9

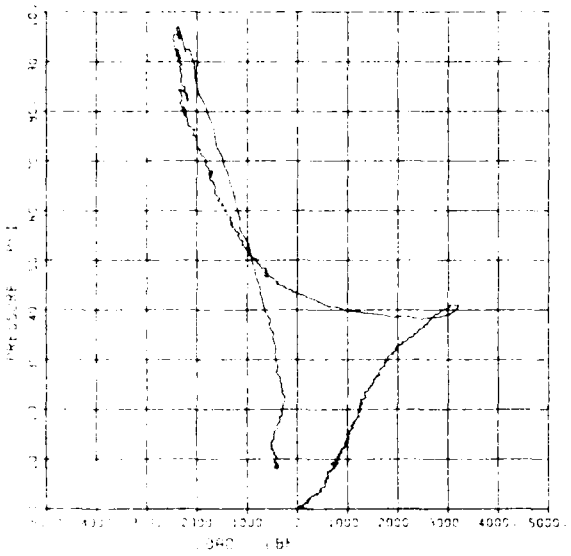

SLAB RESTRAINT 09A
LW-10

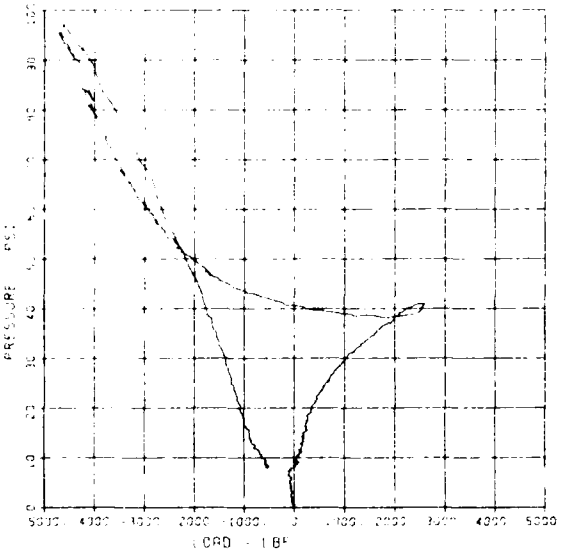

SLAB RESTRAINT 09A
LW-11

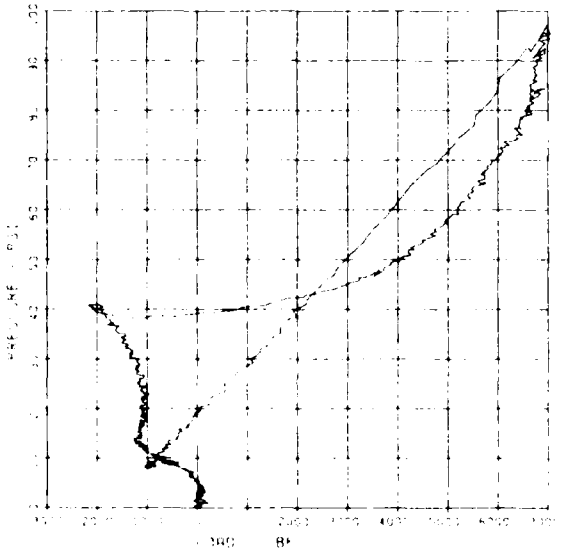

SLAB RESTRAINT 09A
LW-13

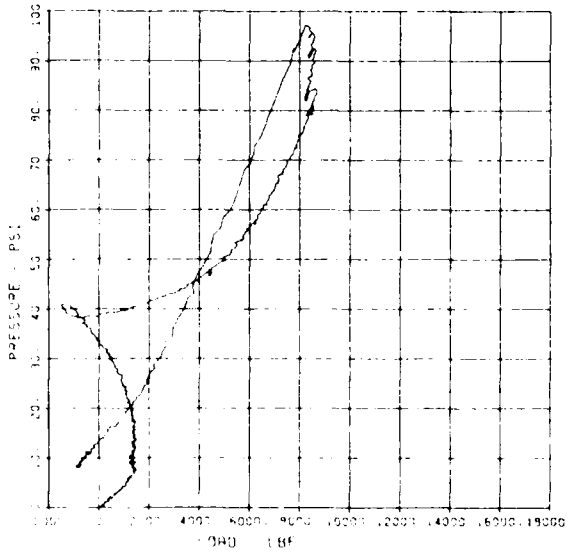

SLAB RESTRAINT 09A
LW-15

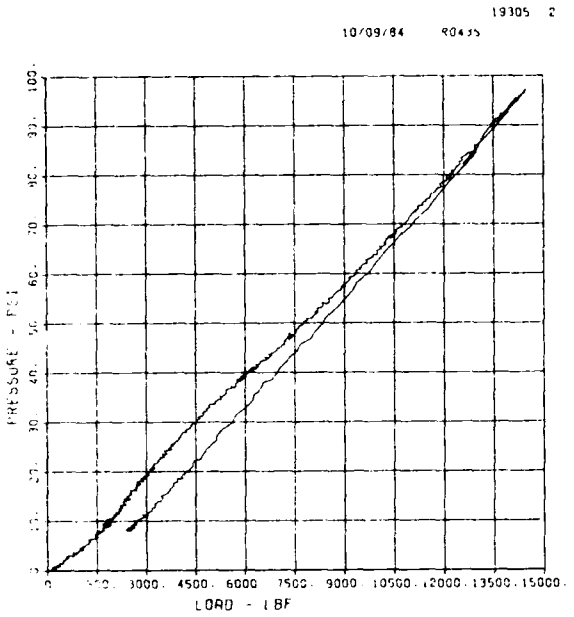

SLAB RESTRAINT 09A
ST-1

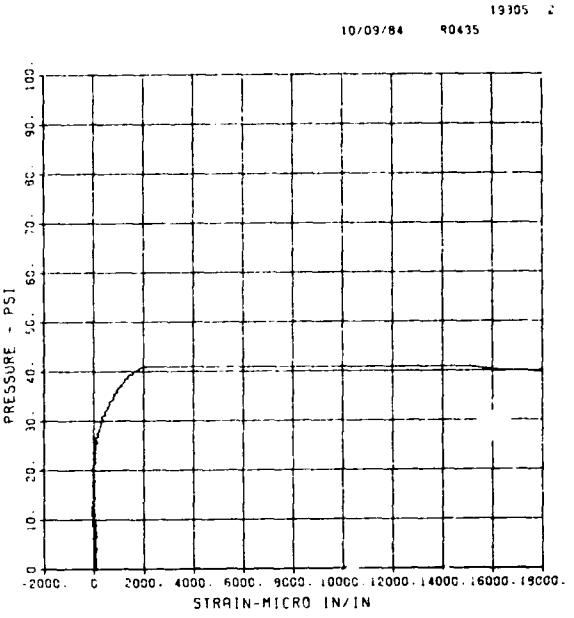

SLAB RESTRAINT 09A
ST-2

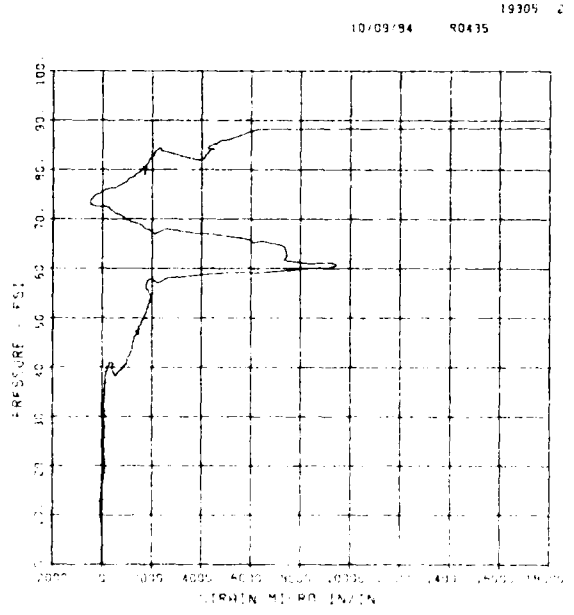

SLAB RESTRAINT 09A
ST-3

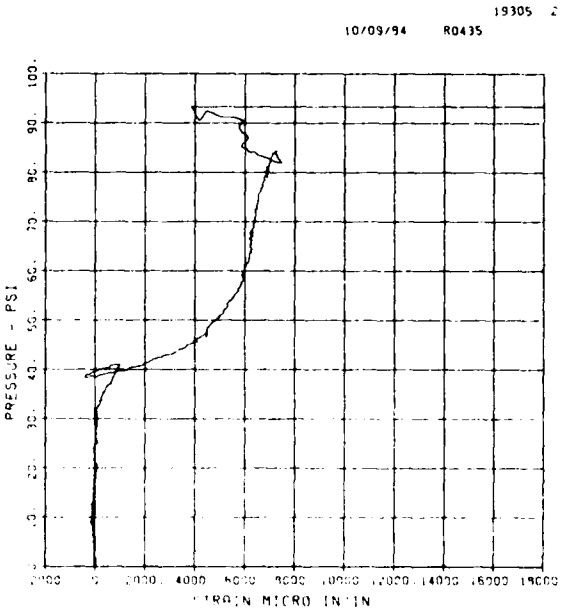

SLAB RESTRAINT C9A
SB-1

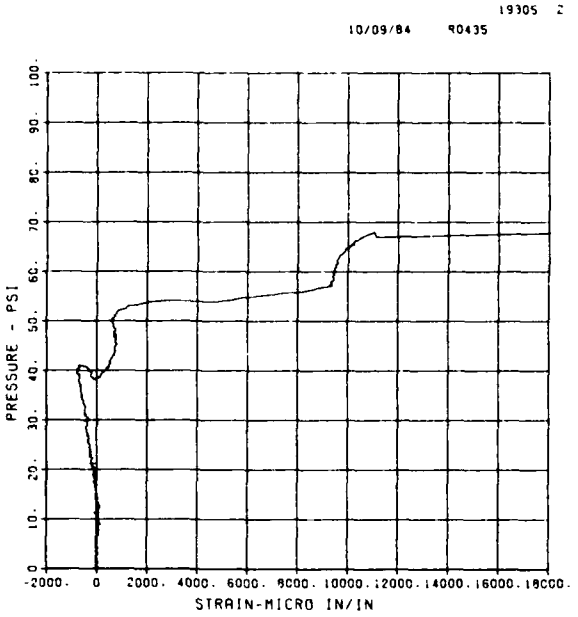

SLAB RESTRAINT C9A
SB-2

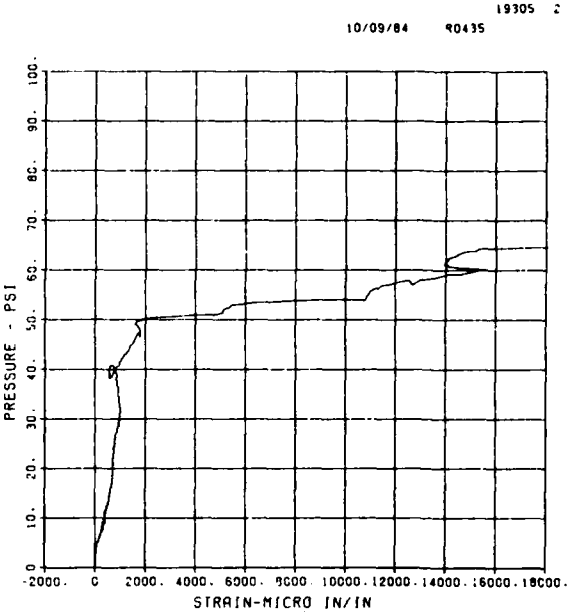

SLAB RESTRAINT C9A
SB-3

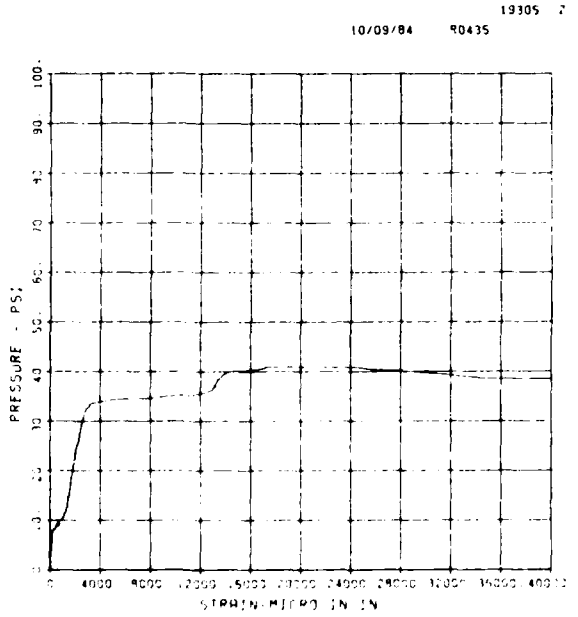

SLAB RESTRAINT C9A
CT-1

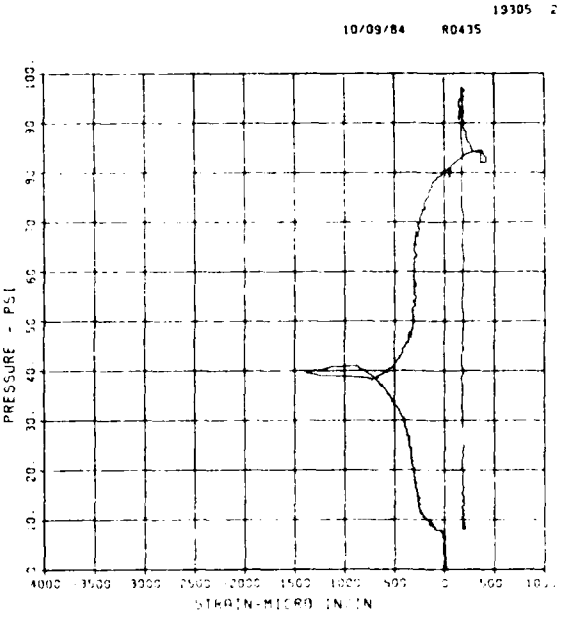

SLAB RESTRAINT C9A
CB-3

19305 2
10/09/84 R0435

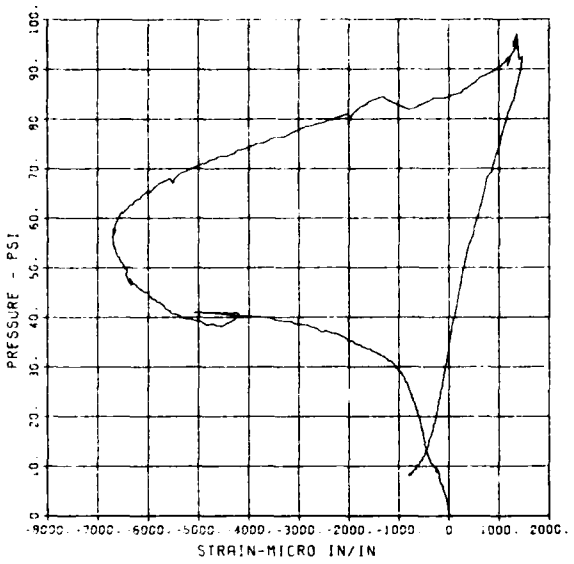

SLAB RESTRAINT C9A
ST-1A

19305 2
10/09/84 R0435

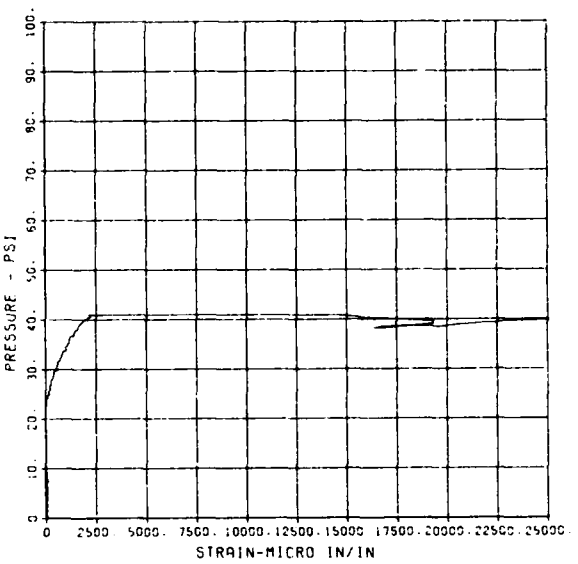

SLAB RESTRAINT C9A
SB-1A

19305 2
10/09/84 R0435

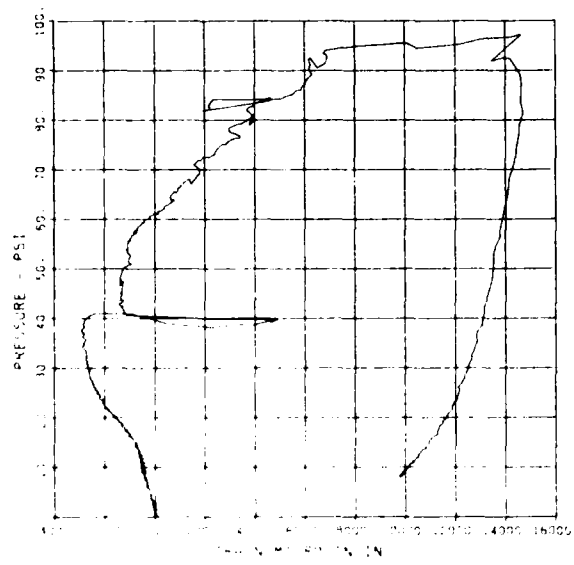

SLAB RESTRAINT C9A
SB-3A

19305 2
10/09/84 R0435

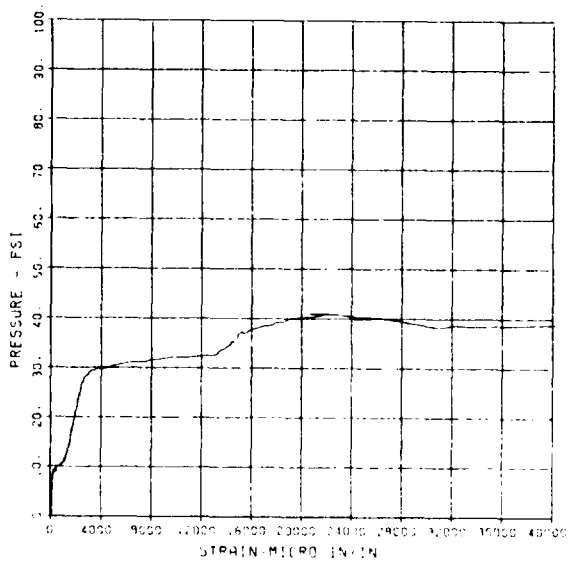

SLAB RESTRAINT G10

SLAB RESTRAINT G10
D-1

20544 1
09/30/84 R0214

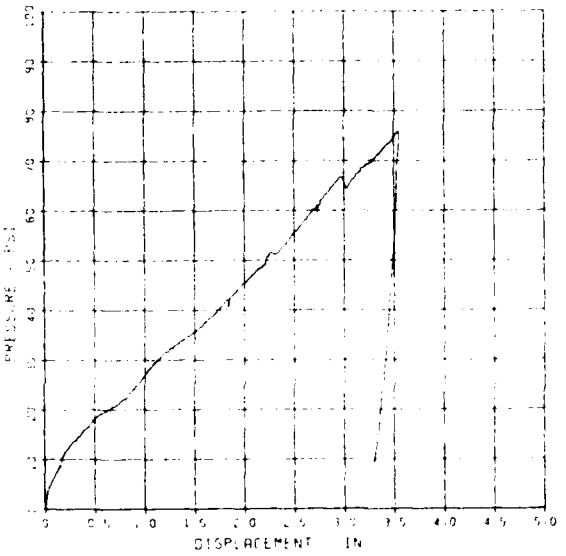

SLAB RESTRAINT G10
D-2

20544 1
09/30/84 R0214

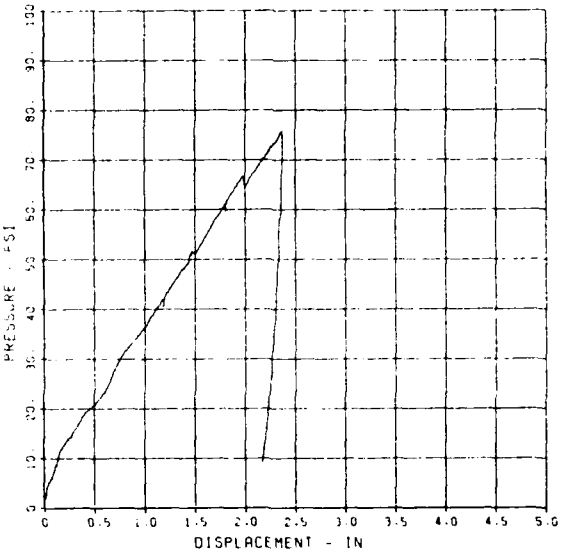

SLAB RESTRAINT G10
D-3

20544 1
09/30/84 R0214

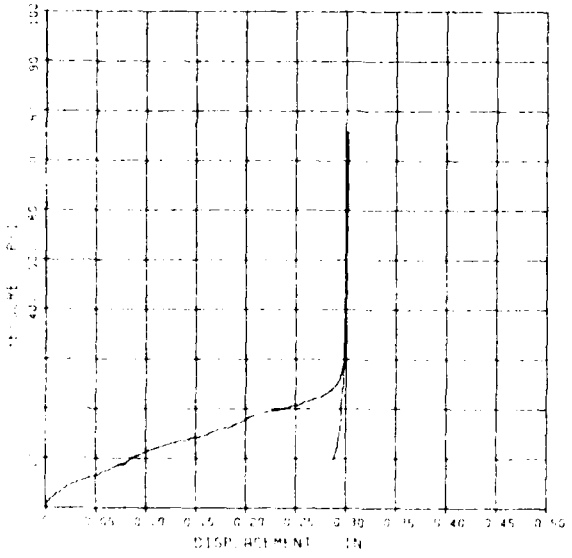

SLAB RESTRAINT G10
D-4

20544 1
09/30/84 R0214

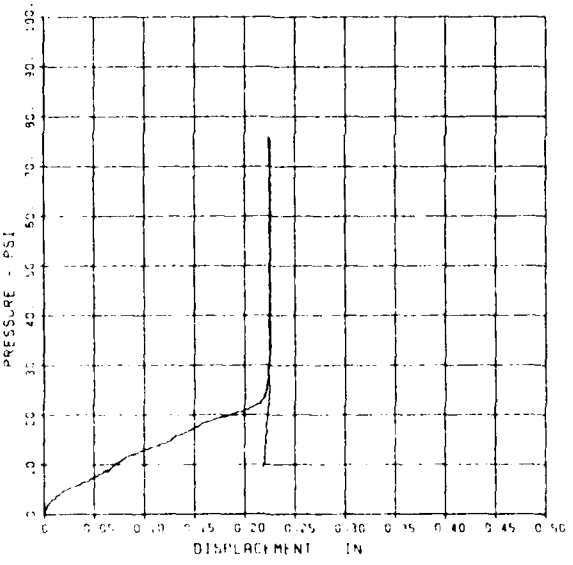

SLAB RESTRAINT G10
LW-1

20544 1
08/30/84 R0214

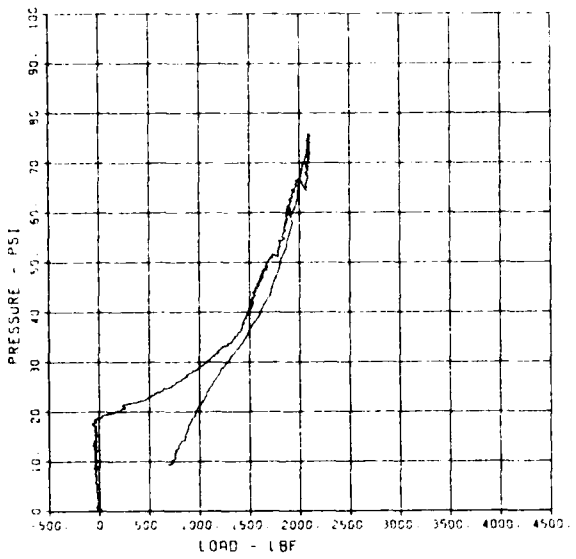

SLAB RESTRAINT G10
LW-2

20544 1
08/30/84 R0214

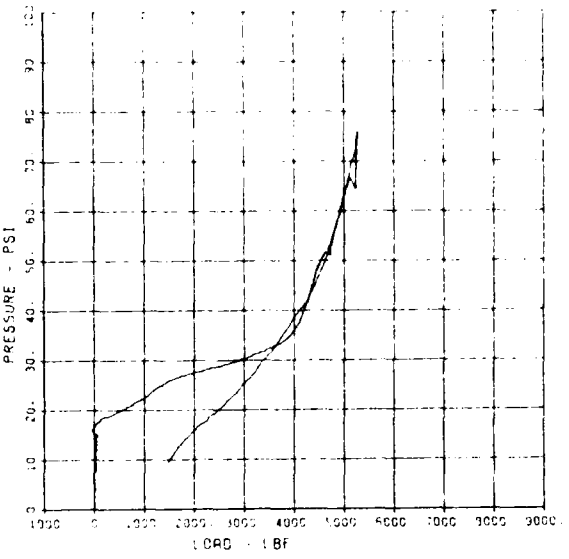

SLAB RESTRAINT G10
LW-3

20544 1
08/30/84 R0214

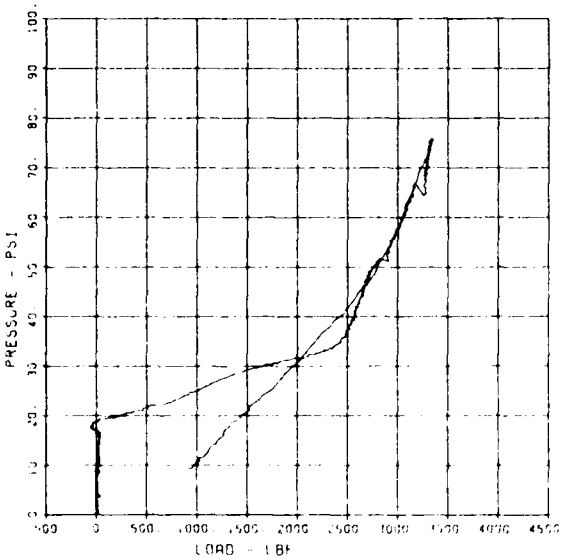

SLAB RESTRAINT G10
LW-4

20544 1
08/30/84 R0214

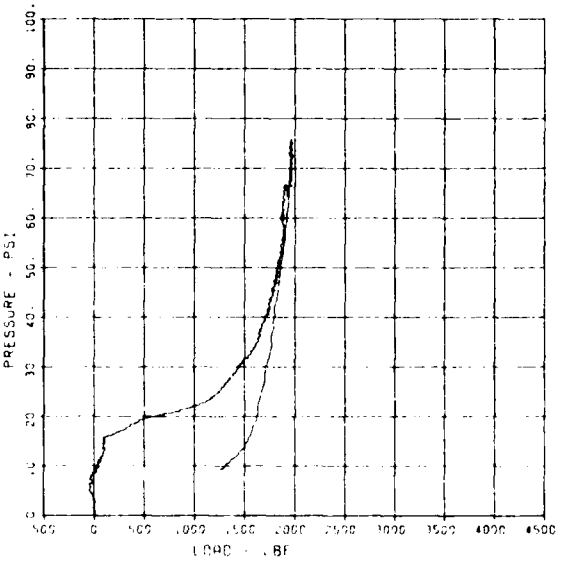

SLAB RESTRAINT G10
LW-5

20544 1
09/30/84 R0214

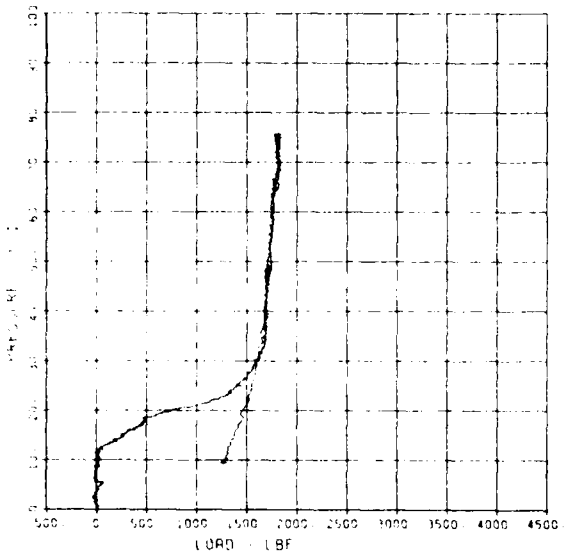

SLAB RESTRAINT G10
LW-6

20544 1
09/30/84 R0214

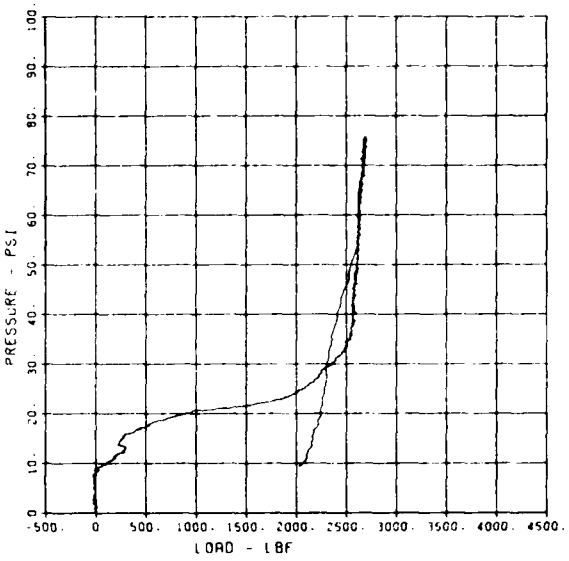

SLAB RESTRAINT G10
LW-7

20544 1
08/30/84 R0214

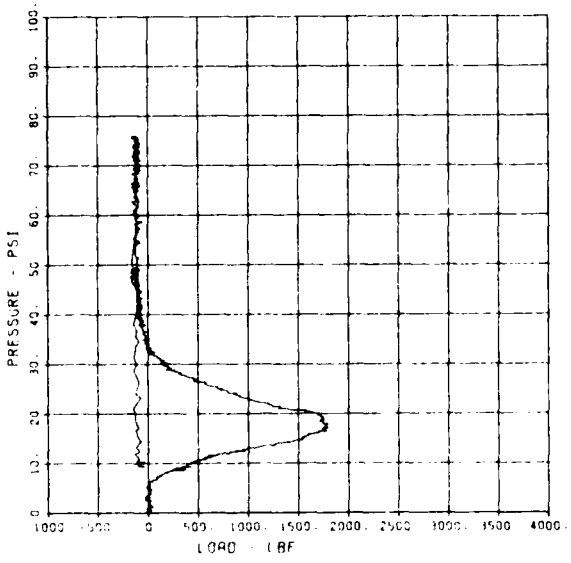

SLAB RESTRAINT G10
LW-8

20544 1
08/30/84 R0214

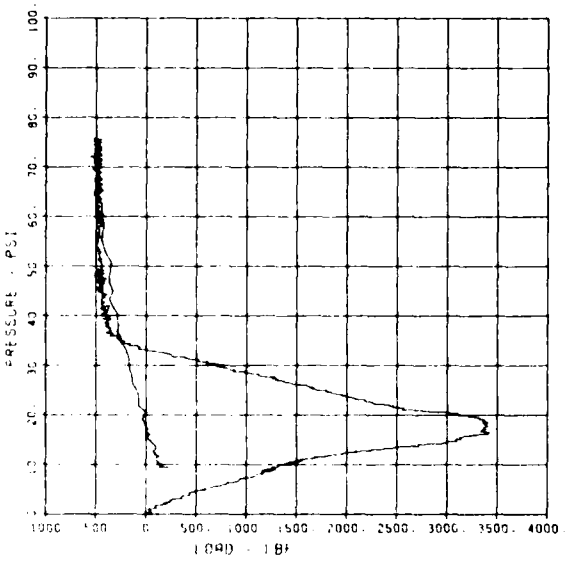

SLAB RESTRAINT G10
LW-9

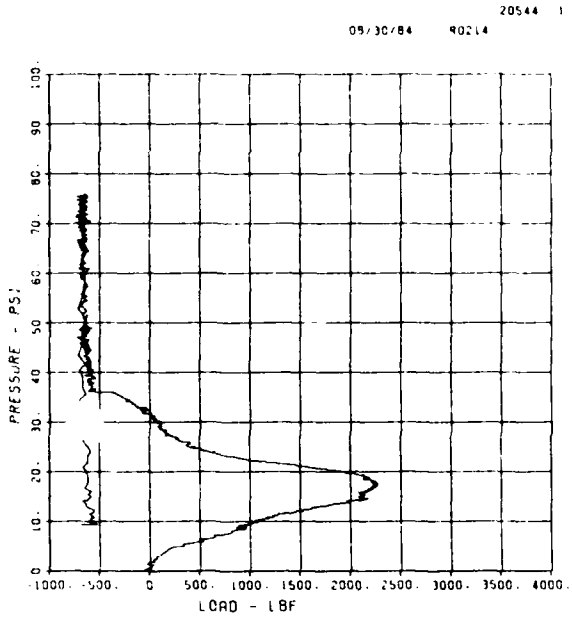

SLAB RESTRAINT G10
LW-10

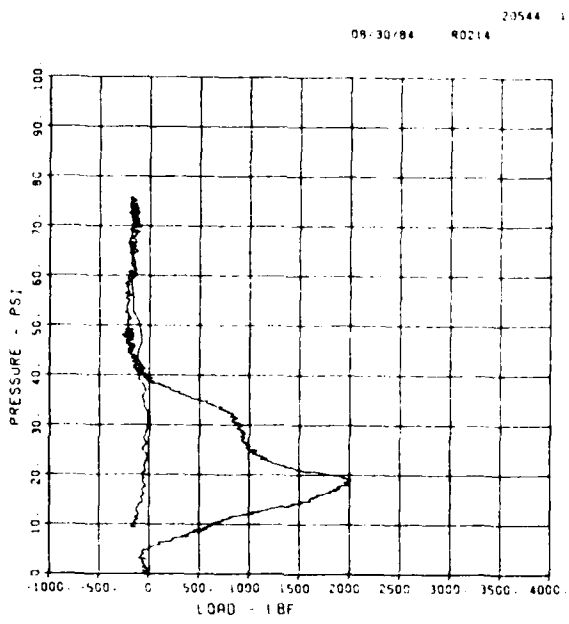

SLAB RESTRAINT G10
LW-11

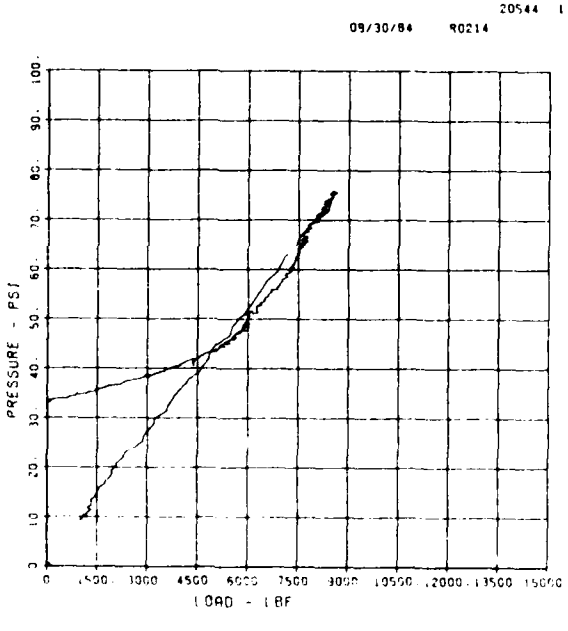

SLAB RESTRAINT G10
LW-12

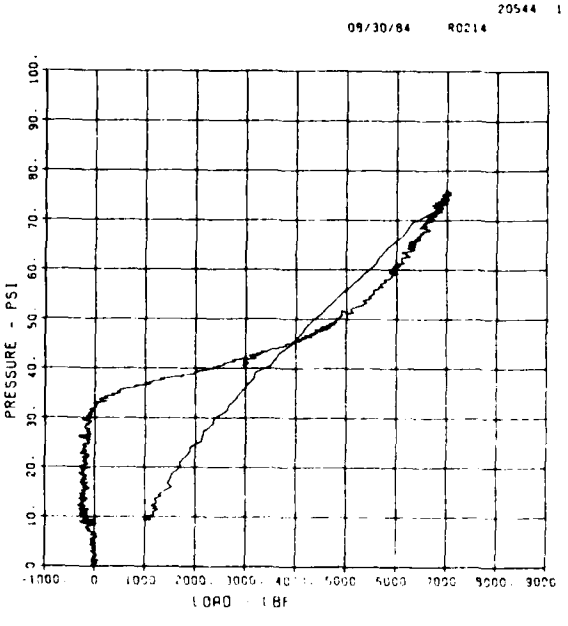

SLAB RESTRAINT G10
LW-13

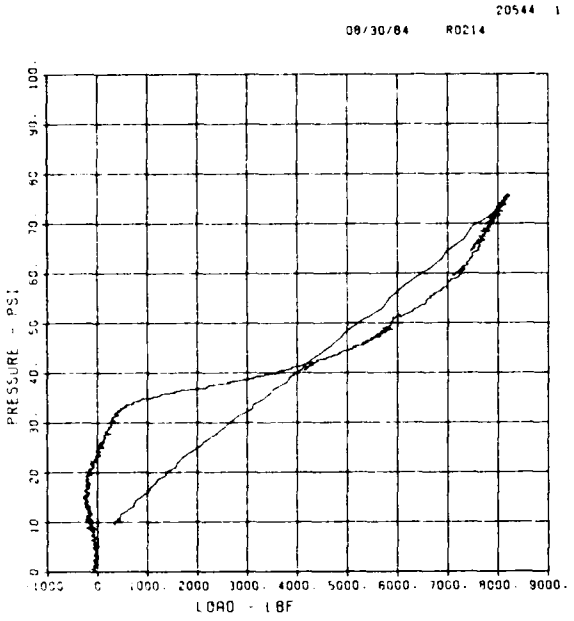

SLAB RESTRAINT G10
LW-14

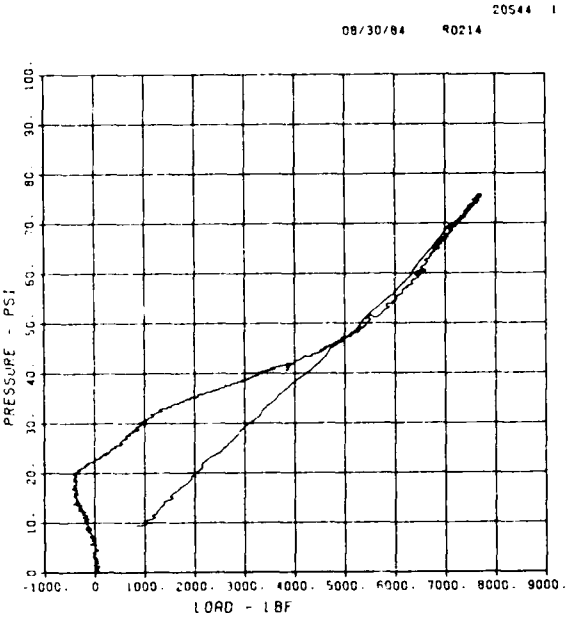

SLAB RESTRAINT G10
LW-15

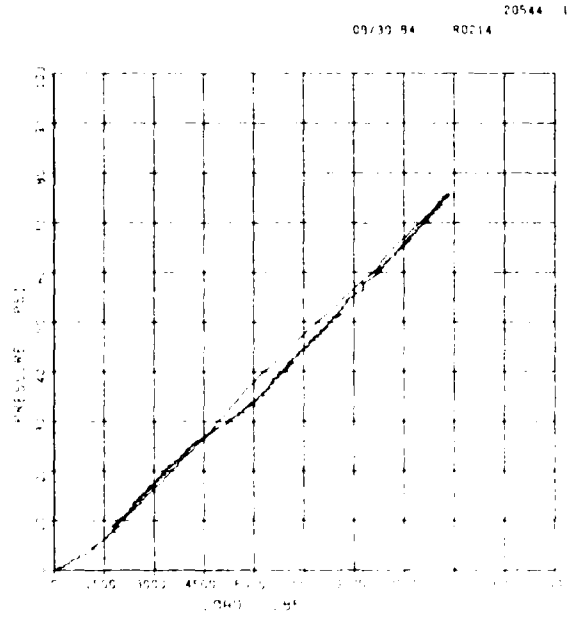

SLAB RESTRAINT G10
LW-16

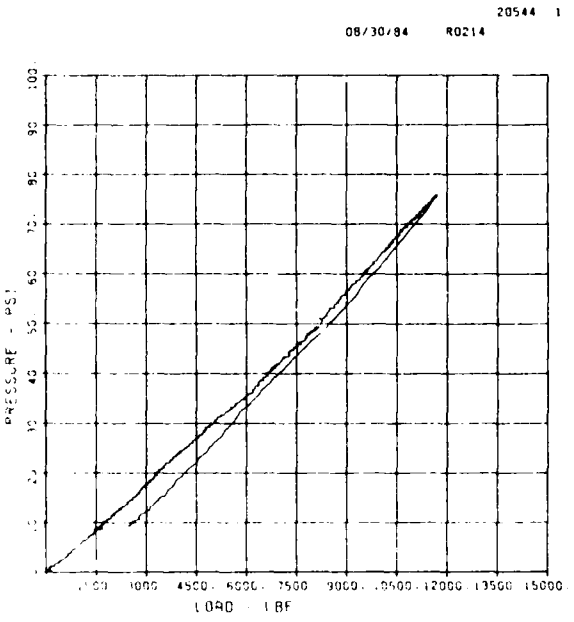

SLAB RESTRAINT C10
ST-1

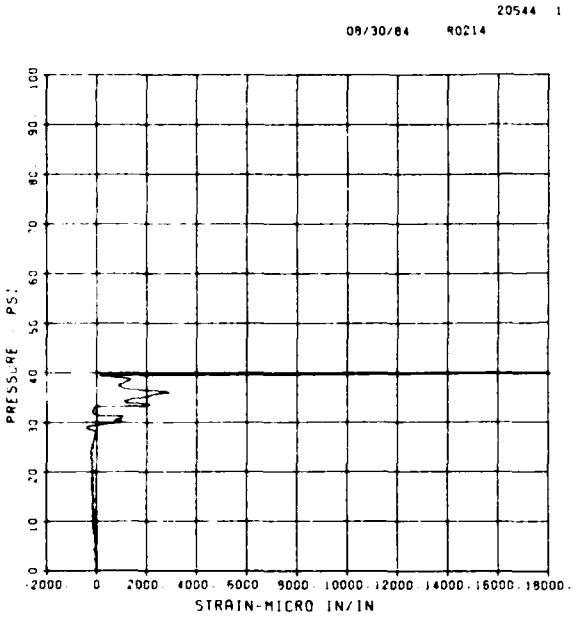

SLAB RESTRAINT C10
ST-2

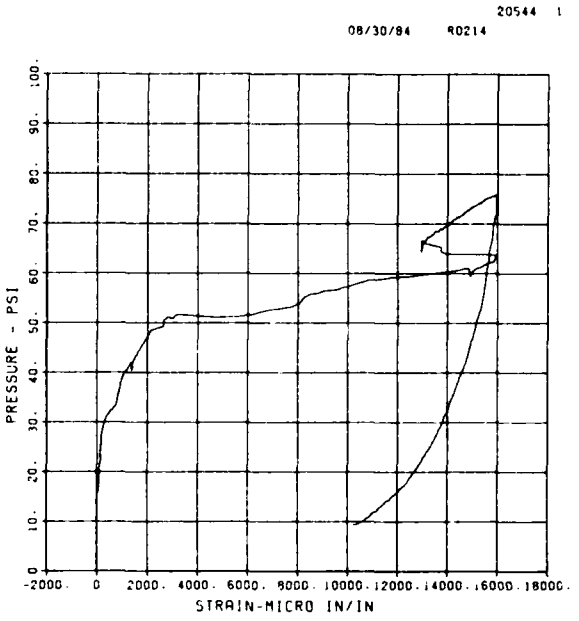

SLAB RESTRAINT C10
ST-3

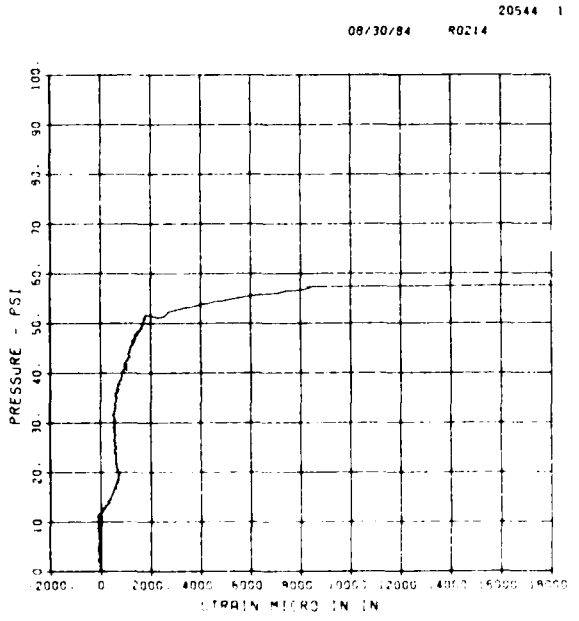

SLAB RESTRAINT C10
SB-1

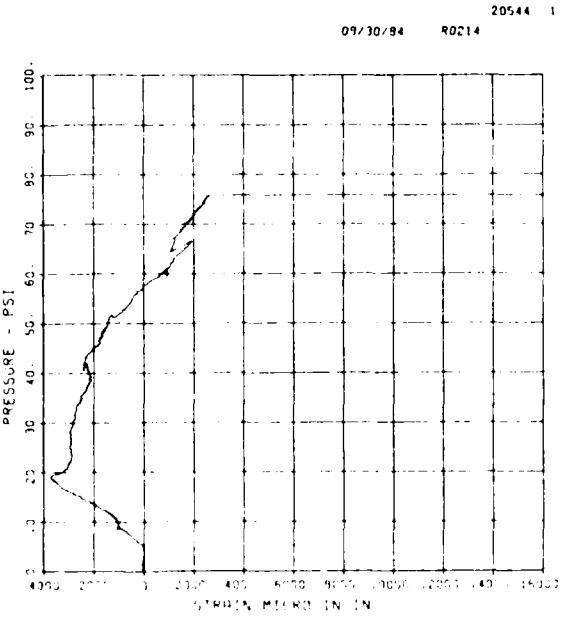

SLAB RESTRAINT G10
SB-2

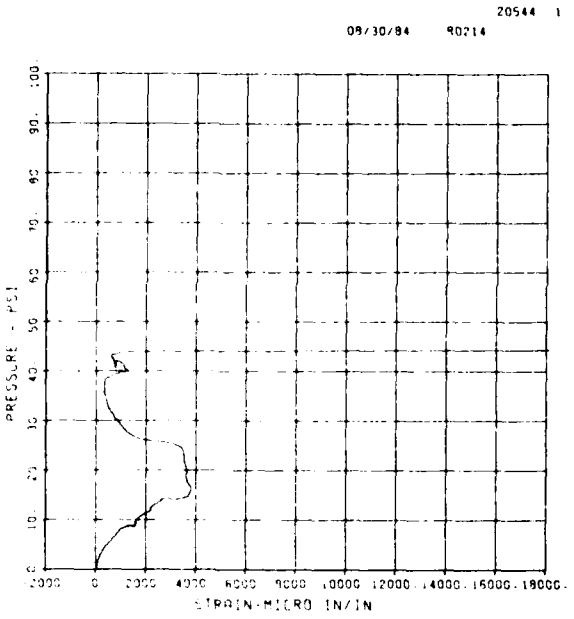

SLAB RESTRAINT G10
SB-3

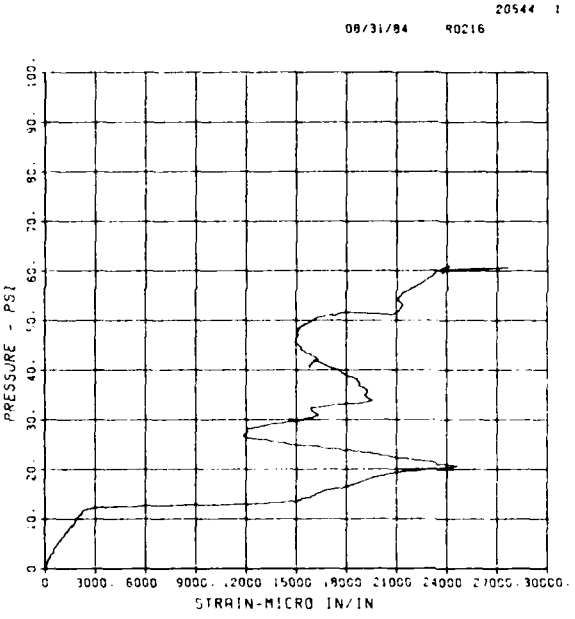

SLAB RESTRAINT G10
ST-1A

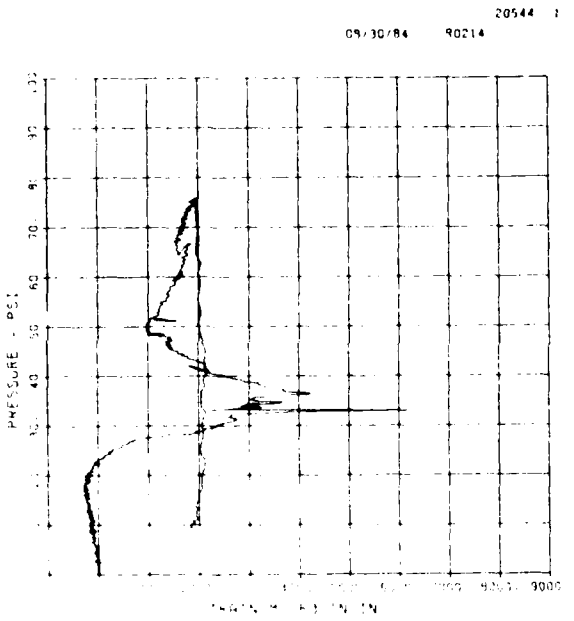

SLAB RESTRAINT G10
SB-1A

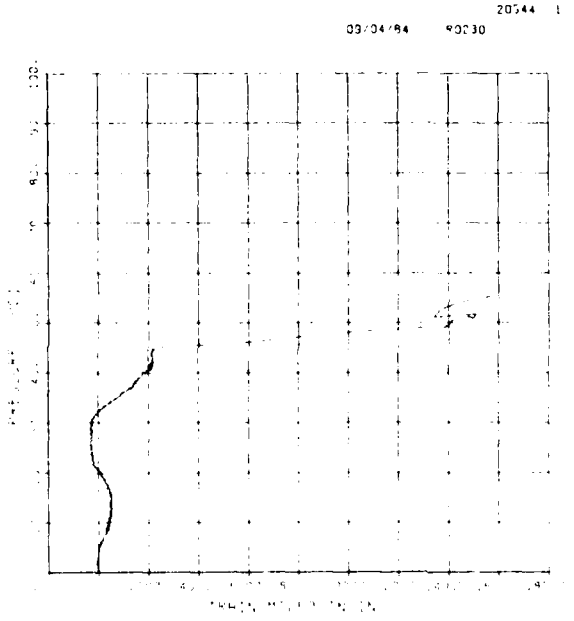

SLAB RESTRAINT S/O
SB-3A

20544

09/04/94 90230

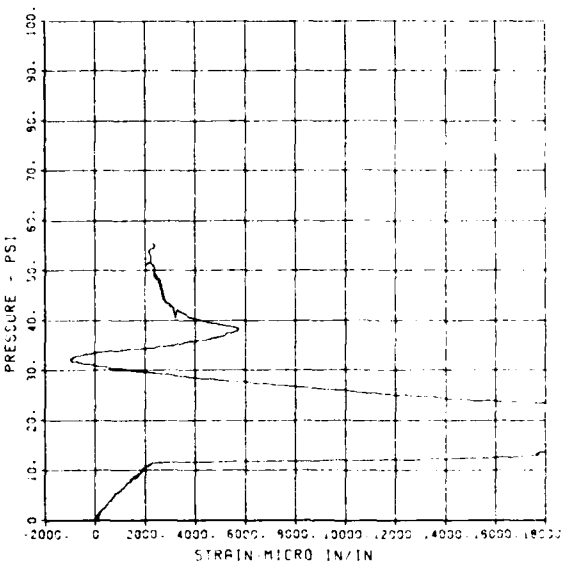

SLAB RESTRAINT G10A

SLAB RESTRAINT C10A
D-1

20723 1
09/29/84 R0199

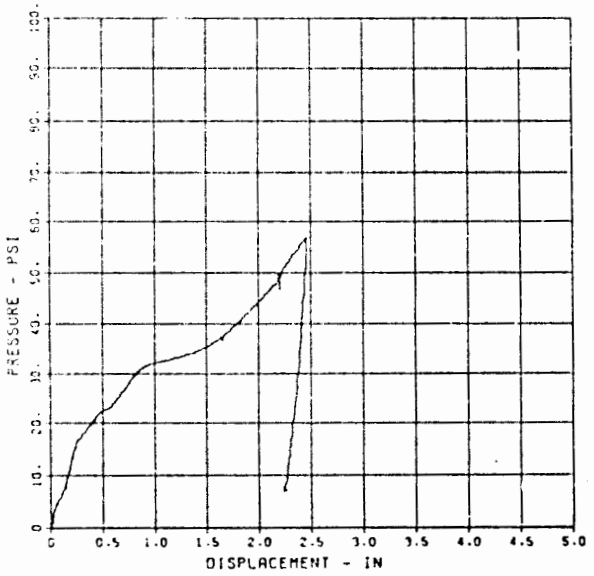

SLAB RESTRAINT C10A
D-2

20723 1
09/29/84 R0199

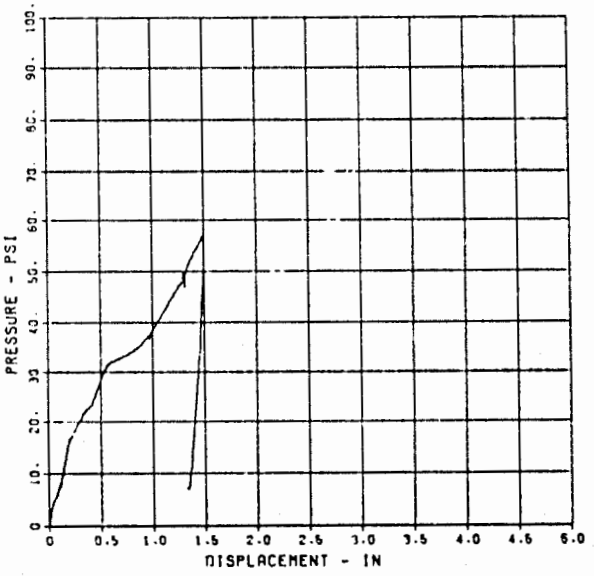

SLAB RESTRAINT C10A
D-3

20723 1
09/29/84 R0199

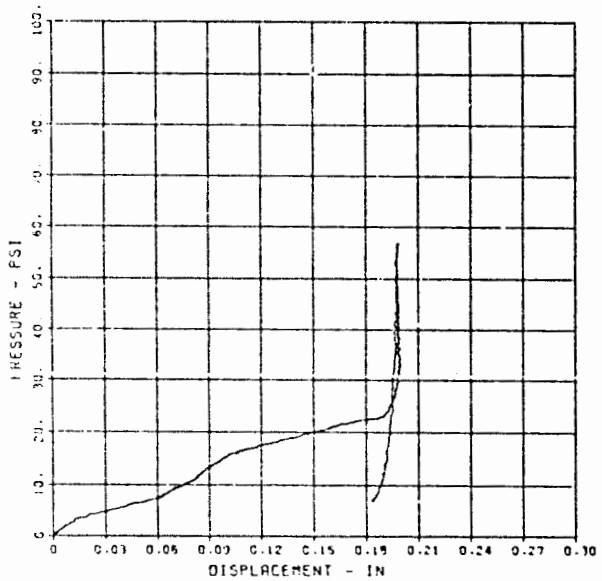

SLAB RESTRAINT C10A
D-4

20723 1
09/29/84 R0199

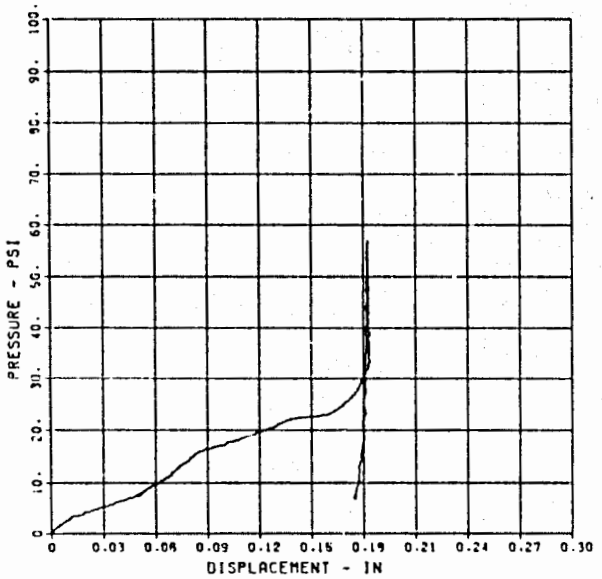

SLAB RESTRAINT G10A
LW-1

20723 1
09/29/94 R0199

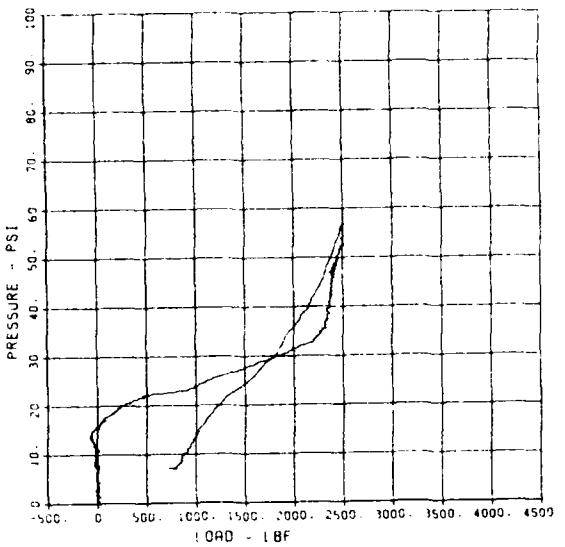

SLAB RESTRAINT G10A
LW-2

20723 1
09/29/94 R0199

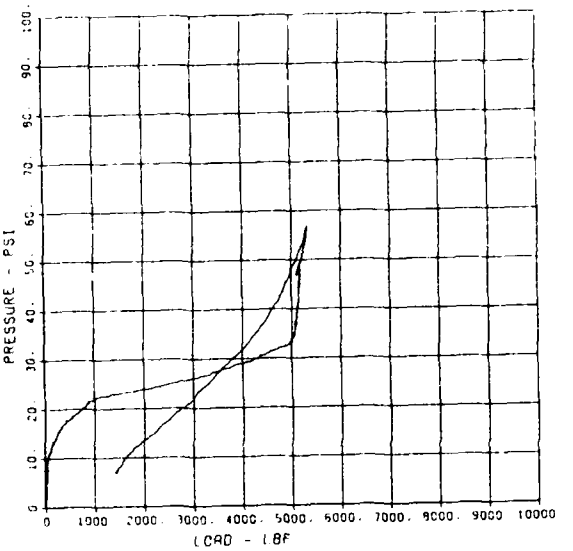

SLAB RESTRAINT G10A
LW-3

20723 1
09/29/94 R0199

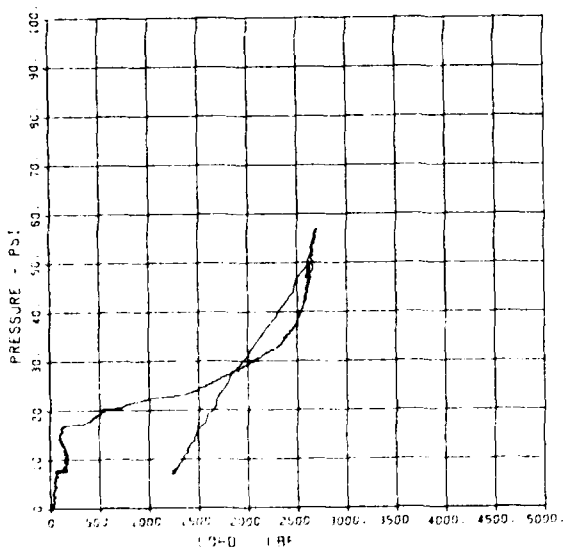

SLAB RESTRAINT G10A
LW-4

20723 1
09/29/94 R0199

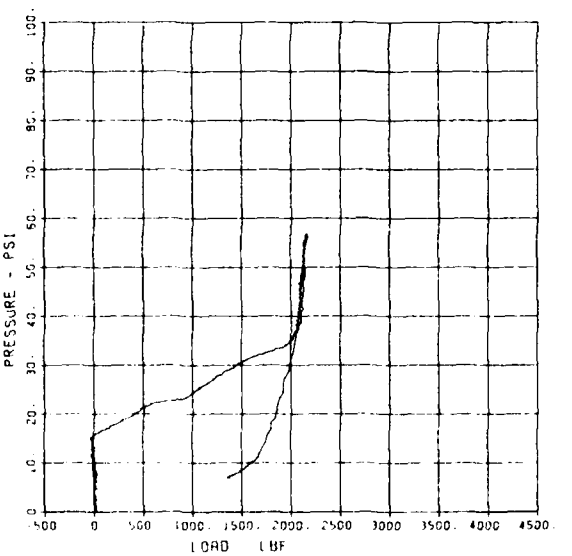

SLAB RESTRAINT C10A
LW-5

20723 1
08/29/84 R0199

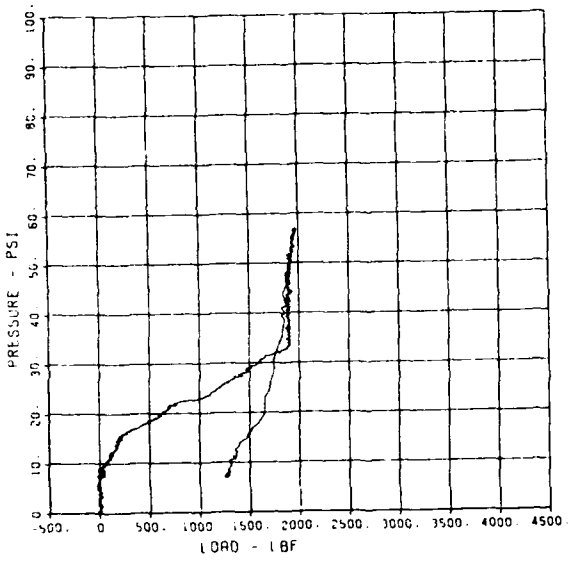

SLAB RESTRAINT C10A
LW-6

20723 1
08/29/84 R0199

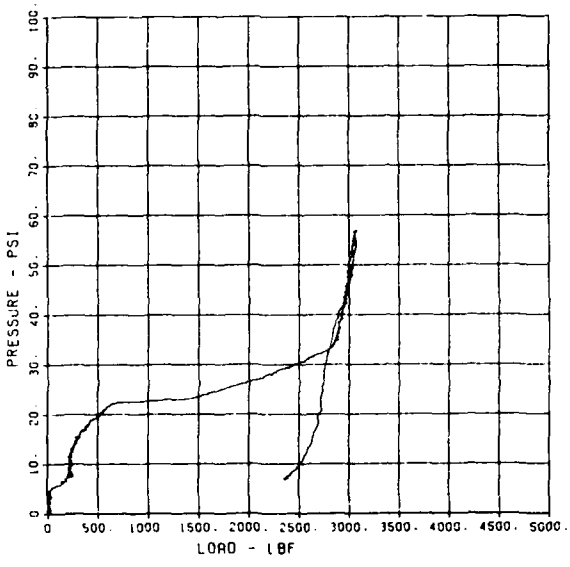

SLAB RESTRAINT C10A
LW-7

20723 1
08/29/84 R0199

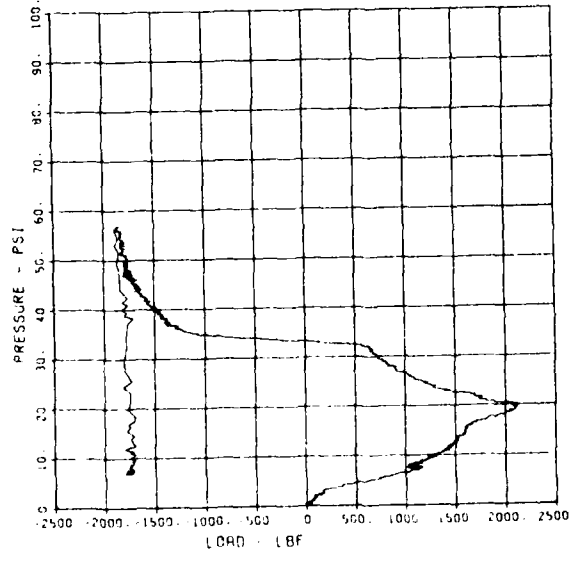

SLAB RESTRAINT C10A
LW-8

20723 1
08/29/84 R0199

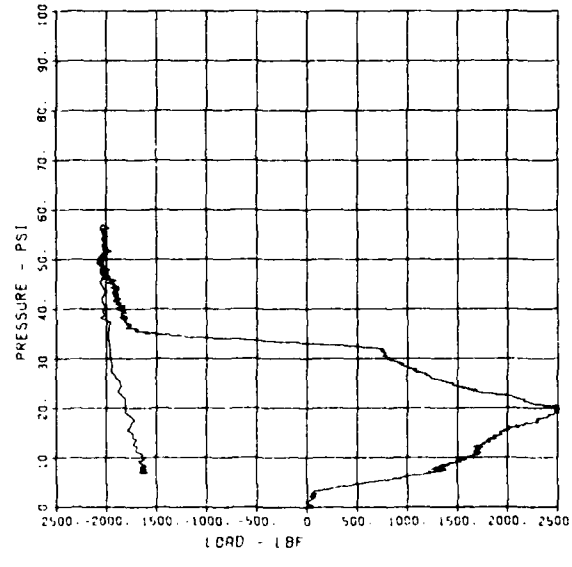

SLAB RESTRAINT C10A
LW-9

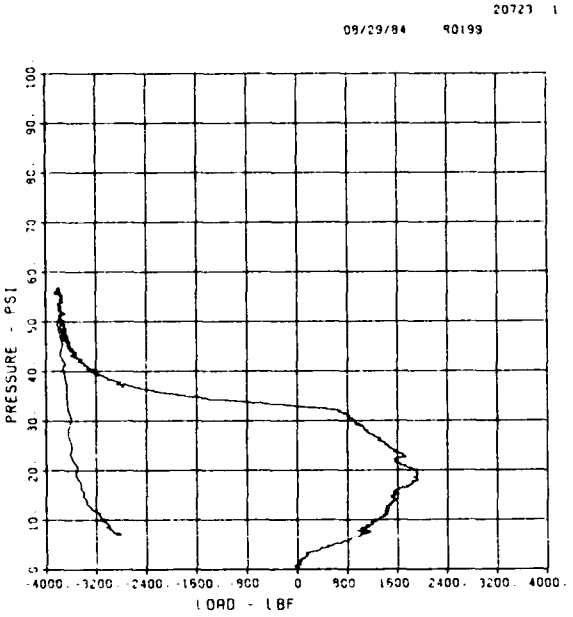

SLAB RESTRAINT C10A
LW-10

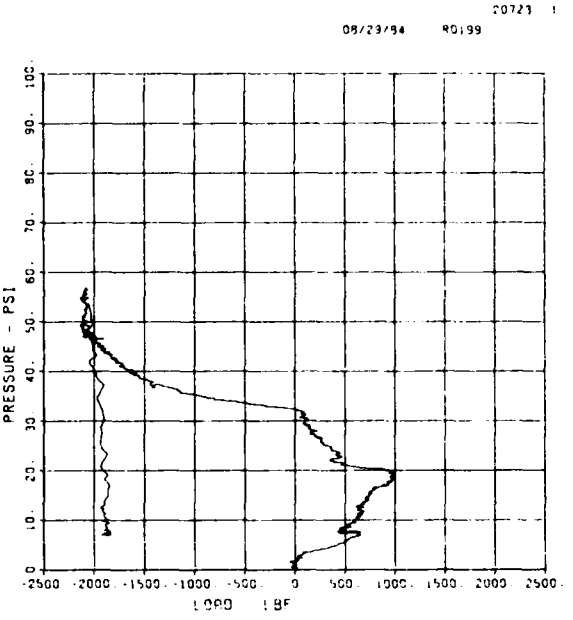

SLAB RESTRAINT C10A
LW-11

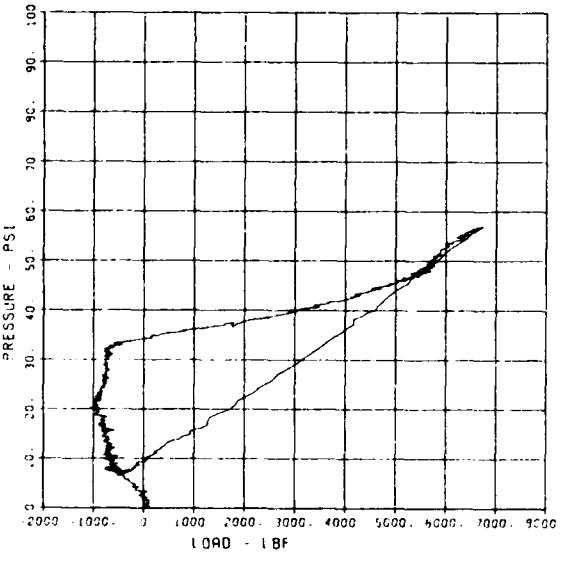

SLAB RESTRAINT C10A
LW-12

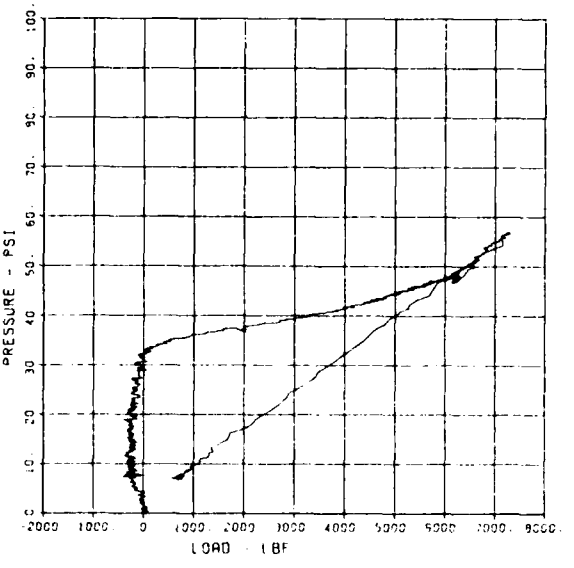

SLAB RESTRAINT C10A
LW-13

20723 1
09/29/94 R0199

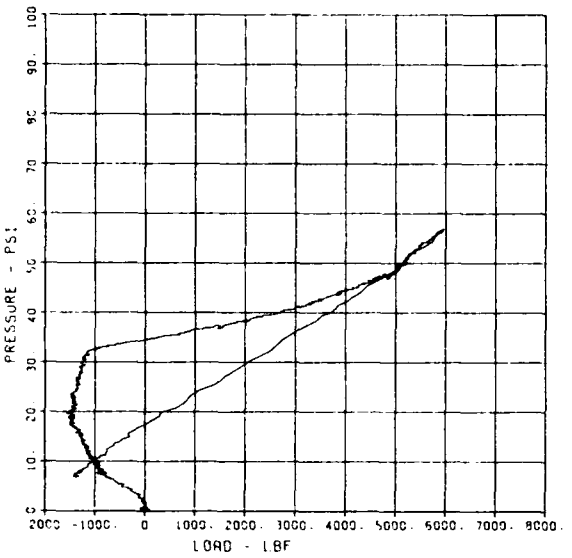

SLAB RESTRAINT C10A
LW-14

20723 1
09/29/94 R0199

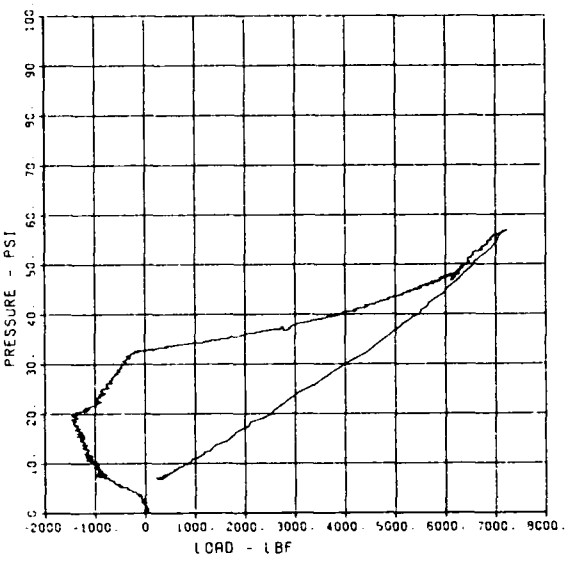

SLAB RESTRAINT C10A
LW-15

20723 1
09/29/94 R0199

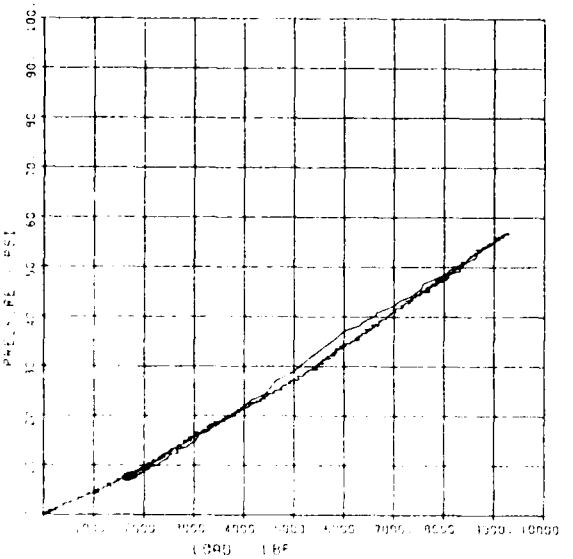

SLAB RESTRAINT C10A
LW-16

20723 1
09/29/84 R0199

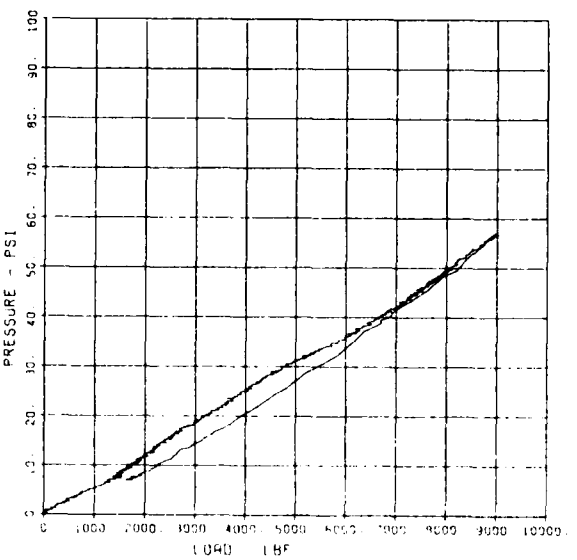

SLAB RESTRAINT C10A
ST-1

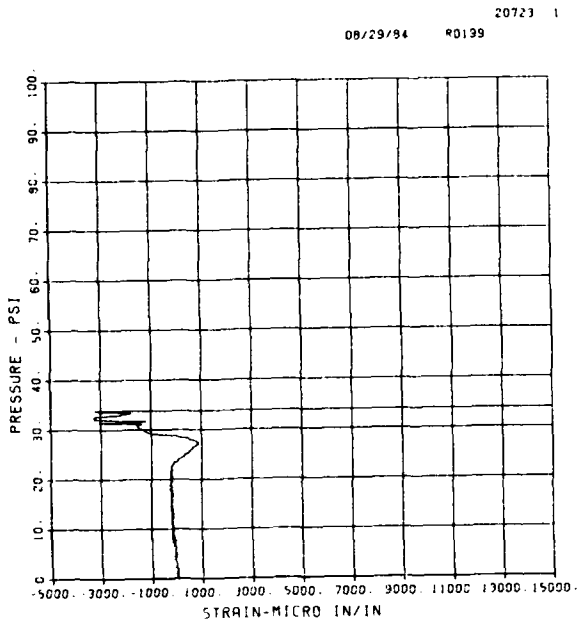

SLAB RESTRAINT C10A
ST-2

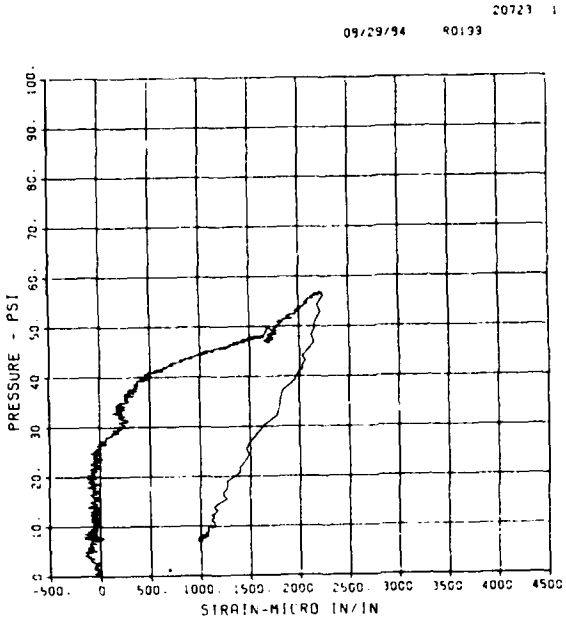

SLAB RESTRAINT C10A
ST-3

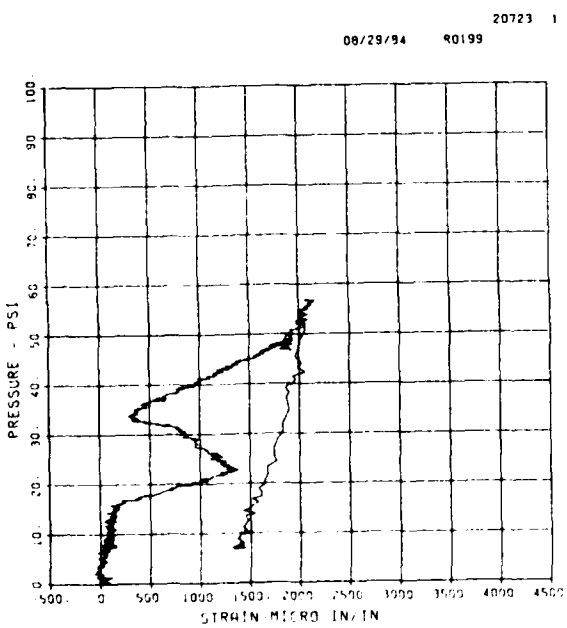

SLAB RESTRAINT C10A
SB-1

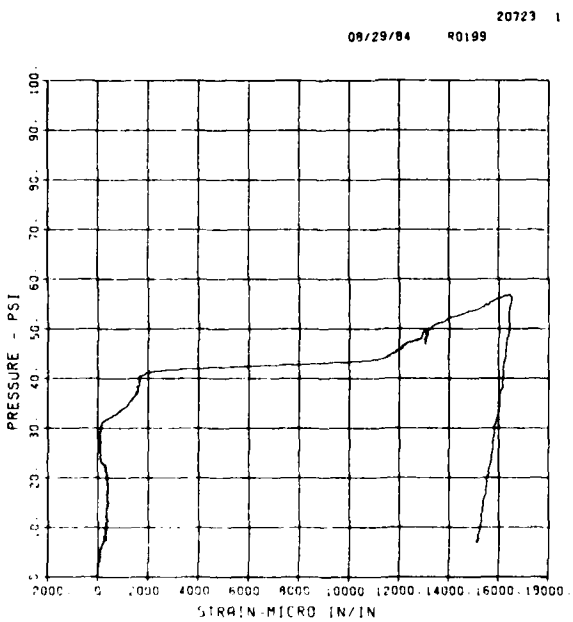

SLAB RESTRAINT C10A
SB-2

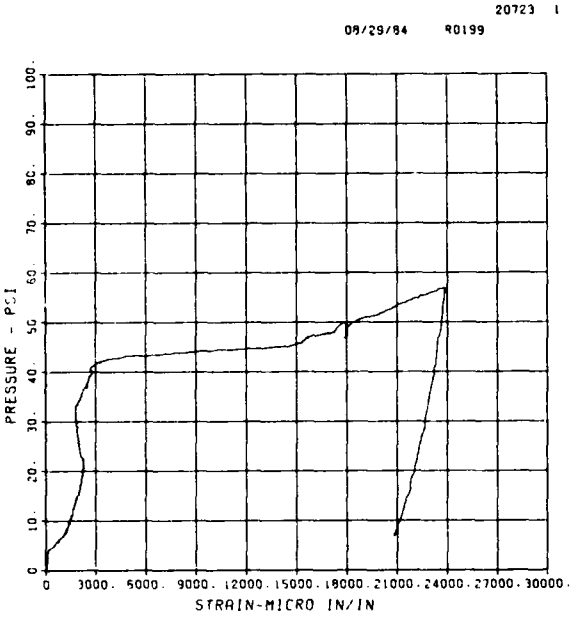

SLAB RESTRAINT C10A
SB-3

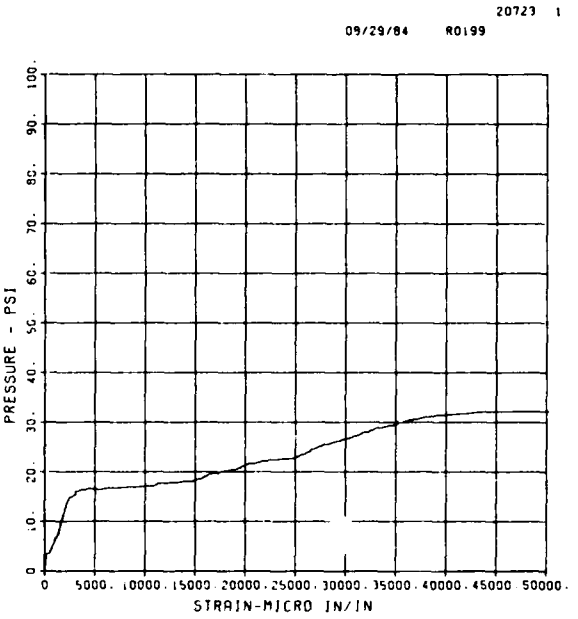

SLAB RESTRAINT C10A
SB-1A

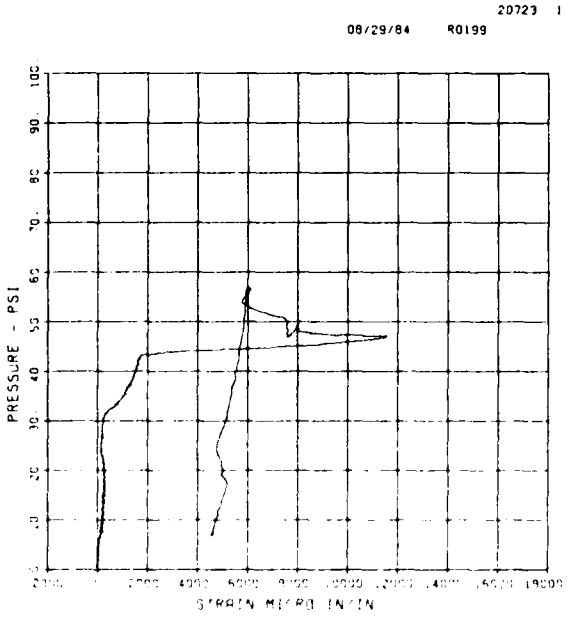

SLAB RESTRAINT C10A
SB-3A

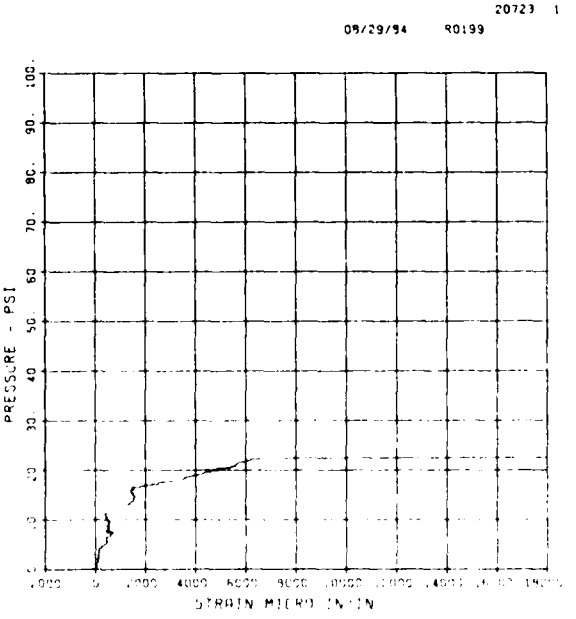

SLAB RESTRAINT G11

SLAB RESTRAINT G11
G-1

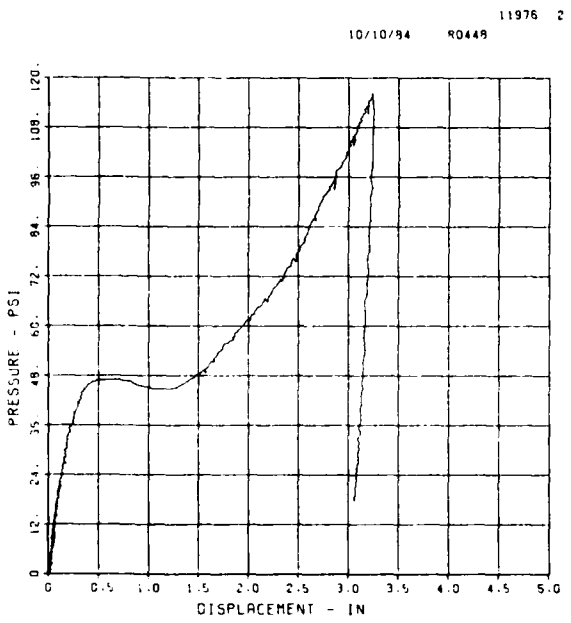

SLAB RESTRAINT G11
G-2

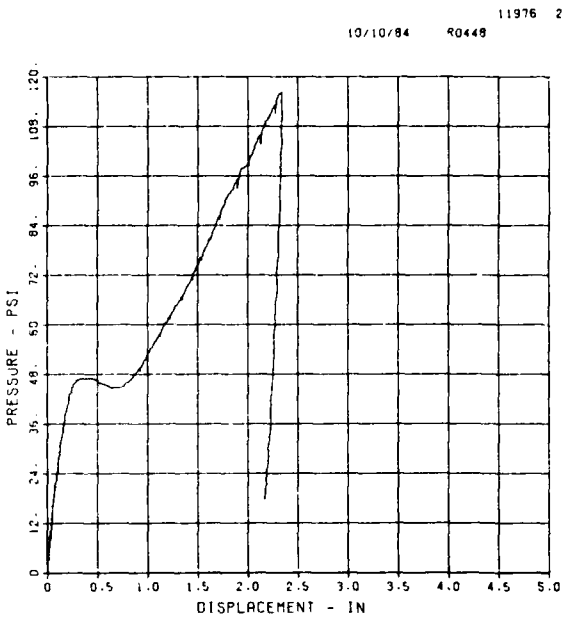

SLAB RESTRAINT G11
G-3

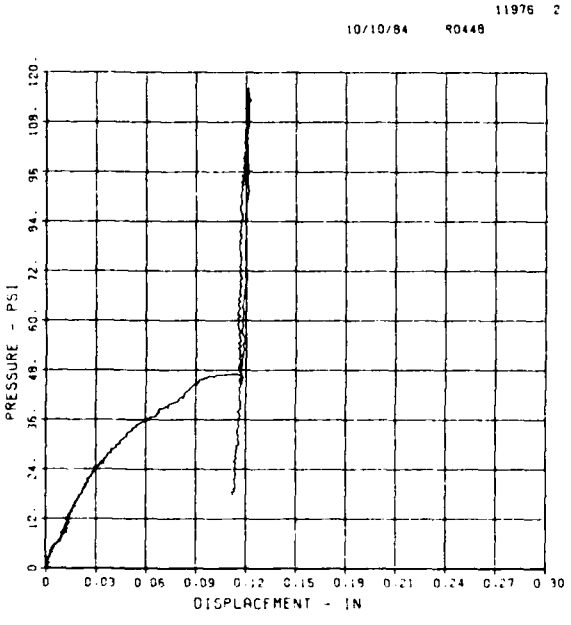

SLAB RESTRAINT G11
G-4

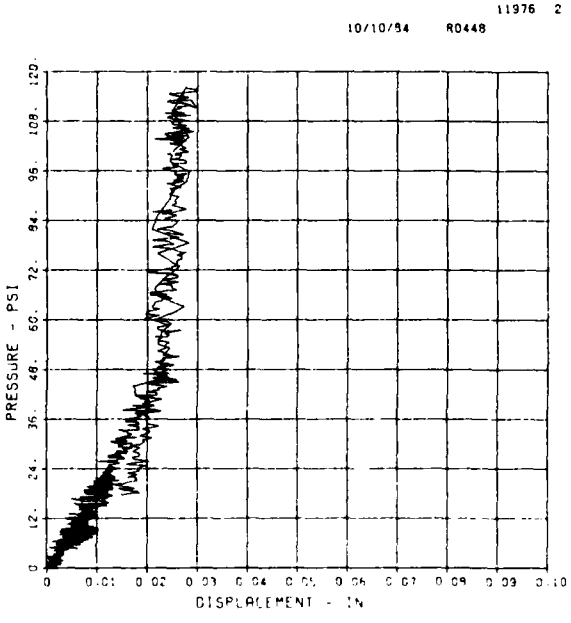

SLAB RESTRAINT G11
LW-1

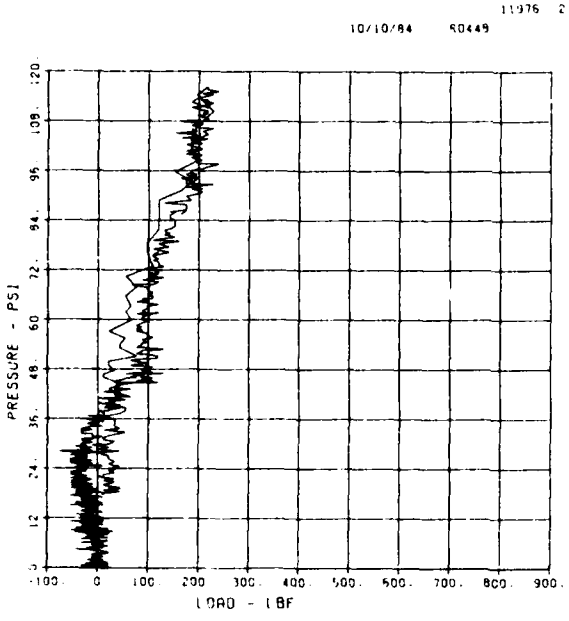

SLAB RESTRAINT G11
LW-2

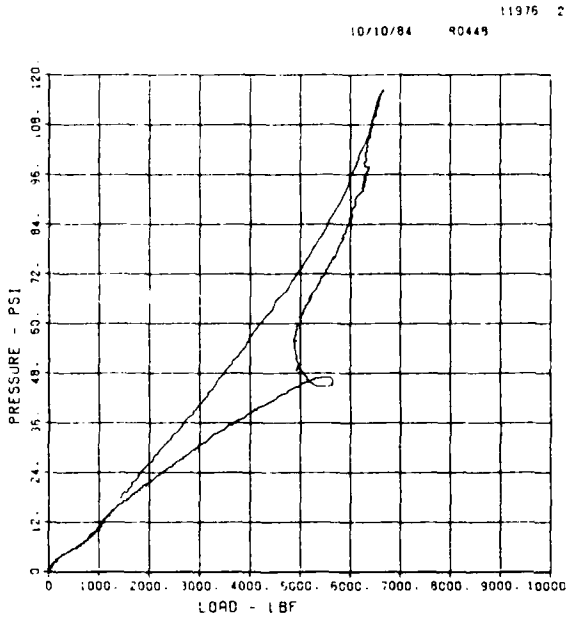

SLAB RESTRAINT G11
LW-3

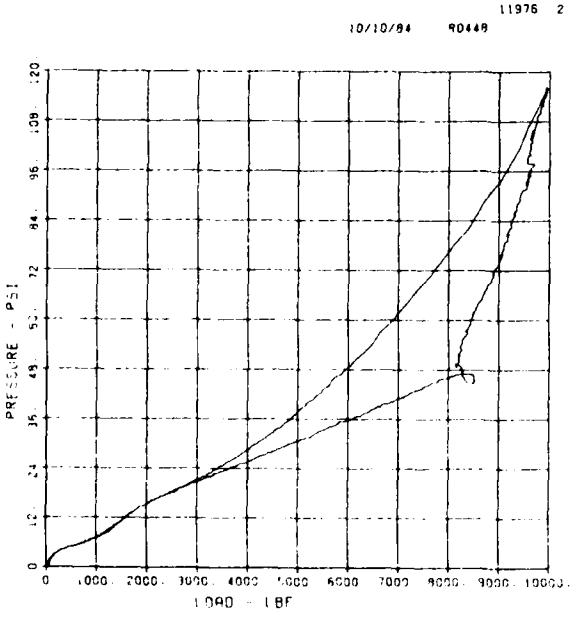

SLAB RESTRAINT G11
LW-4

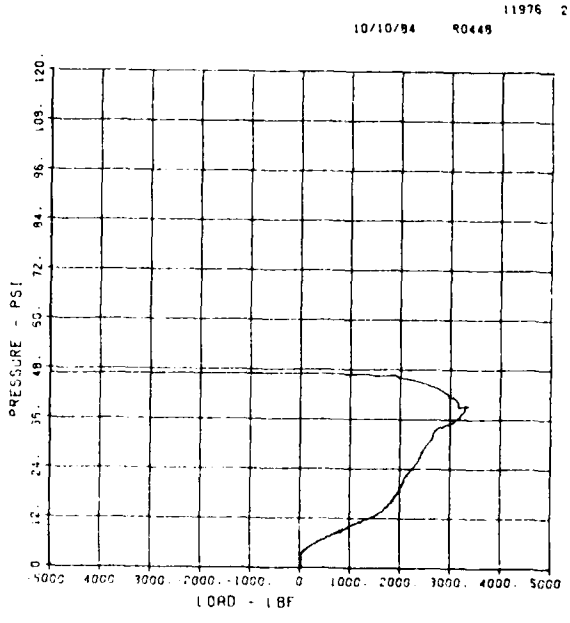

SLAB RESTRAINT G11
LW-6

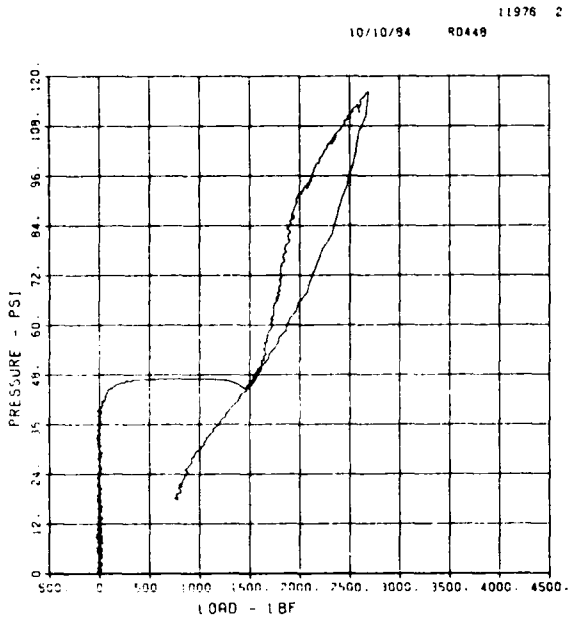

SLAB RESTRAINT G11
LW-7

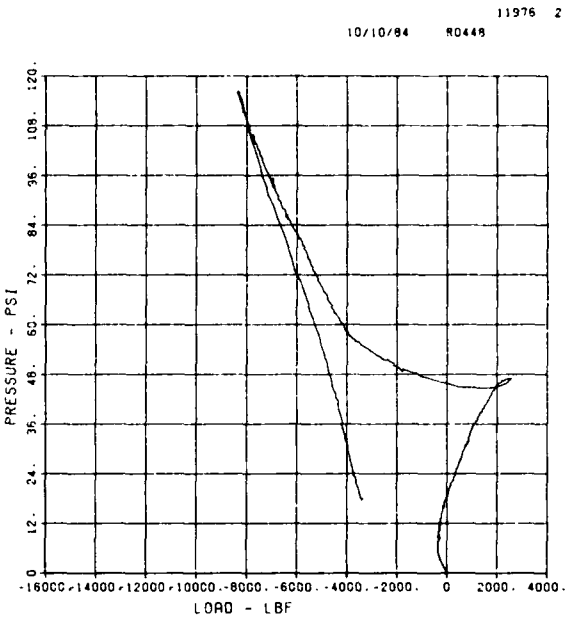

SLAB RESTRAINT G11
LW-8

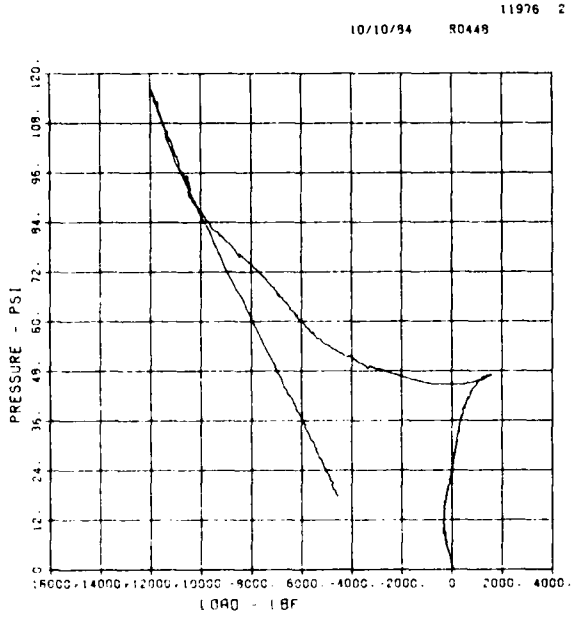

SLAB RESTRAINT G11
LW-9

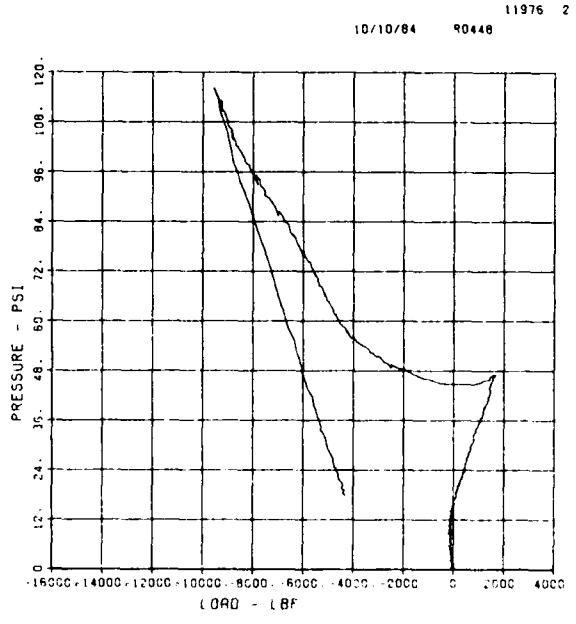

SLAB RESTRAINT G11
LW-10

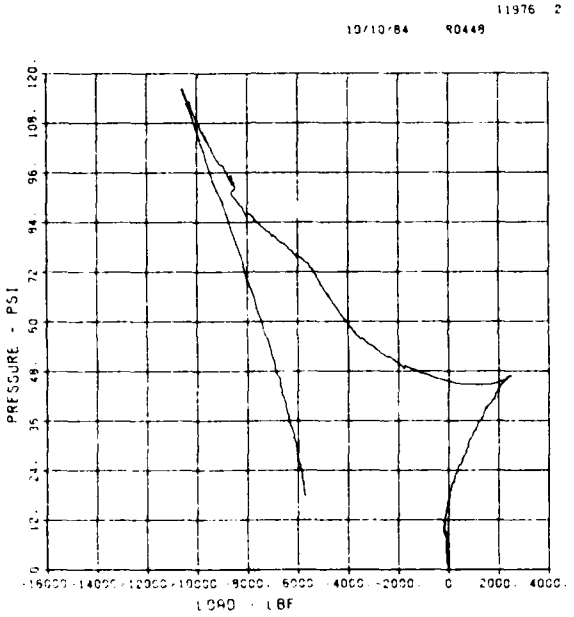

SLAB RESTRAINT G11
LW-11

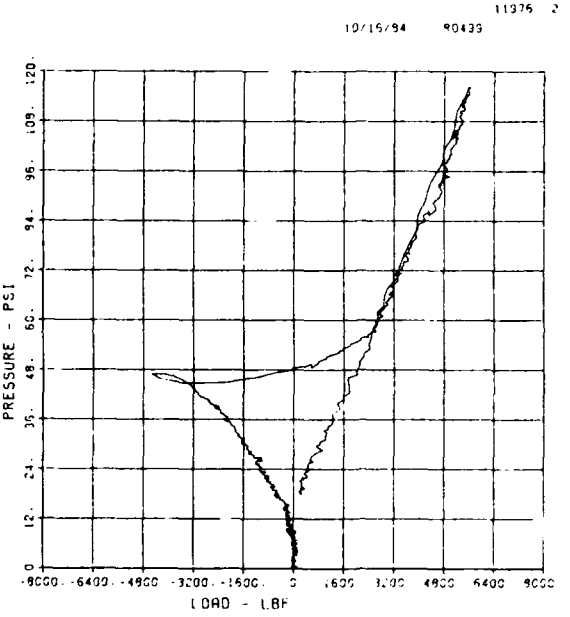

SLAB RESTRAINT G11
LW-13

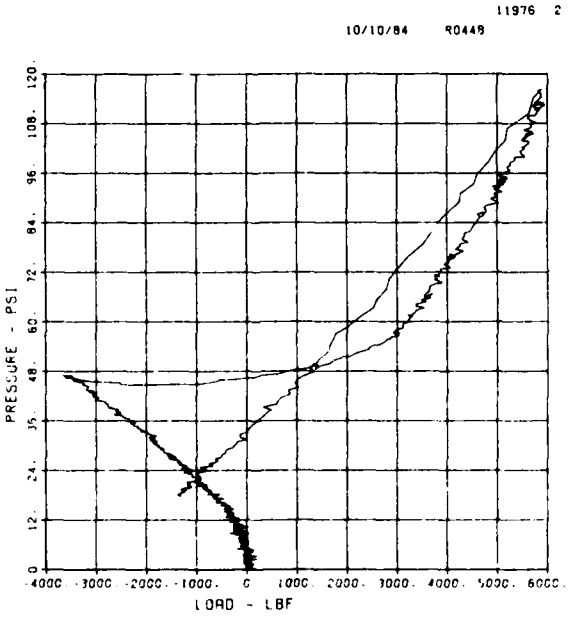

SLAB RESTRAINT G11
LW-14

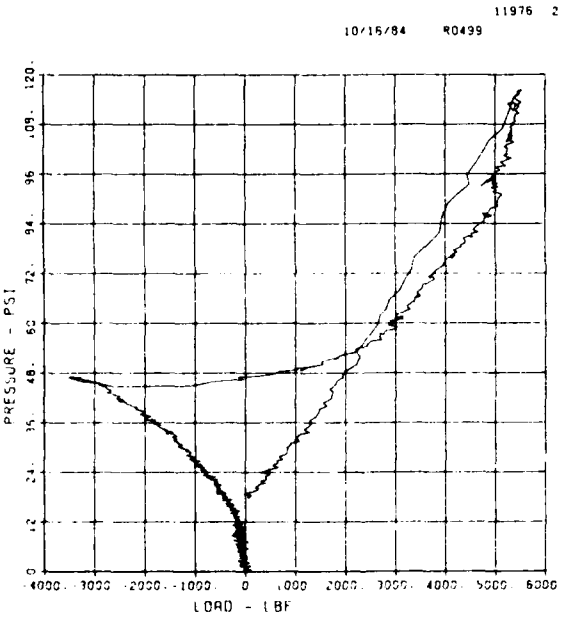

SLAB RESTRAINT G11
LW-15

11976 2
10/10/84 R0449

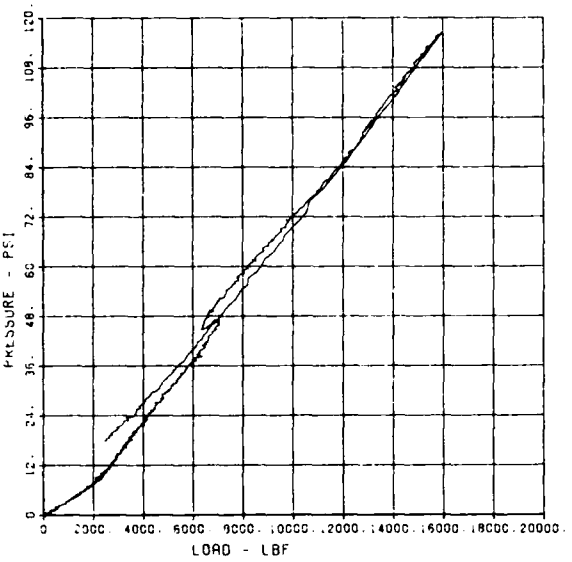

SLAB RESTRAINT G11
ST-1

11976 2
10/10/84 R0449

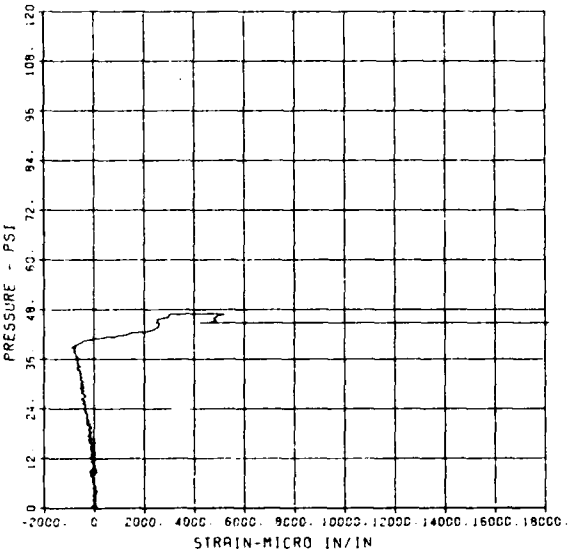

SLAB RESTRAINT G11
ST-2

11976 2
10/10/84 R0449

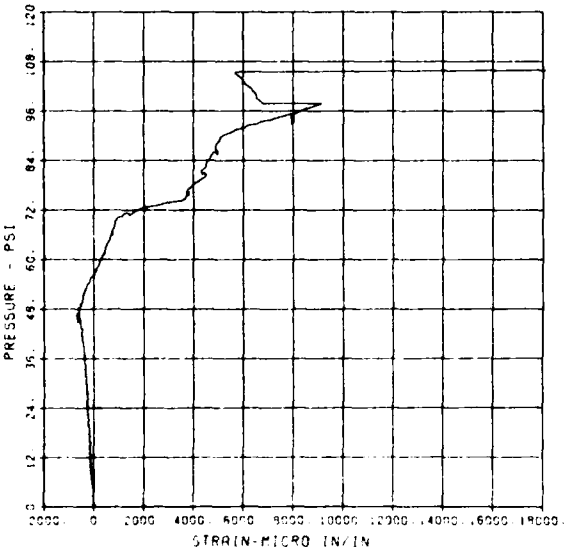

SLAB RESTRAINT G11
ST-3

11976 2
10/10/84 R0449

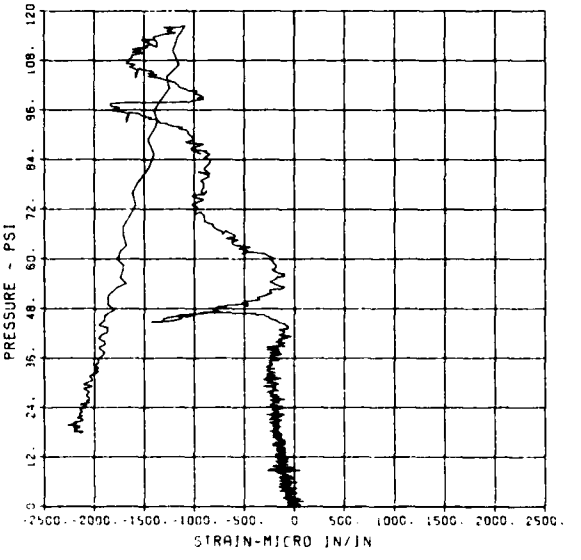

SLAB RESTRAINT G11
SB-1'

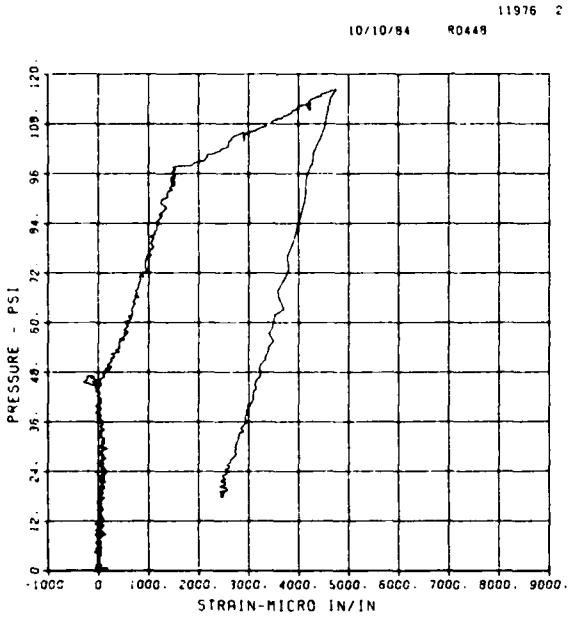

SLAB RESTRAINT G11
SB-2'

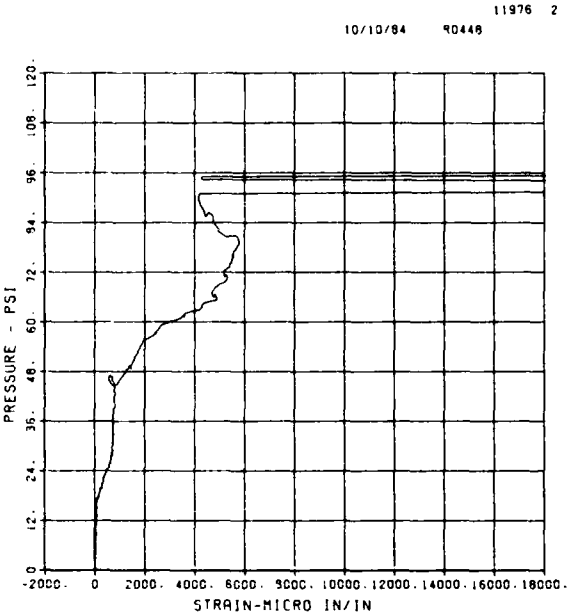

SLAB RESTRAINT G11
SB-3'

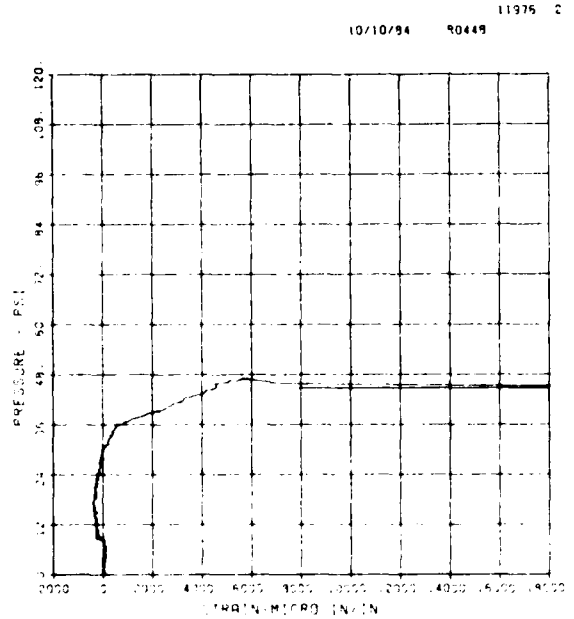

SLAB RESTRAINT G11
CT-1

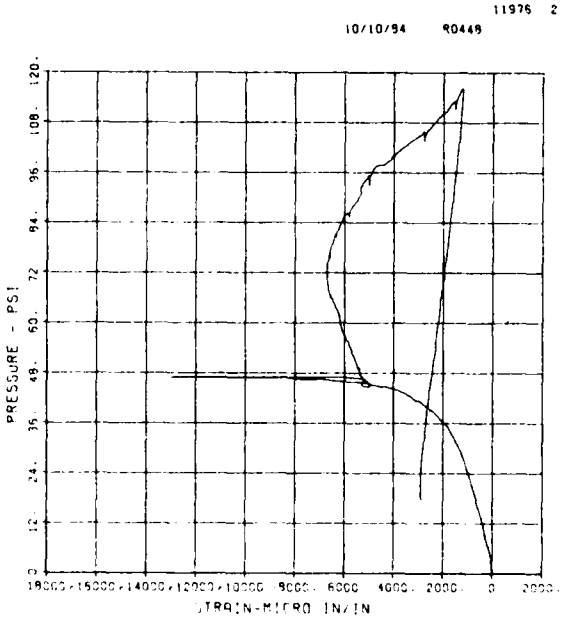

SLAB RESTRAINT G11
CB-3

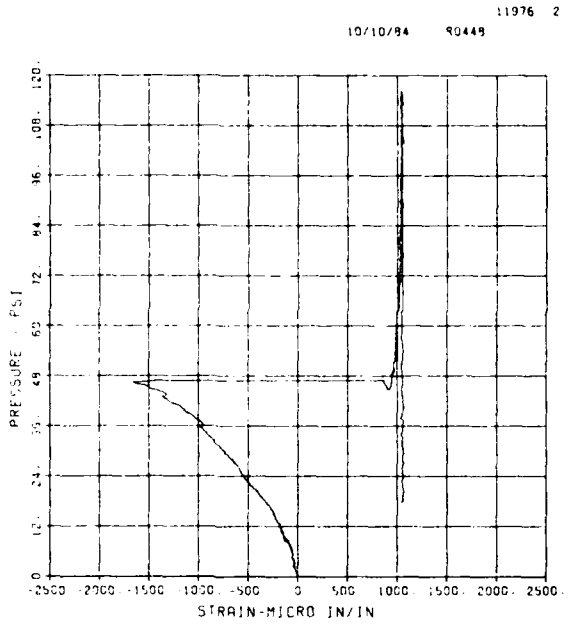

SLAB RESTRAINT G11
SB1A

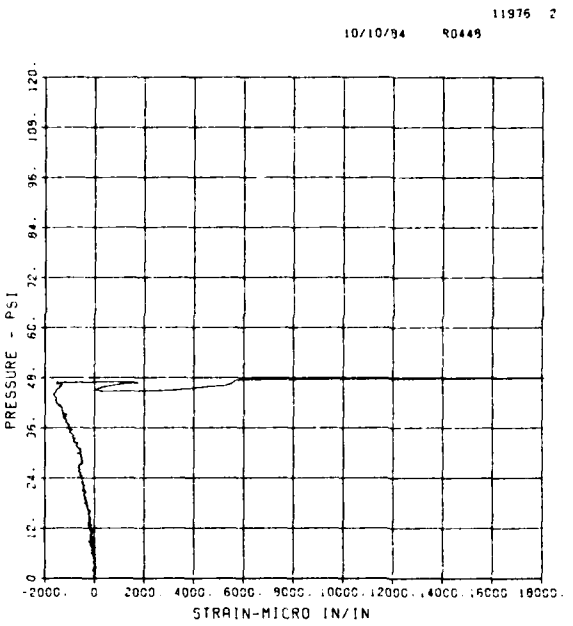

SLAB RESTRAINT G11
SB3'A

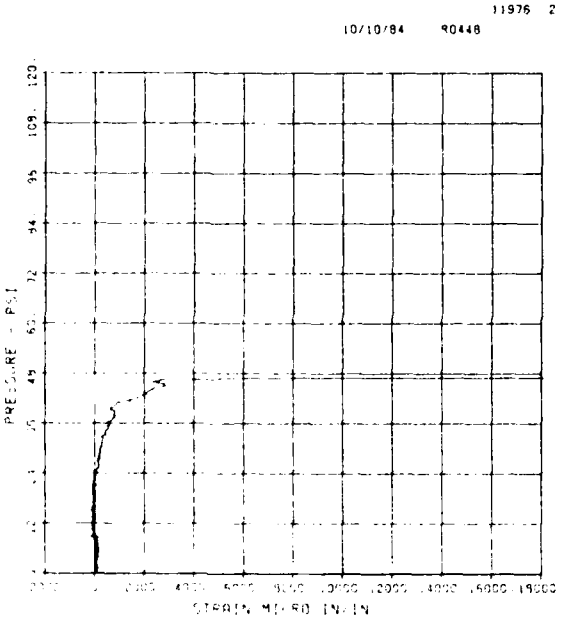

SLAB RESTRAINT G11
SF3A

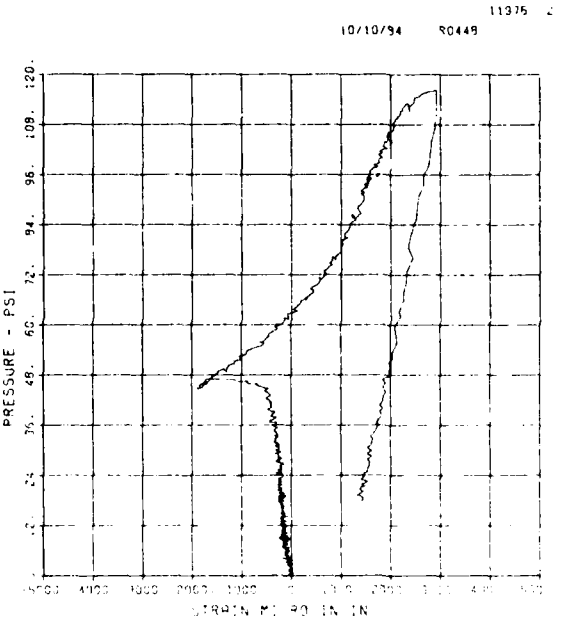

SLAB RESTRAINT G12

SLAB RESTRAINT G12
D-1

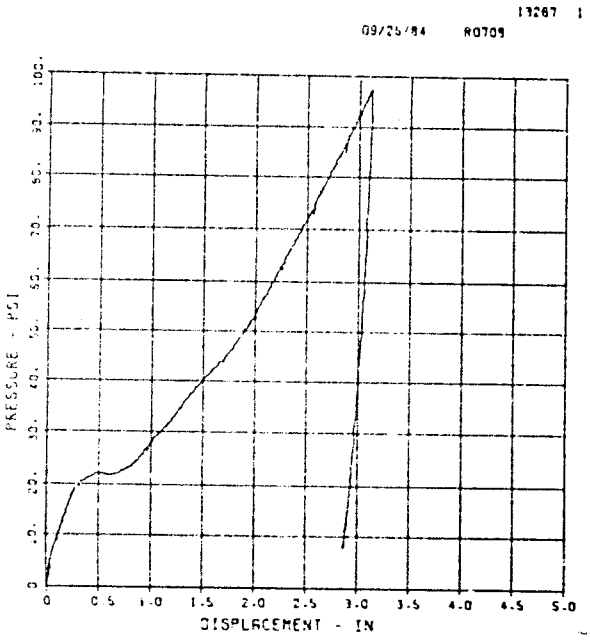

SLAB RESTRAINT G12
D-2

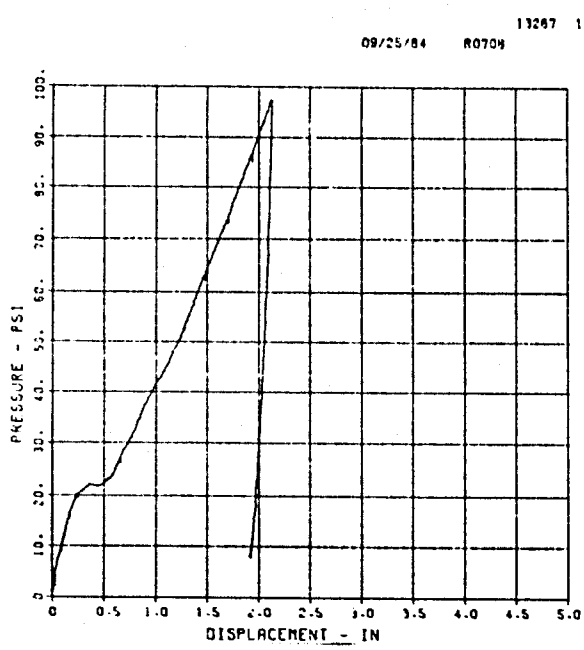

SLAB RESTRAINT G12
D-3

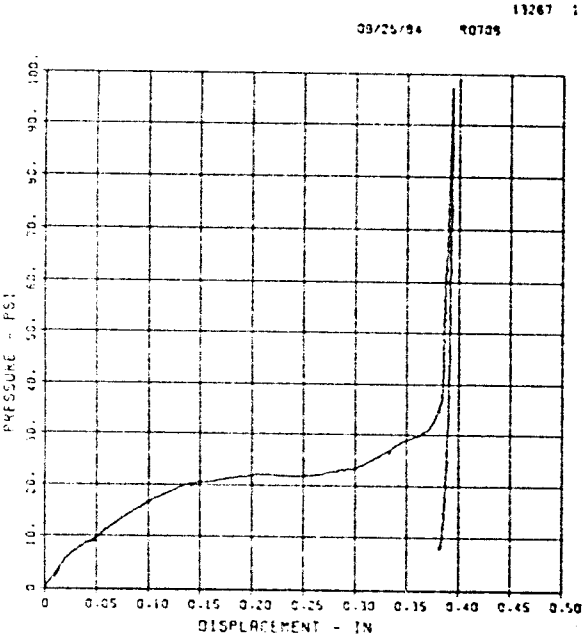

SLAB RESTRAINT G12
D-4

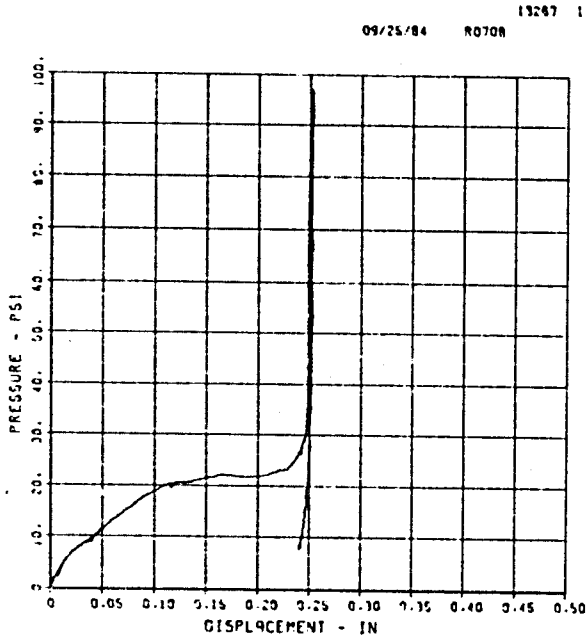

SLAB RESTRAINT G12
LW-1

13267 1
09/25/84 R0709

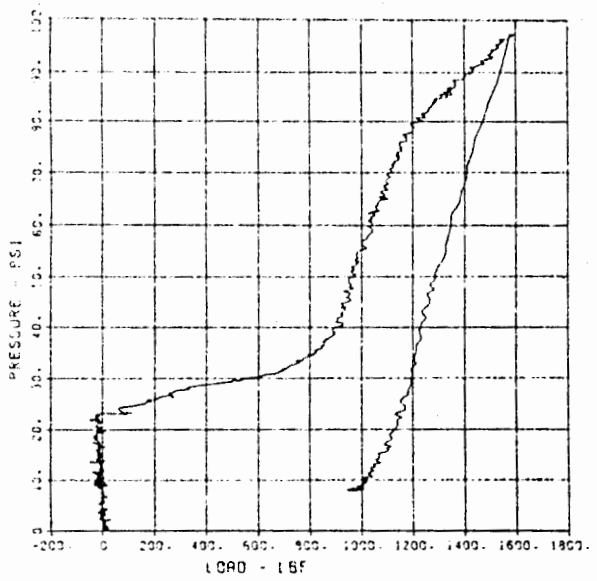

SLAB RESTRAINT G12
LW-2

13267 1
09/25/84 R0709

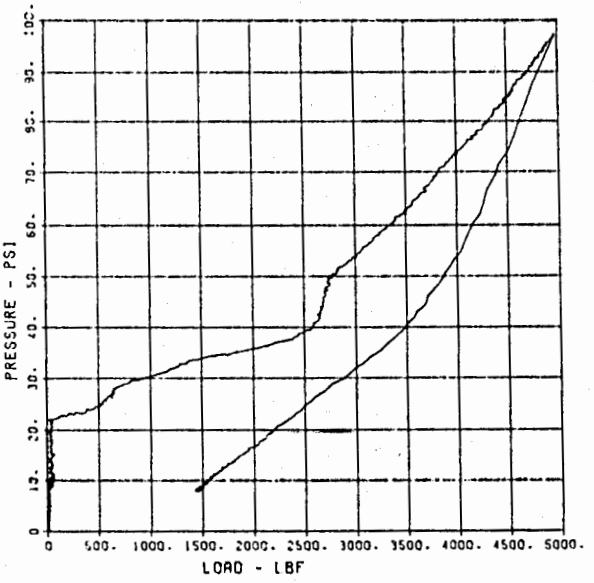

SLAB RESTRAINT G12
LW-3

13267 1
09/25/84 R0709

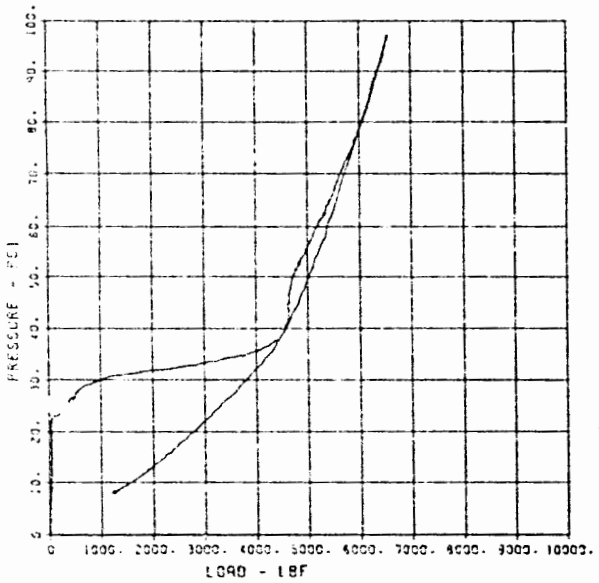

SLAB RESTRAINT G12
LW-4

13267 1
09/25/84 R0709

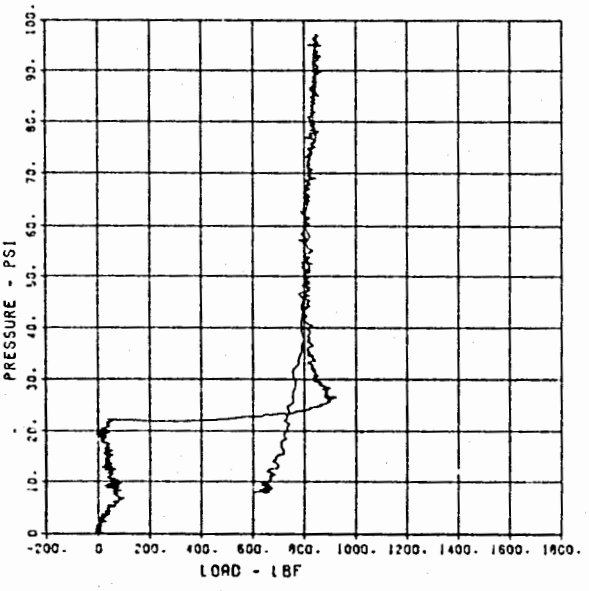

SLAB RESTRAINT G12
LW-5

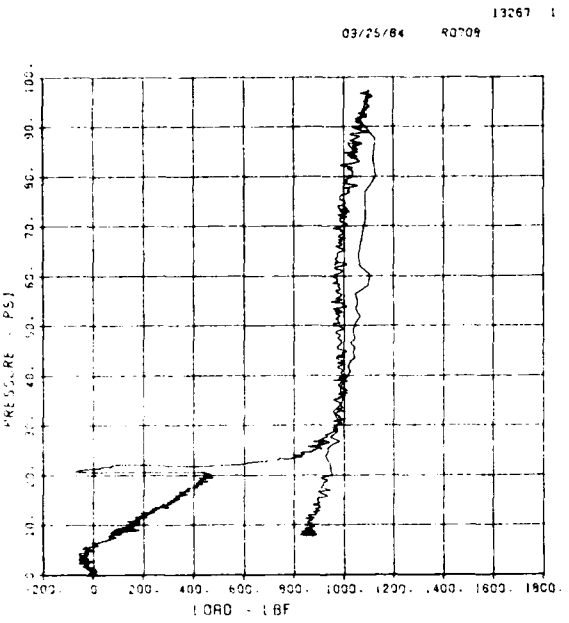

SLAB RESTRAINT G12
LW-6

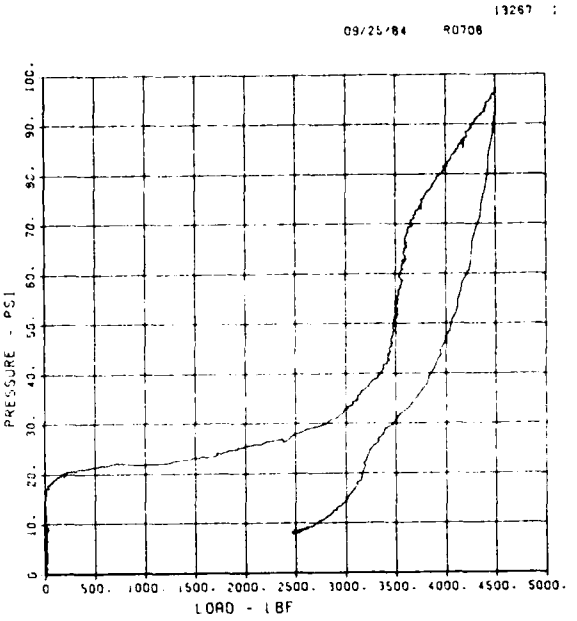

SLAB RESTRAINT G12
LW-11

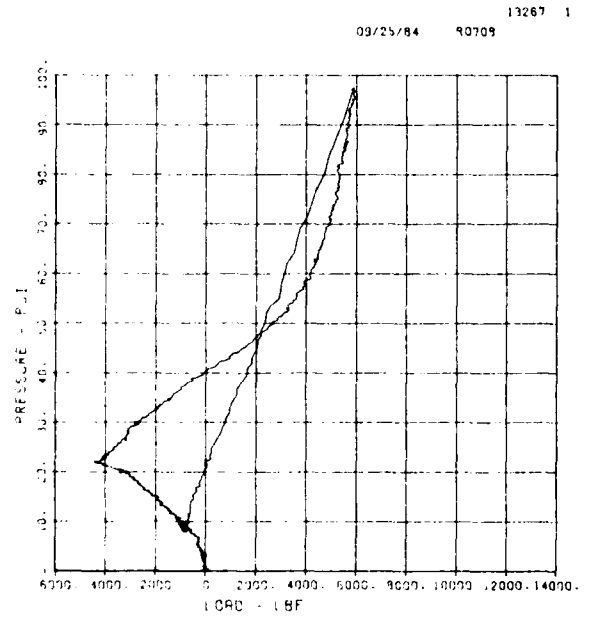

SLAB RESTRAINT G12
LW-12

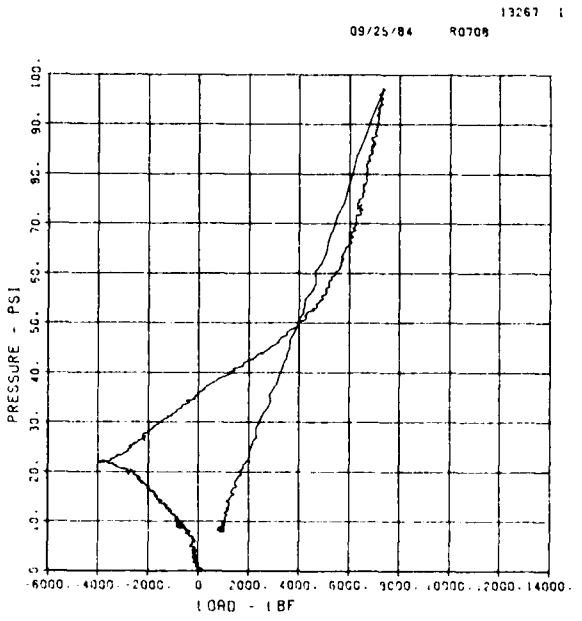

SLAB RESTRAINT G12
LW-13

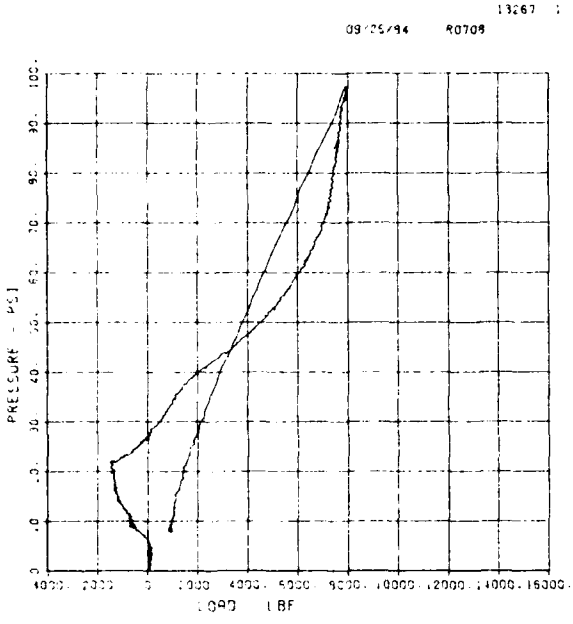

SLAB RESTRAINT G12
LW-14

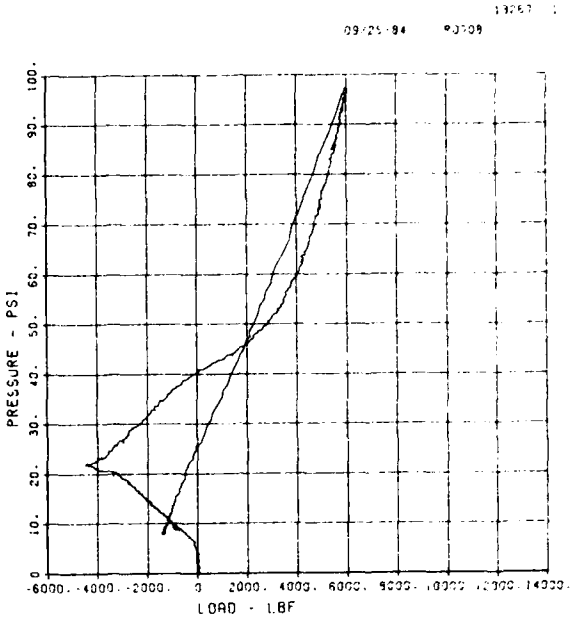

SLAB RESTRAINT G12
LW-15

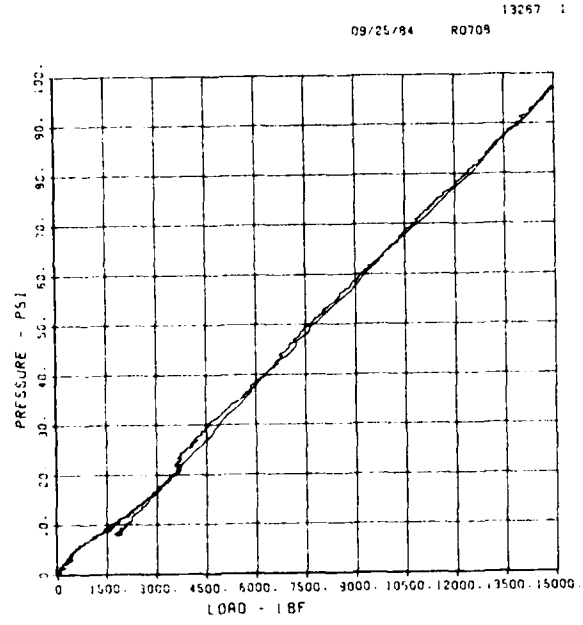

SLAB RESTRAINT G12
ST-1

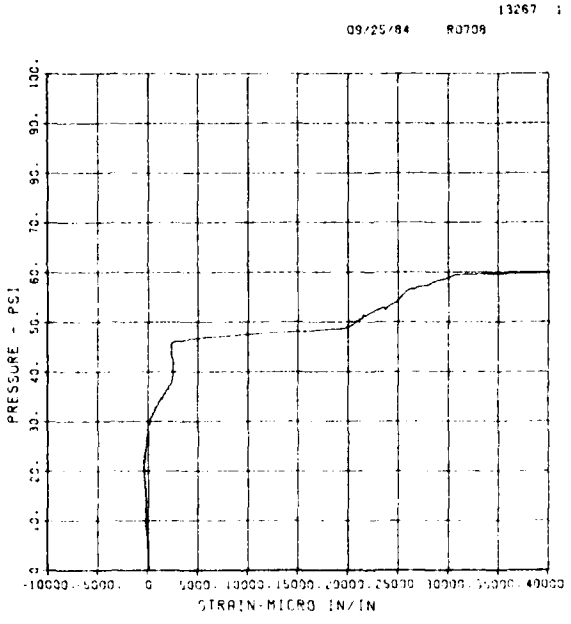

SLAB RESTRAINT G12
ST-2

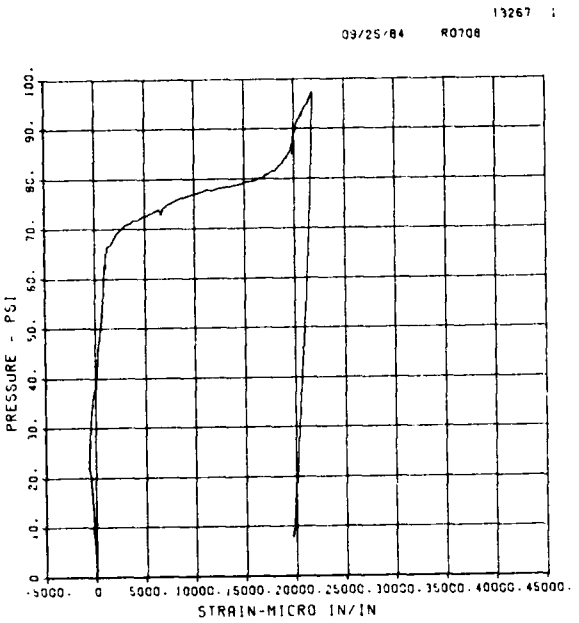

SLAB RESTRAINT G12
ST-3

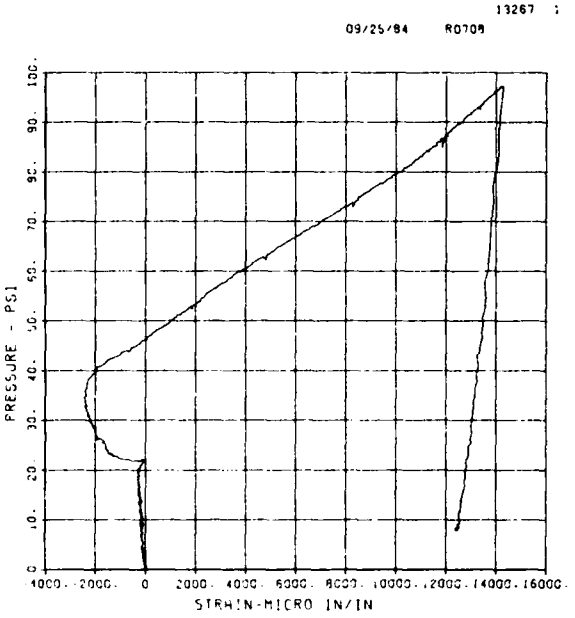

SLAB RESTRAINT G12
SB-1

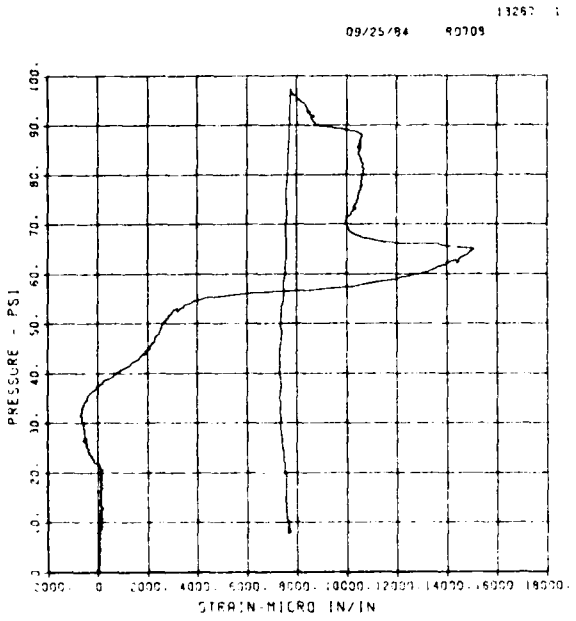

SLAB RESTRAINT G12
SB-2

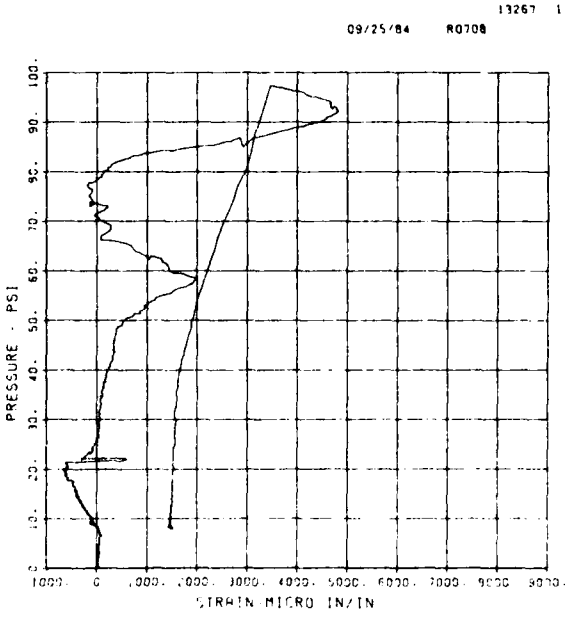

SLAB RESTRAINT G12
SR-3

13267
09/25/84 R0708

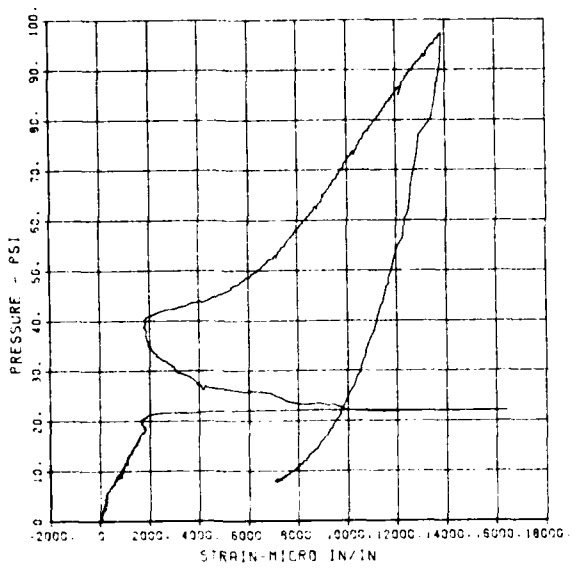

SLAB RESTRAINT G12
C6

13267
09/25/84 R0708

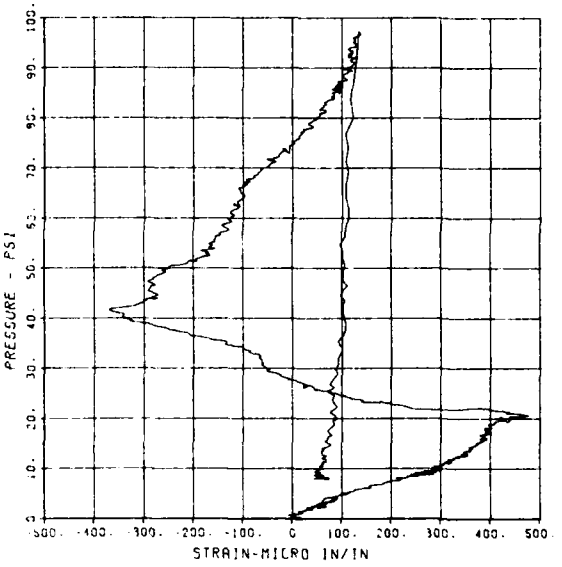

SLAB RESTRAINT G12

13267
09/25/84 R0708

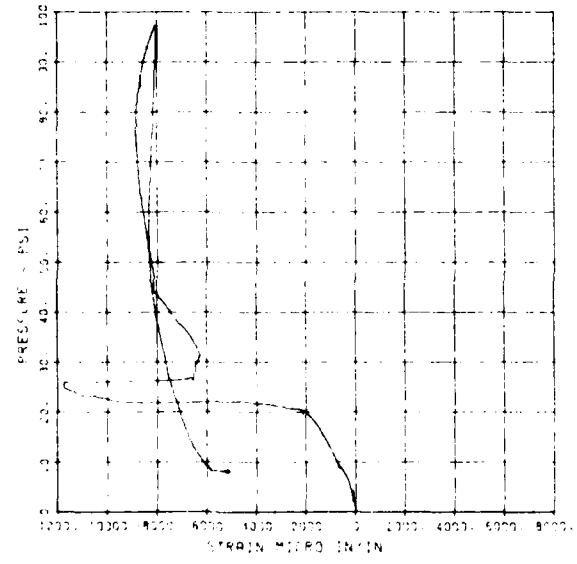

SLAB RESTRAINT G12

13267
09/25/84 R0708

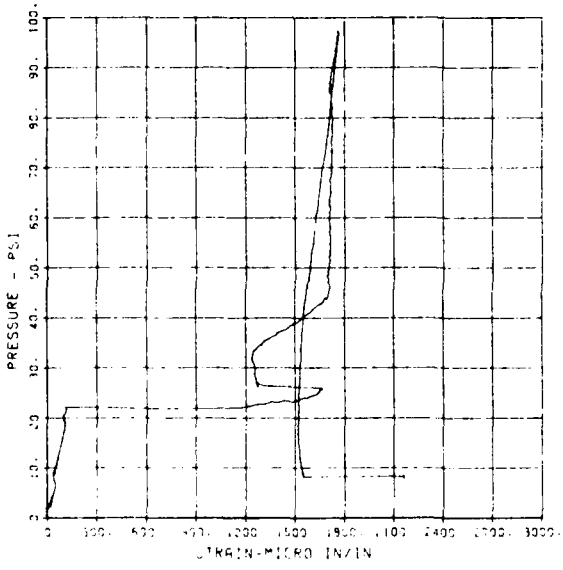

DISTRIBUTION LIST

Director, Federal Emergency Management Agency
25 cys ATTN: Mr. Tom Provenzano
500 C St. SW
Washington, DC 20472

Commander, US Army Engineer District, Wilmington
ATTN: Pat Burns/Library
PO Box 1890
Wilmington, N. C. 28402

Headquarters, Department of Energy
ATTN: Library/G-049 MA-232.2/GTN
Washington, DC 20545

National Bureau of Standards
ATTN: Mr. Samuel Kramer
Dr. Lewis V. Spencer
Washington, DC 20234

Associate Director, Natural Resources and
Commercial Services
Office of Science & Technology
ATTN: Mr. Phillip M. Smith
Executive Office Building
Washington, DC 20500

Director, Office of Administration
Program Planning and Control
Department of Housing and Urban Development
ATTN: Mr. Bert Greenglass
Washington, DC 20410

Director, Defense Nuclear Agency
ATTN: SPTD/Mr. Tom Kennedy
STTL/Technical Library
Washington, DC 20305

Director, Defense Intelligence Agency
ATTN: Mr. Carl Wiehle (DB-4C2)
Washington, DC 20301

Assistant Secretary of the Army (R&D)
ATTN: Assistant for Research
Washington, DC 20301

Office, Chief of Engineers,
Department of the Army
ATTN: DAEN-RDZ-A
DAEN-ECE-D
Washington, DC 20314

Sandia Corporation
ATTN: Dr. Clarence R. Mehl
Dept. 5230
Box 5800, Sandia Base
Albuquerque, N. Mex. 87115

Director, US Army Engineer Waterways
Experiment Station
ATTN: Dr S. A. Kiger
Mr. Bill Huff
Mr. Stan Woodson
3 cys Library
PO Box 631
Vicksburg, Miss. 39180

Defense Technical Information Center
12 cys ATTN: (DTIC-DDAB/Mr. Myer B. Kahn)
Cameron Station
Alexandria, Va. 22314

Commander, US Army Materials and Mechanics
Research Center
ATTN: Technical Library
Watertown, Mass. 02172

Command and Control Technical Center
Department of Defense
Room 2E312 Pentagon
Washington, DC 20301

Los Alamos Scientific Laboratory
ATTN: Report Library MS-364
PO Box 1663
Los Alamos, N. Mex. 87544

Director, Ballistic Research Laboratory
ATTN: (DRXBR-TBD/Mr. George Coulter)
Aberdeen Proving Ground, Md. 21005

Commanding Officer, Office of Naval Research
Department of the Navy
Washington, DC 20390

Commanding Officer
US Naval Civil Engineering Laboratory
Naval Construction Battalion Center
ATTN: Library (Code L08A)
Port Hueneme, Calif. 93043

Commander, Air Force Weapons Laboratory/SUL
ATTN: Technical Library
Kirtland Air Force Base, N. Mex. 87117

Civil Engineering Center
AF/PRECET
Tyndall AFB, Fla. 32403

University of Florida
Civil Defense Technical Services
College of Engineering
Department of Engineering
Gainesville, Fla. 32601

Technical Reports Library
Kurt F. Wendt Library
College of Engineering
University of Wisconsin
Madison, Wisc. 53706

Agbabian Associates
250 N. Nash Street
El Segundo, Calif. 90245

AT&T Bell Laboratories
ATTN: Mr. E. Witt
Whippany, N. J. 07981

James E. Beck & Associates
4216 Los Palos Avenue
Palo Alto, Calif. 94306

Chamberlain Manufacturing Corp.
GARD, Inc.
7449 N. Natchez Avenue
Niles, Ill. 60648

ITT Research Institute
ATTN: Mr. A. Longinow
10 West 35th Street
Chicago, Ill. 60616

H. L. Murphy Associates
Box 1727
San Mateo, Calif. 94401

RAND Corporation
ATTN: Document Library
1700 Main Street
Santa Monica, Calif. 90401

Research Triangle Institute
ATTN: Mr. Edward L. Hill
PO Box 12194
Research Triangle Park, N. C. 27709

Scientific Services, Inc.
517 East Bayshore Drive
Redwood City, Calif. 94060

US Army Engineer Division, Huntsville
10 cys ATTN: Mr. Paul Lahoud
PO Box 1600, West Station
Huntsville, AL 35807

EFFECTS OF EDGE RESTRAINT ON SLAB BEHAVIOR, Unclassified, US Army Engineer Waterways Experiment Station, February 1986, 251 pp.

This study was performed in conjunction with a Federal Emergency Management Agency program to plan, design, and construct keyworker blast shelters which would be used in high-risk areas of the country during and after a nuclear attack. The shelters considered in this study were box-type structures in which damage is much more likely to occur in the roof slab than in the walls or floor. In this part of the program, the effect of edge restraint on slab behavior was investigated. The primary objective was to determine the effects of partial rotational restraint on slab strength, ductility, and mechanism of failure.

Sixteen one-way, reinforced concrete plate elements were tested in a reaction structure under uniform static water pressure. A "thick-slab" group consisted of eight slabs with span-thickness ratios of 10.4, while eight slabs in the "thin-slab" group had span-thickness ratios of 14.8. The following conclusions were reached at the completion of testing: (1) thrusts enhanced the flexural capacities of slabs with small rotational freedoms as long as the lateral stiffness was sufficient to develop in-plane forces; (2) the deflections at which the peak capacities were achieved were significantly different for slabs with varied rotational freedoms; (3) for larger rotational freedoms, the peak capacities occurred at large deflections, were significantly lower than the capacities which were predicted by compressive membrane theory, and in some cases, the slabs had no definitive flexural capacity at all; (4) smaller rotational freedoms were necessary to induce a stability failure in the thin slabs; (5) significantly more tensile membrane response occurred in the thin-slab group than in the thick-slab group; and (6) in those slabs which were reinforced with ductile No. 2 bars, average incipient collapse deflection occurred at approximately one-eighth of the span for the thick-slab group and somewhat more than that for the thin-slab group.

EFFECTS OF EDGE RESTRAINT ON SLAB BEHAVIOR, Unclassified, US Army Engineer Waterways Experiment Station, February 1986, 251 pp.

This study was performed in conjunction with a Federal Emergency Management Agency program to plan, design, and construct keyworker blast shelters which would be used in high-risk areas of the country during and after a nuclear attack. The shelters considered in this study were box-type structures in which damage is much more likely to occur in the roof slab than in the walls or floor. In this part of the program, the effect of edge restraint on slab behavior was investigated. The primary objective was to determine the effects of partial rotational restraint on slab strength, ductility, and mechanism of failure.

Sixteen one-way, reinforced concrete plate elements were tested in a reaction structure under uniform static water pressure. A "thick-slab" group consisted of eight slabs with span-thickness ratios of 10.4, while eight slabs in the "thin-slab" group had span-thickness ratios of 14.8. The following conclusions were reached at the completion of testing: (1) thrusts enhanced the flexural capacities of slabs with small rotational freedoms as long as the lateral stiffness was sufficient to develop in-plane forces; (2) the deflections at which the peak capacities were achieved were significantly different for slabs with varied rotational freedoms; (3) for larger rotational freedoms, the peak capacities occurred at large deflections, were significantly lower than the capacities which were predicted by compressive membrane theory, and in some cases, the slabs had no definitive flexural capacity at all; (4) smaller rotational freedoms were necessary to induce a stability failure in the thin slabs; (5) significantly more tensile membrane response occurred in the thin-slab group than in the thick-slab group; and (6) in those slabs which were reinforced with ductile No. 2 bars, average incipient collapse deflection occurred at approximately one-eighth of the span for the thick-slab group and somewhat more than that for the thin-slab group.

EFFECTS OF EDGE RESTRAINT ON SLAB BEHAVIOR, Unclassified, US Army Engineer Waterways Experiment Station, February 1986, 251 pp.

This study was performed in conjunction with a Federal Emergency Management Agency program to plan, design, and construct keyworker blast shelters which would be used in high-risk areas of the country during and after a nuclear attack. The shelters considered in this study were box-type structures in which damage is much more likely to occur in the roof slab than in the walls or floor. In this part of the program, the effect of edge restraint on slab behavior was investigated. The primary objective was to determine the effects of partial rotational restraint on slab strength, ductility, and mechanism of failure.

Sixteen one-way, reinforced concrete plate elements were tested in a reaction structure under uniform static water pressure. A "thick-slab" group consisted of eight slabs with span-thickness ratios of 10.4, while eight slabs in the "thin-slab" group had span-thickness ratios of 14.8. The following conclusions were reached at the completion of testing: (1) thrusts enhanced the flexural capacities of slabs with small rotational freedoms as long as the lateral stiffness was sufficient to develop in-plane forces; (2) the deflections at which the peak capacities were achieved were significantly different for slabs with varied rotational freedoms; (3) for larger rotational freedoms, the peak capacities occurred at large deflections, were significantly lower than the capacities which were predicted by compressive membrane theory, and in some cases, the slabs had no definitive flexural capacity at all; (4) smaller rotational freedoms were necessary to induce a stability failure in the thin slabs; (5) significantly more tensile membrane response occurred in the thin-slab group than in the thick-slab group; and (6) in those slabs which were reinforced with ductile No. 2 bars, average incipient collapse deflection occurred at approximately one-eighth of the span for the thick-slab group and somewhat more than that for the thin-slab group.